Stony Brook University

Mechanism and Inhibition of Bacterial Enoyl-ACP

Reductases: Towards Novel Antibacterial Drugs

A Dissertation Presented

by

Hao Lu

to

The Graduate School

in Partial Fulfillment of the Requirements

for the Degree of

Doctor of Philosophy

in

Chemistry

Stony Brook University

May 2010

Stony Brook University

The Graduate School

Hao Lu

We, the dissertation committee for the above candidate for the

Doctor of Philosophy degree, hereby recommend

Acceptance of this dissertation

Peter J. Tonge – Dissertation Advisor

Professor of Chemistry Department

Dale G. Drueckhammer – Chairperson of Defense

Professor of Chemistry Department

Elizabeth M. Boon – Committee Member of Defense

Assistant Professor of Chemistry Department

Stewart L. Fisher– External Committee Member of Defense

Principal Scientist II of AstraZeneca R&D Boston

This dissertation is accepted by the Graduate School

Lawrence Martin

Dean of the Graduate School

Abstract of the Dissertation

Mechanism and Inhibition of Bacterial Enoyl-ACP

Reductases: Towards Novel Antibacterial Drugs

by

Hao Lu

Doctor of Philosophy

in

Chemistry

Stony Brook University

2010

Resistance to existing antimicrobial agents is a global threat to human health care, and new drugs with novel mechanisms of action are required in order to keep pace with the emergence of drug resistant pathogens. The bacterial fatty acid biosynthesis (FAS-II) pathway represents a validated yet relatively unexploited target for new antibiotic development and consequently there is significant interest in developing potent inhibitors of FAS-II enzymes. In this work

we have focused on the FAS-II enoyl-ACP reductase enzyme which is known to be essential for bacterial survival.

We cloned, expressed and purified the enoyl-ACP reductase from *Francisella tularensis* (ftuFabI). The enzyme was shown to catalyze substrate reduction through a sequential bi bi mechanism and to prefer substrate with long (C12) acyl chains. In addition, a series of diaryl ether inhibitors were designed and synthesized. These compounds are all subnanomolar slow binding inhibitors of ftuFabI with MIC values as low as 0.00018 µg/ml. A linear correlation between the K_i values for enzyme inhibition and the MIC values for inhibiting bacterial growth strongly suggests that ftuFabI is the primary cellular target of these compounds. Finally, we found that the *in vivo* efficacy of the inhibitors correlates best with their residence time on the enzyme but not with their thermodynamic affinity (K_i) for the enzyme, nor with their MIC values for inhibiting bacterial growth *in vitro*. We conclude therefore that residence time is the best predictor of the drug's *in vivo* efficacy.

Studies on enoyl-ACP reductases have also been extended to the pathogen *Burkholderia mallei* which contains both FabI (bmFabI) and FabV (bmFabV) homologues of this enzyme. FabV is a newly discovered member of the

enoyl-ACP reductase family, and so steady-state kinetics together with site directed mutagenesis have been used to study the reaction mechanism of bmFabV and to explore the role of proposed catalytic residues in substrate reduction. Rational drug design together with structure activity relationship (SAR) studies has lead to the identification of several novel bmFabV inhibitors that have submicromolar affinity for the enzyme.

Finally, since there are two enoyl-ACP reductases (bmFabI and bmFabV) in *B. mallei*, the *in vivo* function of both enzymes has been investigated. Cell complementation experiments and kinetic studies suggest that bmFabV might function in unsaturated fatty acid biosynthesis while bmFabI only reduces the intermediates for saturated fatty acid biosynthesis.

Table of Contents

CHAPTER I. FATTY ACID BIOSYNTHESIS AS A NOVEL TARGET FOR DRUG

DISCOVERY

CHAPTER III. MOLECULAR BASIS OF THE SLOW BINDING INHIBITION OF FTUFABI

CHAPTER IV. MECHANISM AND INHIBITION OF THE FABV ENOYL-ACP REDUCTASE FROM *BURKHOLDERIA MALLEI*

CHAPTER V. FUNCTIONAL REPLACEMENT OF THE *E. COLI* FABI ENZYME WITH THE ENOYL-ACP REDUCTASES FROM *B. MALLEI:* EXPLORING THE FUNCTION OF THESE ENZYMES IN UNSATURATED FATTY ACID BIOSYNTHESIS

List of Figures

List of Tables

List of Equations

Equation 1: $v = V_{max}[S]/[K_m(1+[I]/K_i)+[S]]$

Equation 2: $v = V_{max}[S]/[(K_m+[S])(1+[I]/K_i)]$

Equation 2: $v = V_{max}[S]/[K_m+[S](1+[I]/K_i)]$

Equation 4: $v = V_{max}[A][B] / (K_{iA}K_B + K_B[A] + K_A[B] + [A][B])$

Equation 5: $v = V_{max}[S] / (K_m + [S])$

Equation 6: $$\frac{F_e - F_1}{F_e(\text{max}) - F_1(\text{max})} = \frac{(K_d + [E]_0 + [NADH]) - \sqrt{(K_d + [E]_0 + [NADH])^2 - 4K_d[E]_0}}{2[E]_0}$$

Equation 7: $v = v_0/(1+[I]/K_i')$

Equation 8: $K_i' = K_1([NAD^+]+K_{m,NAD})/[NAD^+]$

Equation 9: $K_i' = K_2([NAD^+]+K_{m,NAD})/K_{m,NAD}$

Equation 10: $K_i' = K_2\{(1+[NAD^+]/K_{m,NAD})/[1+ [NAD^+]/(K_{m,NAD}K_1/K_2)]\}$

Equation 11: $K_{m,NAD} = K_{i,NAD}(1 + [NADH]/K_{m,NADH})$

Equation 12: $A_t = A_0 - V_s*t - (v_i - v_s)*(1-\gamma)*\ln\{[1-\gamma*\exp(-k_{obs}*t)]/(1-\gamma)\}/(k_{obs}*\gamma)$

Equation 13: $k_{obs} = k_4 + k_3*[I]/(K_i^{app} + [I])$

List of Abbreviations and Symbols

AccABCD	Acetyl-CoA caboxylase
ACP	Acyl arrier protein
ACPS	*holo*-ACP synthase
B. mallei	*Burkholderia Mallei*
B. subtilis	*Bacillus subtilis*
bmFabV	Enoyl-ACP reductase from *Burkholderia Mallei*
cis-5-*trans*-2-dienoyl-CoA	(2E,5Z)-Dodeca-2,5-dienoyl-CoA
CoA	Coenzyme A
Cr-ACP	Crotonyl-ACP
Cr-CoA	Crotonyl-CoA
Da	Dalton
DD-CoA	Dodecenoyl-CoA
DTNB	5,5'-Dithio-bis(2-nitrobenzoic acid)
DTT	Dithiothreitol

E. coli	*Escherichia coli*
ecFabI	Enoyl-ACP reductase from *Escherichia coli*
Eqn	Equation
ESI	Electrospray ionization
F. tularensis	*Francisella tularensis*
FabA	β-Hydroxyacyl-ACP dehydrases
FabB	β-Ketoacyl synthases I
FabF	β-Ketoacyl synthases II
FabG	β-Ketoacyl-ACP reductase
FabH	β-Ketoacyl synthases III
FabI	Enoyl-ACP reductase
FabK	Enoyl-ACP reductase
FabL	Enoyl-ACP reductase
FabM	*trans*-2, *cis*-3, Enoyl-ACP isomerase
FabV	Enoyl-ACP reductase
FabZ	β-Hydroxyacyl-ACP dehydrases
FAS-I	Eukaryotic fatty acid biosynthesis
FAS-II	Bacterial fatty acid biosynthesis

FDA	Food and Drug Administration
FRET	Fluorescence resonance energy transfer
ftuACP	Acyl carrier protein from *Francisella tularensis*
INH	Isoniazid
InhA	Enoyl-ACP reductase from *Mycobacterium tuberculosis*
IPTG	Isopropyl-1-thio-β-D-galactopyranoside
KatG	Mycobacterial catalase-peroxidase
LB	Luria Broth
LC-MS	Liquid chromatography–mass spectrometry
M. tuberculosis	*Mycobacterium tuberculosis*
MALDI-TOF	Matrix-assisted laser desorption ionization-time of fly
MDCC	7-Diethylamino-3-((((2-maleimidyl) ethyl)amino)carbonyl)coumarin
MDR-TB	Multi-drug resistant tuberculosis
MIC	Minimal inhibitory concentration
MTB	*Mycobacterium tuberculosis*
NAC	*N*-Acetylcysteamine

NAD$^+$	Nicotinamide adenine dinucleotide, oxidized form
NADH	Nicotinamide adenine dinucleotide, reduced form
NADPH	Nicotinamide adenine dinucleotide phosphate, reduced form
NIAID	National Institute of Allergy and Infectious Diseases
NME	New Molecular Entity
O.D. 600	Optical density at 600 nm
ORF	Open reading frame
P. aeruginosa	*Pseudomonas aeruginosa*
pCN-InhA	InhA with *p*-cyanophenylalanine
*pCN*Phe	*p*-Cyanophenylalanine
PCR	Polymerase chain reaction
Res.	Resideue
S. aurues	*Staphylococcus aureus*
S. pneumoniae	*Streptococcus pneumoniae*
saFabI	Enoyl-ACP reductase frm *Staphylococcus aureus*
SAR	Structure activity relationship
SDR	Short chain dehydrogenase/reductase

SDS-PAGE	sodium dodecyl sulfate-polyacrylamide gel electrophoresis
SFA	Saturated fatty acid
TB	Tuberculosis
TCEP	*Tris*(2-carboxyethyl)phosphine
UFA	Unsaturated fatty acid
V. cholerae	*Vibrio cholerae*
vcFabV	Enoyl-ACP reductase from *Vibrio cholerae*
WHO	World Health Organization
WT	Wild type

Acknowledgement

This is a great opportunity to express my respect to a great many people who have contributed to this dissertation. Without you, this dissertation would not have been possible, and because of you, my graduate experience has been one that I will cherish forever.

I would like to gratefully and sincerely thank my advisor Prof. Peter J. Tonge, who has not only provided support and advice but also given me the latitude to explore my own research interests. His mentorship was paramount in providing a well rounded supervision consistent with my long-term career goals, and more importantly in training me a creative and independent thinker. I would also like to thank Prof. Dale G. Drueckhammer and Prof. Boon for serving as my dissertation committee. It is a pleasure to thank them for their precious suggestions in guiding my research. For Dr. Stewart L. Fisher, the outside member of my committee, it was my great honor and pleasure to collaborate with his group. I owe my gratitude to all his intelligent advice and kind help.

I would like to thank my friends in Tonge Group who shared an extraordinarily happy time with me. I will cherish our friendship in my whole life.

And to my parents, you will never know how much I appreciate you. I am proud of being your son.

List of Publications

- **Lu, H.** and Tonge, P. J. "Mechanism and Inhibition of the FabV Enoyl-ACP Reductase from *Burkholderia mallei*" *Biochemistry* **2010**, *49*, 1281-9.

- **Lu, H.**, England, K., am Ende, C., Truglio, J., Luckner, S., Reddy, G., Marlenee, N., Knudson, S., Knudson, D., Bowen, R., Kisker, C., Slayden, R. and Tonge, P. J. "Slow-onset Inhibition of the FabI Enoyl Reductase from *Francisella tularensis*: Residence Time and *In Vivo* Activity" *ACS Chem. Biol.* **2009**, *4*, 221-31.

- **Lu, H.** and Tonge, P. J. "Inhibitors of FabI, an Enzyme Drug Target in the Bacterial Fatty Acid Biosynthesis Pathway" *Acc. Chem. Res.* **2008**, *41*, 11-20. (**Review Article**)

- **Lu, H.** and Tonge, P. J. "Residence Time of Drug-target Complex and Its Critical Role in Modern Drug Discovery". (**Invited Review Article** in *Curr. Opin. Chem. Biol.*, Submitted)

- **Lu, H.**, Liu, N., Reddy, G., Lu, Y., Ng, S., Cheng, K. and Tonge, P. J. "Deciphering the Unsaturated Fatty Acid Biosynthesis Pathway in *Burkholderia mallei*". (In Preparation)

- England, K., am Ende, C., **Lu, H.**, Sullivan, T., Marlenee, N., Bowen, R., Knudson, S., Knudson, D., Tonge, P. J. and Slayden, R. "Substituted Diphenyl Ethers as A Broad-spectrum Platform for the Development of Chemotherapeutics for the Treatment of Tularemia" *J. Antimicrob. Chemother.* **2009**, *64*, 1052-61.

- Boyne, M., Sullivan, T., am Ende, C., **Lu, H.**, Gruppo, V., Heaslip, D., Amin, A., Chatterjee, D., Lenaerts, A., Tonge, P. J. and Slayden, R. "Targeting Fatty Acid Biosynthesis for the Development of Novel Chemotherapeutics against *Mycobacterium Tuberculosis*: Evaluation of A-ring-modified Diphenyl Ethers as High-affinity InhA Inhibitors" *Antimicrob. Agents Chemother.* **2007**, *51*, 3562-7.

Chapter I[*]. Fatty Acid Biosynthesis as A Novel Target for Drug Discovery

The History of Antibiotics and Drug Resistance

The discovery and development of antibiotics are undoubtedly the biggest advances in the history of human medicine. Before the introduction of antimicrobials in the 1940s, the mortality of bacterial infection, for example with *Mycobacterium tuberculosis* (MTB), was as high as 50% (*1*). Followed with the synthesis of the arsenate-based compound Salvarsan by Ehrlich to treat syphilis (*2*), the serendipitous discovery of lysozyme and penicillin by Fleming (*3-4*), and the determination of sulfanilamide as the active metabolite in the dye-based drug Prontosil (*5*), a completely new stage to develop and use antibiotics was initiated. A so called "golden era" (1940-1960) of antibiotic discovery came shortly after that, during which most of the synthetic and natural molecules currently used were first identified and characterized (*6*).

However, the pace to develop new and clinically useful antibiotic has drastically

[*] Part of work in this chapter has been described in a previous publication (*Lu* et al *Acc. Chem. Res.* **2008**, *41*, 11-20.)

slowed down during the past 40 years (7). Only a few classes of new drugs have been introduced to the market from 1960 to 2003 (**Figure 1.1**), such as naladixic acid in 1962 and linezolid in 2000 (*8*). On the other hand, adaption through natural evolution has brought antibiotic resistance across all bacteria species, which is now a major problem for human heath (*9-12*). In the case of tuberculosis (TB), the World Health Organization (WHO) estimates that over 450,000 people world-wide are infected with multi-drug resistant TB (MDR-TB) (*13-14*). In addition, "virtually untreatable" strains which are not only resistant to front-line drugs but also three or four second-line drugs have also emerged (*15*). Hence there is a pressing need to develop new chemotherapeutics with novel mechanism of action to combat drug resistance.
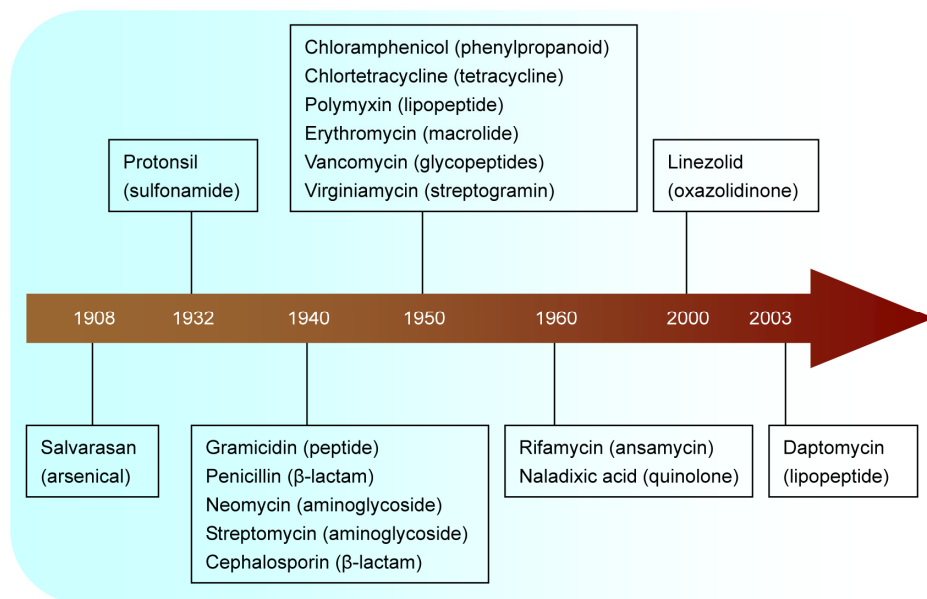
Figure 1.1: Timeline of Antibiotic Discovery. This figure is adapted from (*6*).

A Novel Target for Drug Discovery: the Bacterial Fatty Acid Biosynthesis (FAS-II) Pathway

Although there are many antibiotics now, only a small fraction of metabolic space has been targeted, primarily focusing on DNA replication, transcription and translation as well as in peptidoglycan synthesis (*16-19*). The reason for this concentration is unclear and maybe because most of the metabolic enzymes are not essential (*20*). The vast unexplored space in the whole bacterial genome still provides a promising solution to beat the emerging antibiotic resistant pathogens. Advances in DNA sequencing greatly facilitate the identification of new drug targets. It is expected that in the next few years more than 100 complete bacterial DNA sequences will be known and access to the whole genome sequence will enable many new molecular targets to be identified (*21-22*).

Bacterial fatty acid biosynthesis (FAS-II) pathway (**Figure 1.2**) is a validated yet relatively unexploited drug target. Fatty acids are indispensable components of bacterial cell wall and essential for the viability of microorganisms, but they cannot be scavenged from the host and must be synthesized *de novo* (*21, 23*). In addition, individual enzymes are used to catalyzed each step in the FAS-II pathway, while in eukaryotes all reactions are carried out in the different domains

3

of a single polypeptide (FAS-I) which is therefore fundamentally distinct from the

FAS-II system (*24-25*). Genetic knockout and knockdown experiments combined

with target-specific inhibitor designs have also proved that the FAS-II pathway is

essential for bacterial cell survival (*23, 25*). Finally, crystal structures are available

for most of the enzymes in this pathway from many organisms, which provides a

cornerstone for rational design of new antibiotics (*26*).
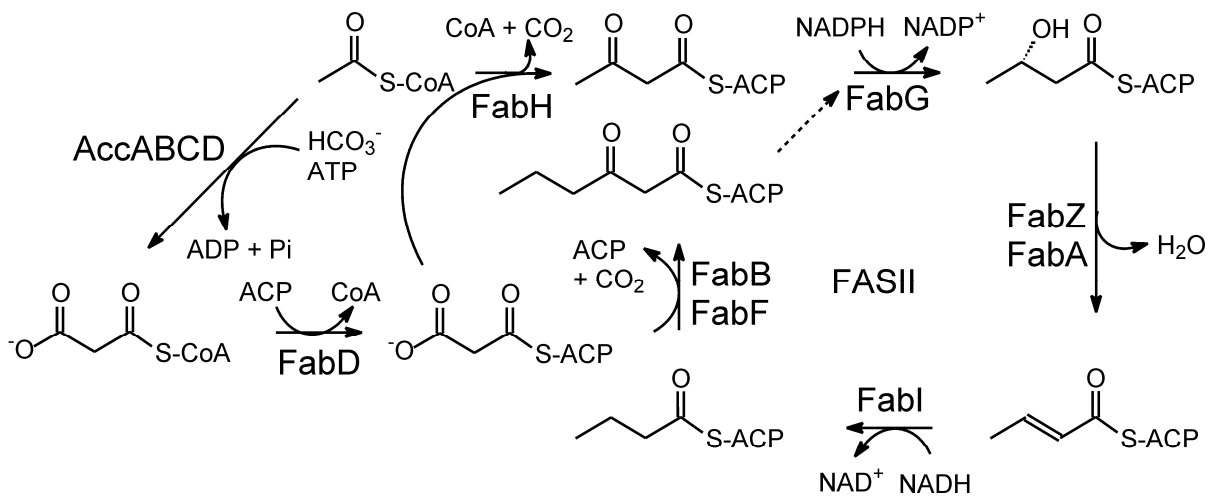
Figure 1.2: The Fatty Acid Biosynthesis Pathway in *E. coli*. AccABCD is the acetyl-CoA carboxylase; FabH is the malonyl-CoA:ACP transacylase; FabG is the β-ketoacyl-ACP reductase; FabA and FabZ are the β-hydroxyacyl-ACP dehydrases; FabI is the enoyl-ACP reductase; FabH, FabB and FabF are the β-ketoacyl-ACP synthases. The initial condensation reaction is catalyzed by FabH, while further rounds of elongation are initiated by FabB or FabF.

Enzymes and Reactions in FAS-II Pathway

The FAS-II pathway is most heavily studied in *E. coli* (**Figure 1.2**) and serves as a paradigm to understand the mechanism of each step. Different organisms use slightly different modules to synthesize fatty acids. For example, gram-positive bacteria do not contain FabA and FabB homologues because they do not synthesize unsaturated fatty acid *de novo*. However, most of the homologues corresponding to *E. coli* FAS-II enzymes are well conserved among all bacteria (*27*).

The first step in the FAS-II pathway is catalyzed by acetyl-CoA carboxylase (AccABCD), a multi-subunit protein catalyzing a biotin-dependent carboxylation reaction via two half reactions. In the first half reaction, the accC subunit activates the CO_2 moiety of a bicarbonate molecule and couples it with biotin to form carboxybiotin. The accA and accD subunits then transfer the activated CO_2 group in carboxybiotin to acetyl-CoA to produce malonyl-CoA. The last subunit forms a covalent bond with biotin and provides a substrate tunnel to connect these two half reactions (*28-30*). The malonyl-CoA that is produced is then converted to malonyl-ACP through a transthioesterifcation reaction catalyzed by malonyl-CoA:ACP transacylase (FabD). This enzyme uses a ping pong mechanism to catalyze the reaction, in which the malonyl group is first attached to

the hydroxyl group of a conserved serine residue in the active site and the CoA moiety is eliminated. Nucleophilic attack to the thiol of acyl carrier protein (ACP) breaks the ester bond between malonyl group and serine hydroxyl group to finally release malonyl-ACP (*31*).

The elongation cycle is initiated by a condensation reaction between acetyl-CoA and malonyl-ACP, which is catalyzed by the β-ketoacyl-ACP synthase III (FabH). An acylated enzyme intermediate is formed by covalently attaching the acetyl group of acetyl-CoA to the active site sulfhydryl in FabH. Malonyl-ACP then condenses with this acetyl group to produce β-ketoacyl-ACP and CO_2 (*26, 32*). The β-ketoacyl-ACP is then reduced at the C3 position to produce β-hydroxyacyl-ACP by β-ketoacyl-ACP reductase (FabG). FabG operates with NADPH as a cofactor and utilizes a Ser-Tyr-Lys triad to catalyze the reduction (*33-34*). The third step in the elongation circle is the dehydration of the β-ketoacyl-ACP to form β-hydroxyacyl-ACP by β-hydroxyacyl-ACP dehydrase (FabA or FabZ). A histidine residue acts as a catalytic base to abstract the proton at the C2 position of the substrate and a catalytic aspartic acid promotes the removal of hydroxyl group, which gives the enoyl-ACP product (*35-36*). Enoyl-ACP reductase (FabI) finishes the elongation cycle by reducing the C2 and C3 carbon-carbon double bond of the enoyl-ACP substrate to a single bond.

6

Unlike FabG, this enzyme uses NADH as cofactor and a Tyr-Tyr-Lys triad for catalysis (*37-38*). This elongation cycle repeats until the required chain length is reached and a thioesterase cleaves the fatty acids for cell wall synthesis. However, it is important to note that in the subsequent elongation cycle β-ketoacyl-ACP synthase II (FabB) and III (FabF) are used to condense malonyl-ACP and acyl-ACP substrates generated from the previous cycle.

The last important enzyme in FAS-II pathway is the acyl carrier protein (ACP) which is one of the most abundant proteins in the cell and acts as the transportation machinery to shuttle substrates among all the enzymes. *apo*-ACP is the product of the *acpP* gene and then converted to its active form by attaching a phosphopantothenyl group from coenzyme A by *holo*-ACP synthase (*39-40*).

The FabI Enoyl-ACP Reductase

Although inhibitors of almost all the FAS-II enzymes have been identified, the enoyl-ACP reductase is most extensively studied as a potential drug target (*41*). In most of the organisms, the enoyl-ACP reductase is the product of the *fabI* gene and uses NADH as the cofactor to catalyze the reduction. The FabI enzymes have been shown to be essential for bacterial growth through the temperature

sensitive mutations and are a key regulator of fatty acid biosynthesis (*42-43*).

FabIs are members of the short-chain alcohol dehydrogenase/reductase (SDR)

superfamily characterized by a catalytic triad that includes a Tyr and a Lys residue

(*44*). In dehydrogenases the third component of this triad is a Ser while in

reductases a Tyr or Phe is most commonly found (*26, 45*). Although the overall

structural homology between the different FabI enzymes is high, variability exists

in a mobile loop of amino acids that covers the active site (the substrate

recognition loop) (*46-47*).

Inhibitors of the FabI Enzymes

FabI inhibitors can generally be divided into two categories based on whether

or not compounds form covalent adducts with the cofactor.

FabI inhibitors that covalently modify the cofactor

Diazaborines are a class of heterocyclic boron-containing compounds (**1**,

Figure 1.3) that form covalent bonds between the boron atom and the 2'-hydroxyl

of the nicotinamide ribose of NAD^+ (*48*). The formed diazaborine-NAD^+ adduct is

a bisubstrate FabI inhibitor which highly resembles the binding model of the

natural enoy-ACP substrate and cofactor and bind tightly to the enzyme (**Figure**

1.4) (*48*). Structure activity relationship (SAR) studies showed that replacement of
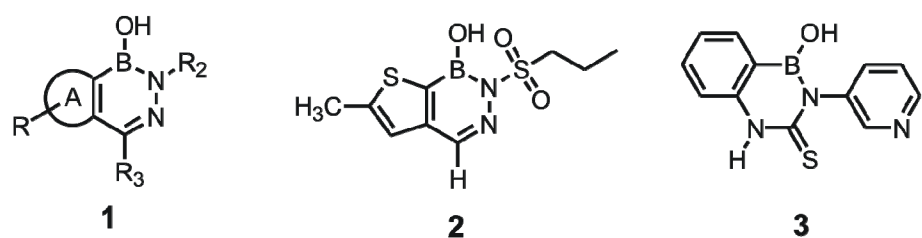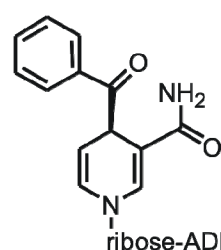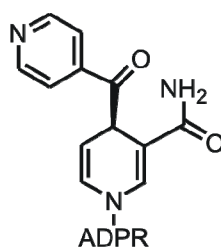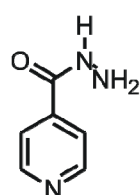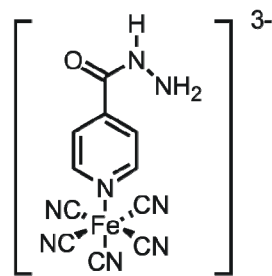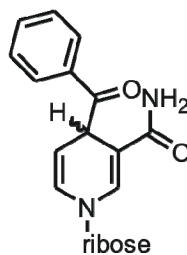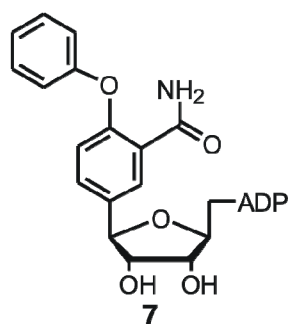
Figure 1.3: FabI Inhibitors Based on Diazaborines and Isoniazid. Structure of the diazaborine skeleton **1**, thiodiazaborine **2** and benzodiazaborine **3**. Ring A in the structure **1** can be benzene, naphthalene, thiophene, furan or pyrrole. Isoniazid **4** reacts with NAD^+ catalyzed by KatG to form the INH-NAD^+ adduct **5**. Compounds **6**-**8** are derivatives of INH-NAD^+ while **9** is a derivative of INH.

the diaza-moiety or the boron atom resulted in complete loss of antibacterial ability and following chemical optimization led to identification of a series of diazaborine derivatives (**2, Figure 1.3**) with antibacterial activity against several organisms, such as *E. coli*, *Salmonella enterica* and *Klebsiella pneumonia* (*49-50*). Later, benzodiazaborine (**3, Figure 1.3**) derivatives were also synthesized and evaluated against *M. tuberculosis* H37R$_v$ with MIC values as low as 8 µg/ml (*51*).

Isoniazid (INH, **4, Figure 1.3**) has been the most effective front line antituberculosis drug since 1952. Though the mode of action of the drug is complex (*52*), from both genetic experiment and crystal structures it is clear that InhA is one of the main cellular targets (*48, 53-54*). INH inhibits InhA through an activation step catalyzed by KatG, the mycobacterial catalase-peroxidase enzyme, resulting in the formation of an adduct with NAD$^+$ (the INH-NAD$^+$ adduct) (**5, Figure 1.3**) (*55*). Structural data has shown that the INH-NAD$^+$ adduct is a bisubstrate inhibitor (**Figure 1.4**), which binds tightly to the enzyme with an overall K$_i$ value of 0.75 nM (*56-57*). Since most INH resistance arises from mutations in KatG, inhibitors that do not require activation by KatG provide a good solution to treat INH-resistant TB (*58*). Compounds (**6-9, Figure 1.3**) mimicking the structure of INH-NAD$^+$ adduction were synthesized and chemical optimization are performed on these compounds to improve binding affinity to InhA (*59-62*).
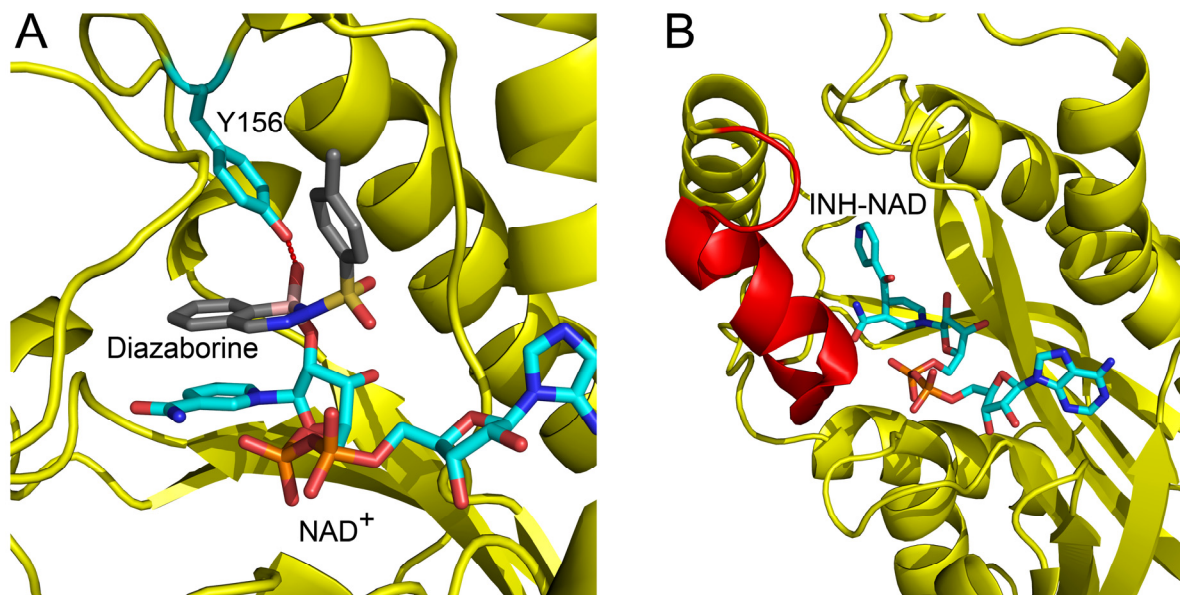
Figure 1.4: Structure of Benzodiazaborine-NAD$^+$ and Isoniazid-NAD$^+$ Adducts Bound to ecFabI and InhA Respectively. A) Structure of the 2-(toluene-4-sulfonyl)-benzodiazaborine NAD$^+$ adduct bound to ecFabI (yellow). A hydrogen bond is shown between the inhibitor and the conserved Tyr, Y156. The diazaborine is colored grey while the NAD$^+$ and Y156 are cyan (1dfg.pdb) (*48*). **B**) Structure of the INH-NAD$^+$ adduct (cyan) bound to InhA (yellow) (1zid.pdb) (*56*). The substrate recognition loop is colored red.

FabI inhibitors that interact noncovalently with the enzyme-cofactor binary complex

Triclosan (**10, Figure 1.5**) is a broad-spectrum antibacterial and antifugal agent included in a wide range of consumer products. However, it was not until recently

that the antibacterial mechanism of triclosan was understood, when it was shown

that triclosan acts as an inhibitor of the FabI enzymes in bacteria (*63-65*). Kinetic

studies revealed that triclosan was a slow, tight-binding inhibitor to FabI from *E.*

coli (ecFabI) with a K_i value as low as 7 pM when it binds to the enzyme-NAD$^+$

binary complex (*66-68*). X-ray crystal structures of FabI-NAD$^+$-triclosan were also

determined by several laboratories showing that the substrate recognition loop

that was disordered in the enzyme-NAD$^+$ binary complex became ordered after

triclosan binding. The loop ordering step was speculated to be the reason for the

high affinity and slow binding inhibition of triclosan to FabIs (*47, 69-70*). In addition

to ecFabI, triclosan (**Figure 1.5**) is also a potent inhibitor of the FabI enzymes

from *Staphylococcus aureus* and *Plasmodium falciparum* (*71-72*). Attempts to

improve the binding affinity and antibacterial activity have involved the synthesis

of a series of triclosan analogues with different substitutents on both of the rings

(*72-75*). However none of these compounds has improved *in vitro* activity

compared to triclosan.

Despite the failure to identify better inhibitors through chemical optimization of

triclosan targeting FabI enzymes, antituberculosis drug development based on

this molecule made great progress. Although triclosan is a picomolar inhibitor of

ecFabI, this compound only weakly inhibits InhA (K_i = 0.2μM) (*76*) and exhibits

Organism	K_i (nM)	MIC (μg/mL)
E. coli	0.007	0.3
S. aureus	5	0.016
P. falciparum	73 (IC_{50})	0.8 (EC_{50})
M. tuberculosis	200	12.5

10
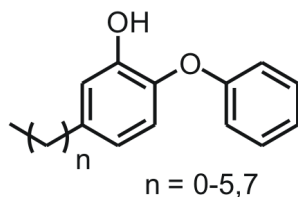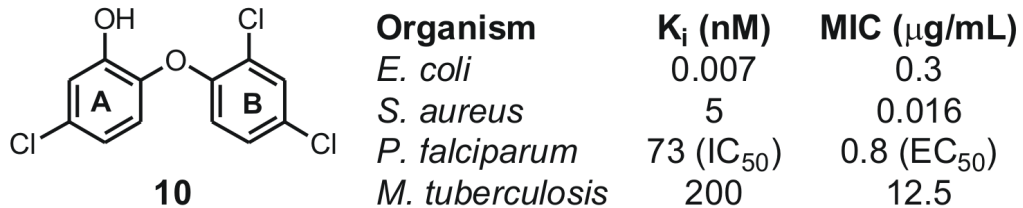
8PP (n = 7)
K_i = 1 nM (InhA)
MIC = 1.9 μg/mL H37$_{Rv}$
& 2.0 μg/mL TN587

n = 0-5,7

11-17

Figure 1.5: Diaryl Ether Inhibitors of FabI. Structure of triclosan **10** and structures of the alkyl diaryl ether inhibitors of InhA (**11**-**17**). Names of the compounds correspond to the length of alkyl chain from 1PP to 8PP. H37R$_V$ is a INH sensitive strain of *M. tuberculosis* and TN587 is a clinical isolated strain of INH-resistant *M. tuberculosis*.

modest bactericidal activity against MTB with an MIC$_{99}$ value of 12.5 µg/ml (*77*).

Analysis of the crystal structure of triclosan binding to InhA revealed that the

chlorine atom in A ring pointed toward a hydrophobic substrate binding pocket

(**Figure 1.6**) (*46*). Consequently, a series of alkyl diaryl ethers were developed

(**Figure 1.5**), the most potent of which (8PP) inhibits InhA with a K_i value of 1nM.

Significantly, this compound is active against both sensitive and INH-resistant
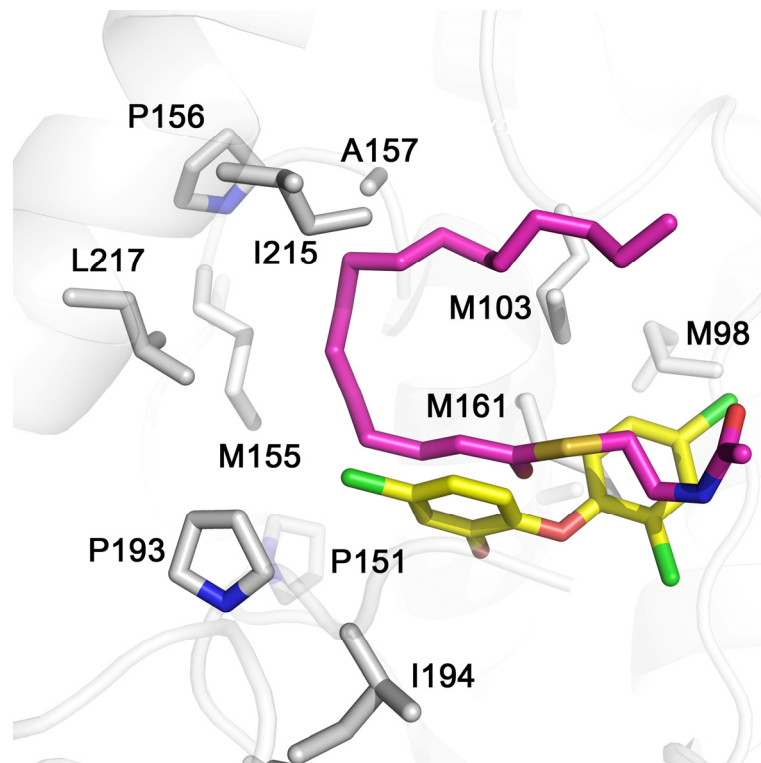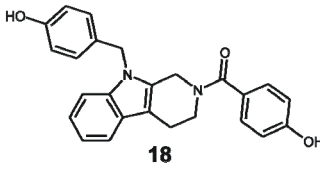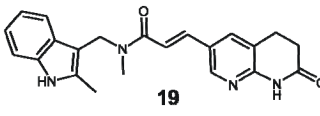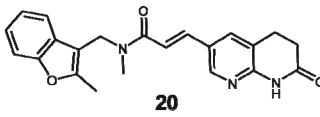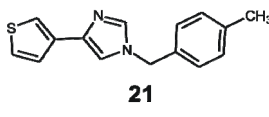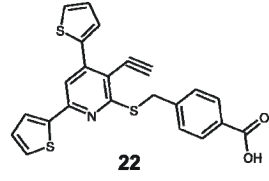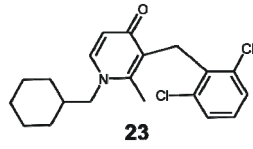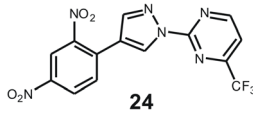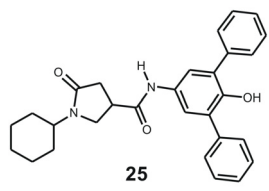
Figure 1.6: Overlay of Triclosan and C16-NAC Fatty Acid Substrate Bound to InhA. Crystal structures of InhA (white) bound with triclosan (2b35.pdb) (*77*) and C16-NAC fatty acid substrate (1brv.pdb) (*46*) were superimposed. For triclosan, carbon atoms are depicted in yellow, chlorine in green and oxygen in red. While the carbon atoms are shown in magenta, oxygen in red and nitrogen in blue for the C16-NAC fatty acid substrate.

strains of *M. tuberculosis* with an MIC$_{99}$ value of 1-2 μg/ml (*77*).

High-throughput screening of over 300,000 compounds in GlaxoSmithKline compound led to the identification of a variety of chemical structures that are potent FabI inhibitors (*78*). Meanwhile, chemical optimization based on structural information resulted in the development of a series of indole inhibitors (**20**) which are currently being optimized by Affinium Pharmacueticals (*79*). These compounds have decent antimicrobial activities against several important pathogens, such as *E. coli*, *S. aureus* and *M. tuberculosis*. The enzyme inhibition data and antibacterial activity are summarized in **Table 1.1** (*79-86*). Crystal structures of these compounds bound to FabI have been solved, demonstrating that they occupy the region of the active site where the enoyl substrate is expected to bind. This suggests that these compounds might also require the presence of the NAD(H) cofactor to form the ternary complex for the enzyme inhibition.

Table 1.1: IC$_{50}$ and MIC Values of FabI Inhibitors Identified from Screening

Chemotype	Representative Structure	IC$_{50}$(µM)/ MIC(µg/ml)	Reference
Indole series	**18**	0.11 / 0.5 (*S. aureus*)	(*79*)
Naphthyridinone Series	**19**	0.05 / 0.016 (*S. aureus*)	(*80*)
Benzofuran Compound	**20**	ND / 0.015 (*S. aureus*)	(*81*)
Imidazole Series	**21**	0.25 / 8 (*S. aureus*)	(*82*)
Thiopyridine Series	**22**	3 / 0.75 (*S. aureus*)	(*83*)
4-Pyridone Series	**23**	0.22 / ND (*E. coli*)	(*84*)
Pyrazole Series (Genz-10850)	**24**	ND / 2.5 (µM) (INH-resistant *M. tuberculosis*)	(*85*)
Pyrrolidine Carboxamide Series	**25**	0.062 / ND (*M. tuberculosis*)	(*86*)

Summary

Aggressive efforts must be made to develop new antimicrobial drugs in order to keep pace with the emergence of organisms that are resistant to current antibiotics, and there must be a concerted effort to identify and inhibit novel drug targets. As discussed above, while a significant fraction of metabolic space is not currently targeted by existing drugs, studies suggest that the range of new 'druggable' targets may be limited. The inhibitor discovery efforts described in this chapter firmly demonstrated that the enoyl reductase FabI is an excellent target for the development of new antibiotics.

References:

1. Dineeen, P., Homan, W. P., and Grafe, W. R. (1976) Tuberculous peritonitis: 43 years' expereince in diagnosis and treatment, *Annu. Surg. 184*, 717-722.

2. Ehrlich, P. (1910) The use and effect of salvarsan, *Deut. Med. Wochenschr. 36*, 2437-2438.

3. Fleming, A. (1929) Lysozyme - a bacteriolytic ferment found normally in tissues and secretions, *Lancet 1*, 217-220.

4. Fleming, A. (1941) Penicillin, *British. Medical. Journal. 1941*, 386-386.

5. Domagk, G. J. (1935) Ein beitrag zur chemotherapie der bakteriellen infektionen, *Deut. Med. Wochenschr. 61*, 250-253.

6. Wright, G. D. (2007) The antibiotic resistome: the nexus of chemical and genetic diversity, *Nat. Rev. 5*, 175-186.

7. Bax, R. P., Anderson, R., Crew, J., Fletcher, P., Johnson, T., Kaplan, E., Knaus, B., Kristinsson, K., Malek, M., and Strandberg, L. (1998) Antibiotic resistance--what can we do?, *Nat. Med. 4*, 545-546.

8. Coates, A., Hu, Y., Bax, R., and Page, C. (2002) The future challenges facing the development of new antimicrobial drugs, *Nat. Rev. Drug Discov. 1*, 895-910.

9.   Cohen, M. L. (1992) Epidemiology of drug resistance: implications for a post-antimicrobial era, *Science 257*, 1050-1055.

10.   McGowan, J. E., Jr. (2006) Resistance in nonfermenting gram-negative bacteria: multidrug resistance to the maximum, *Am. J. Infect. Control 34*, S29-37; discussion S64-73.

11.   Levy, S. B., and Marshall, B. (2004) Antibacterial resistance worldwide: causes, challenges and responses, *Nat. Med. 10*, S122-129.

12.   Livermore, D. M. (2004) The need for new antibiotics, *Clin. Microbiol. Infect. 10 Suppl 4*, 1-9.

13.   Kochi, A. (1991) The global tuberculosis situation and the new control strategy of the World Health Organization, *Tubercle 72*, 1-6.

14.   Bloom, B. R., and Murray, C. J. (1992) Tuberculosis: commentary on a reemergent killer, *Science 257*, 1055-1064.

15.   (2006) "Virtually untreatable" TB found, *BBC News [Online]*.

16.   Williams, D. H. (1996) The glycopeptide story--how to kill the deadly 'superbugs', *Nat. Prod. Rep. 13*, 469-477.

17.   Fourmy, D., Recht, M. I., Blanchard, S. C., and Puglisi, J. D. (1996) Structure of the A site of *Escherichia coli* 16S ribosomal RNA complexed with an aminoglycoside antibiotic, *Science 274*, 1367-1371.

19

18.   Maxwell, A. (1997) DNA gyrase as a drug target, *Trends Mcrobiol. 5*, 102-109.

19.   Walsh, C. (2000) Molecular mechanisms that confer antibacterial drug resistance, *Nature 406*, 775-781.

20.   Becker, D., Selbach, M., Rollenhagen, C., Ballmaier, M., Meyer, T. F., Mann, M., and Bumann, D. (2006) Robust *Salmonella* metabolism limits possibilities for new antimicrobials, *Nature 440*, 303-307.

21.   McDevitt, D., and Rosenberg, M. (2001) Exploiting genomics to discover new antibiotics, *Trends Microbiol. 9*, 611-617.

22.   Taylor, P., and Wright, G. (2008) Novel approaches to discovery of antibacterial agents, *Anim. Health Res. Rev. 9*, 237-246.

23.   Payne, D. J., Warren, P. V., Holmes, D. J., Ji, Y., and Lonsdale, J. T. (2001) Bacterial fatty-acid biosynthesis: a genomics-driven target for antibacterial drug discovery, *Drug Discov. Today 6*, 537-544.

24.   Chirala, S. S., Huang, W. Y., Jayakumar, A., Sakai, K., and Wakil, S. J. (1997) Animal fatty acid synthase: functional mapping and cloning and expression of the domain I constituent activities, *Proc. Natl. Acd. Sci. U.S.A. 94*, 5588-5593.

25.   Campbell, J. W., and Cronan, J. E., Jr. (2001) Bacterial fatty acid

biosynthesis: targets for antibacterial drug discovery, *Annu. Rev. Microbiol. 55*, 305-332.

26.   White, S. W., Zheng, J., Zhang, Y. M., and Rock. (2005) The structural biology of type II fatty acid biosynthesis, *Annu. Rev. Biochem. 74*, 791-831.

27.   Heath, R. J., White, S. W., and Rock, C. O. (2001) Lipid biosynthesis as a target for antibacterial agents, *Prog. Lipid Res. 40*, 467-497.

28.   Cronan, J. E., Jr. and Waldrop, G. L. (2002) Multi-subunit acetyl-CoA carboxylases, *Prog. Lipid Res. 41*, 407-435.

29.   Li, S. J., and Cronan, J. E., Jr. (1992) The gene encoding the biotin carboxylase subunit of *Escherichia coli* acetyl-CoA carboxylase, *The Journal of biological chemistry 267*, 855-863.

30.   Li, S. J., and Cronan, J. E., Jr. (1992) The genes encoding the two carboxyltransferase subunits of *Escherichia coli* acetyl-CoA carboxylase, *J. Biol. Chem. 267*, 16841-16847.

31.   Li, Z., Huang, Y., Fan, H., Zhou, X., Li, S., Bartlam, M., Wang, H., and Rao, Z. (2007) The crystal structure of MCAT from Mycobacterium tuberculosis reveals three new catalytic models, *J. Mol. Biol. 371*, 1075-1083.

32.   Jackowski, S., and Rock, C. O. (1987) Acetoacetyl-acyl carrier protein synthase, a potential regulator of fatty acid biosynthesis in bacteria, *J. Biol.*

Chem. 262, 7927-7931.

33. Price, A. C., Zhang, Y. M., Rock, C. O., and White, S. W. (2001) Structure
     of beta-ketoacyl-acyl carrier protein reductase from *Escherichia coli*:
     negative cooperativity and its structural basis, *Biochemistry 40*,
     12772-12781.

34. Price, A. C., Zhang, Y. M., Rock, C. O., and White, S. W. (2004)
     Cofactor-induced conformational rearrangements establish a catalytically
     competent active site and a proton relay conduit in FabG, *Structure 12*,
     417-428.

35. Leesong, M., Henderson, B. S., Gillig, J. R., Schwab, J. M., and Smith, J. L.
     (1996) Structure of a dehydratase-isomerase from the bacterial pathway
     for biosynthesis of unsaturated fatty acids: two catalytic activities in one
     active site, *Structure 4*, 253-264.

36. Kimber, M. S., Martin, F., Lu, Y., Houston, S., Vedadi, M., Dharamsi, A.,
     Fiebig, K. M., Schmid, M., and Rock, C. O. (2004) The structure of
     (3R)-hydroxyacyl-acyl carrier protein dehydratase (FabZ) from
     Pseudomonas aeruginosa, *J. Biol. Chem. 279*, 52593-52602.

37. Roujeinikova, A., Levy, C. W., Rowsell, S., Sedelnikova, S., Baker, P. J.,
     Minshull, C. A., Mistry, A., Colls, J. G., Camble, R., Stuitje, A. R., Slabas, A.

R., Rafferty, J. B., Pauptit, R. A., Viner, R., and Rice, D. W. (1999) Crystallographic analysis of triclosan bound to enoyl reductase, *J. Mol. Biol. 294*, 527-535.

38.   Roujeinikova, A., Sedelnikova, S., de Boer, G. J., Stuitje, A. R., Slabas, A. R., Rafferty, J. B., and Rice, D. W. (1999) Inhibitor binding studies on enoyl reductase reveal conformational changes related to substrate recognition, *J. Biol. Chem. 274*, 30811-30817.

39.   Rock, C. O., and Cronan, J. E., Jr. (1979) Solubilization, purification, and salt activation of acyl-acyl carrier protein synthetase from *Escherichia coli*, *J. Biol. Chem. 254*, 7116-7122.

40.   Rock, C. O., and Cronan, J. E., Jr. (1979) Re-evaluation of the solution structure of acyl carrier protein, *J. Biol. Chem. 254*, 9778-9785.

41.   Zhang, Y. M., White, S. W., and Rock, C. O. (2006) Inhibiting bacterial fatty acid synthesis, *J. Biol. Chem. 281*, 17541-17544.

42.   Bergler, H., Fuchsbichler, S., Hogenauer, G., and Turnowsky, F. (1996) The enoyl-acyl-carrier-protein reductase (FabI) of *Escherichia coli*, which catalyzes a key regulatory step in fatty acid biosynthesis, accepts NADH and NADPH as cofactors and is inhibited by palmitoyl-CoA, *Eur. J. Biochem. 242*, 689-694.

43. Heath, R. J., and Rock, C. O. (1995) Enoyl-acyl carrier protein reductase (fabI) plays a determinant role in completing cycles of fatty acid elongation in *Escherichia coli*, *J. Biol. Chem. 270*, 26538-26542.

44. Parikh, S., Moynihan, D. P., Xiao, G., and Tonge, P. J. (1999) Roles of tyrosine 158 and lysine 165 in the catalytic mechanism of InhA, the enoyl-ACP reductase from *Mycobacterium tuberculosis*, *Biochemistry 38*, 13623-13634.

45. Rafferty, J. B., Simon, J. W., Baldock, C., Artymiuk, P. J., Baker, P. J., Stuitje, A. R., Slabas, A. R., and Rice, D. W. (1995) Common themes in redox chemistry emerge from the X-ray structure of oilseed rape (*Brassica napus*) enoyl acyl carrier protein reductase, *Structure 3*, 927-938.

46. Rozwarski, D. A., Vilcheze, C., Sugantino, M., Bittman, R., and Sacchettini, J. C. (1999) Crystal structure of the *Mycobacterium tuberculosis* enoyl-ACP reductase, InhA, in complex with NAD^+ and a C16 fatty acyl substrate, *J. Biol. Chem. 274*, 15582-15589.

47. Stewart, M. J., Parikh, S., Xiao, G., Tonge, P. J., and Kisker, C. (1999) Structural basis and mechanism of enoyl reductase inhibition by triclosan, *J. Mol. Biol. 290*, 859-865.

48. Baldock, C., Rafferty, J. B., Sedelnikova, S. E., Baker, P. J., Stuitje, A. R.,

Slabas, A. R., Hawkes, T. R., and Rice, D. W. (1996) A mechanism of drug action revealed by structural studies of enoyl reductase, *Science 274*, 2107-2110.

49.   Grassberger, M. A., Turnowsky, F., and Hildebrandt, J. (1984) Preparation and antibacterial activities of new 1,2,3-diazaborine derivatives and analogues, *J. Med. Chem. 27*, 947-953.

50.   Baldock, C., de Boer, G. J., Rafferty, J. B., Stuitje, A. R., and Rice, D. W. (1998) Mechanism of action of diazaborines, *Biochem. Pharmacol. 55*, 1541-1549.

51.   Davis, M. C., Franzblau, S. G., and Martin, A. R. (1998) Syntheses and evaluation of benzodiazaborine compounds against *M. tuberculosis* H37Rv in vitro, *Bioorg. Med. Chem. Lett. 8*, 843-846.

52.   Slayden, R. A., Lee, R. E., and Barry, C. E., (2000) Isoniazid affects multiple components of the type II fatty acid synthase system of *Mycobacterium tuberculosis*, *Mol. Microbiol. 38*, 514-525.

53.   Banerjee, A., Dubnau, E., Quemard, A., Balasubramanian, V., Um, K. S., Wilson, T., Collins, D., de Lisle, G., and Jacobs, W. R., Jr. (1994) inhA, a gene encoding a target for isoniazid and ethionamide in *Mycobacterium tuberculosis*, *Science 263*, 227-230.

54. Quemard, A., Sacchettini, J. C., Dessen, A., Vilcheze, C., Bittman, R., Jacobs WR, J. r., and Blanchard, J. S. (1995) Enzymatic characterization of the target for isoniazid in *Mycobacterium tuberculosis*, *Biochemistry 34*, 8235-8241.

55. Johnsson, K., King, J., and Schultz, P. G. (1995) Studies on the mechanism of action of isoniazid and ethionamide in the chemotherapy of tuberculosis, *J. Am. Chem. Soc 117*, 5009-5010.

56. Rozwarski, D. A., Grant, G. A., Barton, D. H., Jacobs, W. R., Jr., and Sacchettini, J. C. (1998) Modification of the NADH of the isoniazid target (InhA) from *Mycobacterium tuberculosis*, *Science 279*, 98-102.

57. Rawat, R., Whitty, A., and Tonge, P. J. (2003) The isoniazid-NAD adduct is a slow, tight-binding inhibitor of InhA, the *Mycobacterium tuberculosis* enoyl reductase: adduct affinity and drug resistance, *Proc. Natl. Acd. Sci. U.S.A. 100*, 13881-13886.

58. Ramaswamy, S. V., Reich, R., Dou, S. J., Jasperse, L., Pan, X., Wanger, A., Quitugua, T., and Graviss, E. A. (2003) Single nucleotide polymorphisms in genes associated with isoniazid resistance in *Mycobacterium tuberculosis*, *Antimicrob. Agents Chemother. 47*, 1241-1250.

59. Broussy, S., Bernardes-Genisson, V., Quemard, A., Meunier, B., and

Bernadou, J. (2005) The first chemical synthesis of the core structure of the benzoylhydrazine-NAD adduct, a competitive inhibitor of the *Mycobacterium tuberculosis* enoyl reductase, *J. Org. Chem. 70*, 10502-10510.

60. Bonnac, L., Gao, G. Y., Chen, L., Felczak, K., Bennett, E. M., Xu, H., Kim, T., Liu, N., Oh, H., Tonge, P. J., and Pankiewicz, K. W. (2007) Synthesis of 4-phenoxybenzamide adenine dinucleotide as NAD analogue with inhibitory activity against enoyl-ACP reductase (InhA) of *Mycobacterium tuberculosis*, *Bioorg. Med. Chem. Lett. 17*, 4588-4591.

61. Oliveira, J. S., Sousa, E. H., Basso, L. A., Palaci, M., Dietze, R., Santos, D. S., and Moreira, I. S. (2004) An inorganic iron complex that inhibits wild-type and an isoniazid-resistant mutant 2-*trans*-enoyl-ACP (CoA) reductase from *Mycobacterium tuberculosis*, *Chem. Commun. 7*, 312-313.

62. Oliveira, J. S., de Sousa, E. H., de Souza, O. N., Moreira, I. S., Santos, D. S., and Basso, L. A. (2006) Slow-onset inhibition of 2-*trans*-enoyl-ACP (CoA) reductase from *Mycobacterium tuberculosis* by an inorganic complex, *Curr. Pharm. Des. 12*, 2409-2424.

63. McMurry, L. M., Oethinger, M., and Levy, S. B. (1998) Triclosan targets lipid synthesis, *Nature 394*, 531-532.

64. Heath, R. J., Yu, Y. T., Shapiro, M. A., Olson, E., and Rock, C. O. (1998) Broad spectrum antimicrobial biocides target the FabI component of fatty acid synthesis, *J. Biol. Chem. 273*, 30316-30320.

65. Levy, C. W., Roujeinikova, A., Sedelnikova, S., Baker, P. J., Stuitje, A. R., Slabas, A. R., Rice, D. W., and Rafferty, J. B. (1999) Molecular basis of triclosan activity, *Nature 398*, 383-384.

66. Sivaraman, S., Zwahlen, J., Bell, A. F., Hedstrom, L., and Tonge, P. J. (2003) Structure-activity studies of the inhibition of FabI, the enoyl reductase from *Escherichia coli*, by triclosan: kinetic analysis of mutant FabIs, *Biochemistry 42*, 4406-4413.

67. Sivaraman, S., Sullivan, T. J., Johnson, F., Novichenok, P., Cui, G., Simmerling, C., and Tonge, P. J. (2004) Inhibition of the bacterial enoyl reductase FabI by triclosan: a structure-reactivity analysis of FabI inhibition by triclosan analogues, *J. Med. Chem. 47*, 509-518.

68. Ward, W. H., Holdgate, G. A., Rowsell, S., McLean, E. G., Pauptit, R. A., Clayton, E., Nichols, W. W., Colls, J. G., Minshull, C. A., Jude, D. A., Mistry, A., Timms, D., Camble, R., Hales, N. J., Britton, C. J., and Taylor, I. W. (1999) Kinetic and structural characteristics of the inhibition of enoyl (acyl carrier protein) reductase by triclosan, *Biochemistry 38*, 12514-12525.

69. Qiu, X., Janson, C. A., Court, R. I., Smyth, M. G., Payne, D. J., and Abdel-Meguid, S. S. (1999) Molecular basis for triclosan activity involves a flipping loop in the active site, *Protein Sci. 8*, 2529-2532.

70. Pidugu, L. S., Kapoor, M., Surolia, N., Surolia, A., and Suguna, K. (2004) Structural basis for the variation in triclosan affinity to enoyl reductases, *J. Mol. Biol.343*, 147-155.

71. Xu, H., Sullivan, T. J., Sekiguchi, J., Kirikae, T., Ojima, I., Stratton, C. F., Mao, W., Rock, F. L., Alley, M. R., Johnson, F., Walker, S. G., and Tonge, P. J. (2008) Mechanism and inhibition of saFabI, the enoyl reductase from *Staphylococcus aureus*, *Biochemistry 47*, 4228-4236.

72. Chhibber, M., Kumar, G., Parasuraman, P., Ramya, T. N., Surolia, N., and Surolia, A. (2006) Novel diphenyl ethers: design, docking studies, synthesis and inhibition of enoyl ACP reductase of *Plasmodium falciparum* and *Escherichia coli*, *Bioorg. Med. Chem. 14*, 8086-8098.

73. Freundlich, J. S., Yu, M., Lucumi, E., Kuo, M., Tsai, H. C., Valderramos, J. C., Karagyozov, L., Jacobs, W. R., Jr., Schiehser, G. A., Fidock, D. A., Jacobus, D. P., and Sacchettini, J. C. (2006) Synthesis and biological activity of diaryl ether inhibitors of malarial enoyl acyl carrier protein reductase. Part 2: 2'-substituted triclosan derivatives, *Bioorg. Med. Chem.*

Lett. 16, 2163-2169.

74.   Stone, G. W., Zhang, Q., Castillo, R., Doppalapudi, V. R., Bueno, A. R., Lee, J. Y., Li, Q., Sergeeva, M., Khambatta, G., and Georgopapadakou, N. H. (2004) Mechanism of action of NB2001 and NB2030, novel antibacterial agents activated by beta-lactamases, *Antimicrob. Agents Chemother. 48*, 477-483.

75.   Perozzo, R., Kuo, M., Sidhu, A. S., Valiyaveettil, J. T., Bittman, R., Jacobs, W. R., Jr., Fidock, D. A., and Sacchettini, J. C. (2002) Structural elucidation of the specificity of the antibacterial agent triclosan for malarial enoyl acyl carrier protein reductase, *J. Biol. Chem. 277*, 13106-13114.

76.   Parikh, S. L., Xiao, G., and Tonge, P. J. (2000) Inhibition of InhA, the enoyl reductase from *Mycobacterium tuberculosis*, by triclosan and isoniazid, *Biochemistry 39*, 7645-7650.

77.   Sullivan, T. J., Truglio, J. J., Boyne, M. E., Novichenok, P., Zhang, X., Stratton, C. F., Li, H. J., Kaur, T., Amin, A., Johnson, F., Slayden, R. A., Kisker, C., and Tonge, P. J. (2006) High affinity InhA inhibitors with activity against drug-resistant strains of *Mycobacterium tuberculosis*, *ACS Chem. Biol. 1*, 43-53.

78.   Payne, D. J., Miller, W. H., Berry, V., Brosky, J., Burgess, W. J., Chen, E.,

DeWolf Jr, W. E., Jr., Fosberry, A. P., Greenwood, R., Head, M. S., Heerding, D. A., Janson, C. A., Jaworski, D. D., Keller, P. M., Manley, P. J., Moore, T. D., Newlander, K. A., Pearson, S., Polizzi, B. J., Qiu, X., Rittenhouse, S. F., Slater-Radosti, C., Salyers, K. L., Seefeld, M. A., Smyth, M. G., Takata, D. T., Uzinskas, I. N., Vaidya, K., Wallis, N. G., Winram, S. B., Yuan, C. C., and Huffman, W. F. (2002) Discovery of a novel and potent class of FabI-directed antibacterial agents, *Antimicrob. Agents Chemother. 46*, 3118-3124.

79. Seefeld, M. A., Miller, W. H., Newlander, K. A., Burgess, W. J., Payne, D. J., Rittenhouse, S. F., Moore, T. D., DeWolf, W. E., Jr., Keller, P. M., Qiu, X., Janson, C. A., Vaidya, K., Fosberry, A. P., Smyth, M. G., Jaworski, D. D., Slater-Radosti, C., and Huffman, W. F. (2001) Inhibitors of bacterial enoyl acyl carrier protein reductase (FabI): 2,9-disubstituted 1,2,3,4-tetrahydropyrido[3,4-b]indoles as potential antibacterial agents, *Bioorg. Med. Chem. Lett. 11*, 2241-2244.

80. Seefeld, M. A., Miller, W. H., Newlander, K. A., Burgess, W. J., DeWolf, W. E., Jr., Elkins, P. A., Head, M. S., Jakas, D. R., Janson, C. A., Keller, P. M., Manley, P. J., Moore, T. D., Payne, D. J., Pearson, S., Polizzi, B. J., Qiu, X., Rittenhouse, S. F., Uzinskas, I. N., Wallis, N. G., and Huffman, W. F. (2003)

Indole naphthyridinones as inhibitors of bacterial enoyl-ACP reductases FabI and FabK, *J. Med. Chem. 46*, 1627-1635.

81. Karlowsky, J. A., Laing, N. M., Baudry, T., Kaplan, N., Vaughan, D., Hoban, D. J., and Zhanel, G. G. (2007) *In Vitro* Activity of API-1252, a Novel FabI Inhibitor, against Clinical Isolates of *Staphylococcus aureus* and *Staphylococcus epidermidis*, *Antimicrob. Agents Chemother. 51*, 1580-1581.

82. Heerding, D. A., Chan, G., DeWolf, W. E., Fosberry, A. P., Janson, C. A., Jaworski, D. D., McManus, E., Miller, W. H., Moore, T. D., Payne, D. J., Qiu, X., Rittenhouse, S. F., Slater-Radosti, C., Smith, W., Takata, D. T., Vaidya, K. S., Yuan, C. C., and Huffman, W. F. (2001) 1,4-Disubstituted imidazoles are potential antibacterial agents functioning as inhibitors of enoyl acyl carrier protein reductase (FabI), *Bioorg. Med. Chem. Lett. 11*, 2061-2065.

83. Ling, L. L., Xian, J., Ali, S., Geng, B., Fan, J., Mills, D. M., Arvanites, A. C., Orgueira, H., Ashwell, M. A., Carmel, G., Xiang, Y., and Moir, D. T. (2004) Identification and characterization of inhibitors of bacterial enoyl-acyl carrier protein reductase, *Antimicrob. Agents Chemother. 48*, 1541-1547.

84. Kitagawa, H., Kumura, K., Takahata, S., Iida, M., and Atsumi, K. (2007) 4-Pyridone derivatives as new inhibitors of bacterial enoyl-ACP reductase

FabI, *Bioorg. Med. Chem. 15*, 1106-1116.

85.   Kuo, M. R., Morbidoni, H. R., Alland, D., Sneddon, S. F., Gourlie, B. B., Staveski, M. M., Leonard, M., Gregory, J. S., Janjigian, A. D., Yee, C., Musser, J. M., Kreiswirth, B., Iwamoto, H., Perozzo, R., Jacobs, W. R., Jr., Sacchettini, J. C., and Fidock, D. A. (2003) Targeting tuberculosis and malaria through inhibition of enoyl reductase: compound activity and structural data, *J. Biol. Chem. 278*, 20851-20859.

86.   He, X., Alian, A., Stroud, R., and Ortiz de Montellano, P. R. (2006) Pyrrolidine carboxamides as a novel class of inhibitors of enoyl acyl carrier protein reductase from *Mycobacterium tuberculosis*, *J. Med. Chem. 49*, 6308-6323.

Chapter II[*]. Mechanistic Studies of the FabI enoyl-ACP Reductase from

***Francisella tularensis* (ftuFabI) and Its Inhibition by Diaryl Ether Inhibitors**

Introduction

Tularemia and Francisella tularensis. Tularemia, also known as "rabbit fever", is

a serious infectious disease typically found in animals, especially rodents, rabbits,

and hares. In 1911, an outbreak of this disease in California provided the first

isolation of the gram-negative causative bacterium – *Francisella tularensis* (*1*).

Until now, infections of *F. tularensis* have been reported in many regions including

North America, Japan, Russia and Switzerland. It is known as one of the most

infectious pathogens since susceptible people can be infected by as few as 10

organisms through inoculation or inhalation (*2-4*). The ability of *F. tularensis* to be

aerosolized, coupled with the small numbers of bacteria required to cause

disease and the ability of the bacterium to survive for weeks in a cool, moist

environment, have raised the possibility that this organism could be used

deliberately as a biological weapon. Consequently, NIAID has classified *F. tularensis* as a Category A priority pathogen.

WHO predicted that 250,000 people would be infected if 50 kg of *F. tularensis* was dispersed into a metropolitan area with a population of 5 million humans. Subsequently, one third of the population would have to leave the city, while 1 million people would require antibiotic treatment for at least 10 days (*5*). There is a long history of attempts to develop *F. tularensis* a biological warfare agent. Japanese germ warfare examined the possibility to use this bacterium deliberately between 1932 and 1945 (*6*). After World War II, U.S. military and former Soviet Union also developed bioweapons that can aerosolize *F. tularensis* (*7-8*).

Streptomycin is currently the first line drug used for the treatment of tularemia, while gentamicin may be substituted for patients who are unable to tolerate streptomycin. However neither of them can be orally administrated (*9*). Other antibiotics, such as fluoroquinolones, tetracycline, chloramphenicol and ciprofloxacin, have been proposed, but lack of clinical data or a requirement for longer treatment restricts their use (*5, 10-11*). Taken together, there is an urgent need to develop antibiotics with novel mechanisms of action to treat tularemia.

FAS-II Pathway in F. tularensis. A BLAST search using the genome of *F. tularensis* Schu4 (KEGG) identified open reading frames (ORFs) with high predicted identity to the FAS-II enzymes from *E. coli* (**Table 2.1**). As in *E. coli*, most of the genes encoding the FAS-II enzymes in *F. tularensis* are clustered (FTT1373 – FTT1377) except FabI and FabZ.

The FabI enoyl-ACP reductase from *E. coli* (ecFabI) was initially considered to be the only reductase in bacteria (*12*). While extensive efforts have been made to develop inhibitors of FabI (*13-14*), the subsequent isolation of the FabL, FabK and FabV enoyl-ACP reductases from *Bacillus subtilis*, *Streptococcus pneumoniae* and *Vibrio cholerae* respectively, have reduced the enthusiasm for using FabI as a target for the development of broad spectrum antibacterial agents due to the low structural homology between these four enzymes (*15-17*). However, only one FabI enoyl-ACP reductase homologue (ftuFabI) was found in the *F. tularensis* gene which has a high sequence homology with respect to ecFabI. This confirms our hypothesis that FabI is a good drug target to develop inhibitors for the treatment of tularemia.

Mechanism of Inhibition. Most inhibitors are in rapid reversible equilibrium with their targets. They can bind to the free enzyme and/or different intermediates in

36

Table 2.1: Genes in FAS-II Pathway from *E. coli* and *F. tularensis*

E. Coli Enzyme	*F. tularensis* Homologue	Sequence Identity/Similarity
FabI: enoyl-ACP reductase (262 res.)	FTT0782 (260 res.)	58%/76% over 259 res.
FabH: β-ketoacyl-ACP synthase III (317 res.)	FTT1373 (323 res.)	46%/64% over 322 res.
FabD: malonyl-CoA ACP transacylase (309 res.)	FTT1374 (306 res.)	50%/63% over 306 res.
FabG: β-ketoacyl-ACP reductase (244 res.)	FTT1375 (247 res.)	61%/78% over 246 res.
AcpP: acyl carrier protein (78 res.)	FTT1376 (94 res.)	72%/82% over 70 res.
FabF: β-ketoacyl-ACP synthase II (413 res.)	FTT1377 (419 res.)	56%/75% over 420 res.
FabZ: β-hydroxyacyl-ACP synthase (151 res.)	FTT1570c (163 res.)	44%/62% over 153 res.

the catalytic reaction and thus exhibit different inhibition mechanisms (**Figure 2.1**). If an inhibitor binds exclusively to the free enzyme (E), it is a competitive inhibitor because the binding of the inhibitor and the substrate are mutually exclusive. An inhibitor that only binds to the ES complex or a subsequent species is referred to as uncompetitive. Finally, a noncompetitive inhibitor is one that has a

$$E + S \rightleftharpoons^{K_m} E{\bullet}S \xrightarrow{k_{cat}} E + P$$

$$+ \qquad\qquad +$$

$$I \qquad\qquad I$$

$$\Big\updownarrow K_i \qquad\qquad \Big\updownarrow aK_i$$

$$E{\bullet}I + S \rightleftharpoons^{aK_m} E{\bullet}S{\bullet}I$$
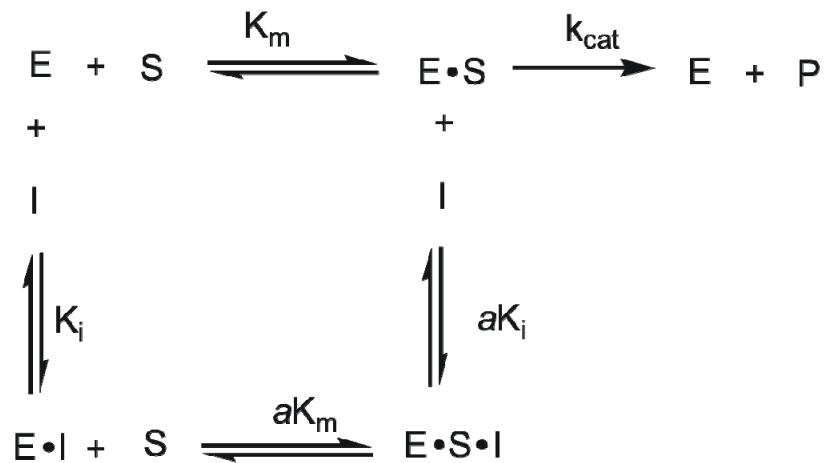
Figure 2.1: Equilibrium Binding Scheme of Different Rapid Reversible Inhibition. K_m is the Michaelis-Menten constant for the substrate; k_{cat} is the turnover number which represents the maximum number of substrate converted to product per active site per unit time; K_i is the inhibition constant and the constant *a* defines the degree to which inhibitor binding affects the affinity of the enzyme for the substrate.

binding affinity for both the free enzyme and the ES complex or subsequent species.

Experimentally, the mechanism of inhibition can be determined by measuring the initial velocities of enzyme reactions by varying the concentration of substrate at several different inhibitor concentrations. A set of double reciprocal lines can be plotted and by examining the point where these lines intersect we can differentiate between inhibition mechanisms (**Figure 2.2**). As we can see, a set of double
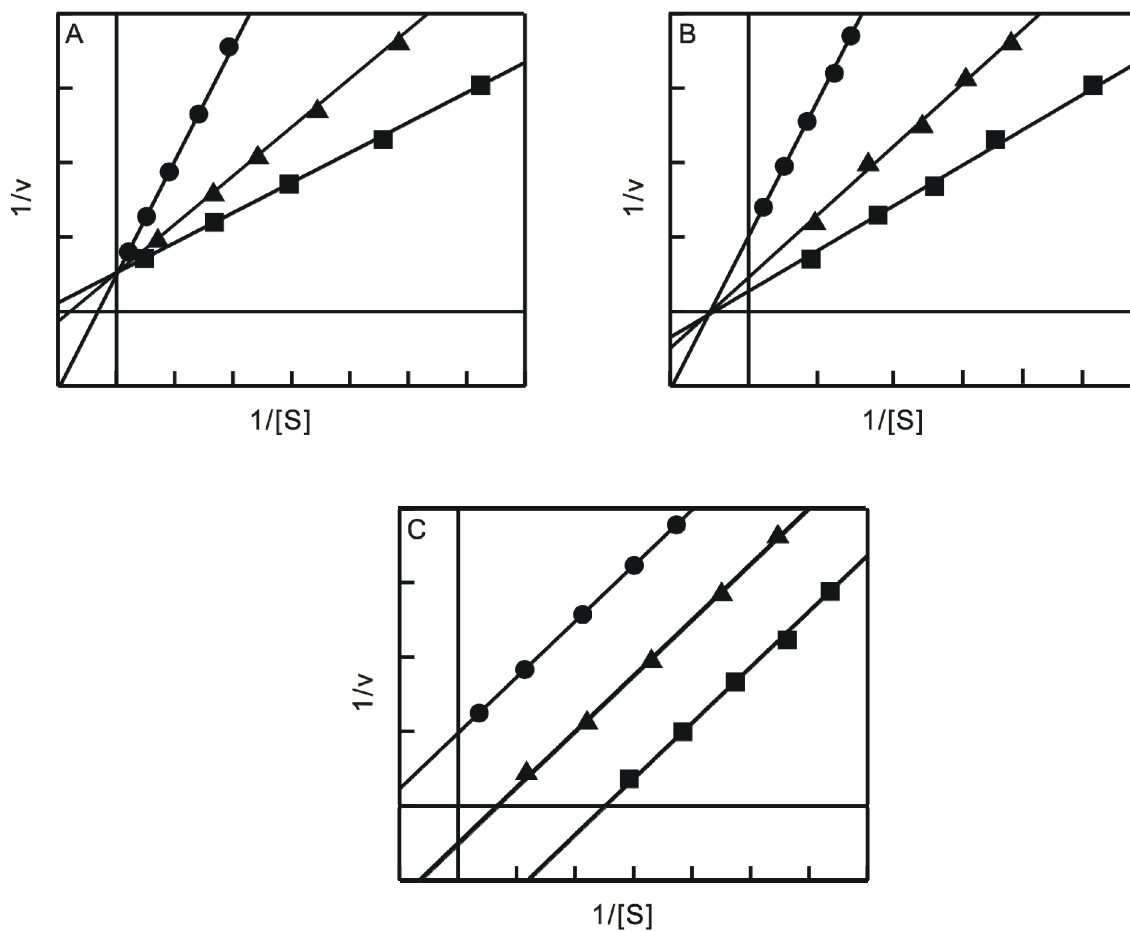
Figure 2.2: Lineweaver-Burk (Double Reciprocal) Plots for Determination of Inhibition Mechanism. A) Competitive Inhibition; **B**) Noncompetitive Inhibition; **C**) Uncompetitive Inhibition. v is the initial velocity and [S] is the concentration of substrate.

reciprocal lines intersecting at the Y-axis indicate that it is a competitive inhibitor (**Figure 2.2A**), while a set of intersecting lines at the X-axis or above suggests a noncompetitive inhibition mechanism (**Figure 2.2B**). Finally, an uncompetitive inhibitor will give a set of parallel lines (**Figure 2.2C**). Inhibition constants of each type of inhibitor can be determined by fitting the initial velocities and substrate concentrations into different equations shown below (eqn **1, 2** and **3**) (*18*).

$v = V_{max}[S]/[K_m(1+[I]/K_i)+[S]]$ (competitive inhibitor , **1**)

$v = V_{max}[S]/[(K_m+[S])(1+[I]/K_i)]$ (noncompetitive inhibitor , **2**)

$v = V_{max}[S]/[K_m+[S](1+[I]/K_i)]$ (uncompetitive inhibitor , **3**)

where [S] is the concentration of the substrate, K_m is the Michaelis-Menten constant for the substrate, V_{max} is the maximum velocity, [I] is the concentration of the inhibitor added and K_i is the inhibition constant.

Slow binding inhibitors associate with and/or dissociate from the target enzymes slowly, thus leading to time dependent inhibition. In order to measure the true affinity of slow binding inhibitors, steady state has to be reached before data collection. Otherwise, the potency of the inhibitors would be underestimated and thus promising inhibitors might be overlooked in SAR studies. There are three common mechanisms proposed for slow binding inhibition (**Figure 2.3**).

A: $E + I \xrightleftharpoons[k_2]{k_1} EI$

B: $E + I \xrightleftharpoons[k_2]{k_1} EI \xrightleftharpoons[k_4]{k_3} E^*I$

C: $E \xrightleftharpoons[k_2]{k_1} E^* + I \xrightleftharpoons[k_4]{k_3} E^*I$
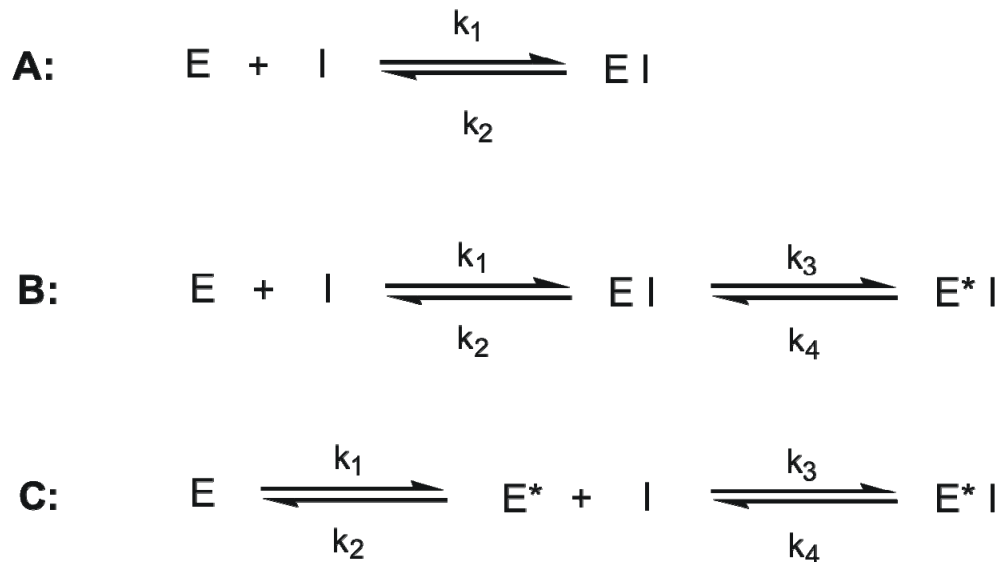
Figure 2.3: Mechanisms of Slow Binding Inhibition. A) A one-step mechanism for which the inherent association rate constant (k_1) or dissociation rate constant (k_2) or both are slow; **B**) A two-step binding mechanism for which the first step is rapid and reversible to form the initial EI complex and the second step is a slow isomerization of the enzyme to form the final E*I complex; **C**) A two-step binding mechanism for which the enzyme is initially in equilibrium between two conformational states and binding with the inhibitor finally shifts the equilibrium to the favorable E* state and forms the E*I complex.

Mechanism **A** illustrates a simple one-step binding and dissociation mechanism governed by the association and dissociation rate constant k_1 and k_2. Slow binding inhibitors undergoing this mechanism behave almost identical to rapid reversible inhibitors except that k_1 and k_2 are much smaller, leading to the time dependent inhibition. Some inhibitors of bacterial protein synthesis and amino acid biosynthesis show this one-step slow binding mechanism (*19-20*). The

second common mechanism of slow binding inhibition is shown in mechanism **B**, where the inhibitor initially binds to a conformation of the enzyme that is less than optimally complementary to the inhibitor and an initial EI complex is formed. Subsequently, the binary E*I complex that is much more stable than the initial EI complex is formed. Generally the first step to form the initial EI encounter complex is considered to be rapid and reversible, while the second step which normally involves a relatively large motion of the enzyme is slow. The isomerization step is the rate determining step, and is controlled by the forward rate constant (k_3) and the reverse rate constant (k_4). To determine the true affinity of the inhibitor, k_3 and k_4, should also be considered since the final E*I complex is much more stable than the initial EI complex. Mechanism **B** is the most commonly found mechanism for the slow binding and high affinity of many pharmacologically active enzyme inhibitors (*21-22*). The last mechanism is represented in mechanism **C**, in which the enzyme is initially in equilibrium between two different conformation states. Only one conformer (E*) is able to bind the inhibitor. After the inhibitor binds to the E* form, the equilibrium shifts to the pool of E* state since E*I complex is preferred. With a sufficient inhibitor concentration and time, all of the enzyme molecules will eventually form the E*I complex. In this mechanism, the

42

interconversion of different enzyme conformational states is the slow step. Mechanism **C** is very unusual and only a few examples have been found (*23-24*).

Progress curve analysis (**Materials and Method**, **Chapter IV**) is the most common way to differentiate different mechanisms of slow binding inhibition (*21-22*). In this method, a pseudo-first-order rate constant (k_{obs}), which is inhibitor concentration dependent, can be measured. A plot of k_{obs} as a function of inhibitor concentration displays a distinguishing feature of each mechanism (**Figure 2.4**). For mechanism **A**, a linear increase of the k_{obs} value can be observed as the inhibitor concentration increases. The value of k_{obs} for mechanism **B** is a compilation of rate constants associated with the initial complex and the final complex. Usually, the value of k_{obs} hyperbolically increases as increasing the concentration of inhibitor. However, if the final complex (E*I) is much more stable than the initial complex (EI) so that the concentration of EI complex is insignificant compared to the concentration of E*I, a linearly correlation between k_{obs} and inhibitor concentration will be observed (*21-22*). In stark contrast to the other two mechanisms, k_{obs} actually decreases when the concentration of inhibitor increases in mechanism **C**. For those inhibitors that take an extraordinarily long time to reach the steady state, preincubation method (**Materials and Method**, **Chapter II**) is used to measure the inhibition constants (*25*).

43
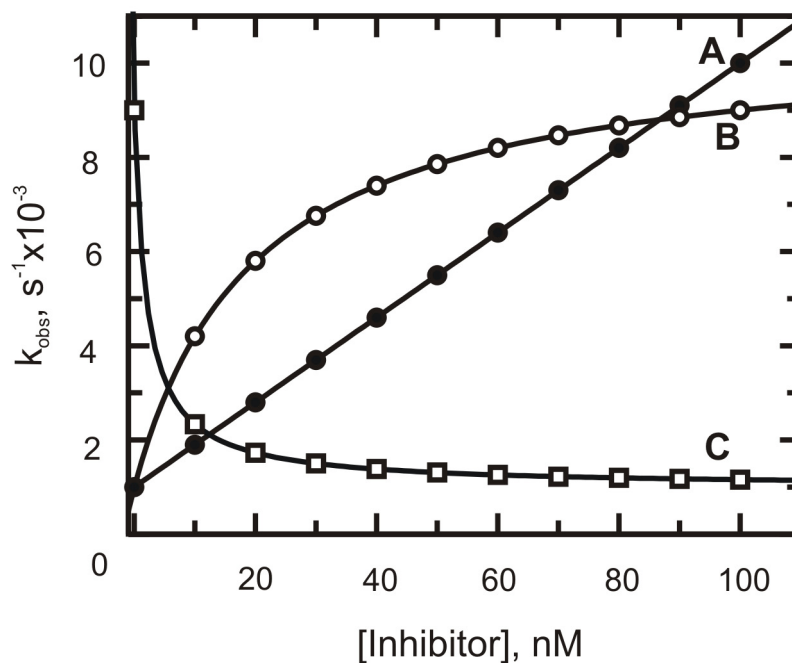
Figure 2.4: Simulation of Pseudo-first-order Rate Constant as A Function of Inhibitor Concentration for Different Slow Binding Mechanisms. A) One-step binding mechanism termed mechanism **A** in the text (●); **B**) Two-step binding mechanism termed mechanism **B** in the text (○); **C**) Two-step binding mechanism termed mechanism **C** in the text (□).

It is worth pointing out that most of the slow binding inhibitors are tight binding inhibitors. This may be due to the stability of the final E*I complex (mechanism **B and C**). Tight binding inhibitors can bind to their target enzymes with such high affinity that the population of free inhibitor molecules is significantly depleted by formation of enzyme-inhibitor complex. In this case, equations (eqn **1**, **2** and **3**)

used to calculate the inhibition constant for classical non-tight binding inhibitors are no longer valid, because one of the most important requirements to apply such equations assumes that the depletion of inhibitor concentration caused by the formation of enzyme-inhibitor complex can be ignored. In order to determine inhibition constants of tight binding inhibitors, the method developed by Morrison should be applied (*22-23*).

Project Goals. In this chapter, the mechanism of the ftuFabI catalyzed reaction will be investigated. Diaryl ethers inhibitors will be synthesized and evaluated based on rational drug design and SAR studies. Antibacterial activity of these inhibitors will also be tested at the cellular level.

Materials and Methods

Materials. His-bind Ni^{2+}-NTA resin and pET vectors were purchased from Novagen while a QuickChange site-directed mutagenesis kit was obtained from Stratagene. Triclosan was a gift from Ciba and all the other inhibitors were available from previous work (*28-29*). *trans*-2-Dodecenoic acid was purchased from TCI. All other chemical reagents were obtained from Sigma-Aldrich.

Cloning, Expression and Purification of ftuFabI. The entire coding region of the gene (FTT 0782) encoding the putative ftuFabI was amplified using the primers 5'-CGC<u>GGATCC</u>ATGGGTTTTCTAGCAGGAAAAAAA-3' (forward) and 5'-CG-C<u>CTCGAG</u>TTGCAAAACATTACCCATAGACAC-3' (reverse) and inserted into Novagen pET23b vector using the 5' BamHI and 3' XhoI restriction sites (underlined) with a His tag at the C-terminus. The constructed plasmid was then purified from XL1Blue cells (Stratagene) using a DNA purification and gel extraction kit from Qiagen Inc., and sequenced using an ABI DNA sequencing.

Protein expression was performed by transforming the plasmid into *E. coli* BL21(DE3)pLysS cells which were then used to inoculate in 10 ml of Luria Broth (LB) media containing 0.2 mg/ml ampicillin in a 50 ml falcon tube. After incubated at 37 $^{\circ}$C overnight in a floor shaker, the culture was used to inoculate 1 liter of LB

media containing ampicillin (0.2 mg/ml) and grown at 37 ^{o}C until the optical density at 600 nm (O.D. 600) increased to ~ 1.0. Induction was achieved by adding 1 mM isopropyl-1-thio-β-D-galactopyranoside (IPTG), followed by expression for 16 h at 25 ºC. Cells were harvested by centrifugation at 5,000 rpm for 25 min at 4 ºC. The cell paste was resuspended in 30 ml of His-binding buffer (5 mM imidazole, 0.5 M NaCl, 20 mM Tris HCl, pH 7.9) and lysed by sonication. Cell debris was removed by centrifugation at 33,000 rpm for 90 min at 4 ºC. The collected supernatant was loaded onto a His-bind column (1.5 cm x 15 cm) containing 4 ml of His-bind resin (Novagen) that has been charged with 9 ml of charge buffer (Ni^{2+}). The column was washed with 60 ml of His-binding buffer and 30 ml of washing buffer (60 mM imidazole, 0.5 M NaCl, 20 mM Tris HCl, pH 7.9). Subsequently, the expressed protein was eluted using a gradient of 20 ml binding buffer and 40 ml elute buffer (1 M imidazole, 0.5 M NaCl, 20 mM Tris HCl, pH 7.9) mixture. Fractions containing the protein after elution were collected and imidazole was removed using a Sephadex G-25 column (1.5 cm x 55 cm) using 30 mM pipes, 150 mM NaCl and 1.0 mM EDTA at pH 8.0, as the eluent. The purity of the protein was determined by 12% sodium dodecyl sulfate-polyacrylamide gel electrophoresis (SDS-PAGE), which gave a molecular weight of approximately 29 kDa for the pure protein. The concentration of the

protein was determined by measuring the absorption at 280 nm using an extinction coefficient (ε) of 16,170 $M^{-1}cm^{-1}$ calculated from the primary sequence. The enzyme was stored at -80°C in the same buffer after freezing with liquid N_2.

Preparation of ftuACP. The ORF (FTT1376) which encodes the putative acyl carrier protein (ACP) in *F. tularensis* was amplified using the primers 5'-GGAATTCCATATGAGTACACATAACGAAGATTCTAAA-3' (forward) and 5'-CCGCTCGAGACCTACATCTTTAGATTCGATATA-3' (reverse). The purified PCR product was then inserted into a Novagen pET23b vector using the 5' BamHI and 3' XhoI restriction sites (underlined) so that the protein would be expressed with a C-terminal His tag. The plasmid construct was then purified and sequenced as described for ftuFabI.

Expression and purification of ftuACP followed a similar protocol to that described above for ftuFabI except that 0.1 M potassium phosphate buffer, pH 8.0 was used for G-25 chromatography. The purified protein was analyzed by 15% SDS-PAGE and MALDI-TOF mass spectrometry. The concentration of the protein was determined by measuring the absorption at 280 nm and by using an extinction coefficient of 2,560 $M^{-1}cm^{-1}$ calculated from the primary sequence. The protein was stored at 4 ^{o}C for over 3 months without losing any activity.

48

Preparation of Crotonyl-ACP (Cr-ACP). Purified ftuACP was concentrated to 900 μM in the reaction buffer (0.1 M potassium phosphate solution at pH 8.0, 3 ml) and an equimolar amount of dithiothreitol was added to the solution. The reaction mixture was then stirred under nitrogen at 0 ^{o}C for 2 h to ensure complete reduction of the ACP thiol group, after which a 1.5-fold molar excess of crotonic anhydride was added to the reaction mixture. After stirring for 15 min at 0 ^{o}C, small molecules were removed from the Cr-ACP by chromatography on a Sephadex G-25 column (0.5 cm x 15 cm) using the PIPES buffer (30 mM pipes, 150 mM NaCl and 1.0 mM EDTA at pH 8.0) as the eluent..

DTNB Assay to Test holo-ACP. An equimolar amount of DTT was added to 1 ml of 900 μM *holo*-ACP in 0.1 M potassium phosphate buffer at pH 8.0. The reaction mixture was stirred at room temperature for 30 min and then a 10-fold excess of 5,5'-dithio-bis(2-nitrobenzoic acid) (DTNB) was added into the mixture. After 30 min, 4 ml of acetone was added to the aqueous solution and the precipitated protein was collected by centrifugation at 13,000 rpm for 10 min at room temperature. One hundred μl of DD-H$_2$O was added to redissolve the protein and 400 μl of acetone was added to precipitate the protein. This step was repeated twice to completely remove the salt from the protein which was finally dissolved in

100 µl of DD-H_2O and analyzed by ESI mass spectrometry.

Preparation of Substrates with Other Acyl Carriers. Crotonyl-CoA (Cr-CoA) and butyryl-CoA were synthesized by coupling free CoA with crotonic anhydride and butyric anhydride, respectively, as described previously (*30*). *trans*-2-Octenoyl-CoA, *trans*-2-decenoyl-CoA and *trans*-2-dodecenoyl-CoA (DD-CoA) were prepared from *trans*-2-octenoic acid, *trans*-decenoic acid and *trans*-dodecenoic acid, respectively, using the mixed anhydride method (*31*). *trans*-2-Dodecenoyl *N*-acetylcysteamine (DD-NAC) was synthesized by coupling *trans*-2-dodecenoic acid and *N*-acetylcysteamine using the mixed anhydride method as described for DD-CoA and purified by flash column chromatography (ethyl acetate : hexane = 1 : 9) (*31*).

Steady-state Kinetic Assays. All kinetic experiments were carried out on a Cary 300 Bio (Varian) spectrophotometer at 25 ^{o}C using 30 mM pipes, 150 mM NaCl and 1.0 mM EDTA, pH 8.0 as the buffer. Kinetic parameters were determined spectrophotometrically by following the oxidation of NADH to NAD^+ at 340 nm (ε = 6,300 $M^{-1}cm^{-1}$).

Initial characterization of the enzyme mechanism was performed in reaction

mixtures containing 10 nM ftuFabI and measuring initial velocities at a fixed concentration of NADH (250 μM) and by varying the concentration of Cr-CoA (76-608 μM), or at a fixed concentration of Cr-CoA (160 μM) and by varying the concentration of NADH (60-250 μM). Double reciprocal plots were then used to differentiate between ping pong or ternary-complex mechanisms.

To further investigate the binding order of substrates, product inhibition studies were performed in which each substrate concentration was varied in the presence of several fixed concentrations of one of the products, NAD^+ (0-1800 μM) or butyryl-CoA (0-1824 μM). The type of inhibition in each case was subsequently determined using a Lineweaver-Burk plot.

Finally the kinetic data in the absence of products were globally fit to the equation for the steady-state sequential bi bi mechanism (eqn **4**) to determine the K_m values for DD-CoA and NADH.

$$v = V_{max}[A][B] / (K_{iA}K_B + K_B[A] + K_A[B] + [A][B]) \tag{4}$$

In eqn **4**, v is the initial velocity, V_{max} is the maximum velocity, [A] and [B] are the concentration of the two substrates, K_A and K_B are the Michaelis constants for A and B respectively, and K_{iA} is the dissociation constant for A. Data analysis was performed using GraFit 4.0 (Erithacus)

For *trans*-2-octenoyl-CoA, *trans*-2-decenoyl-CoA , DD-CoA and DD-NAC, K_m

values were determined by varying the concentration of these substrates at a fixed, saturated concentration of NADH (250 µM). Data sets were fitted to the Michaelis-Menten equation (eqn **5**) using the software program GraFit (Erithacus) to obtain K_m values.

$$v = V_{max}[S] / (K_m + [S])$$ (**5**)

Fluorescence Titration Experiments. Equilibrium fluorescence titration was conducted using a FL3-21 Fluorology-3 spectrofluorometer. The reaction buffer was the same as that used in the steady-state kinetic experiments. A NADH stock solution of 2.86 mM was titrated in 1 µl aliquots into the protein solution (2 ml). The excitation wavelength was 360 nm (5 nm slit width), and the emission wavelength was fixed at 440 nm (1 nm slit width). Dilution of protein concentration was controlled to a minimum (< 1%) and fluorescent differences corresponding to the concentration of NADH in solution was calculated. Since a significant portion of ligand was not free in solution, a quadratic equation (eqn **6**) was used to fit the data.

$$\frac{F_e - F_1}{F_e(\text{max}) - F_1(\text{max})} = \frac{(K_d + [E]_0 + [NADH]) - \sqrt{(K_d + [E]_0 + [NADH])^2 - 4K_d[E]_0}}{2[E]_0}$$ (**6**)

In eqn **6**, F_e and F_1 are the fluorescent intensity in the presence and absence of enzyme, respectively. $F_{e,max}$ and $F_{1,max}$ are the maximum fluorescence intensity in the presence and absence of enzyme, respectively. K_d is the dissociation constant, $[E]_0$ is the total amount of enzyme in solution and [NADH] is the amount of NADH added to the reaction buffer. Grafit 4.0 was used for the data fitting.

Determination of Inhibition Constants of Triclosan and Its Diaryl Ethers Analogues. Since most of the diphenyl ethers are slow binding inhibitors and in each case bind preferentially to the $E\text{-}NAD^+$ form of the enzyme (**Figure 2.5 A**), typical progress curve analysis cannot be used to obtain the inhibition constant since the concentration of NAD^+ varies during the assay. Instead, ftuFabI (10 nM) was preincubated with a fixed concentration of NAD^+, inhibitor (0-1000 µM) and DMSO (1%, V/V) in the presence of 250 µM NADH for 5 h at 4 °C. The mixture was then warmed to room temperature, and the reactions were initiated by the addition of Cr-CoA (160 µM). Eqn **7** was used to estimate the apparent inhibition constant K_i'

$$v = v_0/(1+[I]/K_i') \tag{7}$$

where v_0 is the rate in the absence of inhibitor and [I] is the triclosan concentration.

This experiment was repeated at varying concentrations of NAD^+ (10-200 µM) and the mechanism of inhibition with respect to NAD^+ was determined by fitting the data to eqn **8**-**10**. K_1 and K_2 are defined in panels A and B in **Figure 2.5** and represent the equilibrium constants for inhibitor binding to E-NAD^+ and E-NADH, respectively.

Inhibitor binds exclusively to the E-NAD^+ form

$$K_i' = K_1([NAD^+]+K_{m,NAD})/[NAD^+] \tag{8}$$

Inhibitor binds exclusively to the E-NADH form

$$K_i' = K_2([NAD^+]+K_{m,NAD})/K_{m,NAD} \tag{9}$$

Inhibitor binds both to the E-NAD^+ and E-NADH forms

$$K_i' = K_2\{(1+[NAD^+]/K_{m,NAD})/[1+ [NAD^+]/(K_{m,NAD}K_1/K_2)]\} \tag{10}$$

where the $K_{m,NAD}$ value for NAD^+ was calculated from eqn **11**:

$$K_{m,NAD} = K_{i,NAD}(1 + [NADH]/K_{m,NADH}) \tag{11}$$

and $K_{i,NAD}$ is the dissociation constant of NAD^+. Eqn **11** presumes that NAD^+ is a competitive inhibitor with respect to NADH as was shown by the product inhibition studies.
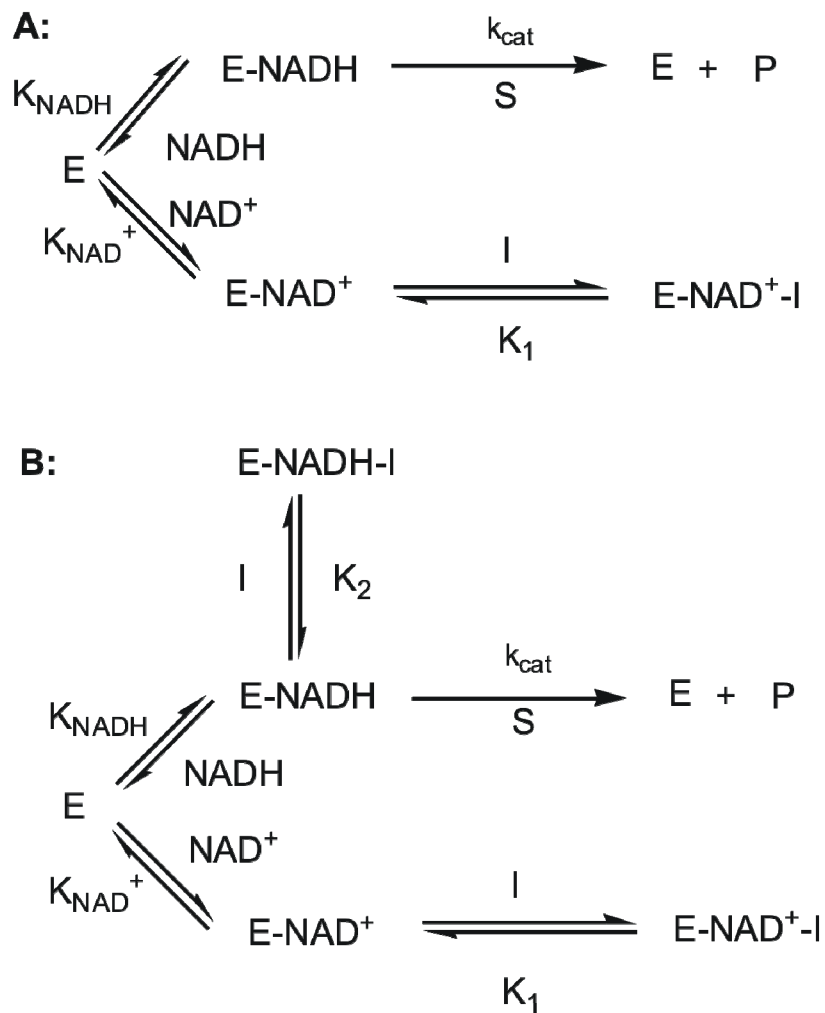
Figure 2.5: Kinetic Schemes for the Interaction of ftuFabI with Inhibitors. A) Inhibitor binds exclusively to the E-NAD$^+$ form of the enzyme with an equilibrium dissociation constant of K_1; **B**) Inhibitor binds to both E-NAD$^+$ and E-NADH forms of the enzyme with equilibrium dissociation constants of K_1 and K_2, respectively.

The mechanism of inhibition with respect to NADH was determined in an analogous fashion by performing the same experiment at various concentrations of NADH (100-500 µM) and at a fixed concentration of NAD^+ (50 µM), and by fitting the data to eqn **8**-**10** using the concentration and K_m value for NADH instead of NAD^+.

For the diaryl ethers that were rapid reversible inhibitors, the concentration of inhibitor in each assay was at least 10-fold larger than the enzyme concentration allowing the inhibition constants to be determined using standard Michaelis-Menten kinetics. Initial velocities were measured using a fixed Cr-CoA concentration (160 µM) and by varying the concentration of NADH and inhibitors. All the inhibitors were shown to be competitive with respect to NADH, and inhibition constants (K_{is}) were calculated by fitting the data to eqn **1**.

$$v = V_{max}[S]/[K_m(1+[I]/K_i)+[S]] \tag{1}$$

where [S] is the concentration of NADH, K_m is the Michaelis-Menten constant for NADH, V_{max} is the maximum velocity, [I] is the concentration of inhibitor added and K_i is the inhibition constant.

Results and Discussion

Cloning, Overexpression and Purification of ftuFabI. The enoyl-ACP reductase

from *F. tularensis* (ftuFabI) was expressed with a C-terminal His tag and purified

from *E. coli* by Ni^{2+}-affinity chromatography. The molecular weight of the purified

protein was around 29 kDa on a 12% SDS-PAGE protein gel (**Figure 2.6**), which

is consistent with the calculated value (28,986 Da).

Lane 1: Lysate from *E. coli*

Lane 2: Eluent from Ni^{2+} His-biding column

Lane 3: Protein Ladder (MW Starndard)

Lane 4: Fraction from G-25 column.
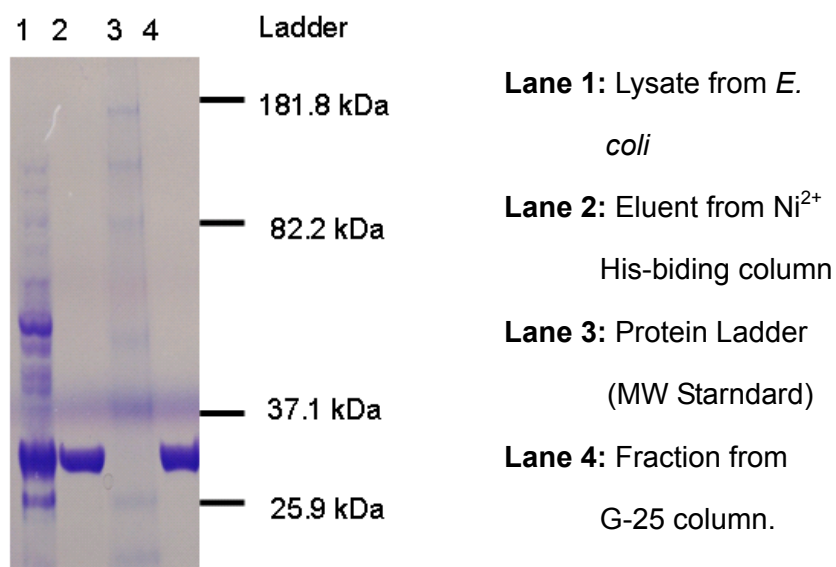
Figure 2.6: 12% SDS-PAGE Showing the Expression and Purification of ftuFabI.

Acylation of holo-ACP to Synthesize Cr-ACP. Acyl carrier proteins (ACP) are

small acidic proteins involved in various biosynthetic pathways including fatty acid

biosynthesis (*32*), peptide and polyketide biosynthesis (*33-34*), posttranslational acylation of proteins (*35*) and the synthesis of oligosaccharides (*36*). In the FAS-II pathway, the fatty acid intermediates are covalently bound to ACP through a thioester bond and these ACP intermediates are recognized as substrates for all the enzymes in the elongation cycle. However, natively expressed ACP (*apo*-ACP) is not the active form of this enzyme. In order to carry fatty acids, a 4'-phosphopantetheine prosthetic group must be attached to a conserved serine residue of *apo*-ACP. This posttranslational modification is catalyzed by the *holo*-ACP synthase (ACPS). The newly modified ACP (*holo*-ACP) has a free sulfhydryl group to form thioester bonds with fatty acyl chains (*37*).

Because the endogenous ACPS from *E. coli* is capable of modifying ACPs from other organisms, both *apo*- and *holo*-ACPs are found in the cell lysate of *E. coli* following the expression of recombinant ACP proteins (*38-40*). However in our attempt to express the ACP protein from *F. tularensis* (ftuACP), only one form was detected by SDS-PAGE. The mass of the purified protein was determined to be 11,934 Da which was 210 Da larger than the calculated value (11,724 Da) of the *apo*-ftuACP. In realization that the first methionine of ACPs was often removed following expression, we speculated that the protein we obtained was purely in its *holo*-form, and indeed the mass of *holo*-ftuACP lacking the first methionine

58

matched the mass of 11,934 Da obtained from the recombinant ACP. To further

substantiate our hypothesis, 5,5'-dithio-bis(2-nitrobenzoic acid) (DTNB) was used

to react with the purified enzyme in the presence of equivalent amounts of DTT. If

the protein is in it *holo*-from, the 5-thio-nitrobenzoyl group from DTNB will be

attached to the free sulfhydryl group and a mass change of 198 Da will be

observed. Upon analysis of ESI mass spectrum, the mass of the reaction product

was determined to be 12196 Da, identical to the calculated mass of

5-thio-nitrobenzoyl-ACP. We concluded that the recombinant ftuACP expressed

from *E. coli* was solely in its *holo*-form. This protein was then directly used to react

with crotonic anhydride to generate Cr-ACP as previously described (*41*). Product

formation was confirmed by MALDI-TOF giving a mass of 12019 Da (Cr-ACP +

NH_4^+).

Catalytic Activity of ftuFabI. Although the *in vivo* substrate of ftuFabI is attached

to the acyl carrier protein (ACP), other enoyl-ACP reductase enzymes also

catalyze the reduction of unsaturated fatty acids esterified to carriers such as CoA

(*25, 42-43*) (**Figure 2.7**). The activity of ftuFabI was demonstrated in an *in vitro*

spectrophotometric assay using its natural substrate and a variety of substrate

mimics, such as fatty acyl chains attached to CoA or NAC, confirming that gene

59
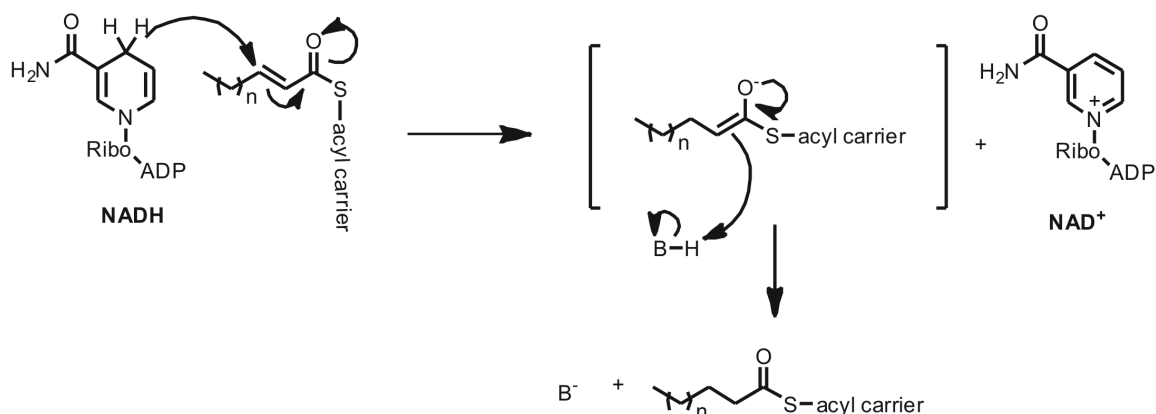
Figure 2.7: Mechanism of the Reduction Reaction Catalyzed by the Enoyl-ACP Reductase. Ribo and ADP refer to ribose and adenosine diphosphate, respectively. The number n is the length of the enoyl chain and the acyl carriers can be ACP, CoA or NAC.

product of FTT0782 is an enoyl-ACP reductase. The steady-state kinetic parameters for the ftuFabI catalyzed reaction are given in **Table 2.2**. For all the substrates with different acyl chain length and acyl carriers, the k_{cat} values were almost the same, indicating that the enzyme modulates the substrate specificity by varying the K_m values. To determine the chain-length specificity, we measured the K_m values of different CoA substrates by varying acyl chain lengths from C4 to C12. It was found that DD-CoA (C12) has the smallest K_m value while Cr-CoA has

Table 2.2: Michaelis Constants of Different Substrates for ftuFabI

Substrate	k_{cat} (s^{-1})	K_m (µM)	k_{cat}/K_m (µM^{-1}s^{-1})
Cr-ACP	20±1	22.0±1.4	0.9±0.1
Cr-CoA	19±1	353±5	0.05±0.01
2-*trans*-Octenoyl-CoA	20±1	33.3±0.4	0.6±0.1
2-*trans*-Decenoyl-CoA	21±1	11.2±0.8	2.1±1
2-*trans*-Dodecenoyl-CoA	20±1	1.7±0.1	9.5±0.6
2-*trans*-Dodecenoyl-NAC	20±1	20.4±0.5	1.0±0.1
NADH	19±1	18.8±0.6	1.0±0.1

the largest K_m value with a 208-fold difference. Substrates with same chain length but different acyl carriers also exhibited different K_m values. The K_m of Cr-CoA was 16-fold larger than Cr-ACP and the K_m of DD-NAC was 12-folder larger than DD-CoA. This trend should result from a decrease in interacting sites between FabI and the acyl carrier. The natural ACP substrate has the largest protein-protein interaction as compared to the substrates attached to CoA or NAC, thus exhibiting the highest affinity with the same acyl chain. Substrate specificity between NADH and NADPH indicated that ftuFabI is an NADH-dependent

enoyl-reductase. This is based on the observation that the k_{cat}/K_m of NADPH is 198-fold lower than the corresponding value of NADH.

Kinetic Mechanism. In order to differentiate between a ternary-complex mechanism and ping pong mechanism, the initial velocity patterns of the two-substrate, two-product reaction were investigated using Cr-CoA as the substrate analogue. Data obtained by varying the concentration of NADH at several different concentrations of Cr-CoA and also varying the concentration of Cr-CoA at several different NADH concentrations, displayed intersecting-line patterns when plotted in double-reciprocal from (**Figure 2.8**). This is a characteristic of the ternary-complex mechanism. Product inhibition studies using NAD$^+$ and butyryl-CoA were explored to determine whether the reaction is an ordered bi bi mechanism or random bi bi mechanism. Double-reciprocal plots indicated that NAD$^+$ was a competitive inhibitor with respect to NADH with a K_i value of 1.5 mM, but showed non-competitive inhibition with respect to Cr-CoA. However, when NADH or Cr-CoA was varied in presence of butyryl-CoA, mixed patterns of inhibition were observed for both substrates (**Figure 2.9**). This combination of product inhibition patterns is indicative of an ordered bi bi mechanism with NADH binding to the enzyme first (*44-45*) (**Figure 2.10**). The

ternary complex steady-state kinetic parameters were obtained by globally fitting

the initial velocity data to eqn 2 for an ordered bi bi mechanism, giving values:

$K_{i,NADH} = 4.8 \pm 0.6$ µM, $K_{m,NADH} = 18.8 \pm 0.6$ µM, $K_{m,Cr\text{-}CoA} = 352.5 \pm 5.0$ µM and $k_{cat} = 19.1 \pm 1.1$ s^{-1}.

The proposed mechanism was also supported by a fluorescence titration

experiment, in which NADH was shown to bind the free enzyme with a K_d of

3.1 ± 0.4 µM.
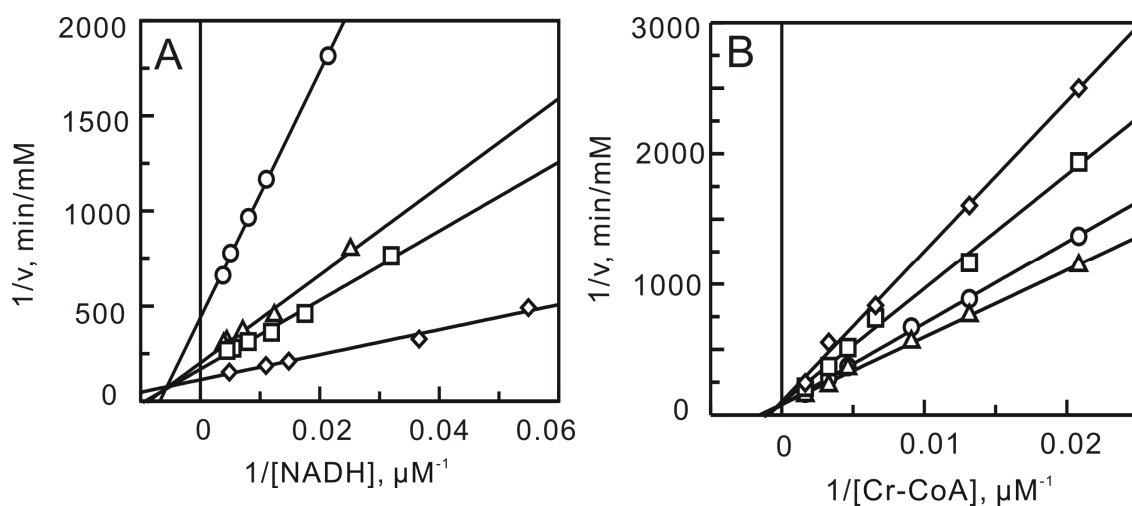
Figure 2.8: Two-substrate Steady-state Kinetics. A) 1/v versus 1/[NADH] double-reciprocal plot while Cr-CoA concentration was fixed at 76 (○), 152 (Δ), 304 (□) and 608µM (◊); **B**) 1/v versus 1/[Cr-CoA] double-reciprocal plot while NADH concentration was fixed at 60 (◊), 90 (□), 200 (○) and 250µM (Δ).
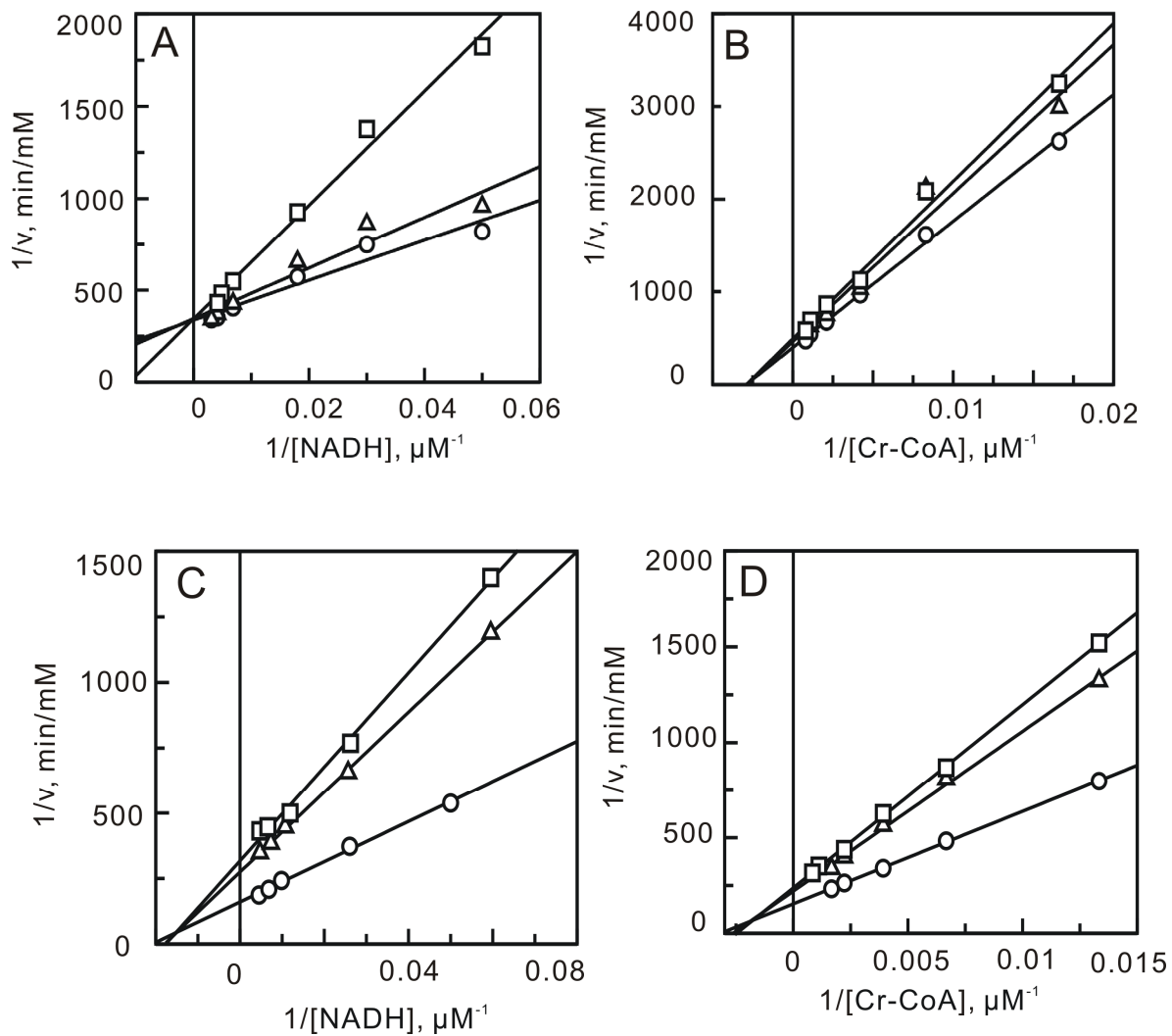
Figure 2.9: Product Inhibition Studies to Determine the Substrate Binding Order. Assays were performed by varying the concentration of one substrate while fixing the concentration of the second substrate in the presence of one product as inhibitor. **A**) NADH varied in presence of NAD$^+$ (0 (○), 800 (Δ) and 1800 μM (□)) with Cr-CoA fixed at 160μM; **B**) Cr-CoA varied in presence of NAD+ (0 (○), 912 (Δ) and 1824 μM (□)) with NADH fixed at 250μM; **C**) NADH varied in presence of butyryl-CoA (0 (○), 250 (Δ) and 500 μM (□)) with Cr-CoA fixed at 160μM; **D**) Cr-CoA varied in presence of butyryl-CoA (0 (○), 912 (Δ) and 1824 μM (□)) with NADH fixed at 250μM.
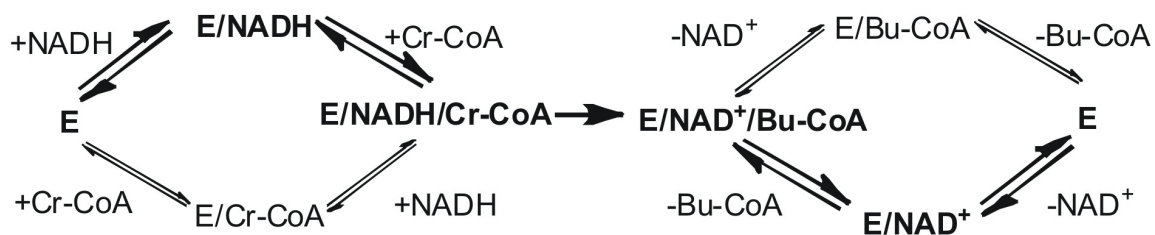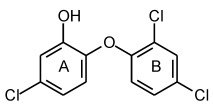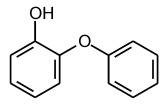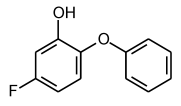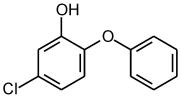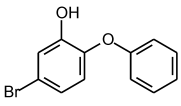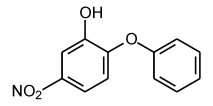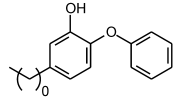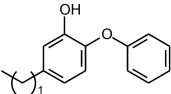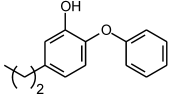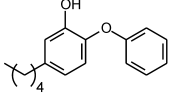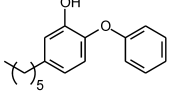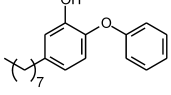
Figure 2.10: Proposed Catalytic Mechanism of the ftuFabI Reaction. Two possible pathways for a sequential bi bi reaction mechanism are shown here. The one we proposed in which NADH binds to the enzyme first and NAD^+ dissociate from the enzyme last is shown in bold. Cr-CoA and Bu-CoA are crotonyl-CoA and butyryl-CoA, respectively.

Structure-Reactivity Analysis of ftuFabI Inhibition by Triclosan and Diaryl Ethers.

Triclosan is a potent inhibitor of FabIs from a variety of organisms (*46-48*). In order to probe the role of specific interactions in the ternary ftuFabI complex, we synthesized a series of diaryl ether compounds (**Table 2.3**). In ecFabI it was found that the B ring points away from the active site and participates in several unfavorable steric interactions with the enzyme based on the observation that 5-chloro-2-phenoxyphenol (**28**) has a 7-fold higher affinity than triclosan (*46*). However, in our studies compound **28** showed a 37-fold decrease in affinity indicating that the two chlorine atoms on ring B form important interactions with ftuFabI. In addition, for the other slow binding inhibitors of ftuFabI that lacked

65

Table 2.3: Enzyme Inhibition and Antibacterial Activity of the ftuFabI Inhibitors

Compound		MIC (µg/ml)	Inhibition Constants and Mode of Inhibition		
			K_1 (nM)[a]	K_2 (nM)[b]	Type of Inhibition
	10	0.000015 ±0	0.051± 0.003	5±35 µM	Slow binding
	26	2.5±0.2	2260±107[c]		Rapid equilibrium
	27	0.32±0.02	289±11[c]		Rapid equilibrium
	28	0.001± 0.001	1.9±0.1	308±6	Slow binding
	29	0.004± 0.001	7.1±0.2	149±2	Slow binding
	30	0.21±0.05	789±13[c]		Rapid equilibrium
	11	0.16±0.07	1.9±0.1	247±5	Slow binding

Structure	No.	K_1[a]	K_2[b]		
	12	0.03± 0.001	2.1±0.1	311±20	Slow binding
	13	0.00018± 0.00014	0.44±0.02	696±70	Slow binding
	15	0.0012± 0.0002	1.3±0.1	525±8	Slow binding
	16	0.16± 0.06	2.7±0.1	331±6	Slow binding
	17	0.66± 0.14	23.6±1.2	192±2	Slow binding
Gentamicin	31	4	ND	ND	ND
Streptomycin	32	2	ND	ND	ND
Doxycycline	33	0.75±0.35	ND	ND	ND

[a]K_1 refers to inhibition constant binding to E-NAD$^+$.
[b]K_2 refers to inhibition constant binding to E-NADH.
[c]K_{is} values for rapid, reversible inhibitors.
ND, not determined.

chlorine atoms on ring B (**28,29,11-17**), binding to both E-NAD$^+$ and E-NADH could be observed. The dependence of K_i' on NAD$^+$ concentration was fit to eqn **10** to obtain the inhibition constants for both forms of the enzyme (**Table 2.3**). These data indicate that the primary effect of removing the B ring chlorines is a specific effect on the affinity of the inhibitor for the E-NAD$^+$ form of the enzyme. Thus, all the Slow binding inhibitors have similar affinities for E-NADH and structural changes to both A and B rings principally modulate the affinity of the analogues for the E-NAD$^+$ product complex. While the precise structural basis for this effect will require additional structural data, one possibility is that the affinity of each inhibitor for the E-NAD$^+$ complex is critically dependent on the precise orientation of the A ring with respect to the oxidized nicotinamide ring and thus the strength of the π-π stacking interaction between inhibitor and cofactor (**Figure 2.11**).

It has been demonstrated that the electronic and steric properties of ring A play a key role in determining the affinity of the diaryl ether inhibitors for ecFabI. The importance of the 5-chloro group on ring A for binding to ftuFabI was initially explored by removing the chlorine to generate analogue **26** which binds 1200-fold less tightly to ftuFabI than does analogue **28**. In addition, analogue **26** was no longer a slow binding inhibitor. To investigate this effect in more detail, we
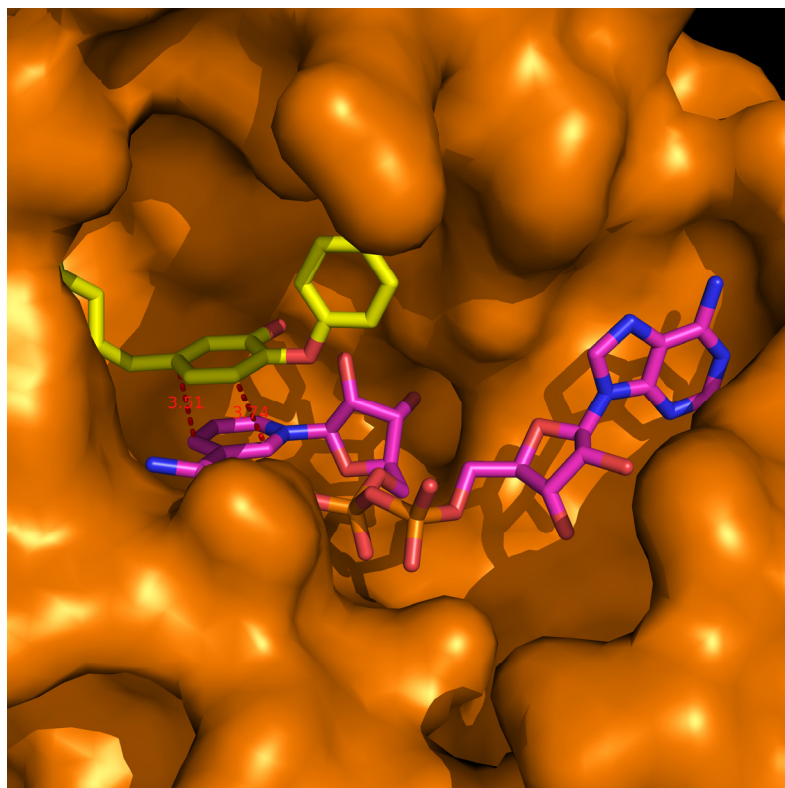
Figure 2.11: Crystal Structure of ftuFabI with Compound 16 and NAD$^+$ Showing the π-π Interaction. The distance of between the A ring of compound **16** and the nicotinamde ring of NAD$^+$ involved in the π-π stacking interaction are measured to be around 3.5 Å (red). The surface of ftuFabI is depicted in orange. For compound **16**, carbon atoms are in yellow and oxygen atoms are in red. For NAD$^+$, carbon atoms are shown in magenta, oxygen in red, nitrogen in blue and phosphorus in orange.

incorporated other halogen atoms into ring A and also replaced the 5-chloro group with alkyl substituents of different lengths (**27,11-13&15-17**). All the alkyl substituted diaryl ethers (**11-13,15-17**) were shown to be slow, tight-binding inhibitors of ftuFabI. Since the 5-chloro substituent points to a hydrophobic pocket for the fatty acid substrate, it is quite possible that replacement of this substituent with a larger and more hydrophobic group will increase the affinity of the inhibitor for the enzyme. However, the data in **Table 2.3** indicate that analogues with smaller alkyl chains generally bound more tightly to the enzyme, with analogue **13** (5-propyl-2-phenoxyphenol) exhibiting the highest affinity for the enzyme.

A remarkable observation is that replacement of the 5-chloro group with a fluorine results in a compound (5-fluoro-2-phenoxyphenol, **27**) that is not a slow binding inhibitor and that exhibits a 150-fold decrease in binding affinity compared to 5-chloro-2-phenoxyphenol (**28**) and 5-methyl-2-phenoxyphenol (**11**). The pKa values of **27** and **28** are almost identical, in agreement with electrostatic potential calculations (*28*), and thus the difference in affinity of **27** and **28** for ftuFabI may arise from the slightly smaller van der Waals radius of fluorine compared to chlorine (0.45 Å), which translates to a ~9 Å^3 reduction in molecular volume of **27** compared to **28**. If the loss of slow binding inhibition is primarily due to the smaller size of the fluorine atom, then replacement of this group with a more bulky

substituent might be expected to restore slow binding and indeed the bromo (**29**) and methyl (**11**) analogs, which have molecular volumes ~5 Å^3 larger than **28**, as well as the propyl (**13**) and pentyl (**15**) analogs, are all slow binding inhibitors. These data are in agreement with previous studies on the ecFabI (*28, 49*), where it was concluded that the shape of the inhibitor was the principal determinant in modulating the affinity of diaryl ether inhibitors for the enzyme. Interestingly, however, incorporation of the larger but more electronegative nitro group (**30**) actually reduced binding affinity 3-fold compared to **27**, and also resulted in a compound that was no longer a slow binding inhibitor. Since **30** has a molecular volume that is only slightly larger (~3 Å^3) than **29** or **11**, the reduction in binding affinity of the nitro analog compared to diaryl ethers bearing, for example, chloro, bromo or methyl substituents, likely results from a decrease in electron density of the A ring and a weakening of the π-π stacking interaction between this ring and the electron deficient positively charged nicotinamide ring of NAD$^+$.

In summary, the SAR studies reflect the subtle interplay of steric and electronic effects that modulate inhibition in the FabI class of enoyl reductases (*28, 49*). For ftuFabI, a 5-chloro or 5-bromo substituent is essential for slow, tight-binding inhibition, while incorporation of hydrophobic alkyl chains of up to three carbons increases the affinity of the inhibitor for the enzyme, presumably due to favorable

71

hydrophobic interactions in the substrate binding pocket. In addition, the π-π stacking interaction between ring A and the NAD$^+$ nicotinamide ring is also important for slow binding enzyme inhibition, as shown by the dramatic impact of introducing a 5-nitro substituent into the inhibitor.

Correlation Between K$_i$ and MIC Values. Minimum inhibitory concentrations (MIC) of triclosan and the diaryl ether inhibitors were obtained against *F. tularensis* LVS. Notably, the diaryl ethers have more favorable MIC values than clinically used drugs (**Table 2.3**). Specifically, the best diaryl ether analog (**13**) is more than 22,000-fold and 4,000-fold more potent than gentamicin and doxycycline, respectively. Significantly, a positive linear correlation between log K$_i$ and log MIC exists for the diaryl ether derivatives (**Figure 2.12**) which strongly suggests that ftuFabI is the primary cellular target for these compounds. Data fitting reveals that the compounds fall into two groups: those with halogen or nitro substituents (**10,26-30**) and those that have alkyl substituents on the A ring (**11-13,15-17**).
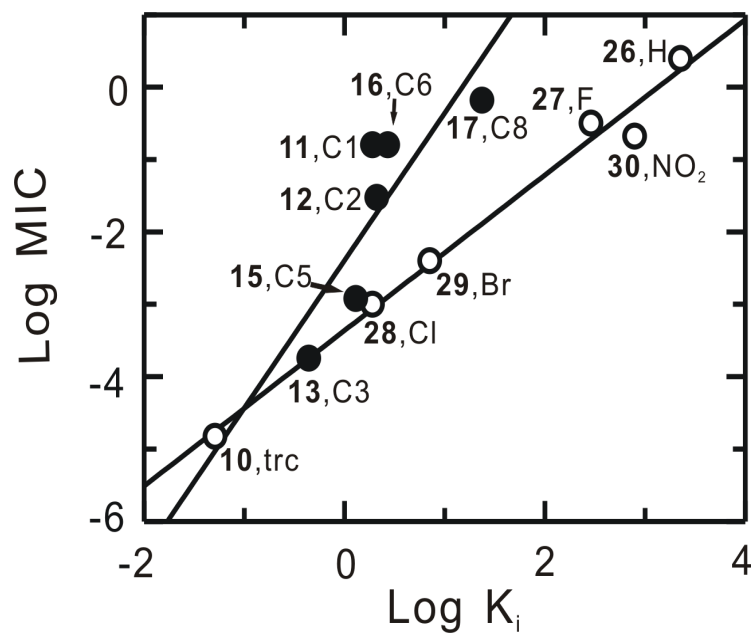
Figure 2.12: Linear Correlation between the logMIC and logK$_i$ Values for Triclosan and the Diaryl Ether Inhibitors. Linear fits are shown for two groups of compounds: **10**,**26**-**30** and **11**-**13**,**15**-**17**.

Conclusions

We successfully cloned, expressed and purified ftuFabI and demonstrated it is an NADH-dependent enoyl-ACP reductase with a sequential bi bi catalytic mechanism. Rational drug design based on the lead compound triclosan identified a group of diaryl ether compounds that are subnanomolar inhibitors of ftuFabI with MIC values as low as 0.00018 µg/ml. Finally $logK_i$ values and logMIC values are linearly correlated, which suggests that ftuFabI is the primary cellular target of these compounds.

References:

1.   McCoy, G. W., and Chapin, C. W. (1912) Further observation on a plague-like disease of rodents with a preliminary note on the causative agent, Bacterium tularensis., *J. Infect. Dis. 25*, 61-72.

2.   Hopla, C. E. (1974) The ecology of tularemia, *Adv. Vet. Sci. Comp. Med. 18*, 25-53.

3.   Oyston, P. C., Sjostedt, A., and Titball, R. W. (2004) Tularaemia: bioterrorism defence renews interest in *Francisella tularensis*, *Nat. Rev. 2*, 967-978.

4.   Ellis, J., Oyston, P. C., Green, M., and Titball, R. W. (2002) Tularemia, *Clin. Microbiol. Rev. 15*, 631-646.

5.   Dennis, D. T., Inglesby, T. V., Henderson, D. A., Bartlett, J. G., Ascher, M. S., Eitzen, E., Fine, A. D., Friedlander, A. M., Hauer, J., Layton, M., Lillibridge, S. R., McDade, J. E., Osterholm, M. T., O'Toole, T., Parker, G., Perl, T. M., Russell, P. K., and Tonat, K. (2001) Tularemia as a biological weapon: medical and public health management, *JAMA 285*, 2763-2773.

6.   Harris, S. (1992) Japanese biological warfare research on humans: a case study of microbiology and ethics, *Annu. N. Y. Acad. Sci. 666*, 21-52.

7.   Christopher, G. W., Cieslak, T. J., Pavlin, J. A., and Eitzen, E. M., Jr. (1997) Biological warfare. A historical perspective, *JAMA 278*, 412-417.

8.   Alibek, K. (1999) The Soviet Union's anti-agricultural biological weapons, *Annu. N. Y. Acad. Sci. 894*, 18-19.

9.   Enderlin, G., Morales, L., Jacobs, R. F., and Cross, J. T. (1994) Streptomycin and alternative agents for the treatment of tularemia: review of the literature, *Clin. Infect. Dis. 19*, 42-47.

10.   Ikaheimo, I., Syrjala, H., Karhukorpi, J., Schildt, R., and Koskela, M. (2000) *In vitro* antibiotic susceptibility of *Francisella tularensis* isolated from humans and animals, *J. Antimicrob. Chemother. 46*, 287-290.

11.   Perez-Castrillon, J. L., Bachiller-Luque, P., Martin-Luquero, M., Mena-Martin, F. J., and Herreros, V. (2001) Tularemia epidemic in northwestern Spain: clinical description and therapeutic response, *Clin. Infect. Dis. 33*, 573-576.

12.   Bergler, H., Wallner, P., Ebeling, A., Leitinger, B., Fuchsbichler, S., Aschauer, H., Kollenz, G., Hogenauer, G., and Turnowsky, F. (1994) Protein EnvM is the NADH-dependent enoyl-ACP reductase (FabI) of *Escherichia coli*, *J. Biol. Chem. 269*, 5493-5496.

13.   Zhang, Y. M., White, S. W., and Rock, C. O. (2006) Inhibiting bacterial fatty

acid synthesis, *J. Biol. Chem. 281*, 17541-17544.

14. Lu, H., and Tonge, P. J. (2008) Inhibitors of FabI, an enzyme drug target in the bacterial fatty acid biosynthesis pathway, *Acc. Chem. Res. 41*, 11-20.

15. Heath, R. J., Su, N., Murphy, C. K., and Rock, C. O. (2000) The enoyl-acyl-carrier-protein reductases FabI and FabL from *Bacillus subtilis*, *J. Biol. Chem. 275*, 40128-40133.

16. Heath, R. J., and Rock, C. O. (2000) A triclosan-resistant bacterial enzyme, *Nature 406*, 145-146.

17. Massengo-Tiasse, R. P., and Cronan, J. E. (2008) *Vibrio cholerae* FabV defines a new class of enoyl-acyl carrier protein reductase, *J. Biol. Chem. 283*, 1308-1316.

18. Sliverman, R. B. (2000) The organic chemistry of enzyme-catalyzed reactions, 1st ed., Academic Press, California, 563-584.

19. Karahalios, P., Kalpaxis, D. L., Fu, H., Katz, L., Wilson, D. N., and Dinos, G. P. (2006) On the mechanism of action of 9-O-arylalkyloxime derivatives of 6-O-mycaminosyltylonolide, a new class of 16-membered macrolide antibiotics, *Mol. Pharmacol. 70*, 1271-1280.

20. Ejim, L. J., Blanchard, J. E., Koteva, K. P., Sumerfield, R., Elowe, N. H., Chechetto, J. D., Brown, E. D., Junop, M. S., and Wright, G. D. (2007)

Inhibitors of bacterial cystathionine beta-lyase: leads for new antimicrobial agents and probes of enzyme structure and function, *J. Med. Chem. 50*, 755-764.

21. Copeland, R. A. (2000) Enzymes: a practical introduction to structure, mechanism and data analysis, 2nd ed., Wiley-VCH, New York, 318-350.

22. Tummino, P. J., and Copeland, R. A. (2008) Residence time of receptor-ligand complexes and its effect on biological function, *Biochemistry 47*, 5481-5492.

23. Halford, S. E. (1971) *Escherichia coli* alkaline phosphatase. An analysis of transient kinetics, *Biochem. J. 125*, 319-327.

24. Fersht, A. (1999) Structure and mechanism in protein science, a guide to enzyme catalysis and protein folding, 1st ed., Freeman, New York, 132-168.

25. Ward, W. H., Holdgate, G. A., Rowsell, S., McLean, E. G., Pauptit, R. A., Clayton, E., Nichols, W. W., Colls, J. G., Minshull, C. A., Jude, D. A., Mistry, A., Timms, D., Camble, R., Hales, N. J., Britton, C. J., and Taylor, I. W. (1999) Kinetic and structural characteristics of the inhibition of enoyl acyl carrier protein reductase by triclosan, *Biochemistry 38*, 12514-12525.

26. Morrison, J. F. (1969) Kinetics of the reversible inhibition of

enzyme-catalysed reactions by tight-binding inhibitors, *Biochim. Biophys. Acta 185*, 269-286.

27.   Copeland, R. A. (2005) Evaluation of enzyme inhibitors in drug discovery: a guide for medicinal chemists and pharmacologists, 1st ed., John Wiley & Son, New Jersey, 178-212.

28.   Sivaraman, S., Sullivan, T. J., Johnson, F., Novichenok, P., Cui, G., Simmerling, C., and Tonge, P. J. (2004) Inhibition of the bacterial enoyl reductase FabI by triclosan: a structure-reactivity analysis of FabI inhibition by triclosan analogues, *J. Med. Chem. 47*, 509-518.

29.   Sullivan, T. J., Truglio, J. J., Boyne, M. E., Novichenok, P., Zhang, X., Stratton, C. F., Li, H. J., Kaur, T., Amin, A., Johnson, F., Slayden, R. A., Kisker, C., and Tonge, P. J. (2006) High affinity InhA inhibitors with activity against drug-resistant strains of *Mycobacterium tuberculosis*, *ACS Chem. Biol. 1*, 43-53.

30.   Hofstein, H. A., Feng, Y., Anderson, V. E., and Tonge, P. J. (1999) Role of glutamate 144 and glutamate 164 in the catalytic mechanism of enoyl-CoA hydratase, *Biochemistry 38*, 9508-9516.

31.   Parikh, S., Moynihan, D. P., Xiao, G., and Tonge, P. J. (1999) Roles of tyrosine 158 and lysine 165 in the catalytic mechanism of InhA, the

enoyl-ACP reductase from *Mycobacterium tuberculosis*, *Biochemistry 38*, 13623-13634.

32.   Magnuson, K., Jackowski, S., Rock, C. O., and Cronan, J. E., Jr. (1993) Regulation of fatty acid biosynthesis in *Escherichia coli*, *Microbiol. Rev. 57*, 522-542.

33.   Baldwin, J. E., Bird, J. W., Field, R. A., O'Callaghan, N. M., Schofield, C. J., and Willis, A. C. (1991) Isolation and partial characterisation of ACV synthetase from *Cephalosporium acremonium* and *Streptomyces clavuligerus*. Evidence for the presence of phosphopantothenate in ACV synthetase, *J. Antibiol. 44*, 241-248.

34.   Summers, R. G., Ali, A., Shen, B., Wessel, W. A., and Hutchinson, C. R. (1995) Malonyl-coenzyme A:acyl carrier protein acyltransferase of *Streptomyces glaucescens*: a possible link between fatty acid and polyketide biosynthesis, *Biochemistry 34*, 9389-9402.

35.   Lawson, D. M., Derewenda, U., Serre, L., Ferri, S., Szittner, R., Wei, Y., Meighen, E. A., and Derewenda, Z. S. (1994) Structure of a myristoyl-ACP-specific thioesterase from *Vibrio harveyi*, *Biochemistry 33*, 9382-9388.

36.   Dotson, G. D., Kaltashov, I. A., Cotter, R. J., and Raetz, C. R. (1998)

Expression cloning of a *Pseudomonas* gene encoding a hydroxydecanoyl-acyl carrier protein-dependent UDP-GlcNAc acyltransferase, *J. Bacteriol. 180*, 330-337.

37.   Lambalot, R. H., and Walsh, C. T. (1995) Cloning, overproduction, and characterization of the *Escherichia coli* holo-acyl carrier protein synthase, *J. Biol. Chem. 270*, 24658-24661.

38.   Haas, J. A., Frederick, M. A., and Fox, B. G. (2000) Chemical and posttranslational modification of *Escherichia coli* acyl carrier protein for preparation of dansyl-acyl carrier proteins, *Protein Expr. Purif. 20*, 274-284.

39.   Schaeffer, M. L., Agnihotri, G., Volker, C., Kallender, H., Brennan, P. J., and Lonsdale, J. T. (2001) Purification and biochemical characterization of the *Mycobacterium tuberculosis* beta-ketoacyl-acyl carrier protein synthases KasA and KasB, *J. Biol. Chem. 276*, 47029-47037.

40.   Broadwater, J. A., and Fox, B. G. (1999) Spinach holo-acyl carrier protein: overproduction and phosphopantetheinylation in *Escherichia coli* BL21(DE3), *in vitro* acylation, and enzymatic desaturation of histidine-tagged isoform I, *Protein Expr. Purif.15*, 314-326.

41.   Shimakata, T., and Stumpf, P. K. (1982) The procaryotic nature of the fatty acid synthetase of developing Carthamus tinctorius L. (Safflower) seeds,

Arch. Biochem. Biophys. 217, 144-154.

42.   Kapoor, M., Dar, M. J., Surolia, A., and Surolia, N. (2001) Kinetic determinants of the interaction of enoyl-ACP reductase from *Plasmodium falciparum* with its substrates and inhibitors, *Biochem. Biophys. Res. Commun. 289*, 832-837.

43.   Quemard, A., Sacchettini, J. C., Dessen, A., Vilcheze, C., Bittman, R., Jacobs WR, J. r., and Blanchard, J. S. (1995) Enzymatic characterization of the target for isoniazid in *Mycobacterium tuberculosis*, *Biochemistry 34*, 8235-8241.

44.   Cleland, W. W. (1963) The kinetics of enzyme-catalyzed reactions with two or more substrates or products. I. Nomenclature and rate equations, *Biochim. Biophys. Acta 67*, 104-137.

45.   Cleland, W. W. (1963) The kinetics of enzyme-catalyzed reactions with two or more substrates or products. II. Inhibition: nomenclature and theory, *Biochim. Biophys. Acta 67*, 173-187.

46.   Sivaraman, S., Zwahlen, J., Bell, A. F., Hedstrom, L., and Tonge, P. J. (2003) Structure-activity studies of the inhibition of FabI, the enoyl reductase from *Escherichia coli*, by triclosan: kinetic analysis of mutant FabIs, *Biochemistry 42*, 4406-4413.

47. Xu, H., Sullivan, T. J., Sekiguchi, J., Kirikae, T., Ojima, I., Stratton, C. F., Mao, W., Rock, F. L., Alley, M. R., Johnson, F., Walker, S. G., and Tonge, P. J. (2008) Mechanism and inhibition of saFabI, the enoyl reductase from *Staphylococcus aureus*, *Biochemistry 47*, 4228-4236.

48. Chhibber, M., Kumar, G., Parasuraman, P., Ramya, T. N., Surolia, N., and Surolia, A. (2006) Novel diphenyl ethers: design, docking studies, synthesis and inhibition of enoyl ACP reductase of *Plasmodium falciparum* and *Escherichia coli*, *Bioorg. Med. Chem. 14*, 8086-8098.

49. Rafi, S. B., Cui, G., Song, K., Cheng, X., Tonge, P. J., and Simmerling, C. (2006) Insight through molecular mechanics Poisson-Boltzmann surface area calculations into the binding affinity of triclosan and three analogues for FabI, the *E. coli* enoyl reductase, *J. Med. Chem. 49*, 4574-4580.

Chapter III[*]. Molecular Basis of the Slow Binding Inhibition of ftuFabI

Introduction

Slow Binding Inhibition and Residence Time. At the molecular level, drug actions require that the drug is physically bound to its physiological target. The longer the drug interacts with its target, the longer the drug effect is maintained, both *in vitro* and *in vivo*. The duration of drug-target interactions is controlled by kinetic constants, the association rate constant (k_{on}) or more critically the dissociation rate constant (k_{off}). Typically, residence time ($t_R = 1/k_{off}$), which is the time required for ~63% dissociation of the remaining drug-target complex, is used to measure the duration of drug-target interactions (*1*). Based on the time scale, drugs can be divided into two types, transient binding drugs and slow binding drugs. For transient binding drugs, the drug-target interaction occurs in a simple bimolecular mechanism (**Figure 3.1,** mechanism **A**) with large k_{on} and k_{off} values. In this scenario commonly observed k_{on} values are diffusion controlled on the

[*] Part of work in this chapter has been described in a previous publication (*Lu* et al *ACS Chem. Biol.* **2009**, *4*, 221-31.)

order of $\sim 10^8$-10^9 $M^{-1}s^{-1}$ and k_{off} values are typically greater than 0.1 s^{-1} depending

on the dissociation constant (K_d) (*2*). It is difficult to measure residence time of

transient binding drugs under experimental conditions since it ranges from

milliseconds to several seconds. However, as the k_{off} value decreases, the time

needed to reach the steady state increases and the equilibrium between free drug,

vacant target and the drug-target complex breaks down. With a sufficiently small

k_{off} value, the residence time of drug can be as long as several days (*3*).

$$\textbf{A.} \quad T \; + \; D \; \underset{k_{off}}{\overset{k_{on}}{\rightleftharpoons}} \; TD$$

$$\textbf{B.} \quad T + D \; \underset{k_2}{\overset{k_1}{\rightleftharpoons}} \; TD \; \underset{k_4}{\overset{k_3}{\rightleftharpoons}} \; T^*D$$
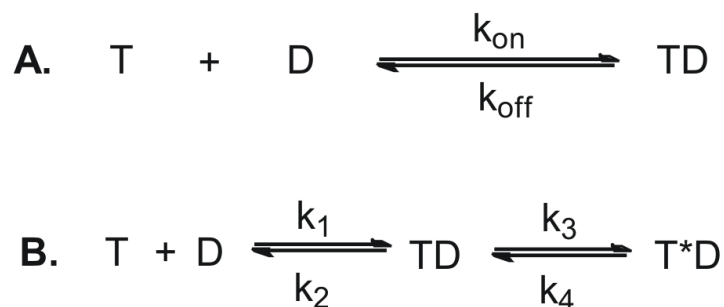
Figure 3.1: Kinetic Schemes for Drug-Target Interaction. T and D refer to target and drug respectively. **A**) A simple one-step mechanism for transient drug binding termed mechanism **A** in the text. k_{on} and k_{off} are both very large. **B**) Induced fit mechanism for slow binding drugs termed mechanism **B** in the text. This is the same mechanism as mechanism **B** in **Figure 2.3**. k_1 and k_2 are the rate constants for the initial complex (TD) formation. k_3 and k_4 are the rate constants for the isomerization step to produce the final complex (T*D). k_1 and k_2 are large, while k_3 and k_4 are small.

Three different mechanisms can account for slow binding inhibition. These include a one step mechanism, induced fit mechanism, and conformational selection mechanism (see **Slow and Tight Binding Inhibitor**, **Chapter II**). Most drugs exhibit time dependent and high affinity inhibition via the induced fit mechanism (**Figure 3.1,** mechanism **B**), such as the HIV protease inhibitor darunavir and the new drug saxagliptin to treat type II diabetes (*4-6*) and thus we will focus our discussion on this mechanism in this chapter. Mechanism **B** involves two steps, beginning with the rapid formation of a drug-target complex with suboptimal interactions between the drug and target. Subsequently, the target will undergo slow isomerization to a new conformation that is more complementary to the drug molecule. The formation and breakdown of the initial complex is normally very fast, while the isomerization is slow and determines the overall duration of drug-target interaction. Because the final complex is thermodynamically more stable than the initial complex, this type of inhibition usually results in high affinity drug binding. Generally, the reverse isomerization is the rate determining step ($k_4 > k_2$ and k_3). Thus, residence time is approximately equal to the reciprocal of rate constant k_4.

Experimentally, there are two different approaches to measure the residence time of slow binding drugs via mechanism **B**. Progress curve analysis is most

commonly used. In this method, time dependent binding of the drug to its target is monitored as a function of time, usually via signals from product formation or changes in fluorescence (*7-8*). Analysis of each progress curve will give a pseudo-first-order rate constant (k_{obs}) which is drug concentration dependent. A plot of k_{obs} versus drug concentration can be used to determine the rate constants of the isomerization step (k_3 and k_4), and the residence time can be simply calculated from k_4 (*9*). Another way of determining residence time involves directly measuring the rate constant of drug-target dissociation. Drug and target are first preincubated at relatively high concentrations for a sufficient period of time such that all target molecules form the final drug-target complex. Excess drug is then removed, and the drug-target complex is diluted to ensure that the concentration of free drug is low. Normally, monitoring the concentration of free radiolabelled drug in solution or the fluorescence signal of the target molecule as a function of time will provide the k_{off} value by fitting into a single decay equation (*7-8*).

Residence Time and Its Correlation with In Vivo Efficacy. Traditionally, initial efforts at the early stages of drug discovery, which includes high throughput screening and lead optimization, focus solely on the optimization of the thermodynamic equilibrium constant (IC_{50} or K_d). The equilibrium constant of

drugs measured in closed systems can sometimes relate to the *in vivo* efficacy. However, since these *in vitro* systems oversimplify the *in vivo* biology by ignoring the fluctuations in drug concentration with time and the duration of drug-target interactions, *in vivo* results often clash with predictions based on *in vitro* measurements. Residence time is an intrinsic property of drugs, which is solely controlled by the kinetic constants and independent of drug concentration. It, thus, provides a critical metric to predict the efficacy of drugs in an open *in vivo* system.

The first paper discussing the use of drug-target time residence time as a tool for drug discovery was published in 1986 (*10*). At the beginning of this century, the importance of residence time in determining the therapeutic window and target selectivity of drugs was emphasized (*3-4, 11-13*). Drugs with long residence time are prevalent in the market. Of 85 New Molecular Entities (NMEs) approved by the FDA between 2001 and 2004 with known targets, 26% show slow binding inhibition (*14*). A survey of 50 drugs demonstrates that drugs with longer residence times have better biological efficacies (*4*). Clearly, there is a strong and direct correlation between residence time and *in vivo* efficacy.

Slow Binding Inhibition and Loop Ordering. Kinetic methods are well developed to characterize the different types of slow binding inhibition (*9, 15*). However the

structural basis for slow binding inhibition remains a mystery. Triclosan inhibition of the FabI enoyl-ACP reductase provides a good model to explore the structural mechanism of slow binding inhibition. Kinetic studies have shown that triclosan and its derivatives are slow, tight binding inhibitors of FabIs from many organisms (*16-20*). Comparison of X-ray crystal structures before and after inhibitor binding reveals that the overall protein structures remain the same except for a "substrate recognition" loop that becomes ordered upon inhibitor binding (*21-22*). In our inhibition studies of ftuFabI, we found that this loop is disordered in the enzyme-NAD$^+$ binary complex. Upon binding of a slow binding inhibitor 5-hexyl-2-phenoxyphenol (**16**) to the enzyme, the loop region forms a helical structure that covers the active site of ftuFabI. Similarly, when a transient binding inhibitor (**Figure 3.2**, **15**) is bound to InhA, the loop region remains disordered. Upon binding of the slow binding inhibitor, PT70 (**34**), the loop region of InhA will adopt an α-helical conformation (**Figure 3.2**) (*23-24*). Hence we have proposed that loop ordering accounts for the isomerization step that occurs in the induced fit mechanism of slow binding inhibition for the FabI enzymes (**Figure 3.1, mechanism B**). However, to date there is no direct evidence showing that the loop ordering is coupled with slow binding inhibition of FabIs. We want to monitor the loop motion using spectroscopic methods to investigate the molecular basis of
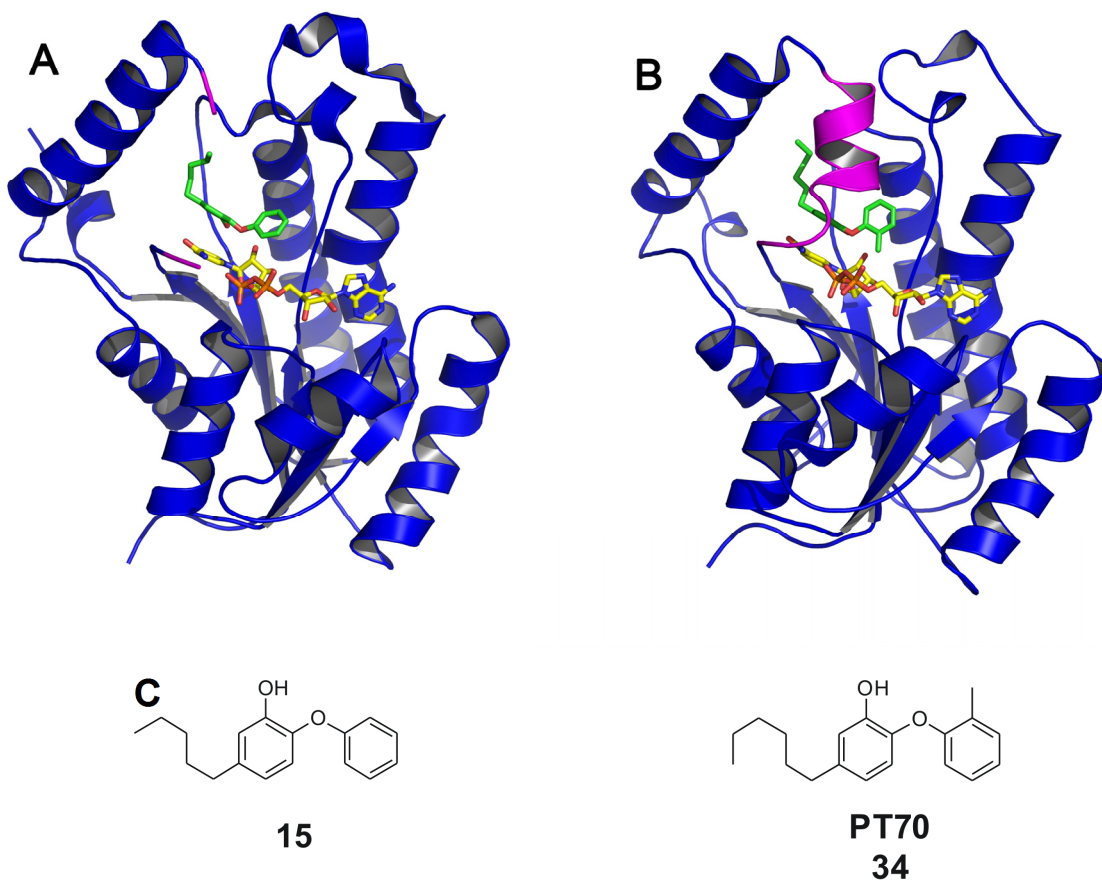
Figure 3.2: Loop Ordering of InhA upon Different Inhibitor Binding. A) Compound **15** (green), a transient binding inhibitor, binds to InhA (blue) with NAD^+ (yellow). The loop ends are marked in magenta. **B)** The structure shows the ternary complex of InhA (blue) with bound NAD^+ (yellow) and a slow binding inhibitor (PT70, **50**) with an ordered helical loop (magenta). Carbon atoms of the inhibitor are depicted in green. **C)** Structure of the two Inhibitors bound to InhA.

slow binding inhibition of the FabI enzymes. This information could be used to optimize residence times of current inhibitors for the development of next generation antibiotics.

Project Goals. In this chapter, the correlation between residence time and *in vivo* efficacy for our ftuFabI inhibitors will be explored. We hypothesize that loop ordering of the enoyl-ACP reductases is coupled with slow binding inhibition. Consequently, we want to modify the loop of enoyl-ACP reductase so that the conformational changes at this region can be monitored. InhA has an extended loop (15 residues) compared to other FabI enzymes (5 to 6 residues), which means less perturbation of native structure should be expected after modification. In addition, our group also has a long term interest in developing slow, tight binding inhibitors of InhA to combat *M. tuberculosis*. Consequently InhA is chosen as the model system to investigate the relationship between slow binding inhibition and loop ordering. The loop of InhA will be modified with different fluorophores and fluorescence spectroscopy will be using to probe the conformational changes of the loop.

Materials and Methods

Materials. His-bind Ni^{2+}-NTA resin and pET 23b vector were purchased from Novagen while a QuickChange site-directed mutagenesis kit was obtained from Stratagene. Triclosan was a gift from Ciba and all the other inhibitors were available from previous work (*23, 25-26*). ftuFabI and crotonyl-CoA (Cr-CoA) were prepared as described in **Chapter II**. 7-Diethylamino-3-((((2-maleimidyl) ethyl)amino)carbonyl)coumarin (MDCC) was purchased from Invitrogen and *p*-cyanophenylalanine was bought from PepTech. All other chemical reagents were obtained from Sigma-Aldrich. DH10B cells, pDule vector and pBAD vector were a gift from Prof. Ryan Mehl at Franklin and Marshall College.

Progress Curve Analysis. Progress curves were used to determine the residence time of drugs tested in the animal model of tularemia. The experiments were performed at 25 °C in 30 mM PIPES buffer pH 7.9 containing 1.0 mM EDTA and 150 mM NaCl. In order to take into account the change in NAD^+ concentration during the assay, reaction mixtures contained 200 μM NAD^+ in addition to ftuFabI (10 nM), Cr-CoA (160 μM), NADH (250 μM), inhibitor and DMSO (1%, V/V). Reactions were allowed to proceed until the progress curve became linear,

indicating that the steady-state velocity had been reached. Low enzyme concentrations were used to ensure only a small fraction of Cr-CoA and NADH was consumed during the course of measurement so that the progress curves were essentially linear in the absence of inhibitor. The resulting progress curves were fit to the integrated rate eqn **12**

$$A_t = A_0 - V_s*t - (v_i - v_s)*(1-\gamma)*\ln\{[1-\gamma*\exp(-k_{obs}*t)]/(1-\gamma)\}/(k_{obs}*\gamma) \tag{12}$$

where $\gamma = [E]*(1-v_s/v_i)^2/[I]$, v_i and v_s are the initial velocity and steady-state velocity; [E] and [I] are the concentration of ftuFabI and inhibitor respectively and k_{obs} is the observed rate constant. Values for v_i, v_s and k_{obs} were extracted by fitting the data to eqn **12** at each inhibitor concentration. Subsequently, K_i^{app} was calculated by fitting the values for k_{obs} to the equation for a two-step inhibition mechanism (eqn **13**) in which the initial rapid binding of the drug to the target is followed by a second slow step resulting in the final drug-target complex (**Figure 3.1,** mechanism **B**).

$$k_{obs} = k_4 + k_3*[I]/(K_i^{app} + [I]) \tag{13}$$

where $K_i^{app} = k_2/k_1$

Expression and Purification of Wild Type InhA and InhA Mutants. The wild type (wt) *InhA* gene inserted in the pET 15b vector was available from previous work

(*27*). Mutations were carried out using the QuikChange mutagenesis kit from Stratagene with the primers listed in **Table 3.1**. After purification from XL1Blue cells (Stratagene) using a DNA purification and gel extraction kit (Qiagen Inc) the correct sequence of InhA mutants C243S and S200C/C253S were confirmed using ABI DNA sequencing.

Table 3.1: Primers Used for Cloning and Mutagenesis

Name	Sequence [a]
C243S forward	5'CAAGACGGTG<u>TCC</u>GCGCTGCTGTCTGAC3'
C243S reversed	5'GTCAGACAGCAGCGC<u>GGA</u>CACCGTCTT3'
S200C/C243S forward	5'GACGCTGGCGA<u>TGT</u>GTGCGATCGTC3'
S200C/C243S reversed	5'GACGATCGCAC<u>ACA</u>TCGCCAGCGTC3'
wt InhA (pBAD) forward	5'CATG<u>CCATGG</u>GCATGACAGGACTCTGGACGGC3'
wt InhA (pBAD) reversed	5'CCC<u>AAGCTT</u>GGAGCAATTGGGTGTGCGCGCC 3'
pCN-InhA (pBAD) forward	5'CTGGCGATGAGT<u>TAG</u>ATCGTCGGCGGTG3'
pCN-InhA (pBAD) reversed	5'CACCGCCGACGAT<u>CTA</u>ACTCATCGCCAG3'

[a] Restriction sites and mutated sites are shown in underline.

Protein expression of wt InhA and the InhA mutants was performed using *E. coli* BL21(DE3)pLysS cells. After transformation, a single colony was used to inoculate 10 ml of Luria Broth (LB) media containing 0.2 mg/ml ampicillin in a 50 ml falcon tube, which was then incubated overnight at 37 °C in a floor shaker. The overnight culture was then used to inoculate 1 l of LB media containing ampicillin (0.2 mg/ml) which was incubated on an orbital shaker at 37 °C until the optical density at 600 nm (O.D. 600) increased to around 1.0. Protein expression was induced by adding 1 mM isopropyl-1-thio-β-D-galactopyranoside (IPTG) and the culture was then shaken at 25 °C for 16 h. Cells were harvested by centrifugation at 5,000 rpm for 25 min at 4 ºC. The cell paste was then resuspended in 30 ml of His-binding buffer (5 mM imidazole, 0.5 M NaCl, 20 mM Tris HCl, pH 7.9) and lysed by sonication. Cell debris was removed by centrifugation at 33,000 rpm for 60 min at 4 ºC. The resulting supernatant was loaded onto a His-bind column (1.5 cm x 15 cm) containing 4 ml of His-bind resin (Novagen) that had been charged with 9 ml of charge buffer (Ni^{2+}). The column was washed with 60 ml of His-binding buffer and 30 ml of wash buffer (60 mM imidazole, 0.5 M NaCl, 20 mM Tris HCl, pH 7.9). Subsequently, the protein was eluted using a gradient of 20 ml binding buffer and 40 ml elute buffer (1 M imidazole, 0.5 M NaCl, 20 mM Tris HCl, pH 7.9). Fractions containing InhA were collected and imidazole was removed

using a Sephadex G-25 column (1.5 cm x 55 cm) using PIPES buffer (30 mM

PIPES, 150 mM NaCl, 1.0 mM EDTA pH 8.0) as the eluent. The purity of the

protein was shown to be >95% by 12% SDS-PAGE, which gave an apparent

molecular weight of ~30 kDa. The concentration of the protein was determined by

measuring the A_{280} and using an extinction coefficient (ε_{280}) of 30,440 $M^{-1}cm^{-1}$

calculated from the primary sequence. The enzyme was stored at -80 °C after

flash freezing with liquid N_2.

7-Diethylamino-3-((((2-maleimidyl)ethyl)amino)carbonyl)coumarin (MDCC)

Labeling of wt InhA. Purified wt InhA protein was transferred into 1 ml of Tris-HCl

buffer (pH = 7.0) with a final concentration of 100 µM. A 10-fold molar excess of

tris(2-carboxyethyl)phosphine (TCEP) was added to the protein solution followed

with an addition of 100 µl of MDCC solution in DMSO (7 mM). The reaction

mixture was stirred at room temperature for 2 h and the labeled protein was then

purified by chromatography on a Sephadex G-25 column (0.5 cm x 15 cm) using

the Tris-HCl buffer.

Cloning, Overexpression and Purification of wt InhA and pCN-InhA Mutant in

pBAD Vector. The *InhA* gene in pET 15b vector (Novagen) was amplified using

the primers listed in **Table 3.1** and inserted into the Invitrogen pBAD/Myc-His C

vector using the 5' NcoI and 3' HindIII restriction sites (underlined) so that a His

tag was encoded at the C-terminus of the coding sequence. After purification from

XL1Blue cells (Stratagene) using a DNA purification and gel extraction kit (Qiagen

Inc) the correct sequence of the insert was confirmed using ABI DNA sequencing.

Mutation for *pCN*-InhA mutant was performed using QuikChange mutagenesis kit

from Stratagene at residue A201 with the primers listed in **Table 3.1.** The plasmid

sequence of the mutant was confirmed with ABI sequencing method.

The protein expression protocol for *pCN*-InhA mutant using the auto-induction

method is described in a previous paper (*28*). Briefly, the pDule vector containing

the tRNA and tRNA synthase for *p*-cyanophenylalanine (*pCN*Phe) incorporation

and appropriate pBAD vector was cotransformed into DH10B cells. A fresh colony

was selected and grown in 10 ml of Luria Broth (LB) media containing 200 µg/ml

ampicillin and 25 µg/ml tetracycline in a 50 ml falcon tube. A 4 l flask with 500 ml

auto-induction media was prewarmed at 37 °C with shaking at 250 rpm.

Antibiotics, ampicillin (200 µg/ml) and tetracycline (25 µg/ml) was added to the

flask followed by addition of 2.5 ml saturated cell culture. After 30 min, *pCN*Phe

dissolved in 4 ml of 0.16 M NaOH solution was added to the cell culture to a final

concentration of 1 mM and incubated at 37 °C with 250 rpm shaking for additional

97

26 h until the optical density at 600 nm (O.D. 600) increased to 3.5-4.0. Cells were harvested by centrifugation at 37 °C at 5,000 rpm for 30 min. Protein purification followed the same procedure described above for the InhA mutants. The purity of the protein was also determined by 12% SDS-PAGE and shown to be >95% pure. The concentration of the protein was determined by measuring the A_{280} and using an extinction coefficient (ε_{280}) of 31,720 $M^{-1}cm^{-1}$ calculated from the primary sequence. The purified protein was also characterized with LC-MS giving a molecular weight of 31,637 Da which is consistent with the calculated value (31,640 Da).

Protein expression, purification and characterization of wt InhA in pBAD vector was performed in the same way as that for *pCN*-InhA mutant except that no *pCN*Phe solution was added. The molecular weight of InhA produced in this way was 31,536 Da (calculated value 31,539 Da).

Steady-state Kinetic Analysis. Steady-state kinetic parameters were determined at 25 °C in 30 mM PIPES buffer pH 7.9 containing 1.0 mM EDTA and 150 mM NaCl. Initial velocities were determined using a Cary 300 Bio (Varian) spectrophotometer to monitor the oxidation of NADH to NAD$^+$ at 340 nm (ε = 6,300 $M^{-1}cm^{-1}$). K_m and k_{cat} values of wt InhA and *pCN*-InhA expressed using the

pBAD vector using DD-CoA as the substrate were determined by varying the concentration of DD-CoA at a fixed concentration of NADH (250 µM). Data sets were then fit to the Michaelis-Menten equation (eqn **5**) using GraFit 4.0 (Erithacus).

$$v = V_{max}[S] / (K_m + [S])$$ (**5**)

where [S] is the substrate and K_m is the Michaelis-Menten constant of the substrate. v is the initial velocity measured and V_{max} is the maximal velocity.

Fluorescence Measurements. Fluorescence spectra of wt InhA and *pCN*-InhA were obtained from 1 ml of enzyme (2 µM) solution containing NAD^+ (120 µM), sodium phosphate (50 mM) and 100 mM NaCl at pH 7.0. The excitation wavelength was fixed at 240 nm (2 nm slit width), and emission spectra were recorded from 250 nm to 400 nm using a Spex FL3-21 Fluorolog-3 spectrofluorimeter. All measurements were carried out at 20 ^{o}C

Results and Discussion

Discrepancies between In Vitro Activity and In Vivo Efficacy. In order to evaluate *in vivo* efficacy of selected compounds against *F. tularensis*, a rapid animal model of tularemia infection was used in collaboration with Prof. Richard Slayden at Colorado State University. Animals under this model are treated for 5 consecutive days, starting from the day of infection, and then monitored for death for an additional 5 days. In general, our experiments showed that all treated animals survived longer than untreated control animals indicating that the diaryl ethers have antibacterial activity and are able to reduce the bacterial load. All selected compounds (**Figure 3.3A**) demonstrated efficacy, with longer median survival values in comparison to untreated control animals whose mean time to death value is 5.2 days (**Figure 3.3B** and **Table 3.2**). While all the other compounds reduced bacterial load and delayed animal death, compound **16** demonstrated greatest efficacy. Importantly, **16** prevented the onset of disease and death of infected animals to the end of the study period of 10 days. In addition, although the median survival values of **10** and **13** are similar, 39% of the animals survived to day 10 when treated with **13** while only 22% survived when **10** was used.
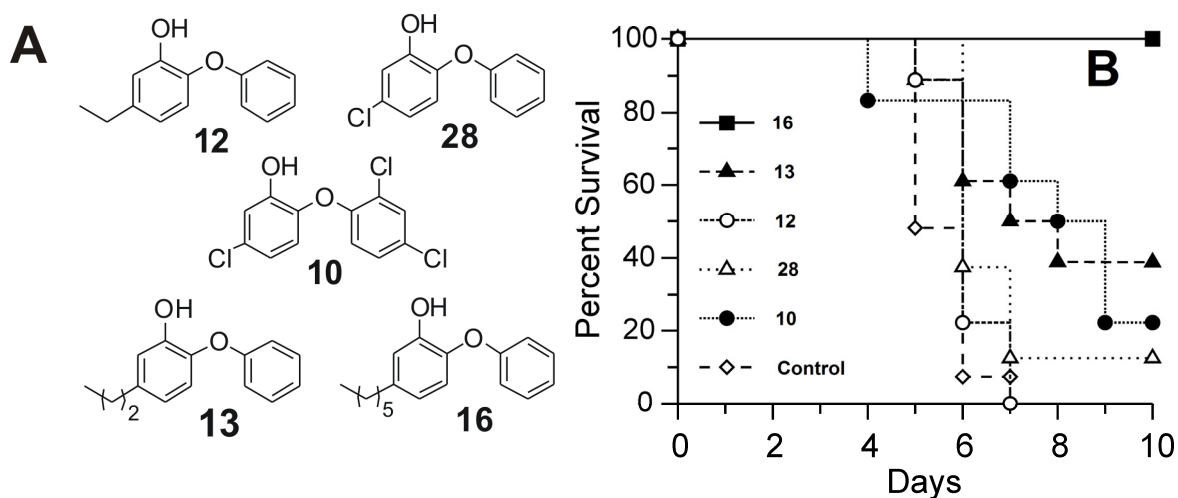
Figure 3.3: Structure of Selected Diaryl Ethers Tested in Animal Model and Survival Plots for Compounds 10, 12, 13, 16 and 28. A) Structure of selected diaryl ethers. **B)** Survival plots for mice infected with *F. tularensis* Schu4.

As mentioned in **Chapter II**, a linear correlation between $logK_i$ and logMIC was observed suggesting that ftuFabI is the target of our compounds in the cell. However, these *in vitro* data give a very poor prediction of the *in vivo* efficacy. For instance, the best *in vitro* compound triclosan only has moderate *in vivo* antibacterial activity, giving a survival percentage of 22%, while compound **16**, which has the highest K_i and MIC values in this series of compounds, can completely rescue mice from death of tularemia infection. Thus, *in vitro* thermodynamic parameters can be misleading when used to predict *in vivo* efficacy.

Table 3.2: Rate Constants for ftuFabI Inhibition as well as *In Vitro* and *In Vivo* Antibacterial Activity of Selected Diaryl Ethers.

Inhibitor	k_4 (min^{-1})	t_R (min)[a]	K_i (nM)[b]	MIC (µg/ml)	Median Survival (Day)	Percent Survival[c]
10	0.025 ± 0.003	40 ± 3	0.051 ± 0.003	0.000015 ± 0	7.8	22
28	0.033 ± 0.002	30 ± 2	1.9±0.1	0.001±0.001	7	11
12	0.048±0.001	21±1	2.1±0.1	0.03 ± 0.001	6.1	0
13	0.017 ± 0.002	59 ± 2	0.44 ± 0.02	0.00018 ± 0.00014	7.8	39
16	0.007 ± 0.002	143 ± 14	2.7 ± 0.1	0.16 ± 0.06	*nd*[d]	100
Control	*na*[e]	*na*	*na*	*na*	5.2	0

[a]Residence time (t_R)= $1/k_{off}$ where k_{off} = $k_2 k_4/(k_2+k_3+k_4)$. In the induced fit mechanism, $k_2 >> k_3$ and k_4, hence $k_{off} \approx k_4$ (*11*).

[b]K_i is the K1 values taken from **Table 2.3** (**Chapter II**).

[c]%survival is percent of animals that survived to day 10.

[d]Not defined, median survival is undefined for **16** since no animals died during the study.

[e]na, not applicable.

Using Residence Time to Predict In Vivo Efficacy. In order to provide further insight into the *in vivo* activity of the compounds, we used progress curve analysis to evaluate the rate constants for formation and breakdown of the final T*D complex (**Figure 3.1,** mechanism **B**) (*9, 15*). Based on the preincubation experiments (**Chapter II**), we already knew that the potency of the slow binding inhibitors increases as the concentration of NAD^+ increases. Hence NAD^+ (200 µM) was added at the beginning of the reaction so that product formation would not affect inhibitor affinity during the reaction. The progress curves showed that the turnover velocity decreased exponentially with time, from an initial velocity v_i to a final steady-state velocity v_s (**Figure 3.4A**). Higher concentrations of inhibitor caused the steady state to be reached more quickly and to give lower values of v_s. This behavior demonstrates that the diaryl ethers are slow binding reversible inhibitors conforming to the induced fit mechanism (*29*). The k_{obs} values obtained from fitting the data to eqn **12** displayed a hyperbolic dependence on the concentration of inhibitor (**Figure 3.4B**). Subsequent nonlinear curve fitting using eqn **13,** gave pre-steady state constants (k_3, k_4, and K_1^{app}) for each inhibitor (**Table 3.2**). Based on the assumption that the rate limiting step for breakdown of the T*D complex is isomerization of TD to T*D (k_4), k_4 can be used to calculate the residence time of the inhibitor on the enzyme. This analysis provided residence
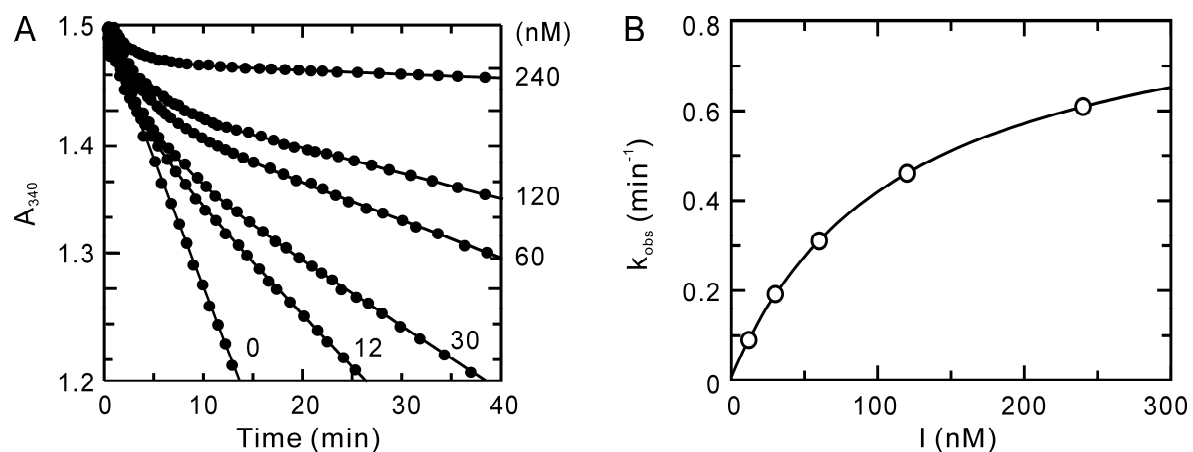
Figure 3.4: Progress Curve Analysis of the Inhibition of ftuFabI by Compound 16. **A**) Time-dependent inactivation of ftuFabI by compound **16**. The solid curves represent the best fit of the data to eqn **12** for slow binding inhibition. **B**) k_{obs} values from **A** plotted as a hyperbolic function of [I].

times of 40, 21, 59 143 and 30 min for **10**, **12**, **13, 16** and **28**, respectively (**Table 3.2**). Interestingly, although triclosan has the highest thermodynamic affinity for ftuFabI and is the most potent compound in the *in vitro* antibacterial assays, compound **16** has the longest residence time on the enzyme. This is significant since **16** is more active in the animal model of infection than triclosan, and thus there is a direct correlation between the residence times of **10** and **16** and the relative antibacterial activity of these compounds in the infected mice. Analysis of the number of animals that survived to day 10 treated with all the selected

104

compounds gave us a linear correlation between residence time and percent survival (**Figure 3.5**), indicating that the enhanced *in vivo* antibacterial activity might be a consequence of the longer residence time of this compound on the enzyme.
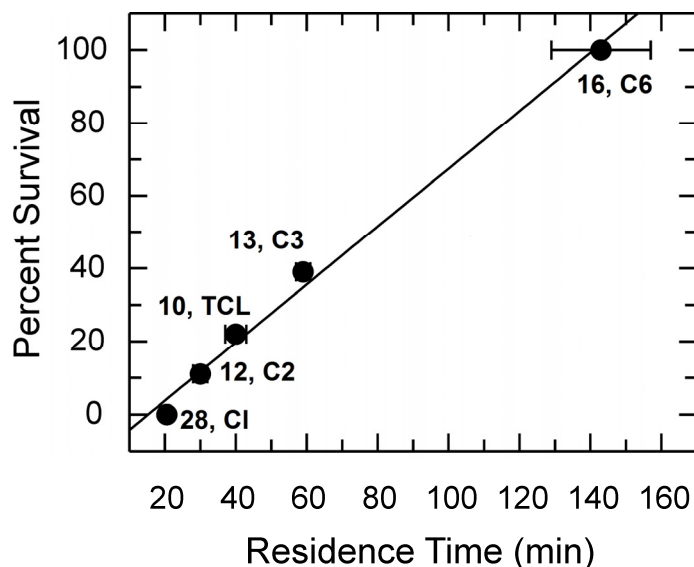
Figure 3.5: Linear Correlation between Percent Survival and Residence Time. A linear fit to the data from **Table 3.2** gave a straight line with r=0.99.

While we are aware that many factors may contribute to differences in the *in vivo* activity of structurally related drugs, and that even minor changes in structure can impact properties such as compound pharmacokinetics, the change in residence time observed between the three compounds evaluated here may have

a critical impact on target selectivity and intracellular activity. The data highlight the issues in translating *in vitro* antibacterial activities, determined at constant drug concentrations, to *in vivo* systems where the drug concentration will fluctuate between doses. These studies have broad implications for drug discovery programs that are largely driven by the measurement of inhibitor activity under equilibrium conditions, and show the benefit of determining both the kinetic and thermodynamics for the formation of drug-target complexes.

Chemical Modification of the Loop of InhA. A simple approach to monitor loop motion of FabI enzymes is to selectively modify the loop region with chemical probes. This method requires a cysteine residue, either native or artificially introduced via mutagenesis, in the loop region which can react with thio-specific dyes (*30-31*). Although, there is no cysteine in the loop, only one native cysteine is found within the whole InhA protein. In addition, InhA has an extended loop containing 16 amino acids (residues 197-211) which is significantly larger than the loop region of other FabIs (5 to 6 residues) (*26*). These characteristics make InhA an ideal model system for understanding the relationship between loop ordering and slow binding inhibition.

InhA mutant C243S plasmid was constructed to replace the native cysteine with

serine and then a second mutation was introduced at loop residue S200, giving the final double mutant S200C/C243S. Both the single and double mutants were expressed and purified, however, neither is stable in the reaction buffer. 95% of the protein in solution precipitated out within 5 min after His tag chromatography. Analysis of the wt InhA crystal structure reveals that C243 is part of a helical structure that closely packs with an adjacent α-helix (**Figure 3.6**). C243 makes van der waals interactions with several residues (I25, V28 and A29) in the neighboring helix, which may play an important role in stabilizing the helix-helix interaction. Thus, mutation at C243 may negatively affect the overall stability of protein folding.

To test if C243 can be modified by chemical dyes, wt InhA was incubated with 7-diethylamino-3-((((2-maleimidyl)ethyl)amino)carbonyl)coumarin (MDCC). After 2 h, a new peak at 430 nm, which is the characteristic absorption maximum of MDCC, appeared in the absorption spectrum suggesting that the native cysteine in wt InhA can react with MDCC. Since the native cysteine is important for the stability of wt InhA and can be modified by the fluorescence probe MDCC, selective labeling of the loop region with thio specific chemical dyes is not likely feasible.
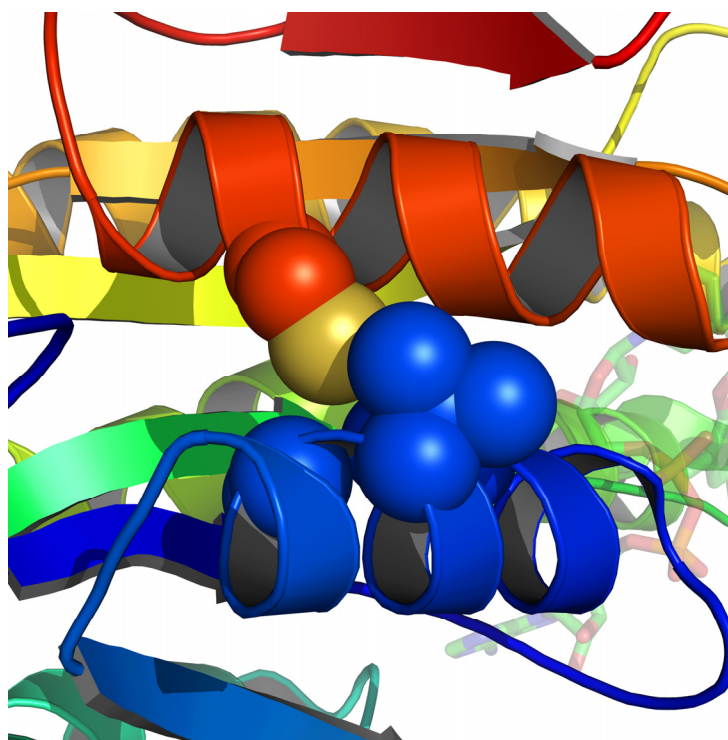
Figure 3.6: Van Der Waals Interactions between C243 and Residues in the Adjacent α-Helix. The structure shows wt InhA bound to PT70 and NAD$^+$. The α-helix containing C243 is depicted in orange, and the neighboring helix is blue. C243 and residues (I25, V28 and A29) involved in van der waals interactions are represented using a sphere model.

Incorporation of pCNPhe into the Loop of InhA. Tools to expand the genetic code with modified tRNA and tRNA synthase allows site-specific incorporation of different unnatural amino acids into target proteins (*32-35*). Despite problems with low yield of the modified protein product, this method provides a higher fidelity of selection and lower perturbation of native structures than other modification techniques (*36*). *pCN*Phe is one of the most widely used unnatural amino acids to study conformational changes of protein. The high fluorescence quantum yield and unique spectroscopic properties enable it to be used as a fluorescence resonance energy transfer (FRET) donor with tryptophan to probe protein dynamics (*37-38*).

Due to the reportedly low yield of incorporating *pCN*Phe into pET vectors(*28*), the gene encoding wt InhA was cloned into a pBAD/Myc His C vector, which is more compatible with the pDule vector containing the corresponding tRNA and tRNA synthase. An amber stop codon (TAG) was introduced to replace the coding sequence of A201, a loop residue in proximity to several tryptophan residues (**Figure 3.7**). Both wt InhA and the *pCN*-InhA mutant were expressed using an autoinduce method, which is able to increase the expression level 5-10 fold (*28*). Purified wt and mutant InhA enzymes were analyzed by LC-MS, and a mass shift of exactly 101 Da was found from wt InhA to *pCN*-InhA confirming the

109

incorporation of *pCN*Phe.

Steady-state kinetics was used to examine the perturbation of the *pCN*Phe on the catalytic activity of InhA. K_m and k_{cat} values of wt InhA and pCN-InhA for DD-CoA were measured. The $k_{cat,DD-CoA}$ and $K_{m,DD-CoA}$ values of *pCN*-InhA were determined to be 312 min^{-1} and 30.3 μM respectively and were comparable to those of wt InhA ($k_{cat,DD-CoA}$ = 651 min^{-1} and $K_{m,DD-CoA}$ = 30 μM). The modest change in kinetic parameters verified that this loop mutant did not significantly alter the kinetics of InhA.

The side chain of *pCN*Phe has absorption maxima at 233 and 280 nm. Since tryptophan has minimal absorbance at 240 nm, *pCN*Phe can be selectively excited at 240 nm in the presence of tryptophan. In addition, the fluorescence emission of *pCN*Phe overlaps with the maximal absorbance of tryptophan at around 280 nm, and thus *pCN*Phe can be used as a FRET donor with tryptophan (*39*). Monitoring the fluorescence emission of tryptophan at 340 nm allows us to readily detect the conformational changes of protein since the efficiency of resonance energy transfer is dependent on the distance between donor and receptor. The Forster distance, for this FRET pair was determined to be around 16 Å. It has also been proved that within 20 Å significant energy transfer can be achieved (*39-40*). From the crystal structure, the distances between A201 and the

three vicinal tryptophan residues were determined to be around 20 Å (**Figure 3.7**). We anticipated that significant energy transfer would occur between *pCN*Phe and these tryptophan residues.

Fluorescence spectra of wt InhA and *pCN*-InhA were taken from 250 to 400 nm with an excitation wavelength of 240 nm. The fluorescence emission spectra were almost identical, both having maximal fluorescence at 335 nm (**Figure 3.8A**). If energy transfer occurs between *pCN*Phe and tryptophan, *pCN*-InhA should have a stronger emission at 335 nm. However, the intensity of emission at this wavelength is similar for both wt InhA (purple trace) and *pCN*-InhA (green trace) (**Figure 3.8A**), indicating that the fluorescence signal at 335 nm is a result of the intrinsic absorbance of tryptophan at 240 nm rather than emission from FRET. The emission peak of *pCN*Phe at 280 nm should be observed if no energy transfer occurs between *pCN*Phe and tryptophan. Since this peak is missing in emission spectrum of *pCN*-InhA protein (**Figure 3.8A**), it is likely that the fluorescence emission of *pCN*Phe is quenched by other residues close to the loop region. To verify this hypothesis, both wt InhA and *pCN*-InhA were unfolded in 8 M urea, and the fluorescence emission spectrum of the denatured protein was recorded (**Figure 3.8B**). A peak at 290 nm, which corresponds to the fluorescence emission of *pCN*Phe, appears in the spectrum of the mutant protein but not for wt
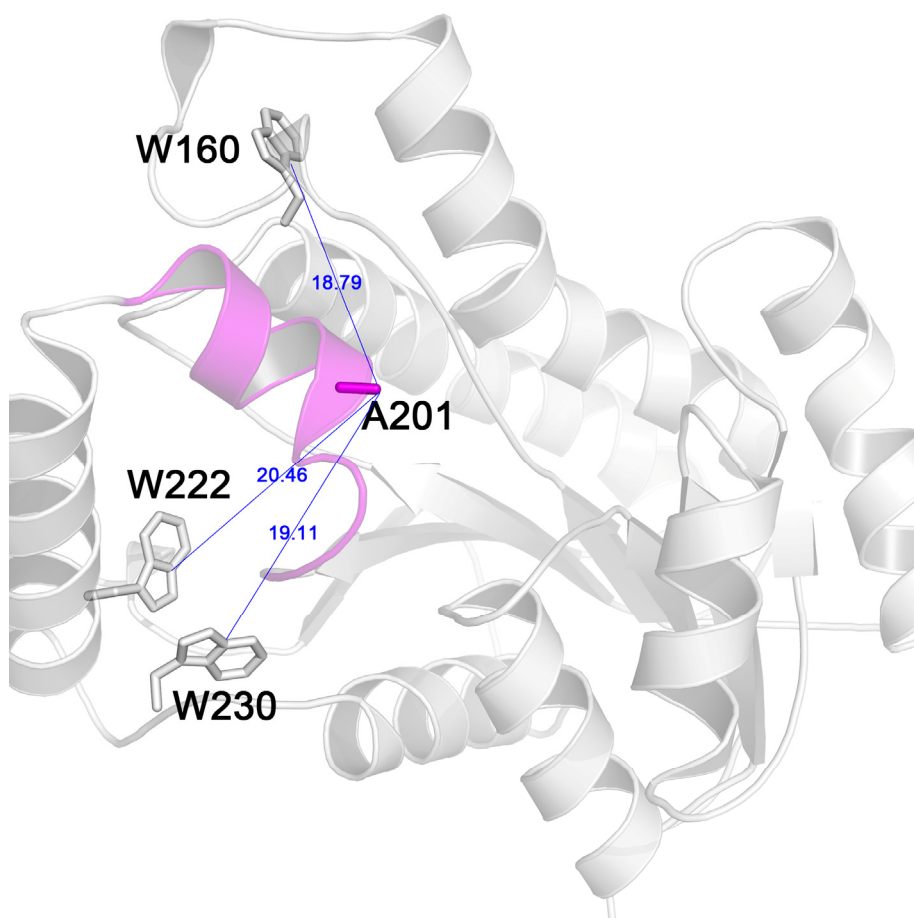
Figure 3.7: Relative Position and Distance of A201 to Neighboring Tryptophan Residues. This is the ternary complex structure of wt InhA (while), PT70 and NAD$^+$ with a ordered loop (magenta). The distance between A201 (magenta) and three neighboring tryptophan residues (W160, W222 and W230) are depicted in blue. Ligand structures have been omitted in this figure.

InhA. In addition, the fluorescence intensity of the *pCN*-InhA mutant (cyan trace) at 335 nm is much stronger than that of wt InhA (purple trace), revealing that FRET between *pCN*Phe and tryptophan probably occur in *pCN*-InhA under the urea induced denaturing condition.
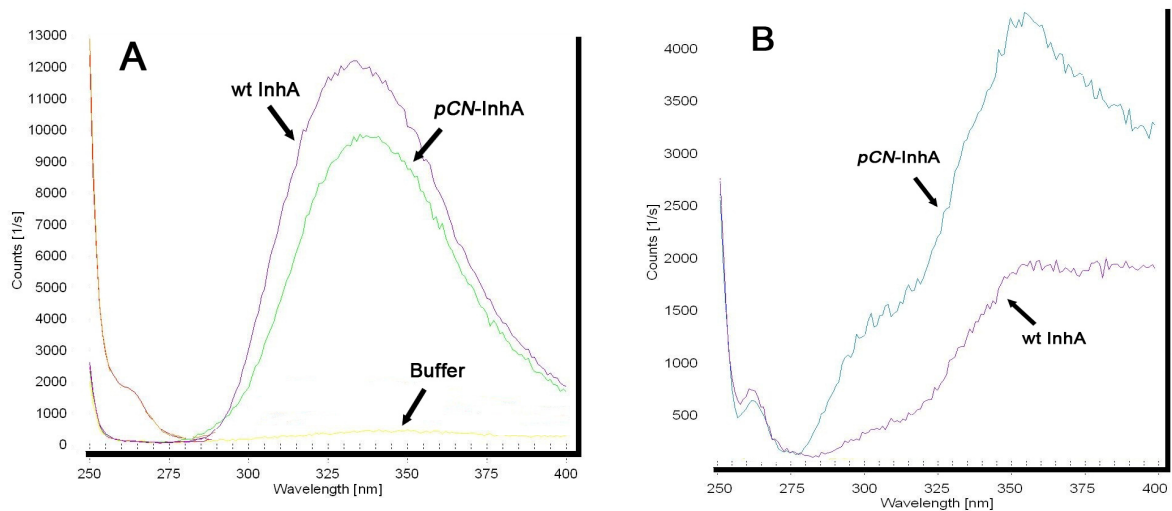
Figure 3.8: Fluorescence Emission Spectra of wt InhA and *pCN*-InhA. A) Emission spectra of proteins under native conditions: wt InhA (purple), *pCN*-InhA (green) and buffer only (yellow); **B**) Emission spectra of proteins under denaturing conditions: wt InhA (cyan) and *pCN*-InhA (purple).

In conclusion, *pCN*Phe was successfully incorporated into the loop region (A201) of InhA. However, the fluorescence signal of *pCN*Phe was quenched, which precludes FRET analysis in the native protein structure. A recent study in using *pCN*Phe and tryptophan as the FRET pair found that neighboring amino acid, such as serine, histidine, and tyrosine, can quench the fluorescence signal from *pCN*Phe (*41*). Since InhA is much larger than most proteins previously studied using this method, the complexity of protein folding and the presence of residues that could potentially quench the fluorescence signal make it very difficult to monitoring the loop motion by FRET.

Conclusions

In our studies of ftuFabI, we found that the *in vivo* antibacterial activity of the lead compounds is linearly correlated to their residence time yet shows no correlation to *in vitro* thermodynamic parameters. We hypothesize that residence time provides higher predictive values for *in vivo* drug efficacy than *in vitro* measurements. The relationship between loop motion and slow binding inhibition of InhA was investigated by selectively labeling the loop region. The importance of the native cysteine in protein stability makes chemical modification at the loop region unfeasible. Genetic approach to incorporate the unnatural amino acid at in the loop was successful. However, the fluorescence signal of *pCN*Phe was quenched under native protein structure, which prevents the possibility to monitor loop conformational changes using FRET.

References:

1.   Zhang, R., and Monsma, F. (2009) The importance of drug-target residence time, *Curr. Opin. Drug Discov. Devel. 12*, 488-496.

2.   Kumar, P., Han, B. C., Shi, Z., Jia, J., Wang, Y. P., Zhang, Y. T., Liang, L., Liu, Q. F., Ji, Z. L., and Chen, Y. Z. (2009) Update of KDBI: Kinetic Data of Bio-molecular Interaction database, *Nucleic Acids Res. 37*, D636-641.

3.   Tummino, P. J., and Copeland, R. A. (2008) Residence time of receptor-ligand complexes and its effect on biological function, *Biochemistry 47*, 5481-5492.

4.   Swinney, D. C. (2004) Biochemical mechanisms of drug action: what does it take for success?, *Nat. Rev. Drug. Discov. 3*, 801-808.

5.   Dierynck, I., De Wit, M., Gustin, E., Keuleers, I., Vandersmissen, J., Hallenberger, S., and Hertogs, K. (2007) Binding kinetics of darunavir to human immunodeficiency virus type 1 protease explain the potent antiviral activity and high genetic barrier, *J. Virol. 81*, 13845-13851.

6.   Kim, Y. B., Kopcho, L. M., Kirby, M. S., Hamann, L. G., Weigelt, C. A., Metzler, W. J., and Marcinkeviciene, J. (2006) Mechanism of Gly-Pro-pNA cleavage catalyzed by dipeptidyl peptidase-IV and its inhibition by saxagliptin (BMS-477118), *Arch. Biochem. Biophys. 445*, 9-18.

7.   Rawat, R., Whitty, A., and Tonge, P. J. (2003) The isoniazid-NAD adduct is a slow, tight-binding inhibitor of InhA, the *Mycobacterium tuberculosis* enoyl reductase: adduct affinity and drug resistance, *Proc. Natl. Acad. Sci. U.S.A. 100*, 13881-13886.

8.   Tsai, Y. C., and Johnson, K. A. (2006) A new paradigm for DNA polymerase specificity, *Biochemistry 45*, 9675-9687.

9.   Copeland, R. (2005) Evaluation of enzyme inhibitors in drug discovery: a guide for medicinal chemists and pharmacologists, 2nd ed., Wiley & Sons, Inc., 144-178.

10.   Leysen, J., and Gommeren, W. (1986) Drug-receptor dissociation time, new tool for drug research: receptr binding affinity and drug-receptor dissociation profiles of Serotonin-S2, dopamine-D2, Histamine-H1 Antagonists, and opiates, *Drug Develop. Res. 8*, 119-131.

11.   Copeland, R. A., Pompliano, D. L., and Meek, T. D. (2006) Drug-target residence time and its implications for lead optimization, *Nat. Rev. Drug Discov. 5*, 730-739.

12.   Swinney, D. (2008) Applications of binding kinetics to drug discovery: translation of binding mechanisms to clinically differentiated therapeutic responses, *Curr. Opin. Pharm. Med. 22*, 23-34.

13. Swinney, D. C. (2009) The role of binding kinetics in therapeutically useful drug action, *Curr. Opin. Drug Discov. Devel. 12*, 31-39.

14. Swinney, D. C. (2006) Biochemical mechanisms of New Molecular Entities (NMEs) approved by United States FDA during 2001-2004: mechanisms leading to optimal efficacy and safety, *Curr. Top. Med. Chem. 6*, 461-478.

15. Morrison, J. F., and Walsh, C. T. (1988) The behavior and significance of slow-binding enzyme inhibitors, *Adv. Enzymol. Relat. Areas Mol. Biol. 61*, 201-301.

16. Lu, H., and Tonge, P. J. (2008) Inhibitors of FabI, an enzyme drug target in the bacterial fatty acid biosynthesis pathway, *Acc. Chem. Res. 41*, 11-20.

17. Ward, W. H., Holdgate, G. A., Rowsell, S., McLean, E. G., Pauptit, R. A., Clayton, E., Nichols, W. W., Colls, J. G., Minshull, C. A., Jude, D. A., Mistry, A., Timms, D., Camble, R., Hales, N. J., Britton, C. J., and Taylor, I. W. (1999) Kinetic and structural characteristics of the inhibition of enoyl acyl carrier protein reductase by triclosan, *Biochemistry 38*, 12514-12525.

18. Kapoor, M., Dar, M. J., Surolia, A., and Surolia, N. (2001) Kinetic determinants of the interaction of enoyl-ACP reductase from *Plasmodium falciparum* with its substrates and inhibitors, *Biochem. Biophys. Res. Commun. 289*, 832-837.

19.   Marcinkeviciene, J., Jiang, W., Kopcho, L. M., Locke, G., Luo, Y., and Copeland, R. A. (2001) Enoyl-ACP reductase (FabI) of *Haemophilus influenzae*: steady-state kinetic mechanism and inhibition by triclosan and hexachlorophene, *Arch. Biochem. Biophys. 390*, 101-108.

20.   Xu, H., Sullivan, T. J., Sekiguchi, J., Kirikae, T., Ojima, I., Stratton, C. F., Mao, W., Rock, F. L., Alley, M. R., Johnson, F., Walker, S. G., and Tonge, P. J. (2008) Mechanism and inhibition of saFabI, the enoyl reductase from *Staphylococcus aureus*, *Biochemistry 47*, 4228-4236.

21.   Stewart, M. J., Parikh, S., Xiao, G., Tonge, P. J., and Kisker, C. (1999) Structural basis and mechanism of enoyl reductase inhibition by triclosan, *J. Mol. Biol. 290*, 859-865.

22.   Pidugu, L. S., Kapoor, M., Surolia, N., Surolia, A., and Suguna, K. (2004) Structural basis for the variation in triclosan affinity to enoyl reductases, *J. Mol. Biol. 343*, 147-155.

23.   am Ende, C. W., Knudson, S. E., Liu, N., Childs, J., Sullivan, T. J., Boyne, M., Xu, H., Gegina, Y., Knudson, D. L., Johnson, F., Peloquin, C. A., Slayden, R. A., and Tonge, P. J. (2008) Synthesis and in vitro antimycobacterial activity of B-ring modified diaryl ether InhA inhibitors, *Bioorg. Med. Chem. Lett. 18*, 3029-3033.

24. Luckner, S., Liu, N., am Ende, C., Tonge, P. J., and Kisker, C. (2010) A slow, tight-binding inhibitor of InhA, the enoyl-ACP reductase from *Mycobacterium tuberculosis*, *J. Biol. Chem.* Epub.

25. Sivaraman, S., Sullivan, T. J., Johnson, F., Novichenok, P., Cui, G., Simmerling, C., and Tonge, P. J. (2004) Inhibition of the bacterial enoyl reductase FabI by triclosan: a structure-reactivity analysis of FabI inhibition by triclosan analogues, *J. Med. Chem. 47*, 509-518.

26. Sullivan, T. J., Truglio, J. J., Boyne, M. E., Novichenok, P., Zhang, X., Stratton, C. F., Li, H. J., Kaur, T., Amin, A., Johnson, F., Slayden, R. A., Kisker, C., and Tonge, P. J. (2006) High affinity InhA inhibitors with activity against drug-resistant strains of *Mycobacterium tuberculosis*, *ACS Chem. Biol. 1*, 43-53.

27. Parikh, S., Moynihan, D. P., Xiao, G., and Tonge, P. J. (1999) Roles of tyrosine 158 and lysine 165 in the catalytic mechanism of InhA, the enoyl-ACP reductase from *Mycobacterium tuberculosis*, *Biochemistry 38*, 13623-13634.

28. Hammill, J. T., Miyake-Stoner, S., Hazen, J. L., Jackson, J. C., and Mehl, R. A. (2007) Preparation of site-specifically labeled fluorinated proteins for 19F-NMR structural characterization, *Nat. Protoc. 2*, 2601-2607.

29.   Morrison, J. F., and Walsh, C. T. (1988) The behavior and significance of slow-binding enzyme inhibitors, *Adv. Enzymol. Relat. Areas Mol. Biol. 61*, 201-301.

30.   Goodson, R. J., and Katre, N. V. (1990) Site-directed pegylation of recombinant interleukin-2 at its glycosylation site, *Biotech. (N. Y.) 8*, 343-346.

31.   Chilkoti, A., Chen, G., Stayton, P. S., and Hoffman, A. S. (1994) Site-specific conjugation of a temperature-sensitive polymer to a genetically-engineered protein, *Bioconjug. Chem. 5*, 504-507.

32.   Zhang, Z., Smith, B. A., Wang, L., Brock, A., Cho, C., and Schultz, P. G. (2003) A new strategy for the site-specific modification of proteins in vivo, *Biochemistry 42*, 6735-6746.

33.   Xie, J., and Schultz, P. G. (2005) Adding amino acids to the genetic repertoire, *Curr. Opin. Chem. Biol. 9*, 548-554.

34.   Xie, J., and Schultz, P. G. (2005) An expanding genetic code, *Methods 36*, 227-238.

35.   Wang, W., Takimoto, J. K., Louie, G. V., Baiga, T. J., Noel, J. P., Lee, K. F., Slesinger, P. A., and Wang, L. (2007) Genetically encoding unnatural amino acids for cellular and neuronal studies, *Nat. Neurosci. 10*,

1063-1072.

36. Wang, L., Xie, J., and Schultz, P. G. (2006) Expanding the genetic code, *Annu. Rev. Biophys. Biomol. Struct. 35*, 225-249.

37. Tang, J., Signarvic, R. S., DeGrado, W. F., and Gai, F. (2007) Role of helix nucleation in the kinetics of binding of mastoparan X to phospholipid bilayers, *Biochemistry 46*, 13856-13863.

38. Miyake-Stoner, S. J., Miller, A. M., Hammill, J. T., Peeler, J. C., Hess, K. R., Mehl, R. A., and Brewer, S. H. (2009) Probing protein folding using site-specifically encoded unnatural amino acids as FRET donors with tryptophan, *Biochemistry 48*, 5953-5962.

39. Tucker, M. J., Oyola, R., and Gai, F. (2005) Conformational distribution of a 14-residue peptide in solution: a fluorescence resonance energy transfer study, *J. Phys. Chem. B 109*, 4788-4795.

40. Aprilakis, K. N., Taskent, H., and Raleigh, D. P. (2007) Use of the novel fluorescent amino acid *p*-cyanophenylalanine offers a direct probe of hydrophobic core formation during the folding of the N-terminal domain of the ribosomal protein L9 and provides evidence for two-state folding, *Biochemistry 46*, 12308-12313.

41. Marek, P., Mukherjee, S., Zanni, M., and Raleigh, D. Residue specific, real

time characterization of lag phase species and fibril growth during amyloid formation: a combined fluorescence and IR studie of *p*-cyanophenylalanine analogues of islet amyloid polypeptide, *J. Mol. Biol.* (submitted).

Chapter IV[*]. Mechanism and Inhibition of the FabV Enoyl-ACP Reductase from *Burkholderia Mallei*

Introduction

Glanders and Burkholderia mallei. Burkholderia mallei is the etiologic agent of glanders, a disease that can date back to 350 *B.C.* (*1*). The bacillus, first isolated in 1882, is a gram-negative, facultative intracellular pathogen (*2*) and is highly infectious, requiring only a few organisms to cause infection in humans. Moreover, the disease can be spread in different ways, such as inhalation, ingestion and inoculation, hence making the bacterium a prevalent agent to be used in biological warfare (*3*). Weaponization of *B. mallei* was reported during the American Civil War, World War I and II as well as the Russian invasion of Afghanistan (*4-6*).

Unfortunately, no vaccine is available to prevent glanders. Current clinical treatment of this disease includes two phases, an initial intensive phase followed

[*] Part of work in this chapter has been described in a previous publication (*Lu* et al *Biochemistry* **2009**, *49*, 1281-9.)

by an eradication phase. A combination of antibiotics, including ceftazimide, amoxicillin-clavulanate and thrimehoprim-sulfamethoxazole, need to be administrated for at least two months to as part of the treatment (*3*). Problems, such as severe side effect, low oral availability and high resistant rate, limit the clinical uses of these chemotherapeutics. Hence, there is an urgent need to develop new antibiotics with a novel mechanism of action.

The FabV Enoyl-ACP Reductase from B. mallei (bmFabV). The majority of the FAS-II enzymes are essential for bacterial viability (*7*) and detailed kinetic studies coupled with high resolution crystal structures have provided a solid foundation for the development of compounds that target this pathway (*8-9*). In particular, the enoyl-ACP reductase, which catalyzes the last reaction in each elongation cycle, has been the most heavily targeted component of the pathway based on the discovery that antibacterial compounds such as triclosan and isoniazid target this enzyme (*10-13*). The FabI enoyl-ACP reductase, exemplified by the enzyme from *E. coli*, was initially considered to be the only reductase in bacteria (*14*), and extensive efforts have been made to develop inhibitors of this enzyme from organisms such as *M. tuberculosis* and *S. aureus* (*15-16*).   However, interests in targeting FabI for the development of an agent with activity against both *S. aureus*

125

and *S. pneumonia* were reduced by the discovery of FabK, an alternative flavin-dependent enoyl-ACP reductase from *S. pneumonia* which was insensitive to the lead FabI inhibitor triclosan (*17*). At around the same time Rock and co-workers also discovered a third enoyl-ACP reductase in *B. subtilis* (FabL) which was homologous to FabI (*18*).

Recently, a fourth isoenzyme (FabV) was identified by Cronan's lab from the gram-negative bacterium *V. cholerae* (vcFabV) (*19*). vcFabV, like FabI and FabL, is a member of the short-chain dehydrogenase/reductase (SDR) superfamily although it is significantly larger than other enzymes in this family. However, there is no convincing sequence homology between FabV and the FabI and FabL enzymes. Subsequent sequence similarity studies revealed that FabV is well conserved among a variety of organisms including several clinically important pathogens, such as *Yersinia pestis*, *Pseudomonas aeruginosa* and *Burkholderia* species (*19*).

Project Goals. To date, no detailed kinetic study has been conducted on any of the FabV enzymes. In this chapter, we will study the catalytic mechanism of the reaction catalyzed by bmFabV. The role of active site residues will be investigated by site direct mutagenesis and steady state kinetics. A series of diaryl ether

126

inhibitors will be designed based on the lead compound triclosan and detailed

inhibition studies of these inhibitors will be conducted.

Materials and Methods

Materials. Biotinylated thrombin and streptavidin agarose were purchased from Invitrogen and QuickChange site-directed mutagenesis kit was obtained from Stratagene. His-bind Ni^{2+}-NTA resin and pET vector were from Novagen. Triclosan was a gift from Ciba while other inhibitors were either synthesized as previously reported (*20-22*) or by Dr. Gopal Reddy. *trans*-2-Dodecenoic acid was purchased from TCI. All other chemical reagents were obtained from Sigma-Aldrich.

Synthesis of DD-CoA, Lauryl-CoA and Cr-ACP. DD-CoA and lauryl-CoA were prepared from *trans*-2-dodecenoic acid and lauric acid respectively, using the mixed anhydride method (*23*). Product formation was confirmed by ESI mass spectrometry. Cr-ACP was synthesized using the same protocol described in **Materials and Method**, **Chapter II**.

Cloning, Expression and Purification of bmFabV. The entire putative *fabV* gene from *Burkholderia mallei* ATCC 23344 strain was amplified using the primers listed in **Table 4.1** and inserted into the Novagen pET15b vector using the 5' NdeI

and 3' BamHI restriction sites (underlined) so that a His tag was encoded at the N-terminus of the coding sequence. After purification from XL1Blue cells (Stratagene) using a DNA purification and gel extraction kit (Qiagen Inc), the correct sequence of the insert was confirmed using ABI DNA sequencing.

Table 4.1: Primers Used for Cloning and Mutagenesis

Name	Sequence[a]
bmFabV forward	5'GGAATTC<u>CATATG</u>ATCATCAAACCGCGCGTAC GC3'
bmFabV reversed	5'CGC<u>GGATCC</u>TCATTCGATCAGATTCGGAATCC G3'
Y235A forward	5'GTCACGCACGACATC<u>GCC</u>TGGAACGGCTCG AT3'
Y235A reversed	5'ATCGAGCCGTTCCA<u>GGC</u>GATGTCGTGCGTGA C3'
Y235S forward	5'ACGCACGACATC<u>TCC</u>TGGAACGGCT3'
Y235S reversed	5'AGCCGTTCCA<u>GGA</u>GATGTCGTGCGT3'
K244A forward	5'ATCGGCGAAGCG<u>GCG</u>AAAGATCTCGACC3'
K244A reversed	5'GGTCGAGATCTTT<u>CGC</u>CGCTTCGCCGAT3'
K244R forward	5'GATCGGCGAAGCG<u>AGG</u>AAAGATCTCGACC3'
K244R reversed	5'GGTCGAGATCTTT<u>CCT</u>CGCTTCGCCGATC3'
K245M forward	5'CGAAGCGAAG<u>ATG</u>GATCTCGACCGC3'
K245M reversed	5'GCGGTCGAGATC<u>CAT</u>CTTCGCTTCG3'
K244A/K245A forward	5'ATCGGCGAAGCG<u>GCGG</u>CAGATCTCGACCG3'
K244A/K245A reversed	5'CGGTCGAGATCTGC<u>CGC</u>CGCTTCGCCGAT3'
ftuACP forward	5'GGAATTC<u>CATATG</u>AGTACACATAACGAAGATT CTAAA3'
ftuACP reversed	5'CCG<u>CTCGAG</u>ACCTACATCTTTAGATTCGATAT A3'

[a]Restriction sites and mutated sites are shown in underline.

Protein expression was performed using *E. coli* BL21(DE3)pLysS cells. After transformation, a single colony was used to inoculate 10 ml of Luria Broth (LB) media containing 0.2 mg/ml ampicillin in a 50 ml falcon tube, which was then incubated overnight at 37 °C in a floor shaker. The overnight culture was then used to inoculate 1 l of LB media containing ampicillin (0.2 mg/ml) which was incubated on an orbital shaker 37 °C until the optical density at 600 nm (O.D. 600) increased to around 1.0. Protein expression was induced by adding 1 mM isopropyl-1-thio-β-D-galactopyranoside (IPTG) and the culture was then shaken at 25 °C for 16 h. Cells were harvested by centrifugation at 5,000 rpm for 25 min at 4 ºC. The cell paste was then resuspended in 30 ml of His-binding buffer (5 mM imidazole, 0.5 M NaCl, 20 mM Tris HCl, pH 7.9) and lysed by sonication. Cell debris was removed by centrifugation at 33,000 rpm for 60 min at 4 ºC. The resulting supernatant was loaded onto a His-bind column (1.5 cm x 15 cm) containing 4 ml of His-bind resin (Novagen) that had been charged with 9 ml of charge buffer (Ni^{2+}). The column was washed with 60 ml of His-binding buffer and 30 ml of wash buffer (60 mM imidazole, 0.5 M NaCl, 20 mM Tris HCl, pH 7.9). Subsequently, the protein was eluted using a gradient of 20 ml binding buffer and 40 ml elute buffer (1 M imidazole, 0.5 M NaCl, 20 mM Tris HCl, pH 7.9). Fractions containing bmFabV were collected and imidazole was removed using a Sephadex

G-25 column (1.5 cm x 55 cm) using PIPES buffer (30 mM PIPES, 150 mM to NaCl, 1.0 mM EDTA pH 8.0) as the eluent. The purity of the protein was shown be >95% by 12% SDS-PAGE, which gave an apparent molecular weight of ~45 kDa. The concentration of the protein was determined by measuring the A_{280} and using an extinction coefficient (ε_{280}) of 42,650 $M^{-1}cm^{-1}$ calculated from the primary sequence. The enzyme was stored at -80 °C after flash freezing with liquid N_2.

To remove the N-terminal His tag, 1 µl of biotinylated thrombin was added to 1 ml of bmFabV (20 µM) in PIPES buffer and the reaction mixture was incubated at room temperature for 16 h. Streptavidin agarose (20 µl) was then added and the solution was incubated for an additional hour, after which the agarose was removed by centrifugation at 13,000 rpm for 10 min. The supernatant was further purified by chromatography on a Sephadex G-25 column (0.5 cm x 15 cm) using PIPES buffer as the eluent and fractions containing bmFabV lacking the His tag were pooled and analyzed by 12% SDS-PAGE.

Site-Directed Mutagenesis, Expression and Purification of bmFabV Mutants. The bmFabV mutants Y235A, Y235S, K244A, K244R, K245M and K244A/K245A were prepared using the QuikChange mutagenesis kit from Stratagene with the primers listed in **Table 4.1**. The sequence of each mutant plasmid was confirmed

by ABI DNA sequencing and the expression and purification of all the mutants followed the same procedure as that described above for the wild-type enzyme.

Steady-state Kinetic Analysis. Steady-state kinetic parameters were determined at 25 °C in 30 mM PIPES buffer pH 7.9 containing 1.0 mM EDTA and 0.62 mM NaCl. The optimum value for ionic strength was determined by varying the concentration of NaCl from 0 to 700 mM while the pH optimum was obtained by varying the pH of the reaction mixture from 6.6 to 8.5. Initial velocities were determined using a Cary 300 Bio (Varian) spectrophotometer to monitor the oxidation of NADH to NAD^+ at 340 nm (ε = 6,300 $M^{-1}cm^{-1}$). Initial characterization of the enzyme mechanism was performed in reaction mixtures containing 5 nM bmFabV and measuring initial velocities at several fixed concentrations of NADH (33 μM, 110 μM and 250 μM) and by varying the concentration of DD-CoA (1.5-35 μM), or at a fixed concentration of DD-CoA (6 μM, 12 μM and 24 μM) and by varying the concentration of NADH (10-352 μM). Double reciprocal plots were then used to differentiate between ping pong or ternary-complex mechanisms.

To further investigate the binding order of substrates, product inhibition studies were performed in which each substrate concentration was varied in the presence of several fixed concentrations of one of the products, NAD^+ (0, 50 and 110 μM)

or lauryl-CoA (0, 50 and 100 μM). The type of inhibition in each case was subsequently determined using a Lineweaver-Burk plot.

Finally the kinetic data in the absence of products were globally fit to the equation for the steady-state sequential bi bi mechanism (eqn **4**) to determine the K_m values for DD-CoA and NADH.

$$v = V_{max}[A][B] / (K_{iA}K_B + K_B[A] + K_A[B] + [A][B]) \tag{4}$$

In eqn **4**, v is the initial velocity, V_{max} is the maximum velocity, [A] and [B] are the concentration of the two substrates, K_A and K_B are the Michaelis constants for A and B respectively, and K_{iA} is the dissociation constant for A. Data analysis was performed using GraFit 4.0 (Erithacus)

K_m values of wild-type bmFabV toward DD-CoA and NADH were also determined by varying the concentration of one substrate at a fixed, saturating, concentration (> 10 x K_m) of the second substrate. Data sets were then fit to the Michaelis-Menten equation (eqn **5**) using GraFit (Erithacus).

$$v = V_{max}[S] / (K_m + [S]) \tag{5}$$

K_m values determined using the above method were found to be very close to those obtained from global fitting. Consequently, all subsequent measurements of K_m utilized initial velocities determined at fixed saturating concentrations of one substrate while the concentration of the other was varied.

Circular Dichroism Spectroscopy. The far-UV CD spectra of the wild-type

bmFabV protein and its mutants were recorded in 50 mM Tris buffer pH 7.9 at 25

°C at a concentration of 10 µM using an AVIV 62 DS spectrometer equipped with

a Peltier temperature control unit. Data analysis was performed using Microsoft

Excel.

Fluorescence Titration of Triclosan Binding to wild-type bmFabV. Equilibrium

fluorescence titrations were conducted using a Spex FL3-21 Fluorolog-3

spectrofluorimeter. One µl aliquots of triclosan (20.0 mM stock in DMSO) were

added to a 1 ml solution of enzyme (2 µM) in the same buffer as that used in the

steady-state kinetic experiments. The excitation wavelength was 295 nm (5 nm

slit width), and the emission wavelength was fixed at 335 nm (1 nm slit width).

Dilution of protein concentration was controlled to minimum (< 1%) and the

change in fluorescence as a function of triclosan concentration was fit to a

quadratic equation (eqn **6**).

$$\frac{F_e - F_1}{F_e(\max) - F_1(\max)} = \frac{(K_d + [E]_0 + [L]) - \sqrt{(K_d + [E]_0 + [L])^2 - 4K_d[E]_0}}{2[E]_0} \qquad \textbf{(6)}$$

In eqn **6**, F_e and F_1 are the fluorescent intensity in the presence and absence of enzyme respectively, $F_{e,max}$ and $F_{1,max}$ are the maximum fluorescence intensity in the presence and absence of enzyme, respectively, K_d is the dissociation constant, $[E]_0$ is the total enzyme concentration and $[L]$ is the amount of triclosan added to the reaction buffer. Data fitting was performed using Grafit.

Progress Curve Analysis. Progress curve analysis was used to determine if triclosan and the inhibitors we synthesized were slow binding inhibitors of bmFabV. FabI from *F. tularensis* (ftuFabI) was used as a model system since it has been shown that triclosan is a slow binding inhibitor of ftuFabI. In the assay, a very low concentration of enzyme (2 nM) and high concentration of substrate (200 μM of DD-CoA and 250 μM of NADH) were used so that initial velocities were linear over a period of 1 h. Since triclosan and other inhibitors bind to enoyl-ACP reductases in the presence of the oxidized cofactor, 100 μM of NAD^+ was added to the reaction so that the concentration of NAD^+ was effectively constant during progress curve data collection. The concentration of inhibitors was 60 μM, and data were collected for 1 h to ensure that the system had reached the steady state. Grafit was used for the data fitting.

135

Inhibition of bmFabV by Triclosan and Other Inhibitors. Initial velocities were measured at a fixed concentration of NADH (250 µM) or DD-CoA (35 µM) and at various concentrations of the second substrate and inhibitor. The equilibrium constant for the uncompetitive inhibition of bmFabV (K_i) was calculated using eqn **4** for the data collected at a fixed concentration of one substrate, either DD-CoA or NADH,

$$v = V_{max}[S]/[K_m+[S](1+[I]/K_i)] \tag{3}$$

where [S] is the concentration of varied substrate, K_m is the Michaelis-Menten constant for that substrate , V_{max} is the maximum velocity, [I] is the concentration of inhibitor added and K_i is the inhibition constant.

Similarly, the equilibrium constant for the competitive inhibition of bmFabV was calculated using eqn **1** for the data collected at a fixed concentration of one substrate, either DD-CoA or NADH,

$$v = V_{max}[S]/[K_m(1+[I]/K_{is})+[S]] \tag{1}$$

where [S] is the concentration of varied substrate, K_m is the Michaelis-Menten constant for that substrate, V_{max} is the maximum velocity, [I] is the concentration of inhibitor added and K_{is} is the inhibition constant.

Results and Discussion

Bioinformatic Analysis. In order to identify putative enoyl-ACP reductase homologues in *B. mallei*, the sequence of FabI from *E. coli* (ecFabI), FabL from *B. subtilis*, FabK from *S. pneumoniae* and FabV from *V. cholerae* (vcFabV) were used as templates for a BLAST analysis of the *B. mallei* ATCC 23344 genome (KEGG). Two open reading frames were identified as ecFabI homologues, one in chromosome 1 (63% identify to ecFabI) and the second in chromosome 2 (42% identity to ecFabI), while a homologue of vcFabV (bmFabV) was also located on chromosome 1 (56% identity to vcFabV). Subsequently the vcFabV homolog was cloned, expressed, purified and shown to catalyze the NADH-dependent reduction of DD-CoA. bmFabV thus has *in vitro* enzymatic activity characteristic of an enoyl-ACP reductase.

Kinetic Mechanism. The optimal ionic strength (0.62 mM) and pH (7.9) values for the enzyme catalyzed reaction were determined by measuring initial velocities at saturating levels (> 10 x K_m) of both DD-CoA and NADH. The Michaelis-Menten constants for DD-CoA and NADH were then determined by varying the concentration of one substrate at a saturating concentration of the second

137

substrate. The values of k_{cat}, $K_{m,NADH}$, and $K_{m,DD-CoA}$ obtained using this method were 930 ± 6 min^{-1}, 28.7 ± 1.2 μM and 2.4 ± 0.1 μM, respectively, which are close to the values obtained from global fitting (see below). Due to reports that vcFabV has a much higher activity after the C-terminal His tag was removed, we then

Table 4.2: Kinetic Parameters for wt and Mutant bmFabV Enzymes

Enzyme	k_{cat} (min^{-1})	K_m (μM)		k_{cat}/K_m (μM^{-1}min^{-1})
		DD-CoA	NADH	DD-CoA
wt without His tag	1728 ± 10	4.4 ± 0.3	ND	392 ± 27
wt with His tag	1242 ± 30	2.5 ± 0.4	23 ± 3	497 ± 79
Y235A	5.0 ± 0.1	2.7 ± 0.2	23 ± 2	1.8 ± 0.1
Y235S	6.1 ± 0.3	2.2 ± 0.1	6 ± 1	2.8 ± 0.1
K244A	11 ± 1	7.2 ± 0.6	66 ± 2	1.5 ± 0.1
K244R	1.3 ± 0.1	7.6 ± 0.7	69 ± 1	0.17 ± 0.01
K245M	18 ± 1	28 ± 2	28 ± 2	0.64 ± 0.03
K244A/K245A	ND	ND	65 ± 4	0.023 ± 0.002

determined the kinetic parameters of bmFabV after thrombin was used to remove the N-terminal His tag. Subsequently we found that bmFabV lacking the N-terminal His tag had k_{cat} and $K_{m,DD-CoA}$ values of 1728 ± 10 min^{-1} and 4.4 ± 0.3 µM (**Table 4.2**), respectively, indicating that the His tag did not have a dramatic effect on activity. Consequently, all subsequent kinetic experiments were performed using enzymes bearing an N-terminal His tag.

To demonstrate that the recombinant enzyme is also capable of catalyzing the reduction of ACP substrates, the ACP from *F. tularensis* Schu4 (ftuACP), which is 68% identical to the putative ACP from *B. mallei*, was expressed and purified. The values of $k_{cat,}$ $K_{m,NADH,}$ and $K_{m,cr-ACP}$ obtained were 1299 ± 29 min^{-1}, 31 ± 4 µM and 25.1 ± 2 µM, respectively.

After optimizing the ionic strength and pH, a matrix of initial velocities was measured at different concentrations of DD-CoA and NADH, and the kinetic data were then analyzed using double-reciprocal plots. Similar to other enoyl-ACP reductases, these studies confirmed that bmFabV catalyzes substrate reduction through a ternary-complex mechanism, since all the lines in the double-reciprocal plot intersect with each other at a single point (**Figure 4.1**) (*24-27*). To further investigate the order of substrate binding, product inhibition studies using NAD$^+$ and lauryl-CoA were performed. Analysis of the results from double-reciprocal
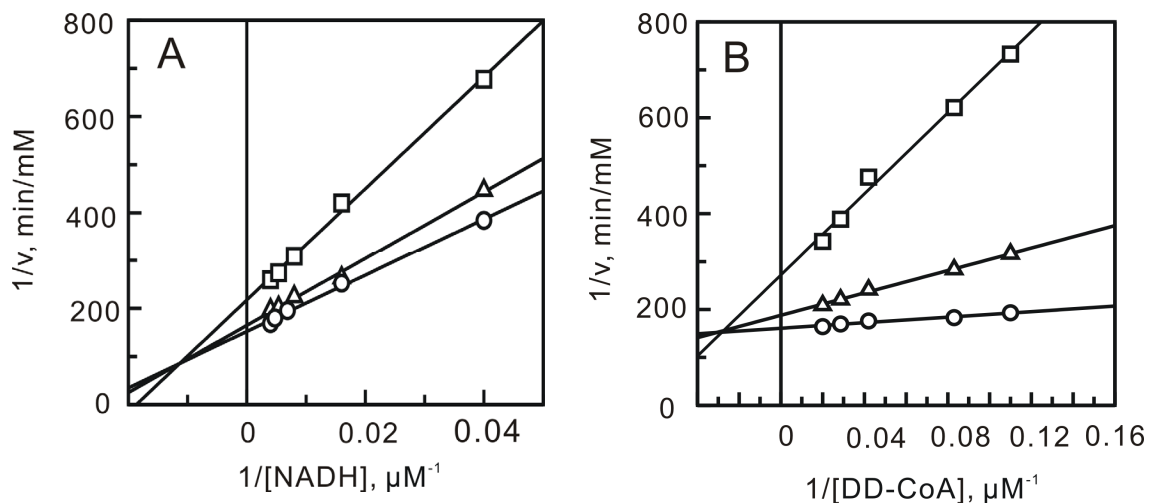
Figure 4.1: Two-substrate Steady-state Kinetics. A) 1/v versus 1/[NADH] double-reciprocal plots in which the DD-CoA concentration was fixed at 6 (□), 12 (Δ) and 24 μM (○); **B**) 1/v versus 1/[DD-CoA] double-reciprocal plots in which the NADH concentration was fixed at 33 (□), 110 (Δ) and 250 μM (○).

plots indicated that NAD^+ was a competitive inhibitor with respect to NADH, but was a non-competitive inhibitor with respect to DD-CoA. However, when NADH or DD-CoA was varied in the presence of lauryl-CoA, mixed patterns of inhibition were observed for both substrates (**Figure 4.2**). This combination of product inhibition patterns is indicative of a sequential bi bi mechanism with NADH binding to the enzyme first. The ternary complex steady-state kinetic parameters were subsequently obtained by globally fitting the initial velocity data to eqn **4** for an ordered bi bi mechanism, giving $K_{i,NADH}$ 13.0 ± 4.1 μM, $K_{m,NADH}$ 23.2 ± 3.4 μM, $K_{m,DD-CoA}$ 2.5 ± 0.4 μM and k_{cat} 1242 ± 30 min^{-1} (**Table 4.2**). Due to the
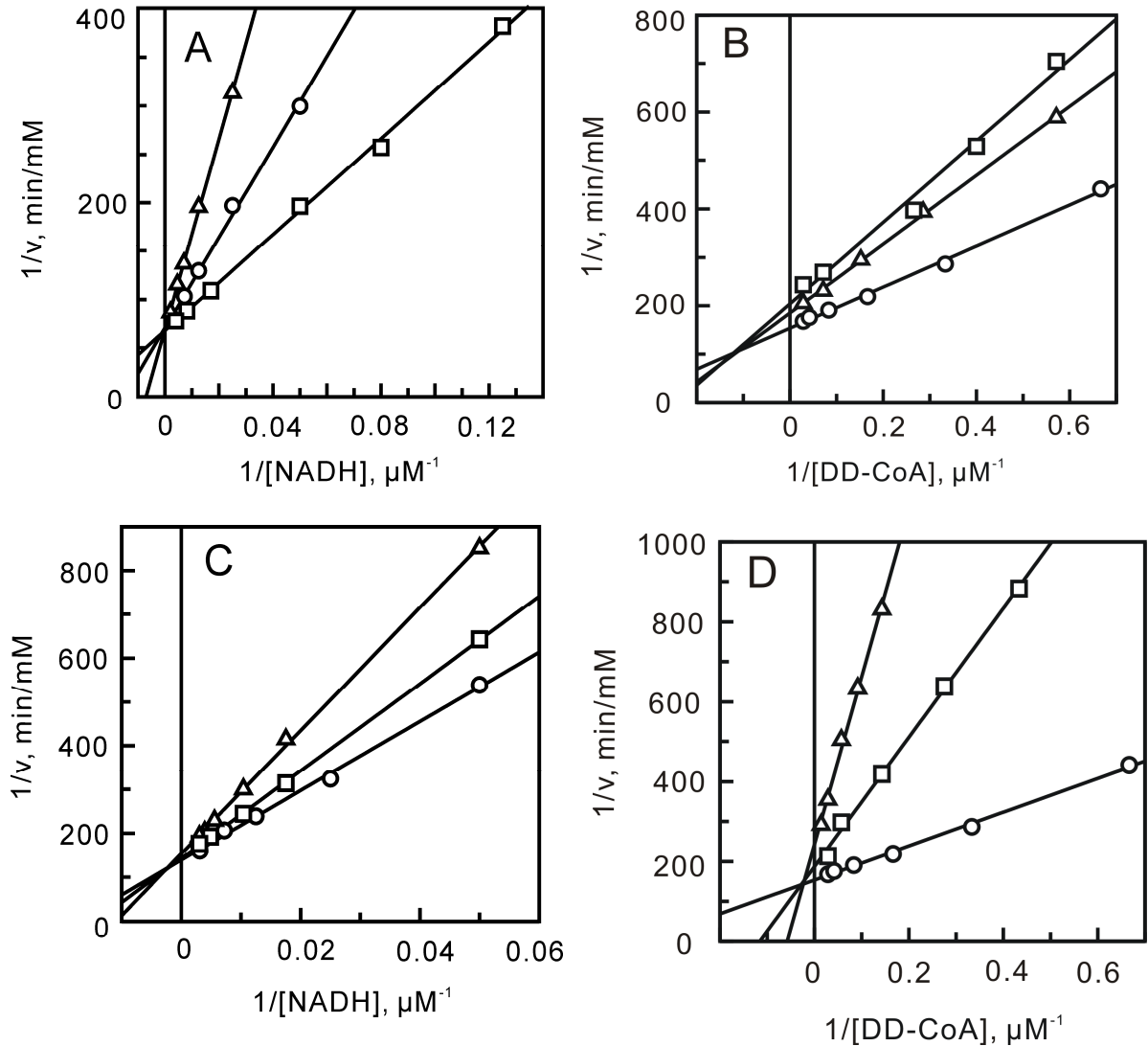
Figure 4.2: Product Inhibition Studies to Determine the Substrate Binding Order. A) NADH varied in the presence of NAD^+ (0 (□), 55 (○) and 110 μM (Δ)) with DD-CoA fixed at 35 μM; **B**) DD-CoA varied in the presence of NAD^+ (0 (○), 55 (Δ) and 110 μM (□)) with NADH fixed at 250 μM; **C**) NADH varied in the presence of lauryl-CoA (0 (○), 50 (□) and 100 μM (Δ)) with DD-CoA fixed at 35 μM; **D**) DD-CoA varied in the presence of lauryl-CoA (0 (○), 50 (□) and 100 μM (Δ)) with NADH fixed at 250 μM.

similarity in kinetic parameters obtained from global fitting and when only one of the substrates was varied at a saturating level of the second substrate, we subsequently analyzed the impact of site-directed mutagenesis by determining kinetic parameters at a single fixed concentration of one substrate while varying the second substrate.

Taken together, the steady state kinetic data reveal that bmFabV functions as an enoyl-ACP reductase, possessing even higher catalytic activity than other enoyl-ACP reductases characterized previously (*23, 27-29*). bmFabV catalyzes substrate reduction through a sequential bi bi mechanism with NADH binding first. This suggests that NADH forms part of the enoyl substrate binding site as seen in several other FabI enoyl-ACP reductases (*26, 30*). In addition, we found that the N-terminal His tag in bmFabV did not have a dramatic effect on catalytic activity as reported for the C-terminal His tag in vcFabV.

Active-site Residues and Catalytic Mechanism. The FabI and FabV enoyl-ACP reductases are members of the short-chain dehydrogenase/reductase (SDR) superfamily (*31-34*). In this family a catalytic tyrosine and lysine are found in a Tyr-$(Xaa)_n$-Lys motif, where n is generally 3 for the dehydrogenases and 6 for enoyl-ACP reductases. The variation in n is thought to relate to the difference in

chemistry between reduction of a carbonyl group, and a carbon-carbon double bond conjugated to a thioester. Analysis of the bmFabV sequence suggests the presence of an even more extended active-site motif, Tyr-(Xaa)$_8$-Lys, involving Y235 and K244. In addition, unlike other SDR reductases, K244 is followed by a second lysine (K245), which is conserved in the FabV homologues from a variety of organisms including *Burkholderia* sp., *Yersinia* sp. and *Clostridium acetobutylicum* (**Figure 4.3**).To investigate the roles of these residues in

```
                        *              *           **
ecFabI   142  L T L S Y L G A E R A I P N Y N - - V M G L A K A S L E A N V R  171
bsFabL   137  V S I S S L G S I R Y L E N Y T - - T V G V S K A A L E A L T R  166
bmFabV   221  T A F T Y L G E Q V T H D I Y W N G S I G E A K K D L D R T V L  252
ypFabV   221  T A F T Y L G E K I T H D I Y W N G S I G A A K K D L D Q K V L  252
caFabV   221  I A Y S Y I G S P R T Y K I Y R E G T I G I A K K D L E D K A K  252
paFabV   221  T A F T Y L G E K I T H D I Y W N G S I G A A K K D L D Q K V L  252
vpFabV   221  T A F T Y L G E R I T H D I Y W N G S I G A A K K D L D Q K V L  252
mfFabV   220  T A F T Y L G E K I T H D I Y W N G T I G A A K K D L D Q R V L  251
etFabV   221  T A F T Y L G E K I T H D I Y W N G S I G E A K K D L D K R V L  252
vcFabV   227  I A F S Y M G P D V T H P I Y L D G T L G R A K I D L H Q T S H  258
                        *              *           **
```

Figure 4. 3: Sequence Alignment of Active Site Residues of the Enoyl-ACP Reductases. Organisms include *Escherichia coli*, *Bacillus subtilis*, *Burkholderia mallei*, *Yesinia pestis*, *Clostridium acetobutylicum*, *Pseudomonas aeruginosa*, *Variovorax paradoxus*, *Methylobacillus flagellatus*, *Erwinia tasmaniensis* and *Vibrio cholerae*. Conserved residues are labeled with an asterisk. The sequence alignment was performed using Clustal W (*35*), and the figure was made using Jalview (*36*).

143

catalysis, the following mutant enzymes were expressed and purified: Y235A, Y235S, K244A, K244R, K245M and K244A/K245A. CD spectra of the wild-type and mutant proteins were superimposable, suggesting that the alteration in catalytic activity resulting from mutagenesis was not a result of major alteration in changes in the protein. Subsequently the kinetic parameters of the mutant enzymes were determined (**Table 4.2**).

Y235 in bmFabV is homologous to the conserved tyrosine that is found in all members of the SDR superfamily (*23, 37*). Replacement of this conserved tyrosine with phenylalanine in the dehydrogenases, such as 3β/17β-hydroxysteroid dehydrogenase, results in an enzyme with virtually no activity (*37*), consistent with the notion that this residue plays a critical role in substrate oxidation/reduction. In contrast, equivalent mutations in the FabI enzymes from *E. coli* (ecFabI; Y156F) and *M. tuberculosis* (InhA; Y158F) result in much more modest decreases in k_{cat} values of 7- and 21-fold, without substantially affecting the K_m value for the substrate (*23, 38*). These data have raised questions concerning the importance of the conserved tyrosine in the enoyl-ACP reductases (*39*), and indeed Anderson and coworkers have suggested that the enolate formed during reduction of the enoyl thioester does not need to be stabilized to a great extent by the enzyme (*40*). Consistent with this idea, the

Y158S InhA enzyme has wild-type activity (*23*), although it now appears that a second tyrosine in ecFabI (Y146) may be involved in transition state stabilization (*39*). This latter residue, which constitutes the third residue in the SDR 'triad', is a phenylalanine in mycobacterial FabI enzymes and is a serine in the dehydrogenases (*23, 37*).

Returning to bmFabV, replacement of Y235 with alanine gave a k_{cat}/K_m value of 1.8 ± 0.1 $\mu M^{-1}min^{-1}$, which is 280-fold lower than the wild-type enzyme. This decrease in k_{cat}/K_m primarily results from a reduction in k_{cat}, suggesting that Y235 plays a crucial role in substrate reduction. To further investigate the catalytic role of Y235, this residue was replaced by a serine. However, unlike InhA, this mutant could not restore the activity of bmFabV, and instead resulted in an enzyme with similar activity to the Y235A mutant. Although the pKa values of the Y235 hydroxyl group and of the S235 mutant in the enzyme are unknown, the pKa values of these side chains differ by ~ 4.5 log in solution, suggesting that the acidity of Y235 is important for the function of this residue in catalysis.

In the SDR enzymes, the primary function of the active site lysine is to bind the cofactor through hydrogen bonds formed with the nicotinamide ribose. In addition, this lysine is also thought to interact directly with the conserved tyrosine in the dehydrogenases, facilitating protonation of the substrate carbonyl by the tyrosine

(*37*). In bmFabV, the K244A mutant had k_{cat}, $K_{m,DD\text{-}CoA}$ and $K_{m,NADH}$ values of 11 ±

1 min^{-1}, 7.2 ± 0.6 μM and 66 ± 2 μM. This mutation thus causes small (3-fold)

increases in the K_m values for both substrates, together with a 110-fold decrease

in the k_{cat} value for substrate reduction. The corresponding mutation in InhA

(K165A) resulted in an enzyme that was unable to bind cofactor. However, in the

case of InhA, replacement of K165 with arginine completely restored activity. In

contrast the K244R bmFabV enzyme had a k_{cat} value 950-fold smaller than that of

wild-type enzyme and was thus even less active that the K244A mutant. The

modest changes in K_m values coupled with the 10^2-10^3-fold reduction in k_{cat}

values caused by mutation of K244 (**Table 4.2**) thus support differing roles for the

conserved lysine in FabI and FabV. In FabV it appears that K244 plays a much

more direct role in facilitating substrate reduction than does the corresponding

residue in FabI where it functions primarily in cofactor binding. Indeed the function

of both Y235 and K244 in bmFabV is more akin to the role played by the

conserved tyrosine and lysine residues in the dehydrogenases than in the FabI

enzymes.

In bmFabV, a second lysine (K245) is found adjacent to K244. This

lysine-lysine sequence is not observed in other enoyl reductases, but is

conserved in FabV from a variety of organisms (**Figure 4.3**). In order to probe the

146

role of K245, the K245M and K244A/K245A mutants were generated. While the K_m value for NADH was unchanged in the K245M mutant, the K_m value for DD-CoA was increased 10-fold compared to the wild-type enzyme. This mutation also caused a 70-fold reduction in the k_{cat} value for substrate reduction. Although the K244A mutation only resulted in a small 3-fold increase in $K_{m,DDCOA}$, combination of K244A with K245A resulted in an enzyme for which the K_m value for DD-CoA has increased to a value that cannot be measured. In contrast, the K_m values for NADH in the single and double mutants are very similar, suggesting that K245 plays an important role in binding the enoyl substrate.

In summary, we have identified three important active site residues in bmFabV using site directed mutagenesis. The kinetic data support a model in which Y235, K244 and K245 form a hydrogen bond network that is important for substrate reduction. By analogy to the reaction mechanism in the SDR dehydrogenases, we suggest that Y235 is hydrogen bonded to K244/K245, an interaction that would lower the pK_a of Y235 and facilitate the ability of this residue to either stabilize and/or protonate the enolate intermediate formed during substrate reduction. In addition, K244 is thought to interact with both cofactor and acyl substrate, while K245 interacts solely with the acyl substrate. A schematic diagram showing these proposed interactions is given in **Figure 4.4**. This figure has been adapted from
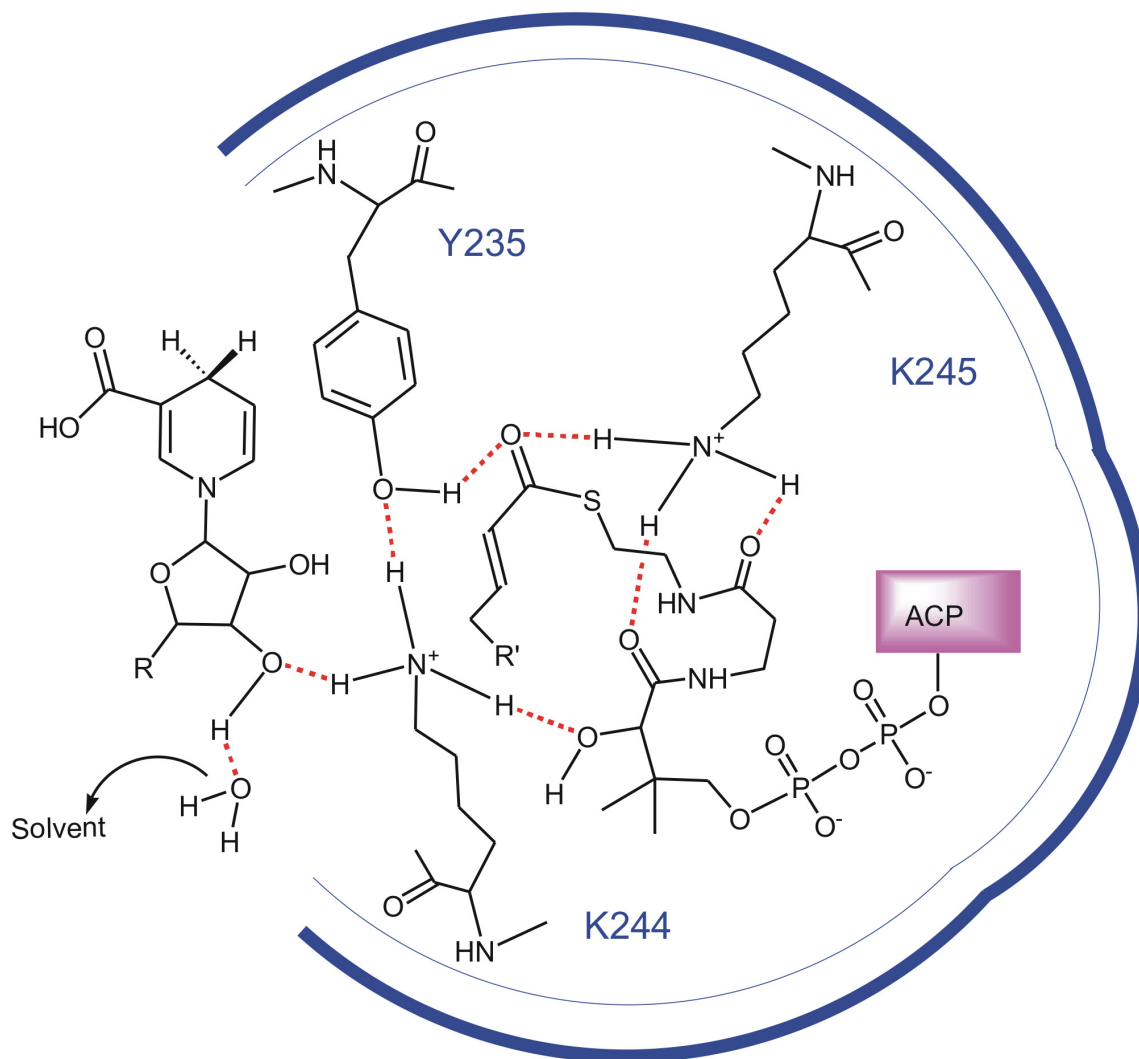
Figure 4.4: Proposed Hydrogen Bonding Network between the Three Active Site Residues (Y235, K244 and K245), Cofactor and the Enoyl–ACP Substrate.

the proposed catalytic mechanism of 3β/17β-hydroxysteroid dehydrogenase in which the conserved tyrosine and lysine residues function together to protonate/deprotonate the substrate (*41*). The interactions that we propose for FabV differ somewhat from those in other FabI enoyl reductases where the conserved lysine is thought to only be involved in cofactor binding.

Inhibition of bmFabV by Triclosan. The diaryl ether triclosan is a potent inhibitor of the FabI enzyme from a variety of organisms. Studies with the FabI enzymes from *E. coli* and *F. tularensis* have revealed that triclosan is a slow binding inhibitor of these organisms, and it is thought that the slow step in formation of the E-I* complex involves ordering of a substrate recognition loop that closes over the active site after triclosan binding (*20, 29, 42-45*). The high affinity of triclosan for the ecFabI and ftuFabI, as well as related FabIs such as the enzyme from *S. aureus*, is generally a hallmark of the FabI enoyl-ACP reductases, with the outlier being the InhA enzyme from *M. tuberculosis*. Triclosan inhibits InhA with a K_i value of only 0.2 µM (*46*) compared to the K_i values of 7 pM, 50 pM and 5 nM for ecFabI, ftuFabI and saFabI, respectively (*15, 28, 38, 43*). In addition triclosan is not a slow binding inhibitor of InhA in contrast to the other enzymes. However a structure-based approach has successfully resulted in diaryl ether-based

inhibitors of InhA with improved affinity (*21*) and that are slow binding inhibitors of the enzyme (*47*). An important distinction between the FabI and FabK enoyl-ACP reductases is the insensitivity of the latter to triclosan (*17*), and Cronan and coworkers have shown that vcFabV is only a weakly inhibited by triclosan (50% inhibition at 12 µM) (*19*). Due to our success in developing high affinity inhibitors of InhA, we were thus very curious to study the inhibition of bmFabV by triclosan.

Previous research in our lab has shown that triclosan is a slow binding inhibitor of ftuFabI (*15*). In a standard progress curve analysis assay, a linear decrease in NADH concentration is observed in the absence of triclosan while a curved line is seen in the presence of inhibitor (**Figure 4.5**). This is a characteristic of slow binding inhibition, since rapid reversible inhibitors are expected to also yield a linear decrease in substrate concentration under similar conditions. In the case of ftuFabI, the initial velocity decreases exponentially with time until a final steady-state velocity is achieved (*48*). However, in the studies with bmFabV, the concentration of NADH decreased linearly with time, which strongly suggests that triclosan is a rapid, reversible inhibitor of bmFabV (**Figure 4.5**).

Initial velocities were subsequently obtained under a range of substrate and inhibitor concentrations, and data analysis revealed that triclosan is an uncompetitive inhibitor with respect to DD-CoA (K_i = 0.42 ± 0.02) and a
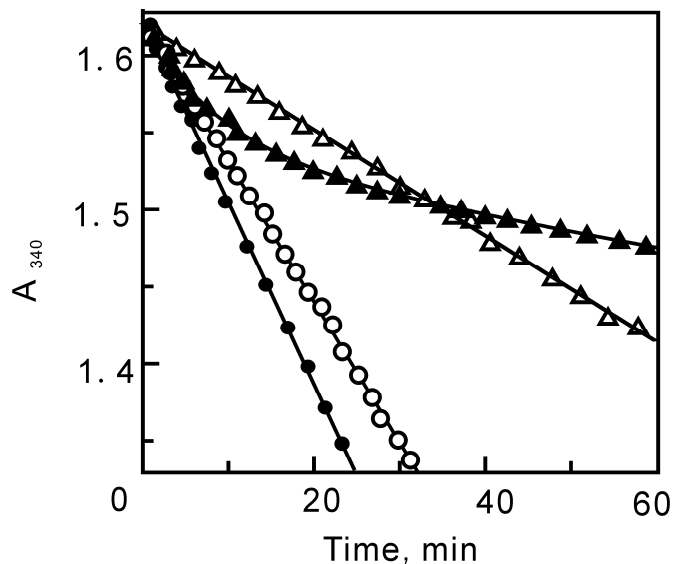
Figure 4.5: Progress Curve Analysis of ftuFabI and bmFabV. Progress curves for ftuFabI (2 nM) in the presence of DD-CoA (200 μM), NADH (250 μM) and either 0 (●) or Δ60 nM (▲) triclosan. Progress curves for bmFabV (2 nM) in the presence of DD-CoA (200 μM), NADH (250μM) and either 0 (○) or 2 μM (Δ) triclosan.

competitive inhibitor with respect to NADH (K_i = 0.48 ± 0.04 μM) (**Figure 4.6**).

Uncompetitive inhibition with respect to DD-CoA indicates that triclosan binds

after DD-CoA. Since we have already shown that bmFabV catalyzes the reaction

through a sequential mechanism with NADH binding first and NAD^+ dissociating

last, triclosan then can only bind to the substrate ternary complex

(E-NADH-DD-CoA), the product ternary complex (E-NAD$^+$-lauryl-CoA) or the

binary product complex (E-NAD$^+$). In addition, since triclosan is a competitive

inhibitor with respect to NADH, triclosan must bind to either the NADH binding site

in the free enzyme or to the E-NAD$^+$ complex. Taken together, we can conclude

that triclosan binds to the E-NAD$^+$ product complex as observed for the FabI class

of enoyl-ACP reductases (*43*). In support of this hypothesis, fluorescence titration
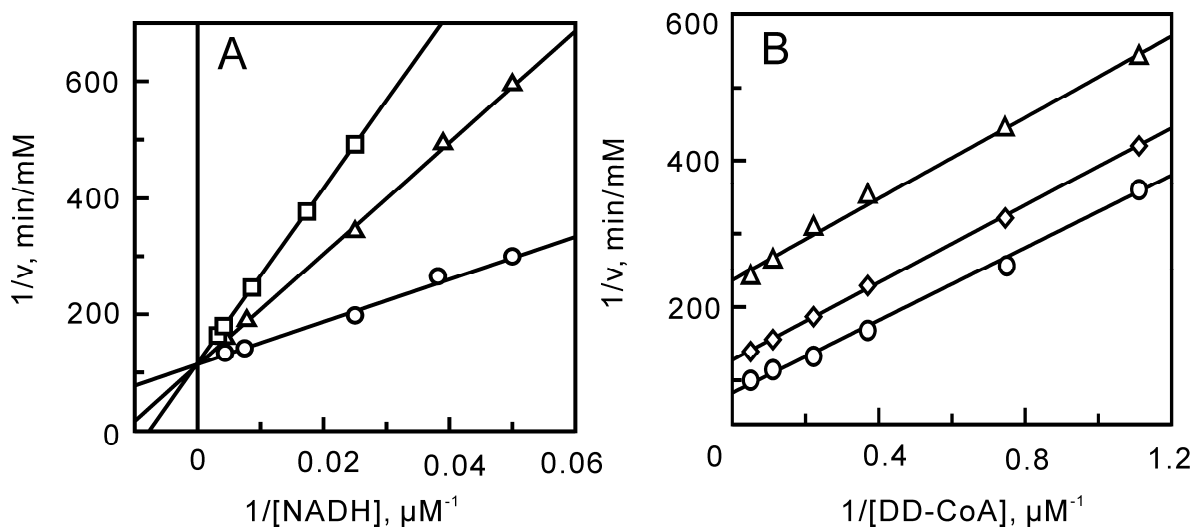
Figure 4.6: Mechanism of bmFabV Inhibition by Triclosan. Assays were performed by varying the concentration of one substrate at a fixed concentration of the second substrate constant and at various concentrations of triclosan. **A**) NADH varied in the presence of triclosan (0 (○), 0.8 (Δ) and 1.6 μM (□)) with DD-CoA fixed at 35 μM; **B**) DD-CoA varied in the presence of triclosan (0 (○), 0.8 (◊) and 1.6 μM (Δ)) with NADH fixed at 250 μM.
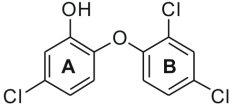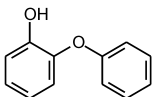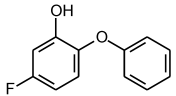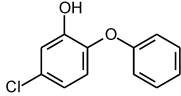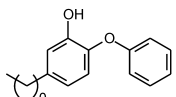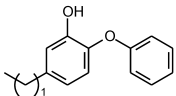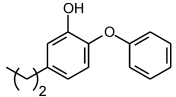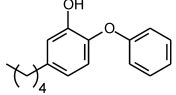
experiments demonstrated that the K_d value for the interaction of triclosan with the free enzyme is larger than 100 μM, which indicates that triclosan binds only weakly to the free enzyme. Finally, the effect of NAD^+ on triclosan binding was investigated by adding NAD^+ to the reaction mixture. When the inhibition of bmFabV by triclosan was measured by varying the concentration of NADH in the presence of 100 μM NAD^+, a 4-fold decrease in the K_i value (0.11 μM) was observed. This means that NAD^+ can potentiate the binding of triclosan to the enzyme by forming an E-NAD^+-triclosan ternary complex. However, the formation and dissociation of this ternary complex must be rapid and reversible, occurring without ordering of the substrate binding loop. The mechanism of inhibition of bmFabV by triclosan thus closely follows that characterized previously for InhA (*46*).
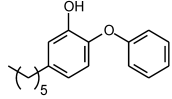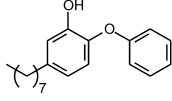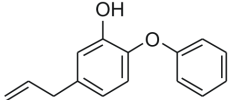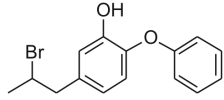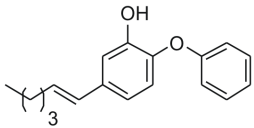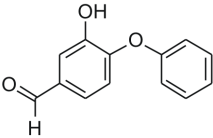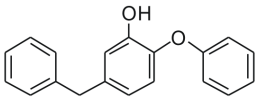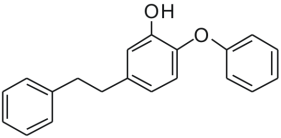
SAR Studies of bmFabV Inhibitors. The K_i for bmFabV inhibition by triclosan is only 0.4 μM, consistent with the suggestion that the resistance of *P. aeruginosa* to triclosan arises from the relative insensitivity of the FabV enzymes to this broad spectrum antibacterial agent (*49*). Given our success at designing high affinity inhibitors of InhA, SAR studies of bmFabV inhibition by triclosan analogues thus

closely follows that conducted previously for InhA (*21*). A series of triclosan analogues were synthesized and the inhibition data are summarized in **Table 4.3**.
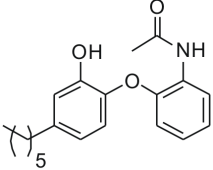
It has been shown that the electronic and steric properties of ring A are critical for the binding affinity of triclosan analogues for InhA (*21*). Initial efforts to explore the importance of the 5-chlorine atom on ring A started with replacing the chlorine with hydrogen to generate analogue **26**. Compared to analogue **28**, the Ki value of **26** increases 11 fold from 1.1 to 12.8 µM indicating that a substituent at the 5-position is important to maintain the binding affinity. To investigate the electronic effect in greater detail, we substituted the chlorine atom with a stronger electron withdrawing group (fluorine) and an electron donating group (methyl group). The resulting compound, 5-fluoro-2-phenoxyphenol (**27**) and 5-methyl-2-phenoxyphenol (**11**) are 5-fold and 3-fold less tightly bound to the enzyme respectively than analogue **26**, which suggests the electronegativity of a substituent at this position is not as important as that in ftuFabI to determine the binding affinity. Different lengths of alkyl groups (**11**-**13**,1**5**-**17**) were then incorporated at the 5-position to study the steric effect and the K_i values of different alkyl diaryl ethers are shown in **Table 4.3**. The binding affinity increases with an increase in the alkyl chain length increases, with analogue **15** (5-pentyl-2-phenoxyphenol) exhibiting the lowest K_i value of 0.11 µM. It has been

154
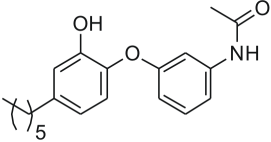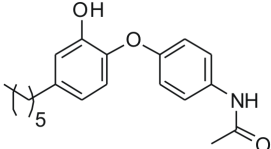
Table 4.3: Inhibition Constant and Mechanism of Triclosan and Its Analogues for bmFabV

Inhibitor		K_i (µM)	Inhibition Mechanism
	10	0.42±0.02	Competitive to NADH & Noncompetitive to DD-CoA

Modification at the 5-position of A ring

Inhibitor		K_i (µM)	Inhibition Mechanism
	26	12.8±0.5	Competitive to NADH
	27	5.3±0.3	Competitive to NADH
	28	1.1±0.1	Competitive to NADH & Noncompetitive to DD-CoA
	11	3.7±0.1	Competitive to NADH
	12	0.28±0.02	Competitive to NADH
	13	0.19±0.01	Competitive to NADH & Noncompetitive to DD-CoA
	15	0.11±0.01	Competitive to NADH & Noncompetitive to DD-CoA
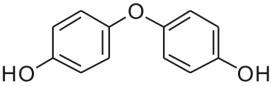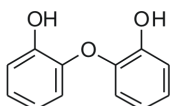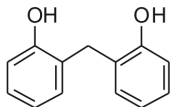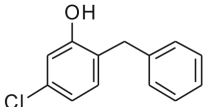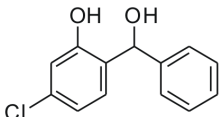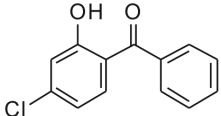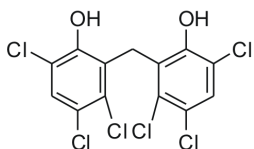
(structure)	**16**	1.6±0.1	Competitive to NADH
(structure)	**17**	6.2±0.2	Competitive to NADH
(structure)	**35**	2.3±0.3	Competitive to NADH
(structure)	**36**	2.1±0.2	Competitive to NADH
(structure)	**37**	20% Inhibition at 30 µM	
(structure)	**38**	No inhibition at 30 µM	
(structure)	**39**	0.21±001	Competitive to NADH
(structure)	**40**	10% Inhibition at 30 µM	

Modification at *ortho*-, *meta*- or *para*-position B ring

(structure)	**41**	3.9±0.5	Competitive to NADH

	42		No inhibition at 30 µM
	43	3.3±0.4	Competitive to NADH

Modification of the bridging atom

	44	2.4±0.05	Competitive to DD-CoA & Noncompetitive to NADH
	45	40.2±0.7	Competitive to NADH
	46	0.97±0.04	Competitive to DD-CoA & Noncompetitive to NADH
	47	2.4±0.2	Competitive to DD-CoA & Noncompetitive to NADH
	48		No inhibition at 30 µM
	49		No inhibition at 30 µM
	50	0.057±0.005	Competitive to DD-CoA & Noncompetitive to NADH

demonstrated that InhA binds most tightly with 5-octyl-2-phenoxyphenol (**17**), while ftuFabI prefers to bind the shorter alkyl chain analogue 5-propyl-2-phenoxyphenol (**13**). Take together, these data suggest that the chlorine atom at the 5-position of ring A might also point to the substrate binding pocket of bmFabV and its hydrophobic pocket is much bigger than that of other FabIs except InhA .

To further examine the steric tolerance of the 5-position, a variety of substituents with higher rigidity were introduced (**35-40**). Analogue **35** with an allylic group and analogue **36** with a 2-bromo-propyl group were 10-fold less potent than their alkyl counterpart (5-propyl-2-phenoxyphenol), which suggests that a flexible chain is preferably accommodated in the binding pocket. The introduction of more bulky group yielded analogues **37** and **40** with weaker inhibition. However, a benzyl substitution at this position generates a potent inhibitor (**39**) with a K_i value of 0.21 μM. Finally, the hypothesis that the substitution at the 5-position extends into the hydrophobic pocket was confirmed by analogue **38** which has no inhibition at 30 μM. The loss of binding affinity might be due to the intolerance of polar group at this binding site. The precise structural basis for these effects will require additional structural data. These data reveal that a bulky and rigid substituent at the 5-position would yield a favorable interaction with the substrate binding pocket.

From previous work, introduction of different function groups on the B ring produced a series of diaryl ether inhibitors that bind weakly to InhA probably due to the unfavorable steric interactions between the substituents and the enzyme (*22*). However, in our studies, deletion of the two chlorine atoms on the B ring (**28)** reduces binding affinity by almost 3 fold compared to triclosan. This suggests that B ring substitutions can possibly have favorable interactions with bmFabV. To carefully study the regio-specificity of possible favorable interactions on the B ring, an amide group was separately incorporated at the *ortho-*, *meta-* and *para*-position. Analogues **41** and **43**, which have *ortho-* and *para-* substitutions respectively, are 4-fold less potent than analogue **28**. Loss of binding affinity might arise from the steric hindrance between the substituents and the enzyme. Finally, the substitution at the *meta*-position of B ring yielded a compound (**42**) with almost no binding affinity. These data suggest that while the *ortho-* and *para-*position can tolerate small substitutions, the *meta*-position might have close contact with the enzyme making substitution at this position less favorable.

The bridging oxygen atom is essential for the binding affinity of diaryl ethers for InhA, as this atom is involved in an important hydrogen bond with the active site Y158 since upon examination of the crystal structure (*21*). The importance of this bridging oxygen for bmFabV was first tested with a commercially available

159

compound 2,2'-methylenediphenol (**46**) and we found that this compound binds with 40 fold higher affinity than does analogue **45**. This observation suggests that the bridging oxygen is not essential for the inhibitor binding to bmFabV. This might result from changes of the binding model between the inhibitors and the enzyme in which the hydrogen bond between the oxygen atom and the active site residue no longer exists. Subsequently we modified the oxygen atom of analogue **28** with different functional groups (**47-49**), however, none of these inhibitors was better than their parent molecule (**28**). Instead, we found that compounds with symmetrical structures (**44**, **46** and **50**) have higher potency for the enzyme inhibition. Our best compound hexachlorophene (**50**) has a Ki value of 57 nM which is 8 fold lower than that of triclosan (0.42 µM).

The structure of hexachlorophene is highly substituted and symmetrical with a carbon as the bridging atom. We speculate that triclosan and hexachlorophene have different models of binding to the enzyme. Detailed inhibition studies were performed with several representative molecules that revealed two distinct inhibition mechanisms. For triclosan and its diaryl ether derivatives, a competitive mechanism with respect to NADH and an uncompetitive mechanism with respect to DD-CoA were observed. However, competitive inhibition with respect to DD-CoA and uncompetitive inhibition with respect to NADH were observed for

hexachlorophene (**50**) and other symmetrical molecules (**44** and **46**). The inhibition studies have shown that triclosan binds to the E-NAD$^+$ product complex. A different inhibition mechanism of hexachlorophene and other symmetrical inhibitors suggests that they might prefer binding to other reaction intermediates. As shown earlier in this chapter, the enzyme catalyzes the reaction through a sequential bi bi mechanism with NADH bound first and NAD$^+$ released in the last step. Competitive inhibition with respect to DD-CoA indicates that these inhibitors only bind to the free E or E-NADH form at the same binding site as DD-CoA. Uncompetitive inhibition with respect to NADH suggests that these inhibitors bind after NADH binds to the enzyme. Together, these data suggests that hexachlorophene and the two other symmetrical inhibitors bind the E-NADH complex (**Figure 4.7**).
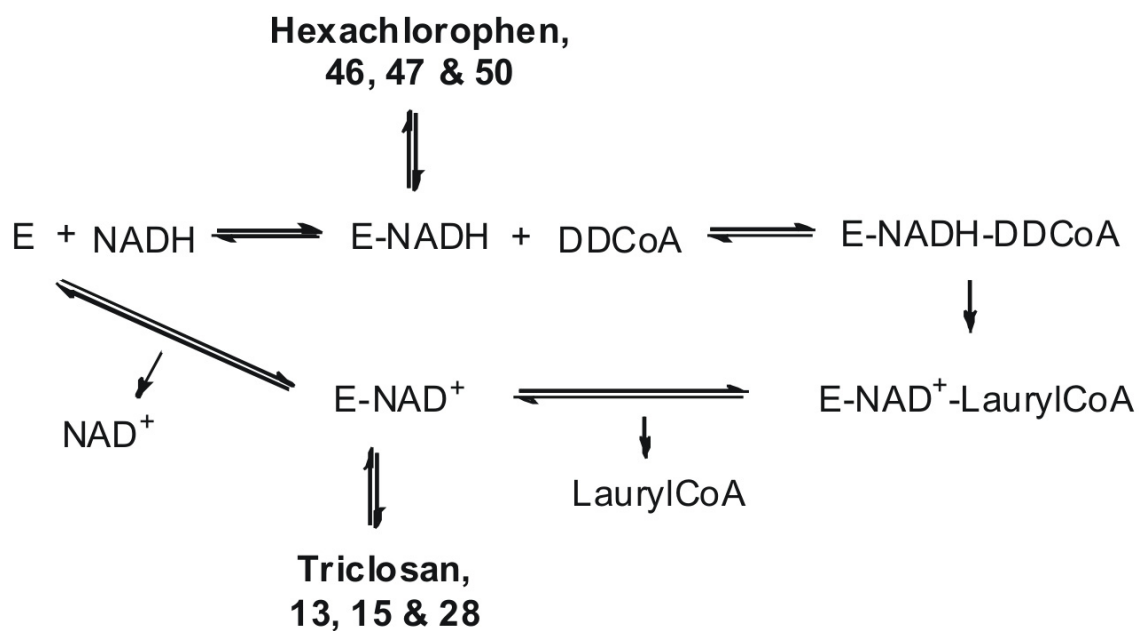
Figure 4.7: Different Binding Modes of Inhibitors during bmFabV Catalyzed Reaction. Triclosan and diaryl ether inhibitors prefer to bind to E-NAD$^+$ product complex, while hexachlorophene and other symmetrical inhibitors bind to E-NADH form preferably.

Conclusions

Here we reported the cloning, expression and purification of bmFabV and demonstrated that it is a NADH dependent enoyl-ACP reductase. The impact of site-directed mutagenesis on catalytic activity is consistent with the fact that bmFabV is a member of the short chain dehydrogenase reductase superfamily. We have studied in detail the mechanism of bmFabV inhibition by this diaryl ether. SAR studies based on triclosan as the lead molecule were performed and identified a series of inhibitors with submicromolar inhibition constants. Inhibition mechanism studies reveal two categories of inhibitors with different enzyme-cofactor preference.

References:

1. Schadewaldt, H. (1975) Discovery of glanders bacillus, *Dtsch. Med. Wochenschr. 100*, 2292-2295.

2. Whitlock, G. C., Estes, D. M., and Torres, A. G. (2007) Glanders: off to the races with *Burkholderia mallei*, *FEMS Microbiol. Lett. 277*, 115-122.

3. Gilad, J., Harary, I., Dushnitsky, T., Schwartz, D., and Amsalem, Y. (2007) *Burkholderia mallei* and *Burkholderia pseudomallei* as bioterrorism agents: national aspects of emergency preparedness, *Isr. Med. Assoc. J. 9*, 499-503.

4. Wheelis, M. (1998) First shots fired in biological warfare, *Nature 395*, 213.

5. Rotz, L. D., Khan, A. S., Lillibridge, S. R., Ostroff, S. M., and Hughes, J. M. (2002) Public health assessment of potential biological terrorism agents, *Emerg. Infect. Dis. 8*, 225-230.

6. Horn, J. K. (2003) Bacterial agents used for bioterrorism, *Surg. Infect. (Larchmt) 4*, 281-287.

7. Heath, R. J., and Rock, C. O. (2004) Fatty acid biosynthesis as a target for novel antibacterials, *Curr. Opin. Investig. Drugs 5*, 146-153.

8. Heath, R. J., White, S. W., and Rock, C. O. (2001) Lipid biosynthesis as a

target for antibacterial agents, *Prog. Lipid Res. 40*, 467-497.

9.   White, S. W., Zheng, J., Zhang, Y. M., and Rock. (2005) The structural biology of type II fatty acid biosynthesis, *Annu. Rev. Biochem. 74*, 791-831.

10.   McMurry, L. M., Oethinger, M., and Levy, S. B. (1998) Triclosan targets lipid synthesis, *Nature 394*, 531-532.

11.   Heath, R. J., Yu, Y. T., Shapiro, M. A., Olson, E., and Rock, C. O. (1998) Broad spectrum antimicrobial biocides target the FabI component of fatty acid synthesis, *J. Biol. Chem. 273*, 30316-30320.

12.   Musser, J. M., Kapur, V., Williams, D. L., Kreiswirth, B. N., van Soolingen, D., and van Embden, J. D. (1996) Characterization of the catalase-peroxidase gene (katG) and inhA locus in isoniazid-resistant and -susceptible strains of *Mycobacterium tuberculosis* by automated DNA sequencing: restricted array of mutations associated with drug resistance, *J. Infect. Dis. 173*, 196-202.

13.   Tonge, P. J., Kisker, C., and Slayden, R. A. (2007) Development of modern InhA inhibitors to combat drug resistant strains of *Mycobacterium tuberculosis*, *Curr. Top. Med. Chem. 7*, 489-498.

14.   Bergler, H., Wallner, P., Ebeling, A., Leitinger, B., Fuchsbichler, S., Aschauer, H., Kollenz, G., Hogenauer, G., and Turnowsky, F. (1994) Protein

EnvM is the NADH-dependent enoyl-ACP reductase (FabI) of *Escherichia coli*, *J. Biol. Chem. 269*, 5493-5496.

15. Lu, H., England, K., am Ende, C., Truglio, J. J., Luckner, S., Reddy, B. G., Marlenee, N. L., Knudson, S. E., Knudson, D. L., Bowen, R. A., Kisker, C., Slayden, R. A., and Tonge, P. J. (2009) Slow-onset inhibition of the FabI enoyl reductase from *Francisella tularensis*: residence time and in vivo activity, *ACS Chem. Biol. 4*, 221-231.

16. Zhang, Y. M., White, S. W., and Rock, C. O. (2006) Inhibiting bacterial fatty acid synthesis, *J. Biol. Chem. 281*, 17541-17544.

17. Heath, R. J., and Rock, C. O. (2000) A triclosan-resistant bacterial enzyme, *Nature 406*, 145-146.

18. Heath, R. J., Su, N., Murphy, C. K., and Rock, C. O. (2000) The enoyl-acyl-carrier-protein reductases FabI and FabL from *Bacillus subtilis*, *J. Biol. Chem. 275*, 40128-40133.

19. Massengo-Tiasse, R. P., and Cronan, J. E. (2008) *Vibrio cholerae* FabV defines a new class of enoyl-acyl carrier protein reductase, *J. Biol. Chem. 283*, 1308-1316.

20. Sivaraman, S., Sullivan, T. J., Johnson, F., Novichenok, P., Cui, G., Simmerling, C., and Tonge, P. J. (2004) Inhibition of the bacterial enoyl

reductase FabI by triclosan: a structure-reactivity analysis of FabI inhibition by triclosan analogues, *J. Med. Chem. 47*, 509-518.

21. Sullivan, T. J., Truglio, J. J., Boyne, M. E., Novichenok, P., Zhang, X., Stratton, C. F., Li, H. J., Kaur, T., Amin, A., Johnson, F., Slayden, R. A., Kisker, C., and Tonge, P. J. (2006) High affinity InhA inhibitors with activity against drug-resistant strains of *Mycobacterium tuberculosis*, *ACS Chem. Biol. 1*, 43-53.

22. am Ende, C. W., Knudson, S. E., Liu, N., Childs, J., Sullivan, T. J., Boyne, M., Xu, H., Gegina, Y., Knudson, D. L., Johnson, F., Peloquin, C. A., Slayden, R. A., and Tonge, P. J. (2008) Synthesis and *in vitro* antimycobacterial activity of B-ring modified diaryl ether InhA inhibitors, *Bioorg. Med. Chem. Lett. 18*, 3029-3033.

23. Parikh, S., Moynihan, D. P., Xiao, G., and Tonge, P. J. (1999) Roles of tyrosine 158 and lysine 165 in the catalytic mechanism of InhA, the enoyl-ACP reductase from *Mycobacterium tuberculosis*, *Biochemistry 38*, 13623-13634.

24. Cleland, W. W. (1963) The kinetics of enzyme-catalyzed reactions with two or more substrates or products. I. Nomenclature and rate equations, *Biochim. Biophys. Acta 67*, 104-137.

25. Cleland, W. W. (1963) The kinetics of enzyme-catalyzed reactions with two or more substrates or products. II. Inhibition: nomenclature and theory, *Biochim. Biophys. Acta 67*, 173-187.

26. Marcinkeviciene, J., Jiang, W., Kopcho, L. M., Locke, G., Luo, Y., and Copeland, R. A. (2001) Enoyl-ACP reductase (FabI) of *Haemophilus influenzae*: steady-state kinetic mechanism and inhibition by triclosan and hexachlorophene, *Arch. Biochem. Biophys. 390*, 101-108.

27. Kapoor, M., Dar, M. J., Surolia, A., and Surolia, N. (2001) Kinetic determinants of the interaction of enoyl-ACP reductase from *Plasmodium falciparum* with its substrates and inhibitors, *Biochem. Biophys. Res. Commun. 289*, 832-837.

28. Xu, H., Sullivan, T. J., Sekiguchi, J., Kirikae, T., Ojima, I., Stratton, C. F., Mao, W., Rock, F. L., Alley, M. R., Johnson, F., Walker, S. G., and Tonge, P. J. (2008) Mechanism and inhibition of saFabI, the enoyl reductase from *Staphylococcus aureus*, *Biochemistry 47*, 4228-4236.

29. Ward, W. H., Holdgate, G. A., Rowsell, S., McLean, E. G., Pauptit, R. A., Clayton, E., Nichols, W. W., Colls, J. G., Minshull, C. A., Jude, D. A., Mistry, A., Timms, D., Camble, R., Hales, N. J., Britton, C. J., and Taylor, I. W. (1999) Kinetic and structural characteristics of the inhibition of enoyl (acyl

carrier protein) reductase by triclosan, *Biochemistry 38*, 12514-12525.

30. Fawcett, T., Copse, C. L., Simon, J. W., and Slabas, A. R. (2000) Kinetic mechanism of NADH-enoyl-ACP reductase from *Brassica napus*, *FEBS Lett. 484*, 65-68.

31. Roujeinikova, A., Levy, C. W., Rowsell, S., Sedelnikova, S., Baker, P. J., Minshull, C. A., Mistry, A., Colls, J. G., Camble, R., Stuitje, A. R., Slabas, A. R., Rafferty, J. B., Pauptit, R. A., Viner, R., and Rice, D. W. (1999) Crystallographic analysis of triclosan bound to enoyl reductase, *J. Mol. Biol. 294*, 527-535.

32. Baldock, C., Rafferty, J. B., Stuitje, A. R., Slabas, A. R., and Rice, D. W. (1998) The X-ray structure of *Escherichia coli* enoyl reductase with bound NAD^+ at 2.1 A resolution, *J. Mol. Biol. 284*, 1529-1546.

33. Rozwarski, D. A., Vilcheze, C., Sugantino, M., Bittman, R., and Sacchettini, J. C. (1999) Crystal structure of the *Mycobacterium tuberculosis* enoyl-ACP reductase, InhA, in complex with NAD^+ and a C16 fatty acyl substrate, *J. Biol. Chem. 274*, 15582-15589.

34. Rafferty, J. B., Simon, J. W., Baldock, C., Artymiuk, P. J., Baker, P. J., Stuitje, A. R., Slabas, A. R., and Rice, D. W. (1995) Common themes in redox chemistry emerge from the X-ray structure of oilseed rape (*Brassica*

napus) enoyl acyl carrier protein reductase, *Structure 3*, 927-938.

35.   Thompson, J. D., Higgins, D. G., and Gibson, T. J. (1994) CLUSTAL W: improving the sensitivity of progressive multiple sequence alignment through sequence weighting, position-specific gap penalties and weight matrix choice, *Nucleic Acids Res. 22*, 4673-4680.

36.   Waterhouse, A. M., Procter, J. B., Martin, D. M., Clamp, M., and Barton, G. J. (2009) Jalview Version 2--a multiple sequence alignment editor and analysis workbench, *Bioinformatics 25*, 1189-1191.

37.   Jornvall, H., Persson, B., Krook, M., Atrian, S., Gonzalez-Duarte, R., Jeffery, J., and Ghosh, D. (1995) Short-chain dehydrogenases/reductases (SDR), *Biochemistry 34*, 6003-6013.

38.   Sivaraman, S., Zwahlen, J., Bell, A. F., Hedstrom, L., and Tonge, P. J. (2003) Structure-activity studies of the inhibition of FabI, the enoyl reductase from *Escherichia coli*, by triclosan: kinetic analysis of mutant FabIs, *Biochemistry 42*, 4406-4413.

39.   Rafi, S., Novichenok, P., Kolappan, S., Zhang, X., Stratton, C. F., Rawat, R., Kisker, C., Simmerling, C., and Tonge, P. J. (2006) Structure of acyl carrier protein bound to FabI, the FASII enoyl reductase from *Escherichia coli*, *The J. Biol. Chem. 281*, 39285-39293.

40. Fillgrove, K. L., and Anderson, V. E. (2001) The mechanism of dienoyl-CoA reduction by 2,4-dienoyl-CoA reductase is stepwise: observation of a dienolate intermediate, *Biochemistry 40*, 12412-12421.

41. Filling, C., Berndt, K. D., Benach, J., Knapp, S., Prozorovski, T., Nordling, E., Ladenstein, R., Jornvall, H., and Oppermann, U. (2002) Critical residues for structure and catalysis in short-chain dehydrogenases/reductases, *J. Biol. Chem. 277*, 25677-25684.

42. Perozzo, R., Kuo, M., Sidhu, A. S., Valiyaveettil, J. T., Bittman, R., Jacobs, W. R., Jr., Fidock, D. A., and Sacchettini, J. C. (2002) Structural elucidation of the specificity of the antibacterial agent triclosan for malarial enoyl acyl carrier protein reductase, *J. Biol. Chem. 277*, 13106-13114.

43. Lu, H., and Tonge, P. J. (2008) Inhibitors of FabI, an enzyme drug target in the bacterial fatty acid biosynthesis pathway, *Acc. Chem. Res. 41*, 11-20.

44. Stewart, M. J., Parikh, S., Xiao, G., Tonge, P. J., and Kisker, C. (1999) Structural basis and mechanism of enoyl reductase inhibition by triclosan, *J. Mol. Biol. 290*, 859-865.

45. Pidugu, L. S., Kapoor, M., Surolia, N., Surolia, A., and Suguna, K. (2004) Structural basis for the variation in triclosan affinity to enoyl reductases, *J. Mol. Biol. 343*, 147-155.

46. Parikh, S. L., Xiao, G., and Tonge, P. J. (2000) Inhibition of InhA, the enoyl reductase from *Mycobacterium tuberculosis*, by triclosan and isoniazid, *Biochemistry 39*, 7645-7650.

47. Luckner, S., Liu, N., am Ende, C., Tonge, P. J., and Kisker, C. (2010) A slow, tight-binding inhibitor of InhA, the enoyl-ACP reductase from *Mycobacterium tuberculosis*, *J. Biol. Chem.* Epub.

48. Rawat, R., Whitty, A., and Tonge, P. J. (2003) The isoniazid-NAD adduct is a slow, tight-binding inhibitor of InhA, the *Mycobacterium tuberculosis* enoyl reductase: adduct affinity and drug resistance, *Proc. Natl. Acad. Sci. U.S.A. 100*, 13881-13886.

49. Zhu, L., Lin, J., Ma, J., Cronan, J. E., and Wang, H. (2010) Triclosan resistance of *Pseudomonas aeruginosa* PAO1 is due to FabV, a triclosan-resistant enoyl-acyl carrier protein reductase, *Antimicrob. Agents Chemother. 54*, 689-698.

Chapter V. Functional Replacement of the *E. coli* FabI Enzyme with the Enoyl-ACP Reductases from *B. mallei:* Exploring the Function of These Enzymes in Unsaturated Fatty Acid Biosynthesis

Introduction

Diversity in Enoyl-ACP Reductases. Most enzymes in the FAS-II pathways are highly conserved among different bacterial strains and the FabI enoyl-ACP reductase was originally considered to be the only enzyme catalyzing the last step in the elongation cycle (*1*). Bacteria using FabI as the only enoyl-ACP reductase are sensitive to triclosan, a potent inhibitor of FabI enzymes (*2-3*). However, other bacteria were later found to be resistant to triclosan, suggesting the presence of a triclosan-resistant enoyl-ACP reductase. This was soon demonstrated by the isolation of a second enoyl-ACP reductase (FabK) from *S. pneumonia*, which is intrinsically resistant to triclosan (*4*). The family of enoyl-ACP reductases was recently expanded by the introduction of two new isoenzymes, FabL and FabV, from *B. subtilis* and *V. cholerae* respectively (*5-6*).

Among all the four enzymes identified, FabI, FabL and FabV are members of the short chain dehydrogenase/reductase (SDR) superfamily which shares a

significantly conserved folding pattern despite the low sequence homology (*7*).

Crystal structures of the FabI enzymes from many organisms have been solved

(**Figure 5.1A**) (*8*). Although no crystal structure was available for the FabL and

FabV enzymes, all SDR enoyl-ACP reductases have a conserved Tyr-(Xaa)$_x$-Lys
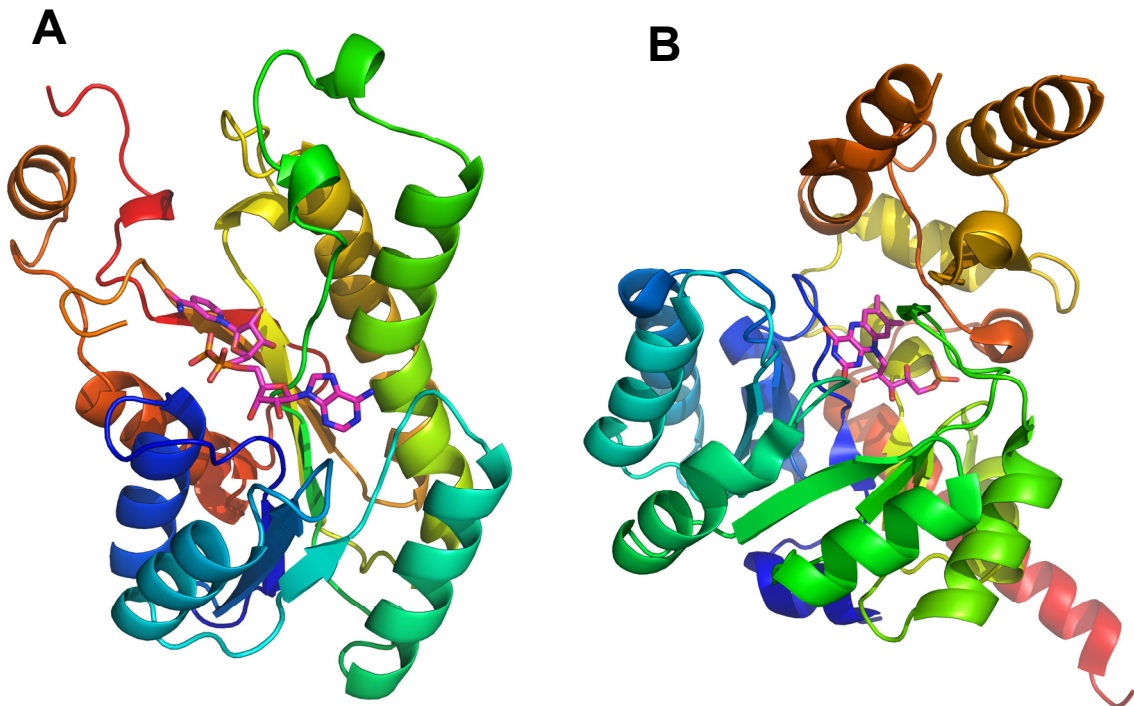
Figure 5.1: Crystal Structures of FabI and FabK from *E. coli* and *S. pneumoniae*. A) ecFabI monomer with NAD$^+$ bound (1DFI.pdb). Carbon atoms of NAD$^+$ are shown in magenta. **B**) FabK monomer from *S. pneumonia* with Flavin bound (2Z6I.pdb). Carbon atoms of flavin are colored in magenta.

motif for catalysis. FabI and FabL have six amino acids between the catalytic

tyrosine and lysine, while the spacing in FabV is eight residues (*9*). NADH is

preferably used as the cofactor in the reactions of all the SDR enoyl-ACP

reductases except the FabI from *S. aureus* that uses NADPH more efficiently as

the hydride source. Unlike the SDR enoyl-ACP reductases, FabK is a

flavin-dependent oxidoredutase which has a triose phosphate isomerase (TIM)

barrel structure (**Figure 5.1B**). The Tyr-$(Xaa)_x$-Lys motif is no longer conserved,

instead an active site histidine is proposed to play an important role in catalysis

(*10*). NADH is still the reductant but only indirectly as it reduces the bound flavin

and the reduced flavin then catalyzes the reduction reaction (*7*).

It is important to note that more than one enoyl-ACP reductase can be found in

certain bacteria. For instance, both of the FabI and FabV enzymes are found in *P.*

aeruginosa (*5, 11*). Although all the enoyl-ACP reductases have been thoroughly

studied *in vitro* by steady state kinetics and X-ray crystallography, the biological

reasons why different bacteria like to use different enoyl-ACP reductases and why

bacteria need more than one enoyl-ACP reductase are still unknown.

Bacterial Unsaturated Fatty Acid (UFA) Biosynthesis. The barrier function of the

cell membrane critically depends on the physical state of the lipid bilayer (*12-13*).

It has been shown that normal cell function requires an appreciable fraction of disordered membrane lipids (*14-15*). In fact, at physiological temperature, the lipid bilayers of most organisms are entirely or mostly fluid (*16-17*). The fluidity of cell membrane was controlled by the ratio between saturated fatty acids (SFAs) and unsaturated fatty acids (UFAs). This ratio was thermally controlled and more UFAs are synthesized at low temperature so that the fluidity of membrane can be maintained in most bacteria (*17*). Although the majority of products synthesized by FAS-II pathway are SFAs, it is also responsible for the biosynthesis of UFAs (*18-19*).

UFA biosynthesis pathway in *E. coli* is the prototype of such pathways. The key players in this pathway are FabA and FabB. As mentioned before, the SFA biosynthesis starts from acetyl-CoA, while the initial point of the UFA biosynthesis is 3-hydroxydecanoyl-ACP (**Figure 5.2A**) (*20*). In this pathway, FabA, a bifunctional enzyme, catalyzes the dehydration and isomerization of 3-hydroxydecanoyl-ACP and yields a *cis*-3-double bond in the product which cannot be reduced by the enoyl-ACP reductase (*21-22*). The *cis*-3-decenoyl-ACP is directly used for the condensation reaction catalyzed by β-ketoacyl transferase in the next elongation cycle. Two β-ketoacyl transferases (FabB and FabF) are found in *E. coli*, however only FabB can condense *cis*-3-decenoyl-ACP with

176
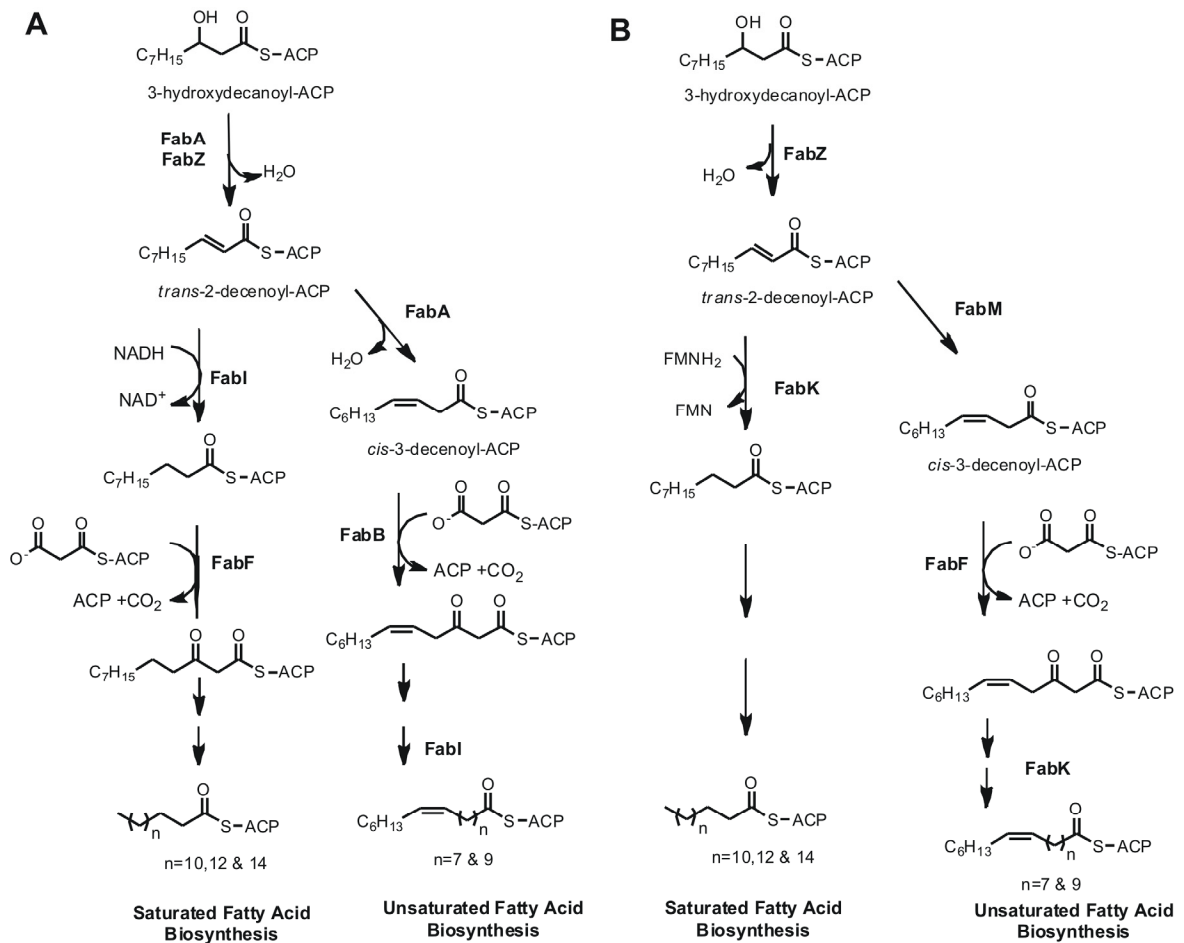
Figure 5.2: Saturated and Unsaturated Fatty Acid Biosynthesis Pathways in *E. coli* and *S. pneumoniae*. Structures of final fatty acids found in the lipids of *E. coli* and *S. pneumoniae*. Enzymes catalyzing each step are in bold. **A**) SFA and UFA biosynthesis pathways in *E coli*; **B**) SFA and UFA biosynthesis pathways in *S. pneumoniae*.

177

malonyl-ACP (*18, 23*). Knockout experiments demonstrated that *fabB* gene is essential for cell growth and *fabB* null mutant grown with exogenous UFAs can still synthesize SFAs (*24-26*). These experiments suggest that only FabB catalyzes some key intermediates in UFA biosynthesis while FabF cannot. Although FabF is not essential for the viability of *E. coli*, knockout of *fabF* gene results an *E. coli* mutant strain that is incapable of synthesizing the C18:1 fatty acid and thermally regulating the fatty acid composition in the lipid. It has been hypothesized that FabF catalyzes the condensation from C16:1 to C18:1 which is the main UFA in the lipid bilayers of *E. coli* (*26-27*). Although the isomerization catalyzed by FabA is essential for the UFA biosynthesis, this is not the rate-determining step. Overexpression of FabA in *E. coli* increases the content of SFAs, while overexpression of FabB can reverse this effect (*28*). The relative level of FabA and FabB gene expression appears to control the basal ratio between UFA and SFA in *E. coli*. However, the expression level of FabI in determining the basal ratio has not been investigated.

A second mechanism to synthesize UFAs was discovered in *S. pneumoniae* by Rock and his coworkers (*29*). Although no FabA or FabB homologue was found, significant amounts of monounsaturated fatty acids were detected in this organism. A new *trans*-2, *cis*-3, enoyl-ACP isomerase (FabM) in the gene cluster

of FAS-II enzymes was then identified (**Figure 5.2B**). Genetic experiments as well kinetic studies demonstrated that this enzyme diverts the fatty acid biosynthesis to UFA branch (*30-31*), while FabF, which is the only β-ketoacyl transferase in *S. pneumoniae*, catalyzes the condensation for both SFA and UFA biosynthesis. Interestingly, complementation of *E. coli fabA* null mutant with FabM plasmid was not able to restore the viability *E. coli* cells, suggesting that FabM cannot compete with FabI to divert the UFA biosynthesis in *E. coli* (*29*).

Recent bacterial genome sequences show that FabA and FabB are only conserved in α- and γ-proteobacteria and FabM is specific for streptococci (*32-33*). Since many other bacteria synthesize UFAs anaerobically, it seems that there are alternative UFA biosynthesis pathways that have not been identified.

The Enoyl-ACP Reductases in B. mallei. A BLAST search using *E. coli* FAS-II enzymes identifies most homologues in *B. mallei* ATCC 23344 (**Table 5.1**). Two FabI homologues were identified from our BLAST search, one in chromosome 1 (FabI1, 63% identify to ecFabI) and the second in chromosome 2 (FabI2, 42% identity to ecFabI), while a homologue of vcFabV (bmFabV) was also located on chromosome 1 (56% identity to FabV from *V. cholerae*). Kinetic measurements demonstrated that both FabI1 and FabV can catalyze the reduction reaction *in*

179

vitro, while FabI2 has no activity. Gene expression experiments shown that FabI1 and FabV are expressed in *B. mallei*, but the expression level of FabI2 is very low (**Figure 5.3**).

Table 5.1: Genes in FAS-II Pathway from *B. mallei* ATCC 23344

Gene ID[a]	Enzyme	Length
BMA1608	**FabI1:** enoyl-ACP reductase	263 residues
BMAA1403	**FabI2:** enoyl-ACP reductase	253 residues
BMA0885	**FabV:** enoyl-ACP reductase	397 residues
BMA0530	**FabH:** β-ketoacyl-ACP synthase III	329 residues
BMA0531	**FabD:** Malonyl-CoA ACP transacylase	310 residues
BMA0532	**FabG:** β-ketoacyl-ACP reductase	249 residues
BMA0533	**AcpP:** Acyl carrier protein	79 residues
BMA0534	**FabF:** β-ketoacyl-ACP synthase II	412 residues
BMA1544	**FabZ:** β-hydroxyacyl-ACP synthase	155 residues

[a]Gene ID obtained from KEGG
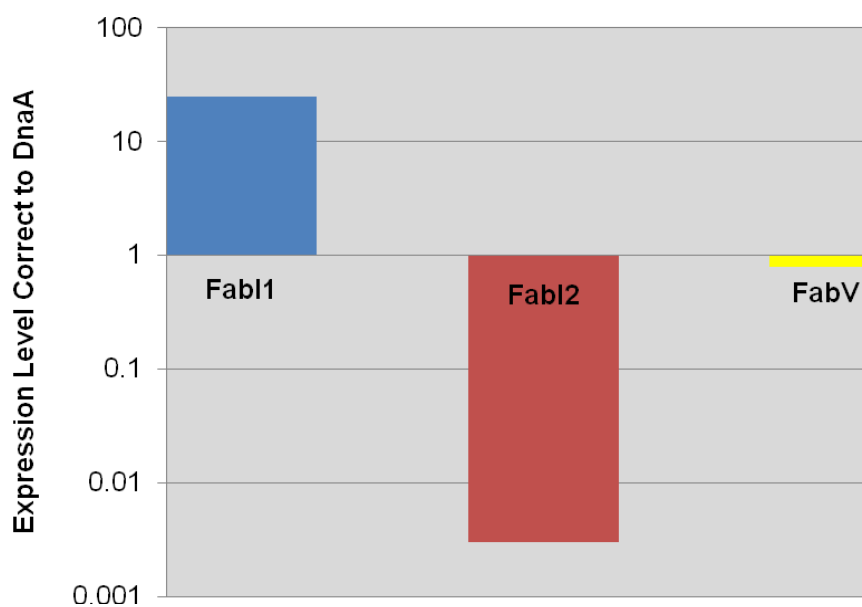
**Figure 5.3: Gene Expression Level of Putative Enoyl-ACP Reductases from
B. mallei.** Expression levels of different genes have been normalized to the
expression level of dnaA. This experiment was done by Dr. Kathleen England at
the Colorado State University.

UFA Biosynthesis in B. mallei. Previous bioinformatic analysis has shown that

FabA and FabB are only found in α- and γ-proteobacteria (*32*). As predicted, FabA

and FabB homologues are not found in *B. mallei* since it is a β-proteobacterium

(**Table 5.1**). There are two possibilities to explain the UFA biosynthesis in this

organism. The first one is that the FabZ and FabF enzymes from *B. mallei* can

functionally replace the activity of *E. coli* FabA and FabB, as is found in

Enterococcus faecalis (*33*). The second possibility is that there is a FabM like

181

isomerase existing in *B. mallei*. A BLAST search in the genome of *B. mallei* identified an ORF (bmaa0541) encoding an enzyme to 31% identical and 50% similar to the FabM enzyme from *S. pneumoniae*, suggesting the existence of a possible FabM homologue in *B. mallei.* However, since FabM cannot compete with the FabI enzyme to make UFAs (*33*), *B. mallei* might need to express another enoyl-ACP reductase (bmFabV) to compete with bmFabI and divert the intermediates to the UFA biosynthesis. We hypothesize that bmFabI serve as the enoyl-ACP reductase in SFA biosynthesis, while bmFabV compete with bmFabI to divert the intermediates into UFA biosynthesis in *B. mallei* (**Figure 5.4**)

Project Goals. In this chapter, the *in vivo* functions of bmFabI and bmFabV, especially their different roles in SFA and UFA biosynthesis, will be explored. In order to substantiate our hypothesis, genes encoding these two enzymes will be transformed into a temperature sensitive *E. coli* strain and kinetic parameters of both enzymes towards different substrates will be determined.
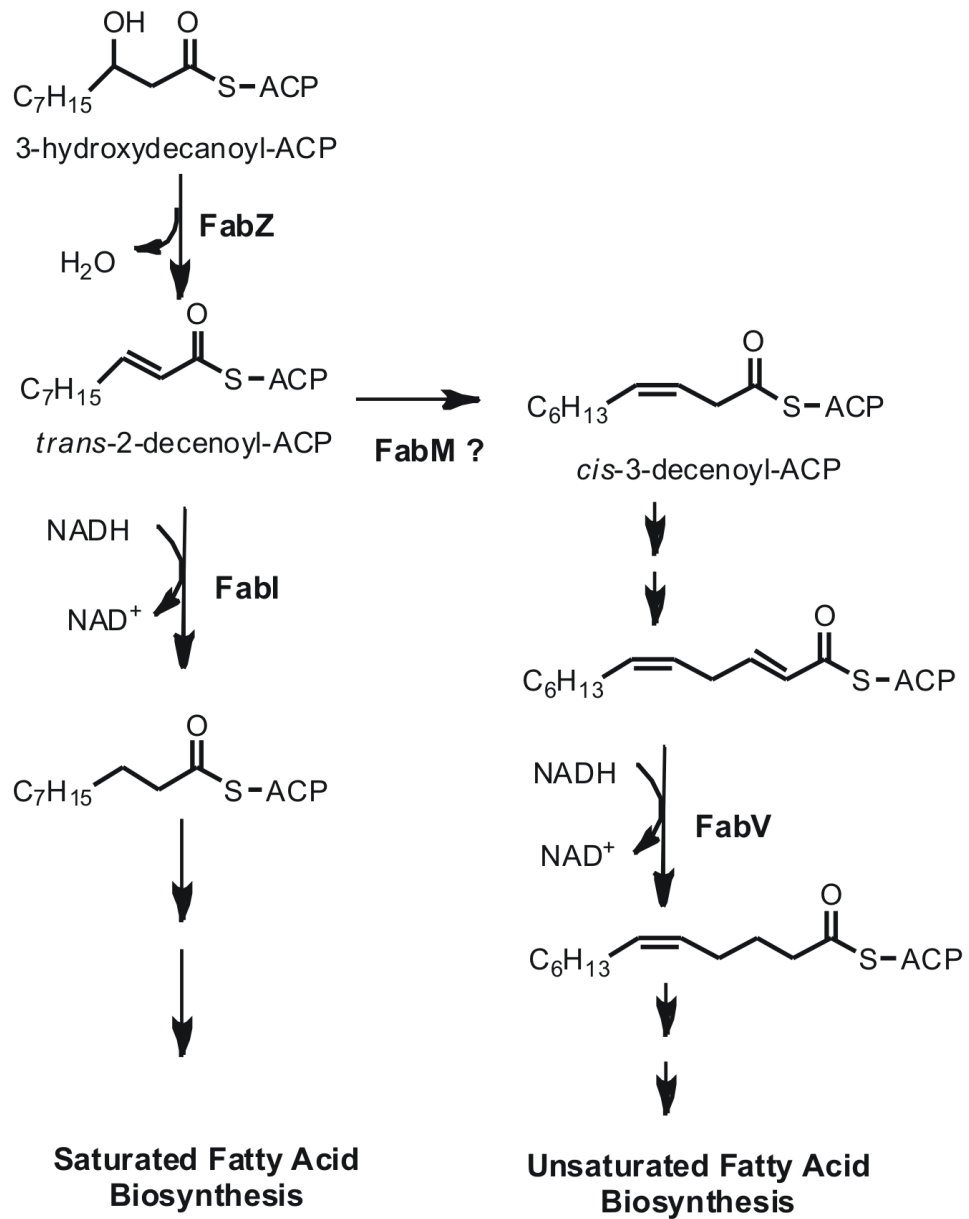
Figure 5.4: Proposed SFA and UFA Biosynthesis Pathway in _B. mallei_.

Materials and Methods

Materials. The temperature sensitive *E. coli* strain (JP1111) was purchased from the Coli Genetic Stock Center at Yale University and pBAD vector and DH10B are gifted by Prof. Ryan Mehl at Franklin and Marshall College. Triclosan was a gift from Ciba while *trans*-2-Dodecenoic acid was purchased from TCI. All other chemical reagents were obtained from Sigma-Aldrich. Crotonyl-CoA (Cr-CoA), *trans*-2-octenoyl-CoA, *trans*-2-decenoyl-CoA, *trans*-2-decenoyl-NAC and DD-CoA were synthesized as described in **Chapter II**. *cis*-3-Decenoyl-NAC and (2E,5Z)-dodeca-2,5-dienoyl-CoA (*cis*-5-*trans*-2-dienoyl-CoA) were synthesized by Dr. Gopal Reddy in our lab.

Construction of Plasmids and Growth Media. Genes of ecFabI, ftuFabI, saFabI, bmFabI and bmFabV were amplified using the primers listed in **Table 5.2** and inserted into the Invitrogen pBAD/Myc-His C vector at different restriction sites (underlined). After purification from XL1Blue cells (Stratagene) using a DNA purification and gel extraction kit (Qiagen Inc). The correct sequence of the insert was confirmed using ABI DNA sequencing. Luria Broth (LB) media was used as the rich media for *E. coli* growth. Ampicillin and L-arabinose were used at a final concentration of 0.2 mg/ml and 0.2% (W/V), respectively.

Expression and Purification of ecFabI, ftuFabI, saFabI, bmFabI and bmFabV. Protein expression and purification protocols for FabI from ecFabI, and *S. aureus* (saFabI) were available from previous work (*2, 34*). The FabI enzyme from *F. tularensis* (ftuFabI) and the FabV enzyme from *B. mallei* (bmFabV) were expressed and purified as described in **Chapter II** and **Chapter IV**, respectively. Recombinant FabI protein from *B. mallei* (bmFabI) was prepared by Nina Liu in our group.

Cloning, Overexpression and Purification of the Putative FabM (bmaa0541). The entire coding region of the gene (bmaa0541) encoded the putative FabM was amplified using the primers 5'-CATG<u>CCATGG</u>GCATGTCCTACCAGACGATTCGC-3' (forward) and 5'-CCC<u>AAGCTT</u>GGCGTCCTTCGAAGCGAGGGGC-3' (reverse) and inserted into the Invitrogen pBAD Myc/His C vector using the 5' NcoI and 3' HindIII restriction sites (underlined) with a His tag at the C-terminus. The constructed plasmid was then purified from XL1Blue cells (Stratagene) using a DNA purification and gel extraction kit from Qiagen Inc., followed with sequencing using ABI DNA sequencing.

Protein expression was performed by transforming the plasmid into *E. coli* DH10B cells which were then grew in 10 ml of Luria Broth (LB) media containing

Table 5.2: Primers Used for Cloning

Primer	Enzyme/Gene ID[a]	Sequence[b]
p^{ecFabI} forward		5'GG<u>GGTACC</u>ATGGTTTTCTTTC CGGTAAGCGC3'
p^{ecFabI} reversed	ecFabI/b1288	5'CG<u>GAATTC</u>TTATTTCAGTTCGA GTTCGTTCAT3'
p^{ftuFabI} forward		5'GG<u>GGTACC</u>ATGGGTTTTCTTT CCGGTAAGCGC3'
p^{ftuFabI} reversed	ftuFabI/FTT_0782	5'CG<u>GAATTC</u>TTATTGCAAAACAT TACCCATAGA3'
p^{saFabI} forward		5'GG<u>GGTACC</u>ATGTTAAATCTTGA AAACAAAACT3'
p^{saFabI} reversed	saFabI/SA0869	5'CCC<u>AAGCTT</u>TTAAATAACGTGA ACAAAGCTGTTGAA 3'
p^{bmFabI} forward		5'GG<u>GGTACC</u>ATGGGCTTTCTCG ACGGTAAAC3'
p^{bmFabI} reversed	bmFabI/BMA1608	5'CG<u>GAATTC</u>TTATTCCTCGAGG CCGGCCAT3'
p^{bmFabV} forward		5'GG<u>GGTACC</u>ATGATCATCAAAC CGCGCGTACGC3'
p^{bmFabV} reversed	bmFabV/BMA0885	5'CCC<u>AAGCTT</u>TCATTCGATCAGA TTCGGAATCCG3'

[a]Gene ID of corresponding enzymes are obtained from KEGG .
[b]Restriction sites are shown in underline.

0.2 mg/ml ampicillin in a 50 ml falcon tube at 37 ^{o}C overnight in a floor shaker.

The culture was used to inoculate 800 ml of LB media containing ampicillin (0.2

mg/ml) and grown at 37 ^{o}C until the optical density at 600 nm (O.D. 600)

increased to around 1.0. Induction was achieved by adding 0.2% L-arabinose for 16 h at 25 °C. Cells were harvested by centrifugation at 5,000 rpm for 15 min at 4 °C. The cell paste was resuspended in 30 ml of His-binding buffer (5 mM imidazole, 0.5 M NaCl, 20 mM Tris HCl, pH 7.9) and lysed by sonication. Cell debris was removed by centrifugation at 33,000 rpm for 60 min at 4 °C. The collected supernatant was loaded onto a His-bind column (1.5 cm x 15 cm) containing 4 ml of His-bind resin (Novagen), charged with 9 ml of charge buffer (Ni^{2+}). The column was washed with 60 ml of His-binding buffer and 30 ml of wash buffer (60 mM imidazole, 0.5 M NaCl, 20 mM Tris HCl, pH 7.9). Subsequently, the expressed protein was eluted using a gradient of 40 ml elute buffer (1 M imidazole, 0.5 M NaCl, 20 mM Tris HCl, pH 7.9) and 20 ml binding buffer mixture. Fractions containing the protein after elution were collected and imidazole was removed using a Sephadex G-25 column (1.5 cm x 55 cm) using 30 mM pipes, 150 mM NaCl and 1.0 mM EDTA at pH 8.0, as the storing buffer. The purity of the protein was judged by 12% sodium dodecyl sulfate-polyacrylamide gel electrophoresis (SDS-PAGE) with the giving a molecular weight of about 32 kDa. The concentration of the protein was determined by measuring the absorption at 280 nm using an extinction coefficient (ε) of 22,310 $M^{-1}cm^{-1}$ calculated from the primary sequence. The enzyme was stored at -80 $^{\circ}$C in the same buffer after

freezing with liquid N_2.

Cell Growth Curve Assay. The temperature sensitive *E. coli* strain (JP1111) was transformed with vectors with or without the enoyl-ACP reductase genes in a LB-ampicillin agar plate at 42 °C. A single colony was picked and used to inoculate 10 ml of Luria Broth (LB) media containing ampicillin and L-arabinose in a 50 ml falcon tube, which was then incubated for 18 h at 42 °C in a floor shaker. The saturated culture was then diluted 100-fold into 50 ml of fresh LB media containing ampicillin and L-arabinose and incubated in an orbital shaker at 42 °C until the cell growth reached the stationary phase. Optical density (O.D. 600) was measured every 30 min and data was processed with Microsoft Excel to obtain the growth curve. All the measurements were repeated for three times and the averages were used as the final readings.

Steady-state Kinetic Analysis. Steady-state kinetic parameters were determined at 25 °C using a Cary 300 Bio (Varian) spectrophotometer. For enoyl-ACP reductases, the reaction buffer used contains 30 mM PIPES, 1.0 mM EDTA and 0.15 mM NaCl at pH 7.9. Initial velocities were determined to monitor the oxidation of NADH to NAD^+ at 340 nm (ε = 6,300 $M^{-1}cm^{-1}$). K_m and k_{cat} values

of the different enoyl-ACP reductases toward DD-CoA and *cis*-5-*trans*-2-dienoyl-CoA were determined by varying the concentration of DD-CoA or *cis*-5-*trans*-2-dienoyl-CoA at a fixed concentration (250 µM) of NADH. Data sets were then fit to the Michaelis-Menten equation (eqn **5**) using GraFit (Erithacus).

$$v = V_{max}[S] / (K_m + [S]) \tag{5}$$

The isomerase activity was measured by monitoring the absorbance at 260 nm (ε = 6,700 $M^{-1}cm^{-1}$). A solution containing 100 µM of substrate (*trans*-2-decenoyl-NAC) or product (*cis*-3-decenoyl-NAC) in 10 mM sodium phosphate buffer (pH 7.0) was placed in a cuvette. Different concentrations (1 µM, 2 µM, 5 µM and 10 µM) of enzyme were added to initiate the reaction.

Results and Discussion

bmFabI and bmFabV Can Replace the Activity of ecFabI In Vivo. The *E. coli* JP1111 strain, also called the *fabI*(Ts) strain, allows cell growth at 30 $^{\circ}$C but blocks growth at 42 $^{\circ}$C. The temperature sensitivity of this strain has been demonstrated to result from a single point mutation at the *fabI* gene (*35-36*). To test the activity of bmFabI and bmFabV *in vivo*, the genes encoding bmFabI and bmFabV were cloned into the arabinose-inducible pBAD vector. The resulting plasmids (p^{bmFabI} and p^{bmFabV}) were introduced in to the temperature sensitive allele and the growth of transformants was examined at 42 $^{\circ}$C without the supplementation of exogenous fatty acids. It has been observed that both transformants can grow at the nonpermissive temperature in the absence of fatty acids (**Figure 5.5**). As a control, p^{ecFabI} vector (ecFabI) and pBAD vector were also transformed into the *E. coli* strain JP1111 separately. Growth of the strain complemented with p^{ecFabI} was observed at 42 $^{\circ}$C, while no growth was found for cells with pBAD vector (**Figure 5.5**). Finally, we also cotransformed p^{bmFabI} and p^{bmFabV} vectors into JP1111 to test the cell growth ability with both of the enoyl-ACP reducases expressed *in vivo*. The resulting cotransformant can also grow at the nonpermissive temperature (**Figure 5.5**). *In vivo* activity of other FabI enzyme, saFabI and ftuFabI were also tested. The *E. coli* strains containing p^{saFabI} and p^{ftuFabI} can both grow at 42 $^{\circ}$C

190

without fatty acid supplementation (**Figure 5.5**).
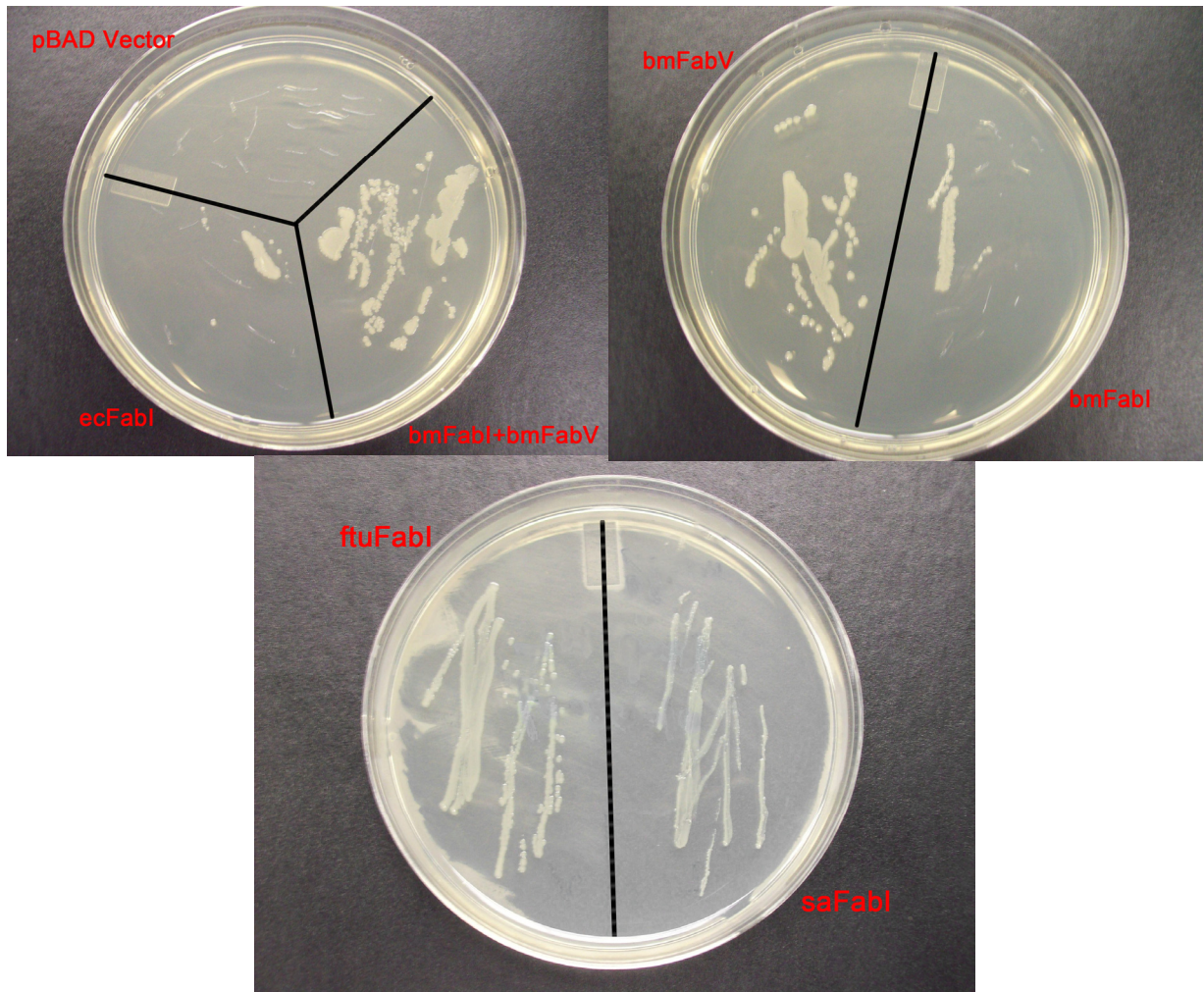
Figure 5.5: Complementation of Arabinose-dependent Growth of *E. coli* Strain JP1111 at 42 °C. Plasmid containing the genes encoding ecFabI, bmFabI, bmFabV, ftuFabI or saFabI were transformed into *E. coli* strain JP1111 which is not able to growth at 42 °C due to a mutation in the *fabI* gene. Ampicillin was used for selection and L-arabinose was used to induce protein expression.

Growth Phenotype of E. coli fabI(Ts) Mutant. It has been demonstrated that bmFabI or/and bmFabV can functionally replace the enoyl-ACP reductase activity of ecFabI in *E. coli*. However, a much lower O.D. 600 value was observed when an overnight culture was prepared from the *E. coli* temperature sensitive cells containing either bmFabI or bmFabV. Cell growth curves at 42 ^{o}C were then determined for *E. coli fal*(Ts) mutant strain containing different plasmids (**Figure 5.6**). As a control, no growth was found for the temperature sensitive strain carrying pBAD vector at 42 ^{o}C, suggesting that the native FabI activity was blocked at the nonpermissive temperature. The growth of *E. coli* strain with *ecfabI* gene was defined as the wt growth. Complementation with both *bmfabI* and *bmfabV* genes together in this strain restores the wt growth. However, a lag at the initial growth phase rate was observed with the complementation of either *bmfabI* or *bmfabV* genes alone.

Although either bmFabI or bmFabV can restore the viability of *E. coli* cells at nonpermissive temperature, the growth phenotypes of these cells are different. More importantly, cotransformation of *bmfabI* and *bmfabV* genes can overcome the growth deficiency of the *fal*(Ts) strain. It has been shown that *fabM* null mutant strain of *S. mutans* has a slower growth rate than that of the wt strain, due, presumably, to an inability to synthesize unsaturated fatty acids (UFAs) (*30*). It is

192

not clear that if the observed lag at the initial phase is a result of the perturbation of UFA biosynthesis in *B. mallei*. These data suggest that both bmFabI and bmFabV are probably required for the normal growth of *B. mallei* cells.
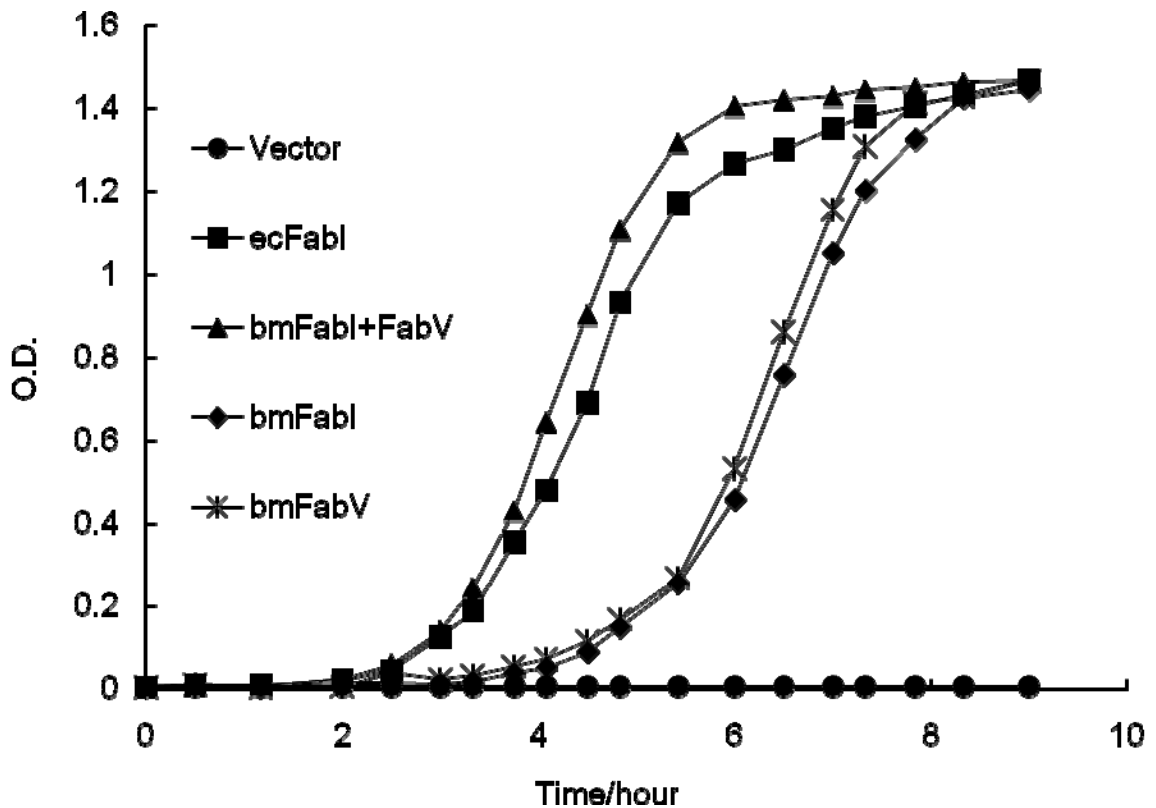
Figure 5.6: Cell Growth Curves of *E. coli* Strain JP1111 Transformed with Different Plasmids at 42 °C. Cells were transformed with different vectors and grown in liquid LB media. Ampicilin (0.2 mg/ml) and L-arabinose (0.2%) were used as antibiotic and inducer respectively.

Substrate Specificity of bmFabI and bmFabV. Recombinant bmFabI and bmFabV enzymes were expressed and purified. Steady state kinetics were used to determine the Michaelis-Menten constants of both enzymes toward different acyl substrates (**Table 5.3**). Both bmFabI and bmFabV have a preference for long acyl chain as the substrate. However, the k_{cat}/K_m values of bmFabV toward shorter acyl substrate, such as Cr-CoA and *trans*-2-octenoyl-CoA, are ~10-fold lower than those of bmFabI, revealing that bmFabV has a lower efficiency for catalyzing the reduction of short acyl substrates (C4 and C8). This inefficiency is overcome when the substrate length increases to twelve carbons. Indeed, the k_{cat}/K_m value of bmFabV toward DD-CoA is 497 $\mu M^{-1}s^{-1}$, almost 2 folds higher than that of bmFabI (300 $\mu M^{-1}s^{-1}$).

As mentioned before, the UFA biosynthesis pathway is initiated from the 3-hydroxydecanoyl-ACP. If the main function of bmFabV *in vivo* is to catalyze the reduction of unsaturated intermediates, it is possible that this enzyme has low catalytic efficiency toward short acyl chain substrates. Instead, SFA biosynthesis starts from acetyl-CoA and the enoyl-ACP reductase in this pathway has to be capable of reducing short acyl substrate such as Cr-ACP. In this case, kinetic data examining the substrate specificity of both enzymes supports the hypothesis that bmFabV might be the enoyl-ACP reductase that reduces intermediates in UFA

194

biosynthesis, while bmFabI is the enzyme that reduces saturated acyl chain intermediates.

Table 5.3: Kinetic Parameters of bmFabI and bmFabV toward Different Substrates

Substrate	bmFabI[a]	bmFabV
	k_{cat}/K_m ($\mu M^{-1}s^{-1}$)	k_{cat}/K_m ($\mu M^{-1}s^{-1}$)
Cr-CoA (C4)	1.2±0.1	0.15±0.01
trans-2-Octenoyl-CoA (C8)	11±1	1.5±0.1
trans-2-Decenoyl-CoA (C10)	60±7	34.2±2.2
trans-2-Dodecenoyl-CoA (C12)	300±18	497±19

[a]Data measured by Nina Liu

Preference of Different Enoyl-ACP Reductases toward the Saturated Acyl Chain Substrate and the Unsaturated Acyl Chain Substrate. To further confirm our hypothesis, two substrates were synthesized by mimicking the intermediates from both the SFA and UFA biosynthesis pathways (**Figure 5.7**). Kinetic parameters of the different enoyl-ACP reductases (ecFabI, ftuFabI, saFabI, bmFabI and

bmFabV) were measured and are shown in **Table 5.4**. As a reference, the percentage of monounsaturated fatty acids from the lipids of corresponding bacteria is also listed.
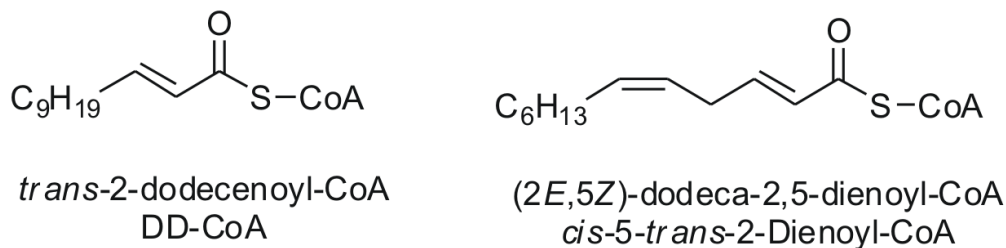
Figure 5.7: Structure of DD-CoA and *cis*-5-*trans*-2-Dienoyl-CoA

The FabI enzymes from *E. coli* and *F. tularensis*, which are the only enoyl-ACP reductase in the corresponding organisms, can efficiently catalyze the reduction of both DD-CoA and *cis*-5-*trans*-2-dienoyl-CoA. Surprisingly, the ratio of k_{cat}/K_m values toward the unsaturated substrate and saturated substrate correlate with their UFA content in the lipids from the respective organism. For saFabI, no activity was observed toward *cis*-5-*trans*-2-dienoyl-CoA, which is also consistent with the data that the lipids of *S. aureus* contains only trace amount of UFAs. These data suggest that bacteria control their UFA/SFA ratio by regulating the activity of the enoyl-AC reductase toward different intermediates in both SFA and

UFA biosynthesis pathways. The argument is debatable in *E. coli* system, since the UFA biosynthesis was proved to be modulated by FabA and FabB enzyme (*18*). However it is reasonable to hypothesize that for bacteria to have a high content of UFAs in their lipids, the enoyl-ACP reductase has to be capable of reducing the unsaturated intermediates in the UFA biosynthesis pathway.

Table 5.4: Kinetic Parameters of Enoyl-ACP Reductases from Different Organisms and Their UFA Content in the Lipid

Enzyme	DD-CoA	*cis*-**5**-*trans*-**2**-Dienoyl-CoA	Ratio[c]	UFA%[d]
	k_{cat}/K_m ($\mu M^{-1}s^{-1}$)	k_{cat}/K_m ($\mu M^{-1}s^{-1}$)		
ecFabI	24±6	8.4±1.3	0.35	33
ftuFabI	570±36	7.6±0.6	0.013	1.2
saFabI	0.8±0.1[a]	inactive[a]	0	trace
bmFabI	300±18[b]	0.92±0.06	0.003	32
bmFabV	497±19	85±3	0.23	

[a]Data measured by Hua Xu

[b]Data measured by Nina Liu

[c]Ratio = *cis*-5-*trans*-2-Dienoyl-CoA / DD-CoA (k_{cat}/K_m values)

[d]Percentage of monounsaturated fatty acid obtained from (*37-40*)

It was found that *B. mallei* have a similarly high UFA content as *E. coli* (**Table 5.4**). However, kinetic experiments have shown that bmFabI can only poorly catalyze reaction of *cis*-5-*trans*-2-dienoyl-CoA. The ratio of k_{cat}/K_m values toward DD-CoA and *cis*-5-*trans*-2-dienoyl-CoA of this enzyme is only 0.003, which is significantly lower than the UFA percentage of this organism. The inefficiency of the bmFabI enzyme to reduce the unsaturated fatty acid chain suggests that there might be another enoyl-ACP reductase that reduces the unsaturated intermediates for UFA biosynthesis. Kinetic data demonstrated that bmFabV can efficiently reduced *cis*-5-*trans*-2-dienoyl-CoA *in vitro* with a 90-fold increase in k_{cat}/K_m value compared to bmFabI.

In Vitro Activity of the Putative trans-2, cis-3, Enoyl-ACP Isomerase from B. mallei. Kinetic data suggests that bmFabV might compete with bmFabI to divert the UFA biosynthesis in *B. mallei*. It has also been shown that FabM from *S. pneumoniae* is not able to compete with ecFabI *in vivo*, since the complementation of FabM in *E coli fabA* null mutant cannot recover the cell viability (*29*). The isomerase in *B. mallei* has not been identified and there are two possibilities. The first possibility is that FabZ from *B. mallei* can function like the *E. coli* FabA enzyme which can catalyze both dehydration and isomerization. The

198

second possibility is that there is a FabM homologue which can catalyze the *trans*-2 to *cis*-3 isomerization. Since FabA and FabB are highly conserved in α- and γ- proteobacteria (*32*), it is more likely that there is a FabM homologue in *B. mallei.* Because FabM cannot compete with bmFabI, the organism has to be able to express another enoyl-ACP reductase (bmFabV) to divert intermediates into UFA biosynthesis.

A BLAST search in the genome of *B. mallei* identified an ORF (bmaa0541) encoding an enzyme to 31% identical and 50% similar to the FabM enzyme from *S. pneumoniae*. We subsequently cloned, expressed and purified this putative FabM enzyme. Since it has previously been shown that isomerization from *trans*-2 to *cis*-3 causes the decrease of absorbance at 260 nm due to the loss of conjugation in the product, we synthesized *trans*-2-decenoly-NAC and tested the activity of the recombinant protein with this substrate (**Figure 5.8**). However,

trans-2-decenoyl-NAC   *cis*-3-decenoyl-NAC
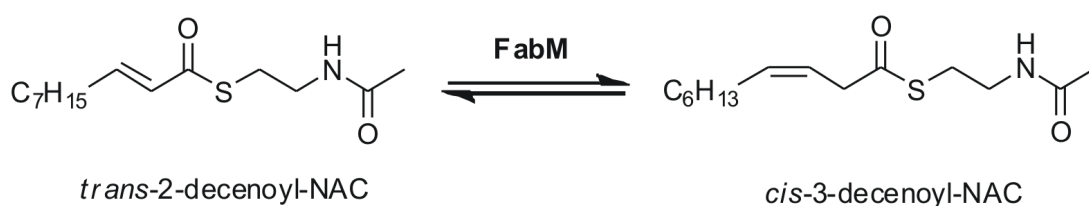
Figure 5.8: Reaction Catalyzed by FabM

the enzyme was inactive toward the synthesized substrate. We then speculate that due to the conjugation in *trans*-2-decenoyl-NAC, the equilibrium of the reaction highly favors to the substrate. Then it is possible that the formation of thermodynamically unfavorable *cis*-3-decenoyl-NAD is so small that the change cannot be observed under our experimental conditions. We then synthesized *cis*-3-decenoyl-NAC and tested the activity of the enzyme. Since the enzymatic reaction is reversible (**Figure 5.8**), increase of absorbance at 260 nm should be observed if the enzyme is active. Unfortunately, still no activity was found. The reason that the enzyme is inactive is still unclear. One possible explanation is that the native structure of this protein has been disturbed because a large segment has been attached at the C-terminus from the encoding sequence of the pBAD vector (25 amino acids). We are currently trying to cut the vector residues and retest its isomerase activity.

Conclusions

We have demonstrated the bmFabI and bmFabV can functionally replace ecFabI in *E. coli*. However, cell growth assay showed that complementation with only one enzyme (bmFabI or bmFabV) results in a lag at initial growth phase of the *E. coli* strain JP1111, indicating the necessity of both enzymes *in vivo*. Kinetic experiments revealed that bmFabV has much lower activity toward the short acyl substrates than bmFabI while bmFabI lacks the capability to reduce the unsaturated intermediates in UFA biosynthesis pathway. Combined together, we hypothesize that bmFabI is the enzyme that reduces the intermediates in SFA biosynthesis, while bmFabV compete with bmFabI to divert the UFA biosynthesis in *B. mallei*

References:

1.   Bergler, H., Wallner, P., Ebeling, A., Leitinger, B., Fuchsbichler, S., Aschauer, H., Kollenz, G., Hogenauer, G., and Turnowsky, F. (1994) Protein EnvM is the NADH-dependent enoyl-ACP reductase (FabI) of *Escherichia coli*, *J. Biol. Chem. 269*, 5493-5496.

2.   Xu, H., Sullivan, T. J., Sekiguchi, J., Kirikae, T., Ojima, I., Stratton, C. F., Mao, W., Rock, F. L., Alley, M. R., Johnson, F., Walker, S. G., and Tonge, P. J. (2008) Mechanism and inhibition of saFabI, the enoyl reductase from *Staphylococcus aureus*, *Biochemistry 47*, 4228-4236.

3.   Lu, H., England, K., am Ende, C., Truglio, J. J., Luckner, S., Reddy, B. G., Marlenee, N. L., Knudson, S. E., Knudson, D. L., Bowen, R. A., Kisker, C., Slayden, R. A., and Tonge, P. J. (2009) Slow-onset inhibition of the FabI enoyl reductase from *Francisella tularensis*: residence time and in vivo activity, *ACS Chem. Biol. 4*, 221-231.

4.   Heath, R. J., and Rock, C. O. (2000) A triclosan-resistant bacterial enzyme, *Nature 406*, 145-146.

5.   Heath, R. J., Su, N., Murphy, C. K., and Rock, C. O. (2000) The enoyl-acyl-carrier-protein reductases FabI and FabL from *Bacillus subtilis*,

J. Biol. Chem. 275, 40128-40133.

6.   Massengo-Tiasse, R. P., and Cronan, J. E. (2008) *Vibrio cholerae* FabV defines a new class of enoyl-acyl carrier protein reductase, *J. Biol. Chem. 283*, 1308-1316.

7.   Massengo-Tiasse, R. P., and Cronan, J. E. (2009) Diversity in enoyl-acyl carrier protein reductases, *Cell Mol. Life Sci. 66*, 1507-1517.

8.   White, S. W., Zheng, J., Zhang, Y. M., and Rock. (2005) The structural biology of type II fatty acid biosynthesis, *Annu. Rev. Biochem. 74*, 791-831.

9.   Lu, H., and Tonge, P. J. (2010) Mechanism and inhibition of the FabV enoyl-ACP reductase from *Burkholderia mallei*, *Biochemistry 49*, 1281-1289.

10.   Saito, J., Yamada, M., Watanabe, T., Iida, M., Kitagawa, H., Takahata, S., Ozawa, T., Takeuchi, Y., and Ohsawa, F. (2008) Crystal structure of enoyl-acyl carrier protein reductase (FabK) from *Streptococcus pneumoniae* reveals the binding mode of an inhibitor, *Protein Sci. 17*, 691-699.

11.   Zhu, L., Lin, J., Ma, J., Cronan, J. E., and Wang, H. (2010) Triclosan resistance of *Pseudomonas aeruginosa* PAO1 is due to FabV, a triclosan-resistant enoyl-acyl carrier protein reductase, *Antimicrob. Agents*

Chemother. 54, 689-698.

12.   Cronan, J. E., Jr., and Gelmann, E. P. (1975) Physical properties of membrane lipids: biological relevance and regulation, *Bacteriol. Rev. 39*, 232-256.

13.   Morein, S., Andersson, A., Rilfors, L., and Lindblom, G. (1996) Wild-type *Escherichia coli* cells regulate the membrane lipid composition in a "window" between gel and non-lamellar structures, *J. Biol. Chem. 271*, 6801-6809.

14.   Cronan, J. E. (2003) Bacterial membrane lipids: where do we stand?, *Annu. Rev. Microbiol. 57*, 203-224.

15.   Mansilla, M. C., and de Mendoza, D. (2005) The *Bacillus subtilis* desaturase: a model to understand phospholipid modification and temperature sensing, *Arch. Microbiol. 183*, 229-235.

16.   Fulco, A. J. (1969) The biosynthesis of unsaturated fatty acids by bacilli. I. Temperature induction of the desaturation reaction, *J. Biol. Chem. 244*, 889-895.

17.   Mansilla, M. C., Cybulski, L. E., Albanesi, D., and de Mendoza, D. (2004) Control of membrane lipid fluidity by molecular thermosensors, *J. Bacteriol. 86*, 6681-6688.

18. Rock, C. O., and Cronan, J. E. (1996) *Escherichia coli* as a model for the regulation of dissociable (type II) fatty acid biosynthesis, *Biochim. Biophys. Acta 1302*, 1-16.

19. Lu, Y. J., Zhang, Y. M., and Rock, C. O. (2004) Product diversity and regulation of type II fatty acid synthases, *Biochem. Cell Biol. 82*, 145-155.

20. Marrakchi, H., Zhang, Y. M., and Rock, C. O. (2002) Mechanistic diversity and regulation of Type II fatty acid synthesis, *Biochem. Soc. Trans. 30*, 1050-1055.

21. Kass, L. R., and Bloch, K. (1967) On the enzymatic synthesis of unsaturated fatty acids in *Escherichia coli*, *Proc. Natl. Acad. Sci. U.S.A. 58*, 1168-1173.

22. Bloch, K. (1969) Enzymic synthesis of monounsaturated fatty acids, *Acc. Chem. Res. 2*, 193-202.

23. Feng, Y., and Cronan, J. E. (2009) *Escherichia coli* unsaturated fatty acid synthesis: complex transcription of the fabA gene and *in vivo* identification of the essential reaction catalyzed by FabB, *J. Biol. Chem. 284*, 29526-29535.

24. Rosenfeld, I. S., D'Agnolo, G., and Vagelos, P. R. (1973) Synthesis of unsaturated fatty acids and the lesion in *fabB* mutants, *J. Biol. Chem. 248*,

2452-2460.

25.   D'Agnolo, G., Rosenfeld, I. S., and Vagelos, P. R. (1975) Multiple forms of beta-ketoacyl-acyl carrier protein synthetase in *Escherichia coli*, *J. Biol. Chem. 250*, 5289-5294.

26.   Garwin, J. L., Klages, A. L., and Cronan, J. E., Jr. (1980) Structural, enzymatic, and genetic studies of beta-ketoacyl-acyl carrier protein synthases I and II of *Escherichia coli*, *J. Biol. Chem. 255*, 11949-11956.

27.   de Mendoza, D., Klages Ulrich, A., and Cronan, J. E., Jr. (1983) Thermal regulation of membrane fluidity in *Escherichia coli*. Effects of overproduction of beta-ketoacyl-acyl carrier protein synthase I, *J. Biol. Chem. 258*, 2098-2101.

28.   Clark, D. P., DeMendoza, D., Polacco, M. L., and Cronan, J. E., Jr. (1983) Beta-hydroxydecanoyl thio ester dehydrase does not catalyze a rate-limiting step in *Escherichia coli* unsaturated fatty acid synthesis, *Biochemistry 22*, 5897-5902.

29.   Marrakchi, H., Choi, K. H., and Rock, C. O. (2002) A new mechanism for anaerobic unsaturated fatty acid formation in *Streptococcus pneumoniae*, *J. Biol. Chem. 277*, 44809-44816.

30.   Fozo, E. M., and Quivey, R. G., Jr. (2004) The fabM gene product of

Streptococcus mutans is responsible for the synthesis of monounsaturated fatty acids and is necessary for survival at low pH, *J. Bacteriol. 186*, 4152-4158.

31. Altabe, S., Lopez, P., and de Mendoza, D. (2007) Isolation and characterization of unsaturated fatty acid auxotrophs of *Streptococcus pneumoniae* and Streptococcus mutans, *J. Bacteriol. 189*, 8139-8144.

32. Campbell, J. W., and Cronan, J. E., Jr. (2001) Bacterial fatty acid biosynthesis: targets for antibacterial drug discovery, *Annu. Rev. Microbiol. 55*, 305-332.

33. Wang, H., and Cronan, J. E. (2004) Functional replacement of the FabA and FabB proteins of *Escherichia coli* fatty acid synthesis by *Enterococcus faecalis* FabZ and FabF homologues, *J. Biol. Chem. 279*, 34489-34495.

34. Rafi, S., Novichenok, P., Kolappan, S., Zhang, X., Stratton, C. F., Rawat, R., Kisker, C., Simmerling, C., and Tonge, P. J. (2006) Structure of acyl carrier protein bound to FabI, the FASII enoyl reductase from *Escherichia coli*, *J. Biol. Chem. 281*, 39285-39293.

35. Bergler, H., Hogenauer, G., and Turnowsky, F. (1992) Sequences of the envM gene and of two mutated alleles in *Escherichia coli*, *J. Gen. Microbiol.138*, 2093-2100.

36. Bergler, H., Fuchsbichler, S., Hogenauer, G., and Turnowsky, F. (1996) The enoyl-acyl-carrier-protein reductase (FabI) of *Escherichia coli*, which catalyzes a key regulatory step in fatty acid biosynthesis, accepts NADH and NADPH as cofactors and is inhibited by palmitoyl-CoA, *Eur. J. Biochem. 242*, 689-694.

37. Patrignani, F., Iucci, L., Belletti, N., Gardini, F., Guerzoni, M. E., and Lanciotti, R. (2008) Effects of sub-lethal concentrations of hexanal and 2-(E)-hexenal on membrane fatty acid composition and volatile compounds of *Listeria monocytogenes*, *Staphylococcus aureus*, *Salmonella enteritidis* and *Escherichia coli*, *Int. J. Food Microbiol. 123*, 1-8.

38. Jantzen, E., Berdal, B. P., and Omland, T. (1979) Cellular fatty acid composition of *Francisella tularensis*, *J. Clin. Microbiol. 10*, 928-930.

39. White, D. C., and Frerman, F. E. (1968) Fatty acid composition of the complex lipids of *Staphylococcus aureus* during the formation of the membrane-bound electron transport system, *J. Bacteriol. 95*, 2198-2209.

40. Vasiurenko, Z. P., Sel'nikova, O. P., Polishchuk, E. I., Samygin, V. M., and Ruban, N. M. (2006) Cellular fatty acid composition of the *Burkholderia mallei* and *Burkholderia pseudomallei* strains as generic feature of Burkholderia, *Mikrobiol. Z. 68*, 33-40.

Bibliography

Chapter I

1.   Dineeen, P., Homan, W. P., and Grafe, W. R. (1976) Tuberculous peritonitis:

        43 years' expereince in diagnosis and treatment, *Annu. Surg. 184*,

        717-722.

2.   Ehrlich, P. (1910) The use and effect of salvarsan, *Deut. Med. Wochenschr.*

        36, 2437-2438.

3.   Fleming, A. (1929) Lysozyme - a bacteriolytic ferment found normally in

        tissues and secretions, *Lancet 1*, 217-220.

4.   Fleming, A. (1941) Penicillin, *British. Medical. Journal. 1941*, 386-386.

5.   Domagk, G. J. (1935) Ein beitrag zur chemotherapie der bakteriellen

        infektionen, *Deut. Med. Wochenschr. 61*, 250-253.

6.   Wright, G. D. (2007) The antibiotic resistome: the nexus of chemical and

        genetic diversity, *Nat. Rev. 5*, 175-186.

7.   Bax, R. P., Anderson, R., Crew, J., Fletcher, P., Johnson, T., Kaplan, E.,

        Knaus, B., Kristinsson, K., Malek, M., and Strandberg, L. (1998) Antibiotic

        resistance--what can we do?, *Nat. Med. 4*, 545-546.

8.   Coates, A., Hu, Y., Bax, R., and Page, C. (2002) The future challenges

        facing the development of new antimicrobial drugs, *Nat. Rev. Drug Discov.*

1, 895-910.

9.   Cohen, M. L. (1992) Epidemiology of drug resistance: implications for a
      post-antimicrobial era, *Science 257*, 1050-1055.

10.   McGowan, J. E., Jr. (2006) Resistance in nonfermenting gram-negative
      bacteria: multidrug resistance to the maximum, *Am. J. Infect. Control 34*,
      S29-37; discussion S64-73.

11.   Levy, S. B., and Marshall, B. (2004) Antibacterial resistance worldwide:
      causes, challenges and responses, *Nat. Med. 10*, S122-129.

12.   Livermore, D. M. (2004) The need for new antibiotics, *Clin. Microbiol. Infect.
      10 Suppl 4*, 1-9.

13.   Kochi, A. (1991) The global tuberculosis situation and the new control
      strategy of the World Health Organization, *Tubercle 72*, 1-6.

14.   Bloom, B. R., and Murray, C. J. (1992) Tuberculosis: commentary on a
      reemergent killer, *Science 257*, 1055-1064.

15.   (2006) "Virtually untreatable" TB found, *BBC News [Online]*.

16.   Williams, D. H. (1996) The glycopeptide story--how to kill the deadly
      'superbugs', *Nat. Prod. Rep. 13*, 469-477.

17.   Fourmy, D., Recht, M. I., Blanchard, S. C., and Puglisi, J. D. (1996)
      Structure of the A site of *Escherichia coli* 16S ribosomal RNA complexed

with an aminoglycoside antibiotic, *Science 274*, 1367-1371.

18. Maxwell, A. (1997) DNA gyrase as a drug target, *Trends Mcrobiol. 5*, 102-109.

19. Walsh, C. (2000) Molecular mechanisms that confer antibacterial drug resistance, *Nature 406*, 775-781.

20. Becker, D., Selbach, M., Rollenhagen, C., Ballmaier, M., Meyer, T. F., Mann, M., and Bumann, D. (2006) Robust *Salmonella* metabolism limits possibilities for new antimicrobials, *Nature 440*, 303-307.

21. McDevitt, D., and Rosenberg, M. (2001) Exploiting genomics to discover new antibiotics, *Trends Microbiol. 9*, 611-617.

22. Alksne, L. E., Burgio, P., Hu, W., Feld, B., Singh, M. P., Tuckman, M., Petersen, P. J., Labthavikul, P., McGlynn, M., Barbieri, L., McDonald, L., Bradford, P., Dushin, R. G., Rothstein, D., and Projan, S. J. (2000) Identification and analysis of bacterial protein secretion inhibitors utilizing a SecA-LacZ reporter fusion system, *Antimicrob. Agents Chemother. 44*, 1418-1427.

23. Payne, D. J., Warren, P. V., Holmes, D. J., Ji, Y., and Lonsdale, J. T. (2001) Bacterial fatty-acid biosynthesis: a genomics-driven target for antibacterial drug discovery, *Drug Discov. Today 6*, 537-544.

24. Chirala, S. S., Huang, W. Y., Jayakumar, A., Sakai, K., and Wakil, S. J. (1997) Animal fatty acid synthase: functional mapping and cloning and expression of the domain I constituent activities, *Proc. Natl. Acd. Sci. U.S.A. 94*, 5588-5593.

25. Campbell, J. W., and Cronan, J. E., Jr. (2001) Bacterial fatty acid biosynthesis: targets for antibacterial drug discovery, *Annu. Rev. Microbiol. 55*, 305-332.

26. White, S. W., Zheng, J., Zhang, Y. M., and Rock. (2005) The structural biology of type II fatty acid biosynthesis, *Annu. Rev. Biochem. 74*, 791-831.

27. Heath, R. J., White, S. W., and Rock, C. O. (2001) Lipid biosynthesis as a target for antibacterial agents, *Prog. Lipid Res. 40*, 467-497.

28. Cronan, J. E., Jr. and Waldrop, G. L. (2002) Multi-subunit acetyl-CoA carboxylases, *Prog. Lipid Res. 41*, 407-435.

29. Li, S. J., and Cronan, J. E., Jr. (1992) The gene encoding the biotin carboxylase subunit of *Escherichia coli* acetyl-CoA carboxylase, *The Journal of biological chemistry 267*, 855-863.

30. Li, S. J., and Cronan, J. E., Jr. (1992) The genes encoding the two carboxyltransferase subunits of *Escherichia coli* acetyl-CoA carboxylase, *J. Biol. Chem. 267*, 16841-16847.

31. Ruch, F. E., and Vagelos, P. R. (1973) Characterization of a malonyl-enzyme intermediate and identification of the malonyl binding site in malonyl coenzyme A-acyl carrier protein transacylase of *Escherichia coli*, *J. Biol. Chem. 248*, 8095-8106.

32. Jackowski, S., and Rock, C. O. (1987) Acetoacetyl-acyl carrier protein synthase, a potential regulator of fatty acid biosynthesis in bacteria, *J. Biol. Chem. 262*, 7927-7931.

33. Price, A. C., Zhang, Y. M., Rock, C. O., and White, S. W. (2001) Structure of beta-ketoacyl-acyl carrier protein reductase from *Escherichia coli*: negative cooperativity and its structural basis, *Biochemistry 40*, 12772-12781.

34. Price, A. C., Zhang, Y. M., Rock, C. O., and White, S. W. (2004) Cofactor-induced conformational rearrangements establish a catalytically competent active site and a proton relay conduit in FabG, *Structure 12*, 417-428.

35. Leesong, M., Henderson, B. S., Gillig, J. R., Schwab, J. M., and Smith, J. L. (1996) Structure of a dehydratase-isomerase from the bacterial pathway for biosynthesis of unsaturated fatty acids: two catalytic activities in one active site, *Structure 4*, 253-264.

36. Kimber, M. S., Martin, F., Lu, Y., Houston, S., Vedadi, M., Dharamsi, A., Fiebig, K. M., Schmid, M., and Rock, C. O. (2004) The structure of (3R)-hydroxyacyl-acyl carrier protein dehydratase (FabZ) from *Pseudomonas aeruginosa*, *J. Biol. Chem. 279*, 52593-52602.

37. Roujeinikova, A., Levy, C. W., Rowsell, S., Sedelnikova, S., Baker, P. J., Minshull, C. A., Mistry, A., Colls, J. G., Camble, R., Stuitje, A. R., Slabas, A. R., Rafferty, J. B., Pauptit, R. A., Viner, R., and Rice, D. W. (1999) Crystallographic analysis of triclosan bound to enoyl reductase, *J. Mol. Biol. 294*, 527-535.

38. Roujeinikova, A., Sedelnikova, S., de Boer, G. J., Stuitje, A. R., Slabas, A. R., Rafferty, J. B., and Rice, D. W. (1999) Inhibitor binding studies on enoyl reductase reveal conformational changes related to substrate recognition, *J. Biol. Chem. 274*, 30811-30817.

39. Rock, C. O., and Cronan, J. E., Jr. (1979) Solubilization, purification, and salt activation of acyl-acyl carrier protein synthetase from *Escherichia coli*, *J. Biol. Chem. 254*, 7116-7122.

40. Rock, C. O., and Cronan, J. E., Jr. (1979) Re-evaluation of the solution structure of acyl carrier protein, *J. Biol. Chem. 254*, 9778-9785.

41. Zhang, Y. M., White, S. W., and Rock, C. O. (2006) Inhibiting bacterial fatty

acid synthesis, *J. Biol. Chem. 281*, 17541-17544.

42.   Bergler, H., Fuchsbichler, S., Hogenauer, G., and Turnowsky, F. (1996) The enoyl-acyl-carrier-protein reductase (FabI) of *Escherichia coli*, which catalyzes a key regulatory step in fatty acid biosynthesis, accepts NADH and NADPH as cofactors and is inhibited by palmitoyl-CoA, *Eur. J. Biochem. 242*, 689-694.

43.   Heath, R. J., and Rock, C. O. (1995) Enoyl-acyl carrier protein reductase (fabI) plays a determinant role in completing cycles of fatty acid elongation in *Escherichia coli*, *J. Biol. Chem. 270*, 26538-26542.

44.   Parikh, S., Moynihan, D. P., Xiao, G., and Tonge, P. J. (1999) Roles of tyrosine 158 and lysine 165 in the catalytic mechanism of InhA, the enoyl-ACP reductase from *Mycobacterium tuberculosis*, *Biochemistry 38*, 13623-13634.

45.   Rafferty, J. B., Simon, J. W., Baldock, C., Artymiuk, P. J., Baker, P. J., Stuitje, A. R., Slabas, A. R., and Rice, D. W. (1995) Common themes in redox chemistry emerge from the X-ray structure of oilseed rape (*Brassica napus*) enoyl acyl carrier protein reductase, *Structure 3*, 927-938.

46.   Rozwarski, D. A., Vilcheze, C., Sugantino, M., Bittman, R., and Sacchettini, J. C. (1999) Crystal structure of the *Mycobacterium tuberculosis*

enoyl-ACP reductase, InhA, in complex with NAD^+ and a C16 fatty acyl substrate, *J. Biol. Chem. 274*, 15582-15589.

47.   Stewart, M. J., Parikh, S., Xiao, G., Tonge, P. J., and Kisker, C. (1999) Structural basis and mechanism of enoyl reductase inhibition by triclosan, *J. Mol. Biol. 290*, 859-865.

48.   Baldock, C., Rafferty, J. B., Sedelnikova, S. E., Baker, P. J., Stuitje, A. R., Slabas, A. R., Hawkes, T. R., and Rice, D. W. (1996) A mechanism of drug action revealed by structural studies of enoyl reductase, *Science 274*, 2107-2110.

49.   Grassberger, M. A., Turnowsky, F., and Hildebrandt, J. (1984) Preparation and antibacterial activities of new 1,2,3-diazaborine derivatives and analogues, *J. Med. Chem. 27*, 947-953.

50.   Baldock, C., de Boer, G. J., Rafferty, J. B., Stuitje, A. R., and Rice, D. W. (1998) Mechanism of action of diazaborines, *Biochem. Pharmacol. 55*, 1541-1549.

51.   Davis, M. C., Franzblau, S. G., and Martin, A. R. (1998) Syntheses and evaluation of benzodiazaborine compounds against *M. tuberculosis* H37Rv in vitro, *Bioorg. Med. Chem. Lett. 8*, 843-846.

52.   Slayden, R. A., Lee, R. E., and Barry, C. E., (2000) Isoniazid affects

multiple components of the type II fatty acid synthase system of *Mycobacterium tuberculosis*, *Mol. Microbiol. 38*, 514-525.

53. Banerjee, A., Dubnau, E., Quemard, A., Balasubramanian, V., Um, K. S., Wilson, T., Collins, D., de Lisle, G., and Jacobs, W. R., Jr. (1994) inhA, a gene encoding a target for isoniazid and ethionamide in *Mycobacterium tuberculosis*, *Science 263*, 227-230.

54. Quemard, A., Sacchettini, J. C., Dessen, A., Vilcheze, C., Bittman, R., Jacobs WR, J. r., and Blanchard, J. S. (1995) Enzymatic characterization of the target for isoniazid in *Mycobacterium tuberculosis*, *Biochemistry 34*, 8235-8241.

55. Johnsson, K., King, J., and Schultz, P. G. (1995) Studies on the mechanism of action of isoniazid and ethionamide in the chemotherapy of tuberculosis, *J. Am. Chem. Soc 117*, 5009-5010.

56. Rozwarski, D. A., Grant, G. A., Barton, D. H., Jacobs, W. R., Jr., and Sacchettini, J. C. (1998) Modification of the NADH of the isoniazid target (InhA) from *Mycobacterium tuberculosis*, *Science 279*, 98-102.

57. Rawat, R., Whitty, A., and Tonge, P. J. (2003) The isoniazid-NAD adduct is a slow, tight-binding inhibitor of InhA, the *Mycobacterium tuberculosis* enoyl reductase: adduct affinity and drug resistance, *Proc. Natl. Acd. Sci.*

U.S.A. 100, 13881-13886.

58. Ramaswamy, S. V., Reich, R., Dou, S. J., Jasperse, L., Pan, X., Wanger, A., Quitugua, T., and Graviss, E. A. (2003) Single nucleotide polymorphisms in genes associated with isoniazid resistance in *Mycobacterium tuberculosis*, *Antimicrob. Agents Chemother. 47*, 1241-1250.

59. Broussy, S., Bernardes-Genisson, V., Quemard, A., Meunier, B., and Bernadou, J. (2005) The first chemical synthesis of the core structure of the benzoylhydrazine-NAD adduct, a competitive inhibitor of the *Mycobacterium tuberculosis* enoyl reductase, *J. Org. Chem. 70*, 10502-10510.

60. Bonnac, L., Gao, G. Y., Chen, L., Felczak, K., Bennett, E. M., Xu, H., Kim, T., Liu, N., Oh, H., Tonge, P. J., and Pankiewicz, K. W. (2007) Synthesis of 4-phenoxybenzamide adenine dinucleotide as NAD analogue with inhibitory activity against enoyl-ACP reductase (InhA) of *Mycobacterium tuberculosis*, *Bioorg. Med. Chem. Lett. 17*, 4588-4591.

61. Oliveira, J. S., Sousa, E. H., Basso, L. A., Palaci, M., Dietze, R., Santos, D. S., and Moreira, I. S. (2004) An inorganic iron complex that inhibits wild-type and an isoniazid-resistant mutant 2-*trans*-enoyl-ACP (CoA) reductase from *Mycobacterium tuberculosis*, *Chem. Commun. 7*, 312-313.

62. Oliveira, J. S., de Sousa, E. H., de Souza, O. N., Moreira, I. S., Santos, D. S., and Basso, L. A. (2006) Slow-onset inhibition of 2-*trans*-enoyl-ACP (CoA) reductase from *Mycobacterium tuberculosis* by an inorganic complex, *Curr. Pharm. Des. 12*, 2409-2424.

63. McMurry, L. M., Oethinger, M., and Levy, S. B. (1998) Triclosan targets lipid synthesis, *Nature 394*, 531-532.

64. Heath, R. J., Yu, Y. T., Shapiro, M. A., Olson, E., and Rock, C. O. (1998) Broad spectrum antimicrobial biocides target the FabI component of fatty acid synthesis, *J. Biol. Chem. 273*, 30316-30320.

65. Levy, C. W., Roujeinikova, A., Sedelnikova, S., Baker, P. J., Stuitje, A. R., Slabas, A. R., Rice, D. W., and Rafferty, J. B. (1999) Molecular basis of triclosan activity, *Nature 398*, 383-384.

66. Sivaraman, S., Zwahlen, J., Bell, A. F., Hedstrom, L., and Tonge, P. J. (2003) Structure-activity studies of the inhibition of FabI, the enoyl reductase from *Escherichia coli*, by triclosan: kinetic analysis of mutant FabIs, *Biochemistry 42*, 4406-4413.

67. Sivaraman, S., Sullivan, T. J., Johnson, F., Novichenok, P., Cui, G., Simmerling, C., and Tonge, P. J. (2004) Inhibition of the bacterial enoyl reductase FabI by triclosan: a structure-reactivity analysis of FabI inhibition

by triclosan analogues, *J. Med. Chem. 47*, 509-518.

68. Ward, W. H., Holdgate, G. A., Rowsell, S., McLean, E. G., Pauptit, R. A., Clayton, E., Nichols, W. W., Colls, J. G., Minshull, C. A., Jude, D. A., Mistry, A., Timms, D., Camble, R., Hales, N. J., Britton, C. J., and Taylor, I. W. (1999) Kinetic and structural characteristics of the inhibition of enoyl (acyl carrier protein) reductase by triclosan, *Biochemistry 38*, 12514-12525.

69. Qiu, X., Janson, C. A., Court, R. I., Smyth, M. G., Payne, D. J., and Abdel-Meguid, S. S. (1999) Molecular basis for triclosan activity involves a flipping loop in the active site, *Protein Sci. 8*, 2529-2532.

70. Pidugu, L. S., Kapoor, M., Surolia, N., Surolia, A., and Suguna, K. (2004) Structural basis for the variation in triclosan affinity to enoyl reductases, *J. Mol. Biol.343*, 147-155.

71. Xu, H., Sullivan, T. J., Sekiguchi, J., Kirikae, T., Ojima, I., Stratton, C. F., Mao, W., Rock, F. L., Alley, M. R., Johnson, F., Walker, S. G., and Tonge, P. J. (2008) Mechanism and inhibition of saFabI, the enoyl reductase from *Staphylococcus aureus*, *Biochemistry 47*, 4228-4236.

72. Chhibber, M., Kumar, G., Parasuraman, P., Ramya, T. N., Surolia, N., and Surolia, A. (2006) Novel diphenyl ethers: design, docking studies, synthesis and inhibition of enoyl ACP reductase of *Plasmodium falciparum*

and *Escherichia coli*, *Bioorg. Med. Chem. 14*, 8086-8098.

73. Freundlich, J. S., Yu, M., Lucumi, E., Kuo, M., Tsai, H. C., Valderramos, J. C., Karagyozov, L., Jacobs, W. R., Jr., Schiehser, G. A., Fidock, D. A., Jacobus, D. P., and Sacchettini, J. C. (2006) Synthesis and biological activity of diaryl ether inhibitors of malarial enoyl acyl carrier protein reductase. Part 2: 2'-substituted triclosan derivatives, *Bioorg. Med. Chem. Lett. 16*, 2163-2169.

74. Stone, G. W., Zhang, Q., Castillo, R., Doppalapudi, V. R., Bueno, A. R., Lee, J. Y., Li, Q., Sergeeva, M., Khambatta, G., and Georgopapadakou, N. H. (2004) Mechanism of action of NB2001 and NB2030, novel antibacterial agents activated by beta-lactamases, *Antimicrob. Agents Chemother. 48*, 477-483.

75. Perozzo, R., Kuo, M., Sidhu, A. S., Valiyaveettil, J. T., Bittman, R., Jacobs, W. R., Jr., Fidock, D. A., and Sacchettini, J. C. (2002) Structural elucidation of the specificity of the antibacterial agent triclosan for malarial enoyl acyl carrier protein reductase, *J. Biol. Chem. 277*, 13106-13114.

76. Parikh, S. L., Xiao, G., and Tonge, P. J. (2000) Inhibition of InhA, the enoyl reductase from *Mycobacterium tuberculosis*, by triclosan and isoniazid, *Biochemistry 39*, 7645-7650.

221

77. Sullivan, T. J., Truglio, J. J., Boyne, M. E., Novichenok, P., Zhang, X., Stratton, C. F., Li, H. J., Kaur, T., Amin, A., Johnson, F., Slayden, R. A., Kisker, C., and Tonge, P. J. (2006) High affinity InhA inhibitors with activity against drug-resistant strains of *Mycobacterium tuberculosis*, *ACS Chem. Biol. 1*, 43-53.

78. Payne, D. J., Miller, W. H., Berry, V., Brosky, J., Burgess, W. J., Chen, E., DeWolf Jr, W. E., Jr., Fosberry, A. P., Greenwood, R., Head, M. S., Heerding, D. A., Janson, C. A., Jaworski, D. D., Keller, P. M., Manley, P. J., Moore, T. D., Newlander, K. A., Pearson, S., Polizzi, B. J., Qiu, X., Rittenhouse, S. F., Slater-Radosti, C., Salyers, K. L., Seefeld, M. A., Smyth, M. G., Takata, D. T., Uzinskas, I. N., Vaidya, K., Wallis, N. G., Winram, S. B., Yuan, C. C., and Huffman, W. F. (2002) Discovery of a novel and potent class of FabI-directed antibacterial agents, *Antimicrob. Agents Chemother. 46*, 3118-3124.

79. Seefeld, M. A., Miller, W. H., Newlander, K. A., Burgess, W. J., Payne, D. J., Rittenhouse, S. F., Moore, T. D., DeWolf, W. E., Jr., Keller, P. M., Qiu, X., Janson, C. A., Vaidya, K., Fosberry, A. P., Smyth, M. G., Jaworski, D. D., Slater-Radosti, C., and Huffman, W. F. (2001) Inhibitors of bacterial enoyl acyl carrier protein reductase (FabI): 2,9-disubstituted

1,2,3,4-tetrahydropyrido[3,4-b]indoles as potential antibacterial agents, *Bioorg. Med. Chem. Lett. 11*, 2241-2244.

80. Seefeld, M. A., Miller, W. H., Newlander, K. A., Burgess, W. J., DeWolf, W. E., Jr., Elkins, P. A., Head, M. S., Jakas, D. R., Janson, C. A., Keller, P. M., Manley, P. J., Moore, T. D., Payne, D. J., Pearson, S., Polizzi, B. J., Qiu, X., Rittenhouse, S. F., Uzinskas, I. N., Wallis, N. G., and Huffman, W. F. (2003) Indole naphthyridinones as inhibitors of bacterial enoyl-ACP reductases FabI and FabK, *J. Med. Chem. 46*, 1627-1635.

81. Karlowsky, J. A., Laing, N. M., Baudry, T., Kaplan, N., Vaughan, D., Hoban, D. J., and Zhanel, G. G. (2007) *In Vitro* Activity of API-1252, a Novel FabI Inhibitor, against Clinical Isolates of *Staphylococcus aureus* and *Staphylococcus epidermidis*, *Antimicrob. Agents Chemother. 51*, 1580-1581.

82. Heerding, D. A., Chan, G., DeWolf, W. E., Fosberry, A. P., Janson, C. A., Jaworski, D. D., McManus, E., Miller, W. H., Moore, T. D., Payne, D. J., Qiu, X., Rittenhouse, S. F., Slater-Radosti, C., Smith, W., Takata, D. T., Vaidya, K. S., Yuan, C. C., and Huffman, W. F. (2001) 1,4-Disubstituted imidazoles are potential antibacterial agents functioning as inhibitors of enoyl acyl carrier protein reductase (FabI), *Bioorg. Med. Chem. Lett. 11*, 2061-2065.

83. Ling, L. L., Xian, J., Ali, S., Geng, B., Fan, J., Mills, D. M., Arvanites, A. C., Orgueira, H., Ashwell, M. A., Carmel, G., Xiang, Y., and Moir, D. T. (2004) Identification and characterization of inhibitors of bacterial enoyl-acyl carrier protein reductase, *Antimicrob. Agents Chemother. 48*, 1541-1547.

84. Kitagawa, H., Kumura, K., Takahata, S., Iida, M., and Atsumi, K. (2007) 4-Pyridone derivatives as new inhibitors of bacterial enoyl-ACP reductase FabI, *Bioorg. Med. Chem. 15*, 1106-1116.

85. Kuo, M. R., Morbidoni, H. R., Alland, D., Sneddon, S. F., Gourlie, B. B., Staveski, M. M., Leonard, M., Gregory, J. S., Janjigian, A. D., Yee, C., Musser, J. M., Kreiswirth, B., Iwamoto, H., Perozzo, R., Jacobs, W. R., Jr., Sacchettini, J. C., and Fidock, D. A. (2003) Targeting tuberculosis and malaria through inhibition of enoyl reductase: compound activity and structural data, *J. Biol. Chem. 278*, 20851-20859.

86. He, X., Alian, A., Stroud, R., and Ortiz de Montellano, P. R. (2006) Pyrrolidine carboxamides as a novel class of inhibitors of enoyl acyl carrier protein reductase from *Mycobacterium tuberculosis*, *J. Med. Chem. 49*, 6308-6323.

Chapter II

1. McCoy, G. W., and Chapin, C. W. (1912) Further observation on a plague-like disease of rodents with a preliminary note on the causative agent, Bacterium tularensis., *J. Infect. Dis. 25*, 61-72.

2. Hopla, C. E. (1974) The ecology of tularemia, *Adv. Vet. Sci. Comp. Med. 18*, 25-53.

3. Oyston, P. C., Sjostedt, A., and Titball, R. W. (2004) Tularaemia: bioterrorism defence renews interest in *Francisella tularensis*, *Nat. Rev. 2*, 967-978.

4. Ellis, J., Oyston, P. C., Green, M., and Titball, R. W. (2002) Tularemia, *Clin. Microbiol. Rev. 15*, 631-646.

5. Dennis, D. T., Inglesby, T. V., Henderson, D. A., Bartlett, J. G., Ascher, M. S., Eitzen, E., Fine, A. D., Friedlander, A. M., Hauer, J., Layton, M., Lillibridge, S. R., McDade, J. E., Osterholm, M. T., O'Toole, T., Parker, G., Perl, T. M., Russell, P. K., and Tonat, K. (2001) Tularemia as a biological weapon: medical and public health management, *JAMA 285*, 2763-2773.

6. Harris, S. (1992) Japanese biological warfare research on humans: a case study of microbiology and ethics, *Annu. N. Y. Acad. Sci. 666*, 21-52.

7. Christopher, G. W., Cieslak, T. J., Pavlin, J. A., and Eitzen, E. M., Jr. (1997)

Biological warfare. A historical perspective, *JAMA 278*, 412-417.

8.   Alibek, K. (1999) The Soviet Union's anti-agricultural biological weapons, *Annu. N. Y. Acad. Sci. 894*, 18-19.

9.   Enderlin, G., Morales, L., Jacobs, R. F., and Cross, J. T. (1994) Streptomycin and alternative agents for the treatment of tularemia: review of the literature, *Clin. Infect. Dis. 19*, 42-47.

10.   Ikaheimo, I., Syrjala, H., Karhukorpi, J., Schildt, R., and Koskela, M. (2000) *In vitro* antibiotic susceptibility of *Francisella tularensis* isolated from humans and animals, *J. Antimicrob. Chemother. 46*, 287-290.

11.   Perez-Castrillon, J. L., Bachiller-Luque, P., Martin-Luquero, M., Mena-Martin, F. J., and Herreros, V. (2001) Tularemia epidemic in northwestern Spain: clinical description and therapeutic response, *Clin. Infect. Dis. 33*, 573-576.

12.   Bergler, H., Wallner, P., Ebeling, A., Leitinger, B., Fuchsbichler, S., Aschauer, H., Kollenz, G., Hogenauer, G., and Turnowsky, F. (1994) Protein EnvM is the NADH-dependent enoyl-ACP reductase (FabI) of *Escherichia coli*, *J. Biol. Chem. 269*, 5493-5496.

13.   Zhang, Y. M., White, S. W., and Rock, C. O. (2006) Inhibiting bacterial fatty acid synthesis, *J. Biol. Chem. 281*, 17541-17544.

14. Lu, H., and Tonge, P. J. (2008) Inhibitors of FabI, an enzyme drug target in the bacterial fatty acid biosynthesis pathway, *Acc. Chem. Res. 41*, 11-20.

15. Heath, R. J., Su, N., Murphy, C. K., and Rock, C. O. (2000) The enoyl-acyl-carrier-protein reductases FabI and FabL from *Bacillus subtilis*, *J. Biol. Chem. 275*, 40128-40133.

16. Heath, R. J., and Rock, C. O. (2000) A triclosan-resistant bacterial enzyme, *Nature 406*, 145-146.

17. Massengo-Tiasse, R. P., and Cronan, J. E. (2008) *Vibrio cholerae* FabV defines a new class of enoyl-acyl carrier protein reductase, *J. Biol. Chem. 283*, 1308-1316.

18. Sliverman, R. B. (2000) The organic chemistry of enzyme-catalyzed reactions, 1st ed., Academic Press, California, 563-584.

19. Karahalios, P., Kalpaxis, D. L., Fu, H., Katz, L., Wilson, D. N., and Dinos, G. P. (2006) On the mechanism of action of 9-O-arylalkyloxime derivatives of 6-O-mycaminosyltylonolide, a new class of 16-membered macrolide antibiotics, *Mol. Pharmacol. 70*, 1271-1280.

20. Ejim, L. J., Blanchard, J. E., Koteva, K. P., Sumerfield, R., Elowe, N. H., Chechetto, J. D., Brown, E. D., Junop, M. S., and Wright, G. D. (2007) Inhibitors of bacterial cystathionine beta-lyase: leads for new antimicrobial

agents and probes of enzyme structure and function, *J. Med. Chem. 50*, 755-764.

21. Copeland, R. A. (2000) Enzymes: a practical introduction to structure, mechanism and data analysis, 2nd ed., Wiley-VCH, New York, 318-350.

22. Tummino, P. J., and Copeland, R. A. (2008) Residence time of receptor-ligand complexes and its effect on biological function, *Biochemistry 47*, 5481-5492.

23. Halford, S. E. (1971) *Escherichia coli* alkaline phosphatase. An analysis of transient kinetics, *Biochem. J. 125*, 319-327.

24. Fersht, A. (1999) Structure and mechanism in protein science, a guide to enzyme catalysis and protein folding, 1st ed., Freeman, New York, 132-168.

25. Ward, W. H., Holdgate, G. A., Rowsell, S., McLean, E. G., Pauptit, R. A., Clayton, E., Nichols, W. W., Colls, J. G., Minshull, C. A., Jude, D. A., Mistry, A., Timms, D., Camble, R., Hales, N. J., Britton, C. J., and Taylor, I. W. (1999) Kinetic and structural characteristics of the inhibition of enoyl acyl carrier protein reductase by triclosan, *Biochemistry 38*, 12514-12525.

26. Morrison, J. F. (1969) Kinetics of the reversible inhibition of enzyme-catalysed reactions by tight-binding inhibitors, *Biochim. Biophys.*

Acta 185, 269-286.

27. Copeland, R. A. (2005) Evaluation of enzyme inhibitors in drug discovery: a guide for medicinal chemists and pharmacologists, 1st ed., John Wiley & Son, New Jersey, 178-212.

28. Sivaraman, S., Sullivan, T. J., Johnson, F., Novichenok, P., Cui, G., Simmerling, C., and Tonge, P. J. (2004) Inhibition of the bacterial enoyl reductase FabI by triclosan: a structure-reactivity analysis of FabI inhibition by triclosan analogues, *J. Med. Chem. 47*, 509-518.

29. Sullivan, T. J., Truglio, J. J., Boyne, M. E., Novichenok, P., Zhang, X., Stratton, C. F., Li, H. J., Kaur, T., Amin, A., Johnson, F., Slayden, R. A., Kisker, C., and Tonge, P. J. (2006) High affinity InhA inhibitors with activity against drug-resistant strains of *Mycobacterium tuberculosis*, *ACS Chem. Biol. 1*, 43-53.

30. Hofstein, H. A., Feng, Y., Anderson, V. E., and Tonge, P. J. (1999) Role of glutamate 144 and glutamate 164 in the catalytic mechanism of enoyl-CoA hydratase, *Biochemistry 38*, 9508-9516.

31. Parikh, S., Moynihan, D. P., Xiao, G., and Tonge, P. J. (1999) Roles of tyrosine 158 and lysine 165 in the catalytic mechanism of InhA, the enoyl-ACP reductase from *Mycobacterium tuberculosis*, *Biochemistry 38*,

13623-13634.

32. Magnuson, K., Jackowski, S., Rock, C. O., and Cronan, J. E., Jr. (1993) Regulation of fatty acid biosynthesis in *Escherichia coli*, *Microbiol. Rev. 57*, 522-542.

33. Baldwin, J. E., Bird, J. W., Field, R. A., O'Callaghan, N. M., Schofield, C. J., and Willis, A. C. (1991) Isolation and partial characterisation of ACV synthetase from *Cephalosporium acremonium* and *Streptomyces clavuligerus*. Evidence for the presence of phosphopantothenate in ACV synthetase,*J. Antibiol. 44*, 241-248.

34. Summers, R. G., Ali, A., Shen, B., Wessel, W. A., and Hutchinson, C. R. (1995) Malonyl-coenzyme A:acyl carrier protein acyltransferase of *Streptomyces glaucescens*: a possible link between fatty acid and polyketide biosynthesis, *Biochemistry 34*, 9389-9402.

35. Lawson, D. M., Derewenda, U., Serre, L., Ferri, S., Szittner, R., Wei, Y., Meighen, E. A., and Derewenda, Z. S. (1994) Structure of a myristoyl-ACP-specific thioesterase from *Vibrio harveyi*, *Biochemistry 33*, 9382-9388.

36. Dotson, G. D., Kaltashov, I. A., Cotter, R. J., and Raetz, C. R. (1998) Expression cloning of a *Pseudomonas* gene encoding a

hydroxydecanoyl-acyl carrier protein-dependent UDP-GlcNAc acyltransferase, *J. Bacteriol. 180*, 330-337.

37. Lambalot, R. H., and Walsh, C. T. (1995) Cloning, overproduction, and characterization of the *Escherichia coli* holo-acyl carrier protein synthase, *J. Biol. Chem. 270*, 24658-24661.

38. Haas, J. A., Frederick, M. A., and Fox, B. G. (2000) Chemical and posttranslational modification of *Escherichia coli* acyl carrier protein for preparation of dansyl-acyl carrier proteins, *Protein Expr. Purif. 20*, 274-284.

39. Schaeffer, M. L., Agnihotri, G., Volker, C., Kallender, H., Brennan, P. J., and Lonsdale, J. T. (2001) Purification and biochemical characterization of the *Mycobacterium tuberculosis* beta-ketoacyl-acyl carrier protein synthases KasA and KasB, *J. Biol. Chem. 276*, 47029-47037.

40. Broadwater, J. A., and Fox, B. G. (1999) Spinach holo-acyl carrier protein: overproduction and phosphopantetheinylation in *Escherichia coli* BL21(DE3), *in vitro* acylation, and enzymatic desaturation of histidine-tagged isoform I, *Protein Expr. Purif.15*, 314-326.

41. Shimakata, T., and Stumpf, P. K. (1982) The procaryotic nature of the fatty acid synthetase of developing Carthamus tinctorius L. (Safflower) seeds, *Arch. Biochem. Biophys. 217*, 144-154.

42. Kapoor, M., Dar, M. J., Surolia, A., and Surolia, N. (2001) Kinetic determinants of the interaction of enoyl-ACP reductase from *Plasmodium falciparum* with its substrates and inhibitors, *Biochem. Biophys. Res. Commun. 289*, 832-837.

43. Quemard, A., Sacchettini, J. C., Dessen, A., Vilcheze, C., Bittman, R., Jacobs WR, J. r., and Blanchard, J. S. (1995) Enzymatic characterization of the target for isoniazid in *Mycobacterium tuberculosis*, *Biochemistry 34*, 8235-8241.

44. Cleland, W. W. (1963) The kinetics of enzyme-catalyzed reactions with two or more substrates or products. I. Nomenclature and rate equations, *Biochim. Biophys. Acta 67*, 104-137.

45. Cleland, W. W. (1963) The kinetics of enzyme-catalyzed reactions with two or more substrates or products. II. Inhibition: nomenclature and theory, *Biochim. Biophys. Acta 67*, 173-187.

46. Sivaraman, S., Zwahlen, J., Bell, A. F., Hedstrom, L., and Tonge, P. J. (2003) Structure-activity studies of the inhibition of FabI, the enoyl reductase from *Escherichia coli*, by triclosan: kinetic analysis of mutant FabIs, *Biochemistry 42*, 4406-4413.

47. Xu, H., Sullivan, T. J., Sekiguchi, J., Kirikae, T., Ojima, I., Stratton, C. F.,

Mao, W., Rock, F. L., Alley, M. R., Johnson, F., Walker, S. G., and Tonge, P. J. (2008) Mechanism and inhibition of saFabI, the enoyl reductase from *Staphylococcus aureus*, *Biochemistry 47*, 4228-4236.

48. Chhibber, M., Kumar, G., Parasuraman, P., Ramya, T. N., Surolia, N., and Surolia, A. (2006) Novel diphenyl ethers: design, docking studies, synthesis and inhibition of enoyl ACP reductase of *Plasmodium falciparum* and *Escherichia coli*, *Bioorg. Med. Chem. 14*, 8086-8098.

49. Rafi, S. B., Cui, G., Song, K., Cheng, X., Tonge, P. J., and Simmerling, C. (2006) Insight through molecular mechanics Poisson-Boltzmann surface area calculations into the binding affinity of triclosan and three analogues for FabI, the *E. coli* enoyl reductase, *J. Med. Chem. 49*, 4574-4580.

Chapter III

1. Zhang, R., and Monsma, F. (2009) The importance of drug-target residence time, *Curr. Opin. Drug Discov. Devel. 12*, 488-496.

2. Kumar, P., Han, B. C., Shi, Z., Jia, J., Wang, Y. P., Zhang, Y. T., Liang, L., Liu, Q. F., Ji, Z. L., and Chen, Y. Z. (2009) Update of KDBI: Kinetic Data of Bio-molecular Interaction database, *Nucleic Acids Res. 37*, D636-641.

3. Tummino, P. J., and Copeland, R. A. (2008) Residence time of

233

receptor-ligand complexes and its effect on biological function, *Biochemistry 47*, 5481-5492.

4.   Swinney, D. C. (2004) Biochemical mechanisms of drug action: what does it take for success?, *Nat. Rev. Drug. Discov. 3*, 801-808.

5.   Dierynck, I., De Wit, M., Gustin, E., Keuleers, I., Vandersmissen, J., Hallenberger, S., and Hertogs, K. (2007) Binding kinetics of darunavir to human immunodeficiency virus type 1 protease explain the potent antiviral activity and high genetic barrier, *J. Virol. 81*, 13845-13851.

6.   Kim, Y. B., Kopcho, L. M., Kirby, M. S., Hamann, L. G., Weigelt, C. A., Metzler, W. J., and Marcinkeviciene, J. (2006) Mechanism of Gly-Pro-pNA cleavage catalyzed by dipeptidyl peptidase-IV and its inhibition by saxagliptin (BMS-477118), *Arch. Biochem. Biophys. 445*, 9-18.

7.   Rawat, R., Whitty, A., and Tonge, P. J. (2003) The isoniazid-NAD adduct is a slow, tight-binding inhibitor of InhA, the *Mycobacterium tuberculosis* enoyl reductase: adduct affinity and drug resistance, *Proc. Natl. Acad. Sci. U.S.A. 100*, 13881-13886.

8.   Tsai, Y. C., and Johnson, K. A. (2006) A new paradigm for DNA polymerase specificity, *Biochemistry 45*, 9675-9687.

9.   Copeland, R. (2005) Evaluation of enzyme inhibitors in drug discovery: a

guide for medicinal chemists and pharmacologists, 2nd ed., Wiley & Sons, Inc., 144-178.

10.   Leysen, J., and Gommeren, W. (1986) Drug-receptor dissociation time, new tool for drug research: receptr binding affinity and drug-receptor dissociation profiles of Serotonin-S2, dopamine-D2, Histamine-H1 Antagonists, and opiates, *Drug Develop. Res. 8*, 119-131.

11.   Copeland, R. A., Pompliano, D. L., and Meek, T. D. (2006) Drug-target residence time and its implications for lead optimization, *Nat. Rev. Drug Discov. 5*, 730-739.

12.   Swinney, D. (2008) Applications of binding kinetics to drug discovery: translation of binding mechanisms to clinically differentiated therapeutic responses, *Curr. Opin. Pharm. Med. 22*, 23-34.

13.   Swinney, D. C. (2009) The role of binding kinetics in therapeutically useful drug action, *Curr. Opin. Drug Discov. Devel. 12*, 31-39.

14.   Swinney, D. C. (2006) Biochemical mechanisms of New Molecular Entities (NMEs) approved by United States FDA during 2001-2004: mechanisms leading to optimal efficacy and safety, *Curr. Top. Med. Chem. 6*, 461-478.

15.   Morrison, J. F., and Walsh, C. T. (1988) The behavior and significance of slow-binding enzyme inhibitors, *Adv. Enzymol. Relat. Areas Mol. Biol. 61*,

201-301.

16. Lu, H., and Tonge, P. J. (2008) Inhibitors of FabI, an enzyme drug target in the bacterial fatty acid biosynthesis pathway, *Acc. Chem. Res. 41*, 11-20.

17. Ward, W. H., Holdgate, G. A., Rowsell, S., McLean, E. G., Pauptit, R. A., Clayton, E., Nichols, W. W., Colls, J. G., Minshull, C. A., Jude, D. A., Mistry, A., Timms, D., Camble, R., Hales, N. J., Britton, C. J., and Taylor, I. W. (1999) Kinetic and structural characteristics of the inhibition of enoyl acyl carrier protein reductase by triclosan, *Biochemistry 38*, 12514-12525.

18. Kapoor, M., Dar, M. J., Surolia, A., and Surolia, N. (2001) Kinetic determinants of the interaction of enoyl-ACP reductase from *Plasmodium falciparum* with its substrates and inhibitors, *Biochem. Biophys. Res. Commun. 289*, 832-837.

19. Marcinkeviciene, J., Jiang, W., Kopcho, L. M., Locke, G., Luo, Y., and Copeland, R. A. (2001) Enoyl-ACP reductase (FabI) of *Haemophilus influenzae*: steady-state kinetic mechanism and inhibition by triclosan and hexachlorophene, *Arch. Biochem. Biophys. 390*, 101-108.

20. Xu, H., Sullivan, T. J., Sekiguchi, J., Kirikae, T., Ojima, I., Stratton, C. F., Mao, W., Rock, F. L., Alley, M. R., Johnson, F., Walker, S. G., and Tonge, P. J. (2008) Mechanism and inhibition of saFabI, the enoyl reductase from

Staphylococcus aureus, *Biochemistry 47*, 4228-4236.

21.   Stewart, M. J., Parikh, S., Xiao, G., Tonge, P. J., and Kisker, C. (1999) Structural basis and mechanism of enoyl reductase inhibition by triclosan, *J. Mol. Biol. 290*, 859-865.

22.   Pidugu, L. S., Kapoor, M., Surolia, N., Surolia, A., and Suguna, K. (2004) Structural basis for the variation in triclosan affinity to enoyl reductases, *J. Mol. Biol. 343*, 147-155.

23.   am Ende, C. W., Knudson, S. E., Liu, N., Childs, J., Sullivan, T. J., Boyne, M., Xu, H., Gegina, Y., Knudson, D. L., Johnson, F., Peloquin, C. A., Slayden, R. A., and Tonge, P. J. (2008) Synthesis and in vitro antimycobacterial activity of B-ring modified diaryl ether InhA inhibitors, *Bioorg. Med. Chem. Lett. 18*, 3029-3033.

24.   Luckner, S., Liu, N., am Ende, C., Tonge, P. J., and Kisker, C. (2010) A slow, tight-binding inhibitor of InhA, the enoyl-ACP reductase from *Mycobacterium tuberculosis*, *J. Biol. Chem.* Epub.

25.   Sivaraman, S., Sullivan, T. J., Johnson, F., Novichenok, P., Cui, G., Simmerling, C., and Tonge, P. J. (2004) Inhibition of the bacterial enoyl reductase FabI by triclosan: a structure-reactivity analysis of FabI inhibition by triclosan analogues, *J. Med. Chem. 47*, 509-518.

26. Sullivan, T. J., Truglio, J. J., Boyne, M. E., Novichenok, P., Zhang, X., Stratton, C. F., Li, H. J., Kaur, T., Amin, A., Johnson, F., Slayden, R. A., Kisker, C., and Tonge, P. J. (2006) High affinity InhA inhibitors with activity against drug-resistant strains of *Mycobacterium tuberculosis*, *ACS Chem. Biol. 1*, 43-53.

27. Parikh, S., Moynihan, D. P., Xiao, G., and Tonge, P. J. (1999) Roles of tyrosine 158 and lysine 165 in the catalytic mechanism of InhA, the enoyl-ACP reductase from *Mycobacterium tuberculosis*, *Biochemistry 38*, 13623-13634.

28. Hammill, J. T., Miyake-Stoner, S., Hazen, J. L., Jackson, J. C., and Mehl, R. A. (2007) Preparation of site-specifically labeled fluorinated proteins for 19F-NMR structural characterization, *Nat. Protoc. 2*, 2601-2607.

29. Morrison, J. F., and Walsh, C. T. (1988) The behavior and significance of slow-binding enzyme inhibitors, *Adv. Enzymol. Relat. Areas Mol. Biol. 61*, 201-301.

30. Goodson, R. J., and Katre, N. V. (1990) Site-directed pegylation of recombinant interleukin-2 at its glycosylation site, *Biotech. (N. Y.) 8*, 343-346.

31. Chilkoti, A., Chen, G., Stayton, P. S., and Hoffman, A. S. (1994)

Site-specific conjugation of a temperature-sensitive polymer to a genetically-engineered protein, *Bioconjug. Chem. 5*, 504-507.

32. Zhang, Z., Smith, B. A., Wang, L., Brock, A., Cho, C., and Schultz, P. G. (2003) A new strategy for the site-specific modification of proteins in vivo, *Biochemistry 42*, 6735-6746.

33. Xie, J., and Schultz, P. G. (2005) Adding amino acids to the genetic repertoire, *Curr. Opin. Chem. Biol. 9*, 548-554.

34. Xie, J., and Schultz, P. G. (2005) An expanding genetic code, *Methods 36*, 227-238.

35. Wang, W., Takimoto, J. K., Louie, G. V., Baiga, T. J., Noel, J. P., Lee, K. F., Slesinger, P. A., and Wang, L. (2007) Genetically encoding unnatural amino acids for cellular and neuronal studies, *Nat. Neurosci. 10*, 1063-1072.

36. Wang, L., Xie, J., and Schultz, P. G. (2006) Expanding the genetic code, *Annu. Rev. Biophys. Biomol. Struct. 35*, 225-249.

37. Tang, J., Signarvic, R. S., DeGrado, W. F., and Gai, F. (2007) Role of helix nucleation in the kinetics of binding of mastoparan X to phospholipid bilayers, *Biochemistry 46*, 13856-13863.

38. Miyake-Stoner, S. J., Miller, A. M., Hammill, J. T., Peeler, J. C., Hess, K. R.,

Mehl, R. A., and Brewer, S. H. (2009) Probing protein folding using site-specifically encoded unnatural amino acids as FRET donors with tryptophan, *Biochemistry 48*, 5953-5962.

39.   Tucker, M. J., Oyola, R., and Gai, F. (2005) Conformational distribution of a 14-residue peptide in solution: a fluorescence resonance energy transfer study, *J. Phys. Chem. B 109*, 4788-4795.

40.   Aprilakis, K. N., Taskent, H., and Raleigh, D. P. (2007) Use of the novel fluorescent amino acid *p*-cyanophenylalanine offers a direct probe of hydrophobic core formation during the folding of the N-terminal domain of the ribosomal protein L9 and provides evidence for two-state folding, *Biochemistry 46*, 12308-12313.

41.   Marek, P., Mukherjee, S., Zanni, M., and Raleigh, D. Residue specific, real time characterization of lag phase species and fibril growth during amyloid formation: a combined fluorescence and IR studie of *p*-cyanophenylalanine analogues of islet amyloid polypeptide, *J. Mol. Biol.* (submitted).

Chapter IV

1.   Schadewaldt, H. (1975) Discovery of glanders bacillus, *Dtsch. Med. Wochenschr. 100*, 2292-2295.

2.   Whitlock, G. C., Estes, D. M., and Torres, A. G. (2007) Glanders: off to the races with *Burkholderia mallei*, *FEMS Microbiol. Lett. 277*, 115-122.

3.   Gilad, J., Harary, I., Dushnitsky, T., Schwartz, D., and Amsalem, Y. (2007) *Burkholderia mallei* and *Burkholderia pseudomallei* as bioterrorism agents: national aspects of emergency preparedness, *Isr. Med. Assoc. J. 9*, 499-503.

4.   Wheelis, M. (1998) First shots fired in biological warfare, *Nature 395*, 213.

5.   Rotz, L. D., Khan, A. S., Lillibridge, S. R., Ostroff, S. M., and Hughes, J. M. (2002) Public health assessment of potential biological terrorism agents, *Emerg. Infect. Dis. 8*, 225-230.

6.   Horn, J. K. (2003) Bacterial agents used for bioterrorism, *Surg. Infect. (Larchmt) 4*, 281-287.

7.   Heath, R. J., and Rock, C. O. (2004) Fatty acid biosynthesis as a target for novel antibacterials, *Curr. Opin. Investig. Drugs 5*, 146-153.

8.   Heath, R. J., White, S. W., and Rock, C. O. (2001) Lipid biosynthesis as a target for antibacterial agents, *Prog. Lipid Res. 40*, 467-497.

9.   White, S. W., Zheng, J., Zhang, Y. M., and Rock. (2005) The structural biology of type II fatty acid biosynthesis, *Annu. Rev. Biochem. 74*, 791-831.

10.   McMurry, L. M., Oethinger, M., and Levy, S. B. (1998) Triclosan targets lipid

synthesis, *Nature 394*, 531-532.

11. Heath, R. J., Yu, Y. T., Shapiro, M. A., Olson, E., and Rock, C. O. (1998) Broad spectrum antimicrobial biocides target the FabI component of fatty acid synthesis, *J. Biol. Chem. 273*, 30316-30320.

12. Musser, J. M., Kapur, V., Williams, D. L., Kreiswirth, B. N., van Soolingen, D., and van Embden, J. D. (1996) Characterization of the catalase-peroxidase gene (katG) and inhA locus in isoniazid-resistant and -susceptible strains of *Mycobacterium tuberculosis* by automated DNA sequencing: restricted array of mutations associated with drug resistance, *J. Infect. Dis. 173*, 196-202.

13. Tonge, P. J., Kisker, C., and Slayden, R. A. (2007) Development of modern InhA inhibitors to combat drug resistant strains of *Mycobacterium tuberculosis*, *Curr. Top. Med. Chem. 7*, 489-498.

14. Bergler, H., Wallner, P., Ebeling, A., Leitinger, B., Fuchsbichler, S., Aschauer, H., Kollenz, G., Hogenauer, G., and Turnowsky, F. (1994) Protein EnvM is the NADH-dependent enoyl-ACP reductase (FabI) of *Escherichia coli*, *J. Biol. Chem. 269*, 5493-5496.

15. Lu, H., England, K., am Ende, C., Truglio, J. J., Luckner, S., Reddy, B. G., Marlenee, N. L., Knudson, S. E., Knudson, D. L., Bowen, R. A., Kisker, C.,

Slayden, R. A., and Tonge, P. J. (2009) Slow-onset inhibition of the FabI enoyl reductase from *Francisella tularensis*: residence time and in vivo activity, *ACS Chem. Biol. 4*, 221-231.

16. Zhang, Y. M., White, S. W., and Rock, C. O. (2006) Inhibiting bacterial fatty acid synthesis, *J. Biol. Chem. 281*, 17541-17544.

17. Heath, R. J., and Rock, C. O. (2000) A triclosan-resistant bacterial enzyme, *Nature 406*, 145-146.

18. Heath, R. J., Su, N., Murphy, C. K., and Rock, C. O. (2000) The enoyl-acyl-carrier-protein reductases FabI and FabL from *Bacillus subtilis*, *J. Biol. Chem. 275*, 40128-40133.

19. Massengo-Tiasse, R. P., and Cronan, J. E. (2008) *Vibrio cholerae* FabV defines a new class of enoyl-acyl carrier protein reductase, *J. Biol. Chem. 283*, 1308-1316.

20. Sivaraman, S., Sullivan, T. J., Johnson, F., Novichenok, P., Cui, G., Simmerling, C., and Tonge, P. J. (2004) Inhibition of the bacterial enoyl reductase FabI by triclosan: a structure-reactivity analysis of FabI inhibition by triclosan analogues, *J. Med. Chem. 47*, 509-518.

21. Sullivan, T. J., Truglio, J. J., Boyne, M. E., Novichenok, P., Zhang, X., Stratton, C. F., Li, H. J., Kaur, T., Amin, A., Johnson, F., Slayden, R. A.,

Kisker, C., and Tonge, P. J. (2006) High affinity InhA inhibitors with activity against drug-resistant strains of *Mycobacterium tuberculosis*, *ACS Chem. Biol. 1*, 43-53.

22. am Ende, C. W., Knudson, S. E., Liu, N., Childs, J., Sullivan, T. J., Boyne, M., Xu, H., Gegina, Y., Knudson, D. L., Johnson, F., Peloquin, C. A., Slayden, R. A., and Tonge, P. J. (2008) Synthesis and *in vitro* antimycobacterial activity of B-ring modified diaryl ether InhA inhibitors, *Bioorg. Med. Chem. Lett. 18*, 3029-3033.

23. Parikh, S., Moynihan, D. P., Xiao, G., and Tonge, P. J. (1999) Roles of tyrosine 158 and lysine 165 in the catalytic mechanism of InhA, the enoyl-ACP reductase from *Mycobacterium tuberculosis*, *Biochemistry 38*, 13623-13634.

24. Cleland, W. W. (1963) The kinetics of enzyme-catalyzed reactions with two or more substrates or products. I. Nomenclature and rate equations, *Biochim. Biophys. Acta 67*, 104-137.

25. Cleland, W. W. (1963) The kinetics of enzyme-catalyzed reactions with two or more substrates or products. II. Inhibition: nomenclature and theory, *Biochim. Biophys. Acta 67*, 173-187.

26. Marcinkeviciene, J., Jiang, W., Kopcho, L. M., Locke, G., Luo, Y., and

Copeland, R. A. (2001) Enoyl-ACP reductase (FabI) of *Haemophilus influenzae*: steady-state kinetic mechanism and inhibition by triclosan and hexachlorophene, *Arch. Biochem. Biophys. 390*, 101-108.

27. Kapoor, M., Dar, M. J., Surolia, A., and Surolia, N. (2001) Kinetic determinants of the interaction of enoyl-ACP reductase from *Plasmodium falciparum* with its substrates and inhibitors, *Biochem. Biophys. Res. Commun. 289*, 832-837.

28. Xu, H., Sullivan, T. J., Sekiguchi, J., Kirikae, T., Ojima, I., Stratton, C. F., Mao, W., Rock, F. L., Alley, M. R., Johnson, F., Walker, S. G., and Tonge, P. J. (2008) Mechanism and inhibition of saFabI, the enoyl reductase from *Staphylococcus aureus*, *Biochemistry 47*, 4228-4236.

29. Ward, W. H., Holdgate, G. A., Rowsell, S., McLean, E. G., Pauptit, R. A., Clayton, E., Nichols, W. W., Colls, J. G., Minshull, C. A., Jude, D. A., Mistry, A., Timms, D., Camble, R., Hales, N. J., Britton, C. J., and Taylor, I. W. (1999) Kinetic and structural characteristics of the inhibition of enoyl (acyl carrier protein) reductase by triclosan, *Biochemistry 38*, 12514-12525.

30. Fawcett, T., Copse, C. L., Simon, J. W., and Slabas, A. R. (2000) Kinetic mechanism of NADH-enoyl-ACP reductase from *Brassica napus*, *FEBS Lett. 484*, 65-68.

31. Roujeinikova, A., Levy, C. W., Rowsell, S., Sedelnikova, S., Baker, P. J., Minshull, C. A., Mistry, A., Colls, J. G., Camble, R., Stuitje, A. R., Slabas, A. R., Rafferty, J. B., Pauptit, R. A., Viner, R., and Rice, D. W. (1999) Crystallographic analysis of triclosan bound to enoyl reductase, *J. Mol. Biol. 294*, 527-535.

32. Baldock, C., Rafferty, J. B., Stuitje, A. R., Slabas, A. R., and Rice, D. W. (1998) The X-ray structure of *Escherichia coli* enoyl reductase with bound NAD$^+$ at 2.1 A resolution, *J. Mol. Biol. 284*, 1529-1546.

33. Rozwarski, D. A., Vilcheze, C., Sugantino, M., Bittman, R., and Sacchettini, J. C. (1999) Crystal structure of the *Mycobacterium tuberculosis* enoyl-ACP reductase, InhA, in complex with NAD$^+$ and a C16 fatty acyl substrate, *J. Biol. Chem. 274*, 15582-15589.

34. Rafferty, J. B., Simon, J. W., Baldock, C., Artymiuk, P. J., Baker, P. J., Stuitje, A. R., Slabas, A. R., and Rice, D. W. (1995) Common themes in redox chemistry emerge from the X-ray structure of oilseed rape (*Brassica napus*) enoyl acyl carrier protein reductase, *Structure 3*, 927-938.

35. Thompson, J. D., Higgins, D. G., and Gibson, T. J. (1994) CLUSTAL W: improving the sensitivity of progressive multiple sequence alignment through sequence weighting, position-specific gap penalties and weight

matrix choice, *Nucleic Acids Res. 22*, 4673-4680.

36.   Waterhouse, A. M., Procter, J. B., Martin, D. M., Clamp, M., and Barton, G. J. (2009) Jalview Version 2--a multiple sequence alignment editor and analysis workbench, *Bioinformatics 25*, 1189-1191.

37.   Jornvall, H., Persson, B., Krook, M., Atrian, S., Gonzalez-Duarte, R., Jeffery, J., and Ghosh, D. (1995) Short-chain dehydrogenases/reductases (SDR), *Biochemistry 34*, 6003-6013.

38.   Sivaraman, S., Zwahlen, J., Bell, A. F., Hedstrom, L., and Tonge, P. J. (2003) Structure-activity studies of the inhibition of FabI, the enoyl reductase from *Escherichia coli*, by triclosan: kinetic analysis of mutant FabIs, *Biochemistry 42*, 4406-4413.

39.   Rafi, S., Novichenok, P., Kolappan, S., Zhang, X., Stratton, C. F., Rawat, R., Kisker, C., Simmerling, C., and Tonge, P. J. (2006) Structure of acyl carrier protein bound to FabI, the FASII enoyl reductase from *Escherichia coli*, *The J. Biol. Chem. 281*, 39285-39293.

40.   Fillgrove, K. L., and Anderson, V. E. (2001) The mechanism of dienoyl-CoA reduction by 2,4-dienoyl-CoA reductase is stepwise: observation of a dienolate intermediate, *Biochemistry 40*, 12412-12421.

41.   Filling, C., Berndt, K. D., Benach, J., Knapp, S., Prozorovski, T., Nordling,

E., Ladenstein, R., Jornvall, H., and Oppermann, U. (2002) Critical residues for structure and catalysis in short-chain dehydrogenases/reductases, *J. Biol. Chem. 277*, 25677-25684.

42. Perozzo, R., Kuo, M., Sidhu, A. S., Valiyaveettil, J. T., Bittman, R., Jacobs, W. R., Jr., Fidock, D. A., and Sacchettini, J. C. (2002) Structural elucidation of the specificity of the antibacterial agent triclosan for malarial enoyl acyl carrier protein reductase, *J. Biol. Chem. 277*, 13106-13114.

43. Lu, H., and Tonge, P. J. (2008) Inhibitors of FabI, an enzyme drug target in the bacterial fatty acid biosynthesis pathway, *Acc. Chem. Res. 41*, 11-20.

44. Stewart, M. J., Parikh, S., Xiao, G., Tonge, P. J., and Kisker, C. (1999) Structural basis and mechanism of enoyl reductase inhibition by triclosan, *J. Mol. Biol. 290*, 859-865.

45. Pidugu, L. S., Kapoor, M., Surolia, N., Surolia, A., and Suguna, K. (2004) Structural basis for the variation in triclosan affinity to enoyl reductases, *J. Mol. Biol. 343*, 147-155.

46. Parikh, S. L., Xiao, G., and Tonge, P. J. (2000) Inhibition of InhA, the enoyl reductase from *Mycobacterium tuberculosis*, by triclosan and isoniazid, *Biochemistry 39*, 7645-7650.

47. Luckner, S., Liu, N., am Ende, C., Tonge, P. J., and Kisker, C. (2010) A slow,

tight-binding inhibitor of InhA, the enoyl-ACP reductase from *Mycobacterium tuberculosis*, *J. Biol. Chem.* Epub.

48.   Rawat, R., Whitty, A., and Tonge, P. J. (2003) The isoniazid-NAD adduct is a slow, tight-binding inhibitor of InhA, the *Mycobacterium tuberculosis* enoyl reductase: adduct affinity and drug resistance, *Proc. Natl. Acad. Sci. U.S.A. 100*, 13881-13886.

49.   Zhu, L., Lin, J., Ma, J., Cronan, J. E., and Wang, H. (2010) Triclosan resistance of *Pseudomonas aeruginosa* PAO1 is due to FabV, a triclosan-resistant enoyl-acyl carrier protein reductase, *Antimicrob. Agents Chemother. 54*, 689-698.

Chapter V

1.   Bergler, H., Wallner, P., Ebeling, A., Leitinger, B., Fuchsbichler, S., Aschauer, H., Kollenz, G., Hogenauer, G., and Turnowsky, F. (1994) Protein EnvM is the NADH-dependent enoyl-ACP reductase (FabI) of *Escherichia coli*, *J. Biol. Chem. 269*, 5493-5496.

2.   Xu, H., Sullivan, T. J., Sekiguchi, J., Kirikae, T., Ojima, I., Stratton, C. F., Mao, W., Rock, F. L., Alley, M. R., Johnson, F., Walker, S. G., and Tonge, P. J. (2008) Mechanism and inhibition of saFabI, the enoyl reductase from

Staphylococcus aureus, *Biochemistry 47*, 4228-4236.

3.   Lu, H., England, K., am Ende, C., Truglio, J. J., Luckner, S., Reddy, B. G.,

Marlenee, N. L., Knudson, S. E., Knudson, D. L., Bowen, R. A., Kisker, C.,

Slayden, R. A., and Tonge, P. J. (2009) Slow-onset inhibition of the FabI

enoyl reductase from *Francisella tularensis*: residence time and in vivo

activity, *ACS Chem. Biol. 4*, 221-231.

4.   Heath, R. J., and Rock, C. O. (2000) A triclosan-resistant bacterial enzyme,

Nature 406, 145-146.

5.   Heath, R. J., Su, N., Murphy, C. K., and Rock, C. O. (2000) The

enoyl-acyl-carrier-protein reductases FabI and FabL from *Bacillus subtilis*,

J. Biol. Chem. 275, 40128-40133.

6.   Massengo-Tiasse, R. P., and Cronan, J. E. (2008) *Vibrio cholerae* FabV

defines a new class of enoyl-acyl carrier protein reductase, *J. Biol. Chem.

283*, 1308-1316.

7.   Massengo-Tiasse, R. P., and Cronan, J. E. (2009) Diversity in enoyl-acyl

carrier protein reductases, *Cell Mol. Life Sci. 66*, 1507-1517.

8.   White, S. W., Zheng, J., Zhang, Y. M., and Rock. (2005) The structural

biology of type II fatty acid biosynthesis, *Annu. Rev. Biochem. 74*, 791-831.

9.   Lu, H., and Tonge, P. J. (2010) Mechanism and inhibition of the FabV

enoyl-ACP reductase from *Burkholderia mallei*, *Biochemistry 49*, 1281-1289.

10.   Saito, J., Yamada, M., Watanabe, T., Iida, M., Kitagawa, H., Takahata, S., Ozawa, T., Takeuchi, Y., and Ohsawa, F. (2008) Crystal structure of enoyl-acyl carrier protein reductase (FabK) from *Streptococcus pneumoniae* reveals the binding mode of an inhibitor, *Protein Sci. 17*, 691-699.

11.   Zhu, L., Lin, J., Ma, J., Cronan, J. E., and Wang, H. (2010) Triclosan resistance of *Pseudomonas aeruginosa* PAO1 is due to FabV, a triclosan-resistant enoyl-acyl carrier protein reductase, *Antimicrob. Agents Chemother. 54*, 689-698.

12.   Cronan, J. E., Jr., and Gelmann, E. P. (1975) Physical properties of membrane lipids: biological relevance and regulation, *Bacteriol. Rev. 39*, 232-256.

13.   Morein, S., Andersson, A., Rilfors, L., and Lindblom, G. (1996) Wild-type *Escherichia coli* cells regulate the membrane lipid composition in a "window" between gel and non-lamellar structures, *J. Biol. Chem. 271*, 6801-6809.

14.   Cronan, J. E. (2003) Bacterial membrane lipids: where do we stand?, *Annu.*

Rev. Microbiol. 57, 203-224.

15. Mansilla, M. C., and de Mendoza, D. (2005) The *Bacillus subtilis* desaturase: a model to understand phospholipid modification and temperature sensing, *Arch. Microbiol. 183*, 229-235.

16. Fulco, A. J. (1969) The biosynthesis of unsaturated fatty acids by bacilli. I. Temperature induction of the desaturation reaction, *J. Biol. Chem. 244*, 889-895.

17. Mansilla, M. C., Cybulski, L. E., Albanesi, D., and de Mendoza, D. (2004) Control of membrane lipid fluidity by molecular thermosensors, *J. Bacteriol. 86*, 6681-6688.

18. Rock, C. O., and Cronan, J. E. (1996) *Escherichia coli* as a model for the regulation of dissociable (type II) fatty acid biosynthesis, *Biochim. Biophys. Acta 1302*, 1-16.

19. Lu, Y. J., Zhang, Y. M., and Rock, C. O. (2004) Product diversity and regulation of type II fatty acid synthases, *Biochem. Cell Biol. 82*, 145-155.

20. Marrakchi, H., Zhang, Y. M., and Rock, C. O. (2002) Mechanistic diversity and regulation of Type II fatty acid synthesis, *Biochem. Soc. Trans. 30*, 1050-1055.

21. Kass, L. R., and Bloch, K. (1967) On the enzymatic synthesis of

unsaturated fatty acids in *Escherichia coli*, *Proc. Natl. Acad. Sci. U.S.A. 58*, 1168-1173.

22. Bloch, K. (1969) Enzymic synthesis of monounsaturated fatty acids, *Acc. Chem. Res. 2*, 193-202.

23. Feng, Y., and Cronan, J. E. (2009) *Escherichia coli* unsaturated fatty acid synthesis: complex transcription of the fabA gene and *in vivo* identification of the essential reaction catalyzed by FabB, *J. Biol. Chem. 284*, 29526-29535.

24. Rosenfeld, I. S., D'Agnolo, G., and Vagelos, P. R. (1973) Synthesis of unsaturated fatty acids and the lesion in *fabB* mutants, *J. Biol. Chem. 248*, 2452-2460.

25. D'Agnolo, G., Rosenfeld, I. S., and Vagelos, P. R. (1975) Multiple forms of beta-ketoacyl-acyl carrier protein synthetase in *Escherichia coli*, *J. Biol. Chem. 250*, 5289-5294.

26. Garwin, J. L., Klages, A. L., and Cronan, J. E., Jr. (1980) Structural, enzymatic, and genetic studies of beta-ketoacyl-acyl carrier protein synthases I and II of *Escherichia coli*, *J. Biol. Chem. 255*, 11949-11956.

27. de Mendoza, D., Klages Ulrich, A., and Cronan, J. E., Jr. (1983) Thermal regulation of membrane fluidity in *Escherichia coli*. Effects of

overproduction of beta-ketoacyl-acyl carrier protein synthase I, *J. Biol. Chem. 258*, 2098-2101.

28.   Clark, D. P., DeMendoza, D., Polacco, M. L., and Cronan, J. E., Jr. (1983) Beta-hydroxydecanoyl thio ester dehydrase does not catalyze a rate-limiting step in *Escherichia coli* unsaturated fatty acid synthesis, *Biochemistry 22*, 5897-5902.

29.   Marrakchi, H., Choi, K. H., and Rock, C. O. (2002) A new mechanism for anaerobic unsaturated fatty acid formation in *Streptococcus pneumoniae*, *J. Biol. Chem. 277*, 44809-44816.

30.   Fozo, E. M., and Quivey, R. G., Jr. (2004) The fabM gene product of *Streptococcus mutans* is responsible for the synthesis of monounsaturated fatty acids and is necessary for survival at low pH, *J. Bacteriol. 186*, 4152-4158.

31.   Altabe, S., Lopez, P., and de Mendoza, D. (2007) Isolation and characterization of unsaturated fatty acid auxotrophs of *Streptococcus pneumoniae* and Streptococcus mutans, *J. Bacteriol. 189*, 8139-8144.

32.   Campbell, J. W., and Cronan, J. E., Jr. (2001) Bacterial fatty acid biosynthesis: targets for antibacterial drug discovery, *Annu. Rev. Microbiol. 55*, 305-332.

33. Wang, H., and Cronan, J. E. (2004) Functional replacement of the FabA and FabB proteins of *Escherichia coli* fatty acid synthesis by *Enterococcus faecalis* FabZ and FabF homologues, *J. Biol. Chem. 279*, 34489-34495.

34. Rafi, S., Novichenok, P., Kolappan, S., Zhang, X., Stratton, C. F., Rawat, R., Kisker, C., Simmerling, C., and Tonge, P. J. (2006) Structure of acyl carrier protein bound to FabI, the FASII enoyl reductase from *Escherichia coli*, *J. Biol. Chem. 281*, 39285-39293.

35. Bergler, H., Hogenauer, G., and Turnowsky, F. (1992) Sequences of the envM gene and of two mutated alleles in *Escherichia coli*, *J. Gen. Microbiol.138*, 2093-2100.

36. Bergler, H., Fuchsbichler, S., Hogenauer, G., and Turnowsky, F. (1996) The enoyl-acyl-carrier-protein reductase (FabI) of *Escherichia coli*, which catalyzes a key regulatory step in fatty acid biosynthesis, accepts NADH and NADPH as cofactors and is inhibited by palmitoyl-CoA, *Eur. J. Biochem. 242*, 689-694.

37. Patrignani, F., Iucci, L., Belletti, N., Gardini, F., Guerzoni, M. E., and Lanciotti, R. (2008) Effects of sub-lethal concentrations of hexanal and 2-(E)-hexenal on membrane fatty acid composition and volatile compounds of *Listeria monocytogenes*, *Staphylococcus aureus*, *Salmonella enteritidis*

and *Escherichia coli*, *Int. J. Food Microbiol. 123*, 1-8.

38.   Jantzen, E., Berdal, B. P., and Omland, T. (1979) Cellular fatty acid composition of *Francisella tularensis*, *J. Clin. Microbiol. 10*, 928-930.

39.   White, D. C., and Frerman, F. E. (1968) Fatty acid composition of the complex lipids of *Staphylococcus aureus* during the formation of the membrane-bound electron transport system, *J. Bacteriol. 95*, 2198-2209.

40.   Vasiurenko, Z. P., Sel'nikova, O. P., Polishchuk, E. I., Samygin, V. M., and Ruban, N. M. (2006) Cellular fatty acid composition of the *Burkholderia mallei* and *Burkholderia pseudomallei* strains as generic feature of Burkholderia, *Mikrobiol. Z. 68*, 33-40.